

MODELING CAPACITY: MULTIPLE WEAVING AREAS

By:
Sheida Khademi

DISSERTATION

Submitted in partial fulfillment of the requirements.
for the degree of Doctor of Philosophy at
The University of Texas at Arlington
August 2021

Arlington, Texas

Supervising Committee:
Dr. James C Williams, Supervising Professor
Dr. Behruz Paschai, Co-advisor
Dr. Negin Fraidouni
Dr. Pengfei (Taylor) Li

Copyright © by Sheida Khademi 2021
All Rights Reserved



ACKNOWLEDGEMENTS

First and foremost, I would like to thank my supervisor Prof. Jim Williams from bottom of my heart who supported me for the last five years. His support was not limited to only my dissertation. He was a fabulous mentor and friend who I learned a lot from him. I am so grateful to him for his invaluable guidance, continuous support, and patience during my graduate journey.

My very sincere appreciation also goes to Dr. Behruz Paschai who played a vital role in my PhD achievement. His immense knowledge and deep insight have guided me throughout my dissertation. His brilliant ideas have always been taking me out from my research problems and helping me to solve them. I am truly honored working under his supervision.

I also want to thank Dr. Taylor Li, and Dr. Negin Fraidouni for their kind consent to be on my PhD supervising committee.

Thanks to Dr. Stephen Mattingly and Dr. Ali Abolmaali for their constant help and support all these years. They generously supported my graduate journey.

I also would like to extend my gratitude to my group member, Dr. Saeed Reza Ramezanpour Nargesi for making our group intimate and collaborative environment where we worked together happily.

I would like to acknowledge the funding agencies- National Institute for Transportation and Communities (NITC) for funding my project. I am also thankful to the Dept. of Civil Engineering, for giving me the opportunity to conduct my research work.

Finally, this work is dedicated to my beloved husband, Afshin, who has been a constant source of support and encouragement during the challenges of graduate school and life. I am truly thankful for having him in my life.

I am also thankful to my parents, parents' in-law and my lovely sister, Raha. They have always been there to help and encourage me and my family.

ABSTRACT

Modeling Capacity: Multiple Weaving Areas

Sheida Khademi, Ph.D.

The University of Texas at Arlington, 2021

Supervising Professor: James C Williams

Systematic, well-designed research provides the most effective approach to the solution of many problems facing highway administrators and engineers. Traffic congestion on freeway systems is one significant concern in urban areas throughout the U.S.A. In this era, building new freeways to reduce congestion is less feasible due to the high capital and social costs. Thus, the effective management and operation of existing freeway facilities has become a preferred approach to reduce traffic congestion.

A weaving section is a common design on major highway facilities that always has been an interest to researchers. Weaving areas are characterized by frequent lane changes, which significantly reduce the capacity of the freeway system. The HCM defined weaving capacity as “any combination of flows that causes the density to reach the LOS E/F boundary condition of 43 pc/m/ln for freeways” based on configuration, number of lanes in the weaving section, free-flow speed, length of the weave, and volume ratio (VR).

Weaving sections are often problematic because of the increase in lane changing. These are common design elements on freeway facilities between an on ramp and off ramp with an auxiliary lane. They are located between merge and diverge points, near ramps where a lane is added or dropped, and at multilane ramps. A weaving section is a freeway segment in which traffic flows cross each other without traffic control (Minderhoud et al. 2003).

Traffic demands exceeding segment capacity at weaving areas cause congestion, which affects the operation of the entire freeway section. Traffic operation problems often exist at weaving areas even when traffic demands are less than capacity and may be experienced at lower traffic flows because of the complexity of vehicle interactions, that is, increased lane changing, resulting in a degradation in level of service (LOS) and potential safety problems (Skabardonis et al. 2012).

A significant amount of research has been done to estimate quality of service and capacity in weaving sections. However, little has been done to address multiple weaves.

A multiple weaving area is one where two or more weaving areas overlap. No satisfactory means of estimating capacity has been found. Current procedures make assumptions about where weaving occurs in the individual weaving segments. A multiple weaving area is found when “a series of closely spaced merge and diverge areas create overlapping weaving movements (between different merge-diverge points).” (HCM 2016)

This work examines capacity and quality of service conditions for a specific example of a multiple weave. Capacity is evaluated through micro-simulation by gradually raising flows for a range of geometric and fraction of weaving-traffic conditions. Models are developed to express capacity in terms of lane configuration, flow ratios, traffic mix (heavy traffic percentages), and overall flow rate.

This study will be limited to cases where there are two overlapping weaving movements created by two entry ramps following by an exit ramp.

The study will develop relations for capacity and service volume for a range of geometric, flow conditions, and traffic mix. Geometric conditions will include number of lanes on the main lane entry and each entrance ramp into and exit ramp from the weaving area (n), and distances (L_s) between ramps. Flow conditions will include a range of flows from each of the entry and exit roadways (V) in the multiple weaving area. The traffic mix represents the fraction of heavy vehicles in the traffic stream (PHV).

In order to estimate the capacity of the weaving area, repeated simulations are performed under varying factors, number of lanes, flow range, heavy vehicle percentage, and routing. VISSIM outputs include link evaluation (average values for the link), and data collection (point measurement) files are extracted. These output files allow us to extract parameters, such as space-mean speed for links, to identify the point at which speed start to drop. Also, entry and exit volumes to see if they are the same as the summation of input volume that we specified in the run. The point that speed starts dropping significantly, or the summation of exit or entrance volume is much lower than what we entered in the system, suggests that we have reached the capacity point.

VISSIM simulation runs are done using COM programming. This VISSIM scripting tool will enable the user to automate the analysis process. Using COM programming, this research has been able to performs many more simulation iterations than otherwise would have been possible in the same time period. Not only for the factors but also for the driving behavior parameters (following, lane change, and car following). To estimate capacity, we will consider all possible combinations of car following parameters to see what gives us the maximum capacity.

At the same time, we will adjust different variables/factors we have introduced (number of lanes, flow, etc.) to see which one will give us a higher throughput, which is the capacity.

This work's result will be presented to DOTs and MPOs as a guidebook. The file would be highly useful and money-saving for these agencies as they prefer to obtain higher capacity by managing existing freeways rather than buying rights of ways.

CONTENTS

INTRODUCTION	17
CHAPTER 1: LITERATURE REVIEW	18
MICROSCOPIC ANALYSIS.....	21
CHAPTER 2: CALIBRATION	23
VISSIM INPUT	24
Network Geometry Coding.....	25
Vehicle Types and Traffic Compositions	25
Desired Speed Distributions	25
Vehicle Inputs and Routing	26
VISSIM OUTPUTS	27
SIMULATION.....	28
Running Time and Resolution	28
Number of Runs.....	28
PARAMETER ADJUSTMENT	31
Lane Change Distance (LCD).....	31
Driving Behavior	32
Driving Behavior/ Lane Change	32
Cooperative Lane Change (CLC)	33
Advanced Merge.....	33
The Emergency Stopping Distance.....	33
The Waiting Time before Diffusion.....	33
Minimum Headway (front/rear).....	33
Safety Distance Reduction Factor (SDRF)	34
Driving Behavior/ Car Following Model.....	34
CC0 (Standstill Distance).....	34
CC1 (Headway Time).....	34
CC2, Following Variation.....	35
CC4 and CC5	35
MODEL SELECTION.....	46
VALIDATION.....	47
SENSITIVITY ANALYSIS FOR CALIBRATION PARAMETERS	51
CHAPTER 3: SIMULATION MODELING	54

STAGES	55
VISSIM INPUT	56
Variables	56
Number of Lanes (48 Scenarios)	56
COM PROGRAMMING	61
SIMULATION RUNS AND RESULTS	61
VISSIM OUTPUTS	62
MODELING CAPACITY	63
SCENARIO 1 (S1).....	65
Capacity Estimation Using Link Flows	65
Capacity Conditions for R1-R2.....	66
Capacity Conditions for link R2-R3	68
Capacity by Density	72
Regression Analysis.....	73
R1-R2 Analysis.....	74
R2-R3 Analysis.....	74
Scenario 1 Conclusion	75
SCENARIO 2 through 44	75
Model Extension	88
Significant Factors for Capacity Evaluation: Multiple Weaving Networks	107
CHAPTER 4: ANALYTICAL MODELING	110
Weaving Multiplier.....	111
Determine Weaving Segment Capacity (C).....	112
LINEAR REGRESSION ANALYSIS.....	113
SENSITIVITY ANALYSIS	115
R1-R2 Segment Sensitivity Analysis.....	116
R2-R3 Segment Sensitivity Analysis.....	118
EXTENDED VR.....	119
MOST SIGNIFICANT FLOWS.....	120
OUTCOMES.....	120
Significant Factors Affecting Capacity: Multiple Weaving Networks (VR<0.7).....	120
Weaving Segment Capacity	120
CHAPTER 5: SUMMARY	122

Weaving Segment Capacity	123
REFERENCES	124
APPENDIX A; POSSIBLE LANE GEOMETRIES	128
APPENDIX B; CHARTS	131
APPENDIX C; MOST SIGNIFICANT FLOWS	196

FIGURES

Figure 1: State Highway 360 Northbound	23
Figure 2: Calibration Segment	24
Figure 3: Desired Speed Distribution	26
Figure 4: Time Intervals.....	27
Figure 5: Vehicle Input (7pm)	27
Figure 6: Vehicle Input (8am).....	27
Figure 7: Data Collection Points.....	28
Figure 8: Data Collection Points in VISSIM Network	28
Figure 9: 500 feet High -Density Lane Change Area	32
Figure 10: Model 1- 7pm- Volume.....	37
Figure 11: Model 1- 7pm- Speed.....	38
Figure 12: Model 2- 7pm- Volume.....	39
Figure 13: Model 2- 7 pm – Speed	39
Figure 14: Model 3- 7pm- Volume.....	40
Figure 15: Model 3- 7 pm – Speed	41
Figure 16: Model 4- 7pm- Volume.....	42
Figure 17: Model 4- 7pm- Speed	42
Figure 18: Model 5- 7pm- Volume.....	43
Figure 19: Model 5- 7pm- Speed	44
Figure 20: Model 6- 7pm- Volume.....	45
Figure 21: Model 6- 7pm- Speed	45
Figure 22: Volume Comparison- 8 am	49
Figure 23: Speed Comparison- 8 am	49
Figure 24: Sensitivity Analysis- Volume.....	53
Figure 25: Sensitivity Analysis- Speed.....	53
Figure 26: Multiple Weaving Area Elements	55
Figure 27: Flow Distribution	56
Figure 28: Type A Lane Configurations at The Merge/Diverge Points	59
Figure 29: Type B Lane Configurations at The Merge/Diverge Points.....	59
Figure 30: Multiple Weave Model Network in VISSIM	63
Figure 31: Scenario 1 Lane Geometry	66
Figure 32: Demand vs. Flow for R1-R2 Segment, Excluding VR1=3,000 & 1,500 vph.....	67
Figure 33: Demand vs. Flow for R1-R2 Segment, All Possible Variable Combinations.....	68
Figure 34: Demand vs. Flow for R1-R2 Segment, VF1=3,000 vph and VR1=1,500 vph	68
Figure 35: Demand vs. Flow for R2-R3 Segment, All Possible Variable Combinations.....	69
Figure 36: Demand vs. Flow for R2-R3 Segment, VR1-R2= 4,000/4,500 vph	70
Figure 37: Demand vs. Flow for R2-R3 Segment, VR1-R2= 4,500 vph and VR2= 1,000 vph...	70
Figure 38: Demand vs. Flow for R2-R3 Segment, VR1-R2= 4,000 vph and VR2=1,500 vph....	71
Figure 39: Demand vs. Flow for R2-R3 Segment, VR1-R2= 4,500 vph and VR2=1,500 vph....	71
Figure 40: Density Presentation.....	73
Figure 41: Density Presentation (Saturated).....	73
Figure 42: Scenario 4 Lane Geometry	75

Figure 43: Scenario 5 Lane Geometry	76
Figure 44: Scenario 9 Lane Geometry	77
Figure 45: Scenario 12 Lane Geometry	78
Figure 46: Scenario 15 Lane Geometry	78
Figure 47: Scenario 16 Lane Geometry	79
Figure 48: Scenario 17 Lane Geometry	80
Figure 49: Scenario 20 Lane Geometry	80
Figure 50: Scenario 23 Lane Geometry	81
Figure 51: Scenario 26 Lane Geometry	82
Figure 52: Scenario 27 Lane Geometry	83
Figure 53: Scenario 28 Lane Geometry	83
Figure 54: Scenario 31 Lane Geometry	84
Figure 55: Scenario 34 Lane Geometry	85
Figure 56: Scenario 37 Lane Geometry	85
Figure 57: Scenario 38 Lane Geometry	86
Figure 58: Scenario 39 Lane Geometry	87
Figure 59: Scenario 42 Lane Geometry	88
Figure 60: Scenario 2 Lane Geometry	89
Figure 61: Scenario 3 Lane Geometry	89
Figure 62: Scenario 6 Lane Geometry	90
Figure 63: Scenario 7 Lane Geometry	91
Figure 64: Scenario 10 Lane Geometry	92
Figure 65: Scenario 13 Lane Geometry	92
Figure 66: Scenario 18 Lane Geometry	93
Figure 67: Scenario 21 Lane Geometry	94
Figure 68: Scenario 24 Lane Geometry	95
Figure 69: Scenario 29 Lane Geometry	95
Figure 70: Scenario 35 Lane Geometry	96
Figure 71: Scenario 40 Lane Geometry	97
Figure 72: Scenario 8 Lane Geometry	97
Figure 73: Scenario 11 Lane Geometry	98
Figure 74: Scenario 14 Lane Geometry	99
Figure 75: Scenario 19 Lane Geometry	100
Figure 76: Scenario 22 Lane Geometry	100
Figure 77: Scenario 25 Lane Geometry	101
Figure 78: Scenario 30 Lane Geometry	102
Figure 79: Scenario 32 Lane Geometry	103
Figure 80: Scenario 33 Lane Geometry	103
Figure 81: Scenario 36 Lane Geometry	104
Figure 82: Scenario 41 Lane Geometry	105
Figure 83: Scenario 43 Lane Geometry	105
Figure 84: Scenario 44 Lane Geometry	106
Figure 85: R1-R2 Segment- Sensitivity Analysis for $N_M=0$	116

Figure 86: R1-R2 Segment- Sensitivity Analysis for $N_M=1$	117
Figure 87:R1-R2 Segment- Sensitivity Analysis for $N_M=2$	117
Figure 88: R2-R3 Segment- Sensitivity Analysis for $N_{WL}=2$	118
Figure 89: R2-R3 Segment- Sensitivity Analysis for $N_{WL}=3$	118
Figure 90: Lane Geometry Schematic Number 1	128
Figure 91: Lane Geometry Schematic Number 2	128
Figure 92: Lane Geometry Schematic Number 3	128
Figure 93: Lane Geometry Schematic Number 4	128
Figure 94: Lane Geometry Schematic Number 5	129
Figure 95: Lane Geometry Schematic Number 6	129
Figure 96: Lane Geometry Schematic Number 7	129
Figure 97: Lane Geometry Schematic Number 8	129
Figure 98: Lane Geometry Schematic Number 9	130
Figure 99: Lane Geometry Schematic Number 10	130
Figure 100: Lane Geometry Schematic Number 11	130
Figure 101: Scenario 2, Density.....	131
Figure 102: Scenario 2, R1R2 Flow vs. Demand	131
Figure 103: Scenario 2, R2R3 Flow vs. Demand	132
Figure 104: Scenario 3, Density.....	132
Figure 105: Scenario 3, R1R2 Flow vs. Demand	133
Figure 106: Scenario 3, R2R3 Flow vs. Demand	133
Figure 107: Scenario 4, Density.....	134
Figure 108: Scenario 4, R1R2 Flow vs. Demand	134
Figure 109: Scenario 4, R2R3 Flow vs. Demand	135
Figure 110: Scenario 5, Density.....	135
Figure 111: Scenario 5, R1R2 Flow vs. Demand	136
Figure 112: Scenario 5, R2R3 Flow vs. Demand	136
Figure 113: Scenario 6, Density.....	137
Figure 114: Scenario 6, R1R2 Flow vs. Demand	137
Figure 115: Scenario 6, R2R3 Flow vs. Demand	138
Figure 116: Scenario 7, Density.....	138
Figure 117: Scenario 7, R1R2 Flow vs. Demand	139
Figure 118: Scenario 7, R2R3 Flow vs. Demand	139
Figure 119: Scenario 8, Density.....	140
Figure 120: Scenario 8, R1R2 Flow vs. Demand	140
Figure 121: Scenario 8, R2R3 Flow vs. Demand	141
Figure 122: Scenario 9, Density.....	141
Figure 123: Scenario 9, R1R2 Flow vs. Demand	142
Figure 124: Scenario 9, R2R3 Flow vs. Demand	142
Figure 125: Scenario 10, Density.....	143
Figure 126: Scenario 10, R1R2 Flow vs. Demand	143
Figure 127: Scenario 10, R2R3 Flow vs. Demand	144
Figure 128: Scenario 11, Density.....	144

Figure 129: Scenario 11, R1R2 Flow vs. Demand	145
Figure 130: Scenario 11, R2R3 Flow vs. Demand	145
Figure 131: Scenario 12, Density.....	146
Figure 132: Scenario 12, R1R2 Flow vs. Demand	146
Figure 133: Scenario 12, R2R3 Flow vs. Demand	147
Figure 134: Scenario 13, Density.....	147
Figure 135: Scenario 13, R1R2 Flow vs. Demand	148
Figure 136: Scenario 13, R2R3 Flow vs. Demand	148
Figure 137: Scenario 14, Density.....	149
Figure 138: Scenario 14, R1R2 Flow vs. Demand	149
Figure 139: Scenario 14, R2R3 Flow vs. Demand	150
Figure 140: Scenario 15, Density.....	150
Figure 141: Scenario 15, R1R2 Flow vs. Demand	151
Figure 142: Scenario 15, R2R3 Flow vs. Demand	151
Figure 143: Scenario 16, Density.....	152
Figure 144: Scenario 16, R1R2 Flow vs. Demand	152
Figure 145: Scenario 16, R2R3 Flow vs. Demand	153
Figure 146: Scenario 17, Density.....	153
Figure 147: Scenario 17, Flow vs. Demand.....	154
Figure 148: Scenario 17, R2R3 Flow vs. Demand	154
Figure 149: Scenario 18, Density.....	155
Figure 150: Scenario 18, R1R2 Flow vs. Demand	155
Figure 151: Scenario 18, R2R3 Flow vs. Demand	156
Figure 152: Scenario 19, Density.....	156
Figure 153: Scenario 19, R1R2 Flow vs. Demand	157
Figure 154: Scenario 19, R2R3 Flow vs. Demand	157
Figure 155: Scenario 20, Density.....	158
Figure 156: Scenario 20, R1R2 Flow vs. Demand	158
Figure 157: Scenario 20, R2R3 Flow vs. Demand	159
Figure 158: Scenario 21, Density.....	159
Figure 159: Scenario 21, R1R2 Flow vs. Demand	160
Figure 160: Scenario 21, R2R3 Flow vs. Demand	160
Figure 161: Scenario 22, Density.....	161
Figure 162: Scenario 22, R1R2 Flow vs. Demand	161
Figure 163: Scenario 22, R2R3 Flow vs. Demand	162
Figure 164: Scenario 23, Density.....	162
Figure 165: Scenario 23, R1R2 Flow vs. Demand	163
Figure 166: Scenario 23, R2R3 Flow vs. Demand	163
Figure 167: Scenario 24, Density.....	164
Figure 168: Scenario 24, R1R2 Flow vs. Demand	164
Figure 169: Scenario 24, R2R3 Flow vs. Demand	165
Figure 170: Scenario 25, Density.....	165
Figure 171: Scenario 25, R1R2 Flow vs. Demand	166

Figure 172: Scenario 25, R2R3 Flow vs. Demand	166
Figure 173: Scenario 26, Density.....	167
Figure 174: Scenario 26, R1R2 Flow vs. Demand	167
Figure 175: Scenario 26, R2R3 Flow vs. Demand	168
Figure 176: Scenario 27, Density.....	168
Figure 177: Scenario 27, R1R2 Flow vs. Demand	169
Figure 178: Scenario 27, R2R3 Flow vs. Demand	169
Figure 179: Scenario 28, Density.....	170
Figure 180: Scenario 28, R1R2 Flow vs. Demand	170
Figure 181: Scenario 28, R2R3 Flow vs. Demand	171
Figure 182: Scenario 29, Density.....	171
Figure 183: Scenario 29, R1R2 Flow vs. Demand	172
Figure 184: Scenario 29, R2R3 Flow vs. Demand	172
Figure 185: Scenario 30, Density.....	173
Figure 186: Scenario 30, R1R2 Flow vs. Demand	173
Figure 187: Scenario 30, R2R3 Flow vs. Demand	174
Figure 188: Scenario 31, Density.....	174
Figure 189: Scenario 31, R1R2 Flow vs. Demand	175
Figure 190: Scenario 31, R2R3 Flow vs. Demand	175
Figure 191: Scenario 32, Density.....	176
Figure 192: Scenario 32, R1R2 Flow vs. Demand	176
Figure 193: Scenario 32, R2R3 Flow vs. Demand	177
Figure 194: Scenario 33, Density.....	177
Figure 195: Scenario 33, R1R2 Flow vs. Demand	178
Figure 196: Scenario 33, R2R3 Flow vs. Demand	178
Figure 197: Scenario 34, Density.....	179
Figure 198: Scenario 34, R1R2 Flow vs. Demand	179
Figure 199: Scenario 34, R2R3 Flow vs. Demand	180
Figure 200: Scenario 35, Density.....	180
Figure 201: Scenario 35, R1R2 Flow vs. Demand	181
Figure 202: Scenario 35, R2R3 Flow vs. Demand	181
Figure 203: Scenario 36, Density.....	182
Figure 204: Scenario 36, R1R2 Flow vs. Demand	182
Figure 205: Scenario 36, R2R3 Flow vs. Demand	183
Figure 206: Scenario 37, Density.....	183
Figure 207: Scenario 37, R1R2 Flow vs. Demand	184
Figure 208: Scenario 37, R2R2 Flow vs. Demand	184
Figure 209: Scenario 38, Density.....	185
Figure 210: Scenario 38, R1R2 Flow vs. Demand	185
Figure 211: Scenario 38, R2R3 Flow vs. Demand	186
Figure 212: Scenario 39, Density.....	186
Figure 213: Scenario 39, R1R2 Flow vs. Demand	187
Figure 214: Scenario 39, R2R3 Flow vs. Demand	187

Figure 215: Scenario 40, Density.....	188
Figure 216: Scenario 40, R1R2 Flow vs. Demand	188
Figure 217: Scenario 40, R2R3 Flow vs. Demand	189
Figure 218: Scenario 41, Density.....	189
Figure 219: Scenario 41, R1R2 Flow vs. Demand	190
Figure 220: Scenario 41, R2R3 Flow vs. Demand	190
Figure 221: Scenario 42, Density.....	191
Figure 222: Scenario 42, R1R2 Flow vs. Demand	191
Figure 223: Scenario 42, R2R3 Flow vs. Demand	192
Figure 224: Scenario 43, Density.....	192
Figure 225: Scenario 43, R1R2 Flow vs. Demand	193
Figure 226: Scenario 43, R2R3 Flow vs. Demand	193
Figure 227: Scenario 44, Density.....	194
Figure 228: Scenario 44, R1R2 Flow vs. Demand	194
Figure 229: Scenario 44, R2R3 Flow vs. Demand	195
Figure 230: R1R2 Segment- Removing (F1-F2)- $N_M=0$	196
Figure 231: R1R2 Segment- Removing (F1-F2), $N_M=1$	196
Figure 232: R1R2 Segment- Removing (F1-F2), $N_M=2$	197
Figure 233: R1R2 Segment- Removing (F1-R3), $N_M=0$	197
Figure 234: R1R2 Segment- Removing (F1-R3), $N_M=1$	198
Figure 235: R1R2 Segment- Removing (F1-R3), $N_M=2$	198
Figure 236: R1R2 Segment- Removing (R1-F2), $N_M=0$	199
Figure 237: R1R2 Segment- Removing (R1-F2), $N_M=1$	199
Figure 238: R1R2 Segment- Removing (R1-F2), $N_M=2$	200
Figure 239: R1R2 Segment- Removing (R1-R3), $N_M=0$	200
Figure 240: R1R2 Segment- Removing (R1-R3), $N_M=1$	201
Figure 241: R1R2 Segment- Removing (R1-R3), $N_M=2$	201
Figure 242: R2R3 Segment- Removing (F1-F2), $N_{WL}=2$	202
Figure 243: R2R3 Segment- Removing (F1-F2), $N_{WL}=3$	202
Figure 244: R2R3 Segment- Removing (F1-R3), $N_{WL}=2$	203
Figure 245: R2R3 Segment- Removing (F1-R3), $N_{WL}=3$	203
Figure 246: R2R3 Segment- Removing (R1-F2), $N_{WL}=2$	204
Figure 247: R2R3 Segment- Removing (R1-F2), $N_{WL}=3$	204
Figure 248: R2R3 Segment- Removing (R1-R3), $N_{WL}=2$	205
Figure 249: R2R3 Segment- Removing (R1-R3), $N_{WL}=3$	205
Figure 250: R2R3 Segment- Removing (R2-F2), $N_{WL}=2$	206
Figure 251: R2R3 Segment- Removing (R2-F2), $N_{WL}=3$	206
Figure 252: R2R3 Segment- Removing (R2-R3), $N_{WL}=2$	207
Figure 253: R2R3 Segment- Removing (R2-R3), $N_{WL}=3$	207

TABLES

Table 1: Sample Size (7pm).....	29
Table 2: Freeway Model Calibration Targets (FHA, 2019)	31
Table 3: Lane Change Parameters	34
Table 4: Car Following Parameters	36
Table 5: Car Following Parameters- Model 1.....	37
Table 6: Model 1- 7pm- GEH.....	37
Table 7: Car Following Parameters- Model 2.....	38
Table 8: Model 2- 7pm- GEH.....	39
Table 9: Car Following Parameters- Model 3.....	40
Table 10: Model 3- 7pm- GEH.....	40
Table 11: Car Following Parameters- Model 4.....	41
Table 12: Model 4- 7pm- GEH.....	42
Table 13: Car Following Parameters- Model 5.....	43
Table 14: Model 5- 7pm- GEH.....	43
Table 15: Car Following Parameters- Model 6.....	44
Table 16: Model 6- 7pm- GEH.....	45
Table 17: Raw Score	47
Table 18: Scoring- 7pm	47
Table 19: Sample Size (8am).....	48
Table 20: Car Following Parameters (Validation).....	48
Table 21: GEH Comparison- 8 am	49
Table 22: Models Scoring- 8am.....	50
Table 23: Total Scoring	51
Table 24: Sensitivity Analysis Scenarios.....	52
Table 25: Sensitivity Analysis- GEH.....	53
Table 26: Number of Lanes Range	57
Table 27: Number of Lanes Scenarios.....	57
Table 28: Flow Range (vph)	59
Table 29: Flow Scenarios.....	60
Table 30: Range of Variable for Capacity Estimation.....	62
Table 31: Possible Scenarios	63
Table 32: Number of Lanes and Gore to Gore Distance for S1.....	65
Table 33: Model Summary, R1-R2 Segment.....	74
Table 34: Number of Lanes and Gore to Gore Distance for S4.....	75
Table 35: Number of Lanes and Gore to Gore Distance for S5.....	76
Table 36: Number of Lanes and Gore to Gore Distance for S9.....	77
Table 37: Number of Lanes and Gore to Gore Distance for S15.....	78
Table 38: Number of Lanes and Gore to Gore Distance for S16.....	79
Table 39: Number of Lanes and Gore to Gore Distance for S17.....	80
Table 40: Number of Lanes and Gore to Gore Distance for S20.....	80
Table 41: Number of Lanes and Gore to Gore Distance for S23.....	81
Table 42: Number of Lanes and Gore to Gore Distance for S26.....	82

Table 43: Number of Lanes and Gore to Gore Distance for S27.....	82
Table 44: Number of Lanes and Gore to Gore Distance for S28.....	83
Table 45: Number of Lanes and Gore to Gore Distance for S31.....	84
Table 46: Number of Lanes and Gore to Gore Distance for S37.....	85
Table 47: Number of Lanes and Gore to Gore Distance for S38.....	86
Table 48: Number of Lanes and Gore to Gore Distance for S39.....	87
Table 49: Number of Lanes and Gore to Gore Distance for S42.....	87
Table 50: Range of Flow for Model Extension	88
Table 51: Number of Lanes and Gore to Gore Distance for S2.....	88
Table 52: Number of Lanes and Gore to Gore Distance for S3.....	89
Table 53: Number of Lanes and Gore to Gore Distance for S6.....	90
Table 54: Number of Lanes and Gore to Gore Distance for S7.....	91
Table 55: Number of Lanes and Gore to Gore Distance for S13.....	92
Table 56: Number of Lanes and Gore to Gore Distance for S18.....	93
Table 57: Number of Lanes and Gore to Gore Distance for S21.....	94
Table 58: Number of Lanes and Gore to Gore Distance for S24.....	94
Table 59: Number of Lanes and Gore to Gore Distance for S29.....	95
Table 60: Number of Lanes and Gore to Gore Distance for S35.....	96
Table 61: Number of Lanes and Gore to Gore Distance for S40.....	96
Table 62: Number of Lanes and Gore to Gore Distance for S8.....	97
Table 63: Number of Lanes and Gore to Gore Distance for S11.....	98
Table 64: Number of Lanes and Gore to Gore Distance for S19.....	99
Table 65: Number of Lanes and Gore to Gore Distance for S22.....	100
Table 66: Number of Lanes and Gore to Gore Distance for S25.....	101
Table 67: Number of Lanes and Gore to Gore Distance for S30.....	102
Table 68: Number of Lanes and Gore to Gore Distance for S32.....	102
Table 69: Number of Lanes and Gore to Gore Distance for S33.....	103
Table 70: Number of Lanes and Gore to Gore Distance for S36.....	104
Table 71: Number of Lanes and Gore to Gore Distance for S41.....	105
Table 72: Number of Lanes and Gore to Gore Distance for S43.....	105
Table 74: Significant Factors for Capacity Evaluation.....	107
Table 76: Model Summaries.....	113
Table 77: ANOVA Tables	114
Table 78: Coefficient Tables.....	115

INTRODUCTION

Systematic, well-designed research provides the most effective approach to the solution of many problems facing highway administrators and engineers. Traffic congestion on freeway systems is a significant concern in urban areas throughout the U.S.A. In this era, building new freeways to reduce congestion is less feasible due to the high capital and social costs. Thus, the effective management and operation of existing freeway facilities has become a preferred approach to reduce traffic congestion.

A weaving section is a freeway segment¹ in which traffic flows cross each other without traffic control (Minderhoud et al. 2003). Weaving sections are often problematic because of the increase in lane changing. These are common design elements on freeway facilities between an on ramp and off ramp with an auxiliary lane. They are located between merge and diverge points, near ramps where a lane is added or dropped, and at multilane ramps. As the length of a weaving section increases, the merge and diverge operate independently, and the weaving segment no longer exists.

Traffic demands exceeding segment capacity at weaving areas cause congestion, which affects the operation of the entire freeway section. Traffic operational problems often exist at weaving areas even when traffic demands are less than capacity, and may be experienced at lower traffic flows because of the complexity of vehicle interactions, that is, increased lane changing, resulting in a degradation in level of service (LOS) and potential safety problems (Skabardonis et al. 2012).

A significant amount of research has been done to estimate quality of service and capacity in weaving sections. However, little has been done to address multiple weaves. In these cases, weaving sections on the freeways overlap and may be caused by closely spaced ramps where lanes are added or dropped.

In this work, we examine capacity and quality of service conditions for a specific example of a multiple weave. Capacity is evaluated through micro-simulation by gradually increasing flows for a range of geometric and fraction of weaving-traffic conditions. The simulation model is first calibrated, using a data set for a freeway weave section in Arlington, Texas. Models are developed to express capacity in terms of lane configuration, flow ratios, traffic mix (heavy traffic percentages), and overall flow rate.

¹ Segment is the portions of freeway section where a merge, diverge, or weave influence facility operation (HCM 2016)

CHAPTER 1: LITERATURE REVIEW

This chapter begins with a literature review to provide a background to weaving area research on freeways. The chapter concludes with a brief introduction to microscopic simulation analysis.

The Highway Capacity Manual (HCM) is the authoritative source providing state-of-the-art methodologies for evaluating highway, transit, bicycle, and pedestrian facilities at both the operational and planning levels. It provides deterministic and macroscopic methodologies for estimating measures of traffic operations such as speed, density, and delay, which are used as the foundation for economic and environmental analyses (HCM 2016).

The original Highway Capacity Manual was published in 1950 and became the national guide for the design, analysis, and evaluation of streets and highways in terms of their traffic-carrying capability (HCM 1950). However, its procedures had several shortcomings, including lack of data used to develop weaving models, and the practical application often produced inconsistent results (Skabardonis et al. 2015).

The second edition, 1965, introduced the concept of design/analysis of weaving segments which was based on a relationship between weaving length, total weaving volume, level-of-service (LOS) and lane volume prediction (HCM 1965). It recommended adding an auxiliary lane in order to increase the accuracy of LOS predictions for basic weaving sections, adding a regression-based procedure for ramp cases at levels of service A, B, and C and adding a vehicle-distribution-profile procedure for ramp cases at levels of service D and E. (Pignataro et al. 1975).

Between 1965 and 1985, a speed prediction model was developed which accounted for constrained versus unconstrained flow, and segment configuration (Xu et al. 2020). Since 1985, the core algorithm in the capacity and level of service analysis of weaving sections was the prediction of average weaving and non-weaving operating speeds. In the HCM 1985, and its subsequent update in 1994, speed was directly related to level of service. In HCM 2000, speed was predicted and subsequently converted to density to determine level of service. (NCHRP 3-75)

Research conducted in the 1970s through the 1980s updated the HCM to 4th edition, 2000 (Roess et al. 2000). Although, the 4th edition improved the speed prediction algorithm, still more studies were required to improve estimated weaving and non-weaving speed, calibrate weaving intensity factor, weaving capacity model, maximum possible weaving volume under given geometric and traffic conditions, and maximum possible on-ramp volume (Roess et al. 2000) (Kwon et al. 2000). It also did not consider different weaving flows per incoming leg for capacity value, density limitation, weaving flow rate, and volume ratio (Minderhoud et al. 2000),(Roess et al. 2009).

The HCM 2010 classified the weaving sections into ramp and major weaves (Xu et al. 2020) and proposed a mixture of theoretical and regression models to predict rate of lane changing in the

weaving section, average weaving and non-weaving speed (did not apply to segments with LOS F), and estimated maximum weaving length (Skabardonis et al. 2012).

The HCM 2010 method provided reliable estimations for major weaving sections, but significantly under-predicted the traffic performance at ramp weaving sections (Skabardonis et al. 2012). It also over-predicted density and under-predicted weaving section capacity when the weaving volume is high for a ramp weave (Skabardonis et al. 2015). It did not provide a methodology to assess LOS, density, and space mean speed for oversaturated freeway weaving segments.

In a like manner, the other limitations in HCM 2010 were the assumptions of a fixed capacity throughout under saturated and congested regimes, and ignoring the impact of inclement weather on free-flow speed. (Sajjadi, et al. 2013)

In 2016, the 6th edition of HCM offered a wide spectrum of freeway analyses ranging from freeway segments to facility travel time reliability. However it lacked weave length sensitivity which mainly is because of the absence of this parameter in the non-weaving lane change and speed model (Ahmed et al. 2019).

Chapter 27 of the HCM 2016 supplement, suggests using alternative means to estimate capacity and the quality of service and recommends using simulation. It presented that the heavy-vehicle adjustment factor, f_{HV} , is an effective factor on weaving section capacity estimation.

To overcome the HCM shortcomings in terms of capacity model, several research projects were conducted. Eads et al. (2000) analyzed directional freeway facilities emphasizing time-varying demands and capacities, the implementation and evaluation of freeway geometric and operational improvements, and oversaturated conditions. Kwon, et al. (2000) investigated the behavior of weaving flows and the effects of time-variant traffic conditions on the capacity of weaving areas. The study indicated that the beginning portion of an auxiliary lane in a ramp-weave area is shared by both merging and diverging vehicles, and the length of such a shared area varies depending on the length of a given weave section and the amount of weaving flow. Also, the maximum value of the weaving volume in a ramp-weave area with one auxiliary lane is limited by the maximum through capacity of one lane.

In addition, Zhang et al. (2004) also presented a systematic analysis of the factors that potentially impact the capacity of freeway weaving sections, which include the length of the weaving section, the weaving ratio, the percentage of heavy vehicles, and the speed differential between freeway and ramp traffic.

Furthermore, Rakha et al. (2006) modeled different weaving section configurations for a wide range of weaving section lengths and travel demand distributions. The study considered short lengths (less than 150 m) and long weaving section lengths and accounted for the source and

distribution of weaving flow, and ensured that the capacity of a weaving section reverts to basic freeway capacity when the volume ratio is zero regardless of the weaving section length.

On the other hand, Roess et al. (2009) relied on the prediction of lane-changing activity within the weaving segment to quantify the impact of configuration on resulting speeds and densities. Al-jameel (2011), adopted drivers' behaviors at weaving sections to assess the effect on capacity. To determine weaving section capacity, weaving ratio, volume ratio, weaving configuration, the upstream traffic characteristics, the frequency of lane changes, the length of weaving section and a merging point were investigated.

In the same fashion, Marczak, et al. (2015) proposed an analytical traffic model at the macroscopic level considering the superposition of two merges and two diverges. The model illustrated that the capacity drop related to the weaving lane changes depends on six parameters: free-flow speed, jam density, weave speed in congestion, vehicles' acceleration, relaxation factor, and length of anticipation zone.

To be coupled with the flow related factors, Fitzpatrick et al. (2011) investigated the impact of geometric factors on freeway operation. The study checked ramp spacing, weaving length, decision sight distance, sign spacing needs, and speed relation. Liu et al. (2012) also determined the cross-weaving effect as a function of different roadway geometric configurations as well as traffic conditions. They explored the effect of parameters such as number of lanes, weaving demand, and weaving length. Qi et al. (2018), found that if the weaving segment is followed by an entrance/exit ramp and this ramp has high traffic volume, dropping the auxiliary lane before this entrance/exit ramp is an operationally effective option.

Furthermore, the geometry study by Guo et al. (2020) proposed to split the existing ramp designs to create two merge or diverge points, such that potential conflicts of the freeway and ramp traffic can be distributed spatially. The split design can potentially increase throughput by 6% to 9% and reduce delay by 35% to 80% across different scenarios.

In order to analyze the operations of two-sided weaving segment, Johor, et al. (2018) recognized the maximum weaving length and lane-changing rate as the most important factors. The study found that shorter weaving distances cause less lane-changing activity.

The research by Xu et al. (2020) distinguished between congestion effects caused by high v/c ratios from turbulence caused by merging, diverging, and weaving traffic to address difficulties in calibrating and validating of the speed model, and complex procedure for estimating weaving segment density and level of service.

A sensitivity analysis by Leclercq et al. (2016) estimated the effective capacity at freeway merges in a multilane context which showed that vehicle acceleration and the truck ratio are the most influential parameters for the total capacity.

Most recent studies showed that emerging automated vehicle technology can improve the operations and increase the capacity of weaving sections. A new concept to the field of freeway weaving analysis, driverless car was not presented in the HCM 2010. The great potential of the automated vehicles (lower reaction time) that can reduce headways and the required gaps for lane changing maneuvers will increase the capacity (Shi et al. 2016), (Tilg, et al. 2018).

MICROSCOPIC ANALYSIS

Due to data collection cost, microscopic simulation is an alternative tool to evaluate the operation of weaving areas. The nominated alternative tool could estimate speed, density, capacity, and weaving length given weaving and non-weaving traffic demand. It also offers additional performance measures including delay, stop, queue length, fuel consumption, pollution, and operating cost. Despite macroscopic analysis that yielded only segment-level measures, this tool provided details on point problems. The microscopic analysis: lane changing, density, extent of segregation, and some analytic modeling is important in understanding basic mechanisms and in guiding the macroscopic model development.

The HCM 2010 used deterministic equations developed and calibrated with macroscopic data while microscopic simulation models treat each vehicle as separate object to be propagated through the system. The HCM capacities, densities, etc. expressed in equivalent passenger car unit, whereas the simulation values represented by actual vehicles.

CORSIM is a microscopic simulation model which was significantly affected by car-following parameters, lane-changing aggressiveness factor, and percentage of freeway through vehicles that yield to merging traffic (Skabardonis 2002). Factors that potentially impacted the capacity of freeway weaving sections estimated through CORSIM included the length of the weaving section, the weaving ratio, the percentage of heavy vehicles, and the speed differential between freeway and ramp traffic (Zhang et al. 2004).

Due to significant improvements in computing power and the theoretical aspect of modeling, the newer version of simulation tools has a superior performance. In the project by Chulsu Yang et al. (2011), VISSIM was used to estimate the capacity of two-sided weaving on freeways (one weaving movement must cross all the freeway lanes). The study developed a weaving model considering parameters including time required for lane changing, optimal speed of merging vehicles, and probability of weaving success. The critical factors affecting the distance required for weave turned out to be speed during merging and flow. Using VISSIM, Chao Yang et al. (2012) also showed that the capacity of weaving segments was affected by volume ratio, length of weaving segments, source and distribution of weaving flow and non-weaving flow.

In addition, a methodology was developed by Leyn et al. (2015) to assess the level of service and to find standard parameter sets calibrated for the VISSIM simulation. The ability of microscopic

simulation to demonstrate more accurate capacity estimation in specific situations than calculated by the methods in the HCM can save a considerable amount of investment costs.

The HCM 2016 method relies on the 15 min peak period within the peak hours. The methodology was applicable to managed lanes, work zones, and was the basis of both freeway reliability analysis and the assessment of active traffic and demand management (ATDM) strategies. The methodology was integrated with FREEVAL2 (FREeway EVALuation) computational engine (HCM 2016). FREEVAL is a macroscopic/mesoscopic tool which enables users to implement HCM-based freeway analysis quickly. However, the microscopic simulation tool, VISSIM, models real world conditions with high level of accuracy. Segment density obtained from HCM methods is generally higher than the segment density from VISSIM microsimulation (Jolovic et al. 2016).

This chapter provided a literature survey for weaving sections on freeways and an introduction to microscopic simulation. Calibration and validation of the VISSIM model is covered in Chapter 2. VISSIM was calibrated using a data set from the Dallas/Fort Worth area. In Chapter 3, various scenarios are identified on the basis of lane configuration, number of lanes, and distances between ramps. Then the capacities are estimated by raising the flows until a link output is less than its corresponding input. This condition assumes that the link in question is experiencing queueing. Then, capacity is estimated based on the HCM's definition of capacity, i.e., a density of 43 pc/hr/lane. Capacity modelling is done in Chapter 4, using the simulation results from Chapter 3. Macroscopic models are created for each scenario. A sensitivity analysis is performed for each model (scenario).

² Computerized tool designed to faithfully implement the operational analysis computations for under-saturated and over-saturated directional freeway facilities.

CHAPTER 2: CALIBRATION

Calibration and validation of the VISSIM model is covered in this chapter. VISSIM was calibrated using a data set from the Dallas/Fort Worth area.

DATA

For calibration, data was obtained from the research by Denney and Williams (2005). The research was conducted from 1996 to 2000 with the intention of developing a new method for calculating the capacity and quality of service for weaving zones for the 2000 Highway Capacity Manual.

Specific capacity considerations must be made in weaving areas because drivers from two upstream roadways must merge into a single roadway, and then diverge into two different downstream roadways. Weaving areas are characterized by frequent lane changes, where vehicles compete for the same pavement.

The data was collected for the freeway segment on northbound SH 360 between the entrance from eastbound IH20 to the exit for Mayfield Road in Arlington, Texas (Figure 1). When entering this weaving area, northbound traffic on SH 360 required two lane changes to the right in order to exit at Mayfield.



Figure 1: State Highway 360 Northbound

The above segment was fully modeled all the way back to IH20 due to the level of volume, weaving, and the distance needed for required lane changes. We did not model the exit ramp (to Mayfield) all the way to the signal, as the speed data showed that the right lane operates at free flow (over 70 mph) without any backups caused by the downstream traffic signal. Figure 2 shows the segments which we modeled for calibration purpose with a gore-to-gore distance of 1,460 ft.

In Figure 2, the darker green line is for eastbound IH 20 traffic exiting to go north on IH20 traffic. A dashed line represents where traffic streams merge and diverge.

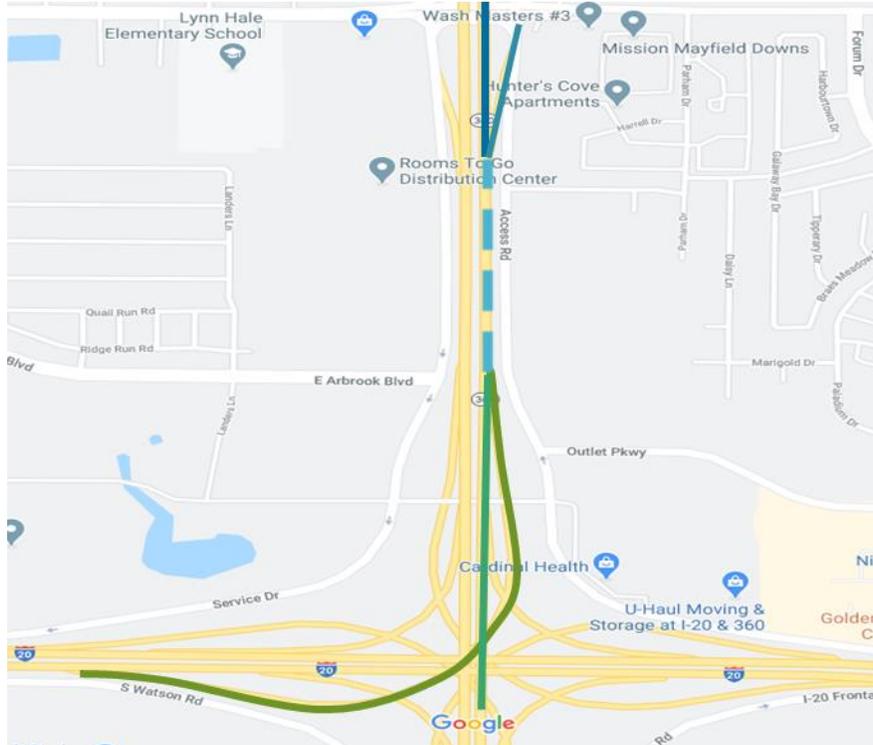


Figure 2: Calibration Segment

The site was subjected to a series of simulation runs for a range of volume and fraction of weaving traffic conditions. The proportion of weaving traffic is derived from the origin-destination information (freeway to freeway, freeway to ramp, etc.), and that for any one run, the sum of the freeway-to-freeway traffic and freeway to ramp traffic was equal to the freeway entry flow. Likewise, ramp to freeway and ramp to ramp flow summation is equal to entry ramp flow.

The weaving lanes were identified as the lanes on each side of the entrance ramp gore (right lane of the freeway and left lane of the two-lane entrance ramp), and the weaving traffic was that whose origin-destination was freeway to ramp or ramp to freeway.

At lower flows, the ramp-to-ramp traffic can largely be sorted into the right lane of the entrance ramp, and the ramp to freeway traffic can be sorted into the left lane of the entrance ramp.

VISSIM INPUT

Simulation is a key element of this research and the VISSIM 2020 platform was selected because of its capabilities. The primary objective of this chapter is to introduce the VISSIM parameters that affect the capacity estimation of the weaving area.

VISSIM is a microscopic, time-step and behavior-based simulation model using deterministic car following logic, and a driver behavior model. In addition, VISSIM simulates traffic flow by moving these “driver-vehicle-units” through a network. Every driver with his/her specific behavior

characteristics is assigned to a specific vehicle. Therefore, the driver behavior corresponds to the technical/mechanical capabilities of his/her vehicle.

Network Geometry Coding

VISSIM networks are based on links and connectors. Links are used to define the width and number of lanes for a given roadway segment. There are different link types, and each link type is represented by its driving behavior model. Connectors are used to connect the links and implicitly have the same link types as the link from which they originate. Since this research focuses on freeway weaving, the link type for this model is freeway.

Vehicle Types and Traffic Compositions

A group of vehicles with similar performance characteristics and driving behavior is defined as a vehicle type. Typically, the following vehicle types are available: car, HGV (truck), bus, tram, pedestrian, and bike. Each vehicle type is characterized by minimum and maximum acceleration, minimum and maximum deceleration, weight, power, and length. Traffic mix is the proportion of each vehicle type present in the source flows. In calibration process, the traffic mix is: 95% car, and 5% HGV (truck).

Desired Speed Distributions

During coding, speed decisions are entered in the model based on actual measured speeds. The available time-mean speed on different lanes indicates that cars travel at speeds between 70 and 80 mph in the free-flowing lanes. Therefore, the desired speed distribution shown in Figure 3 was used in the project. In these simulations, twenty percent of the vehicles have a target speed between 70 and 72 mph; twenty percent of the vehicles are assigned a target speed between 78 and 80 mph, and the remaining vehicles are assigned a speed between 72 and 78 mph.

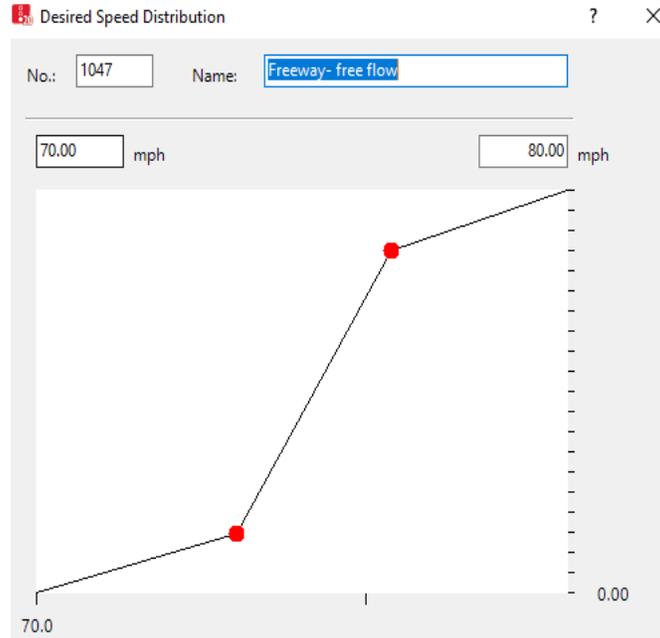


Figure 3: Desired Speed Distribution

Vehicle Inputs and Routing

Vehicle inputs are defined for a specific link and time period in vehicles per hour even if the time is different from one hour. Figure 4 shows time intervals for the calibration process. The total simulation time is 4,200 seconds which includes three time periods for each run; a five-minute time (0-300 seconds), one hour period (300-3900 seconds), followed by a five-minute period (3900-4200 seconds) at the end. The first period is the warm-up time, and the next hour-interval is the actual running time where the simulation outputs are collected. The 5-minute warm up time is included because the network starts empty. Time intervals are defined for vehicle input and vehicle weaving share.

Figures 5 and 6 show vehicle input for different datasets. Data collected for the 7 to 8 pm data has total flows of 3,509 vph for the freeway entry and 3,040 vph for the entrance ramp (Figure 5). Data collected from 8 to 9 am and has total flows of 3,020 vph for freeway entry and 2,578 vph for ramp entry (Figure 6).

Weaving shares are defined based on vehicles' origin-destination matrix. Traffic mix is defined in terms of cars and heavy vehicle classes. In the 7pm dataset, 8% of both classes (car and heavy vehicle) entering at ramp and the exit at off-ramp. For the vehicles entering freeway at 7pm, 6% exit at the off-ramp.

For 8am dataset, ramp to ramp distributions is 4% while freeway to ramp distribution is 96% (for both classes).

Time Intervals		
Count	Start	End
1	0.0	300.0
2	300.0	3900.0
3	3900.0	MAX

Figure 4: Time Intervals

Vehicle Inputs / Vehicle Volumes By Time Interval					
Count	No	Name	Link	Volume(0)	VehComp(0)
1	1	Entrance Ramp	1: Entrance Ramp	3509.0	2: Entrance Ramp
2	2	Main Lane	2: Main Lane Entrance	3040.0	1: Main Lanes

Count	Cont	TimeInt	Volume	VehComp	VolType
1	<input type="checkbox"/>	0-300	3509.0	2: Entrance Ramp	Exact
2	<input checked="" type="checkbox"/>	300-36...	3509.0	2: Entrance Ramp	Exact
3	<input checked="" type="checkbox"/>	3600-...	3509.0	2: Entrance Ramp	Exact
4	<input type="checkbox"/>	0-300	3040.0	1: Main Lanes	Exact
5	<input checked="" type="checkbox"/>	300-36...	3040.0	1: Main Lanes	Exact
6	<input checked="" type="checkbox"/>	3600-...	3040.0	1: Main Lanes	Exact

Figure 5: Vehicle Input (7pm)

Vehicle Inputs / Vehicle Volumes By Time Interval					
Count	No	Name	Link	Volume(0)	VehComp(0)
1	1	Entrance Ramp	1: Entrance Ramp	3020.0	2: Entrance Ramp
2	2	Main Lane	2: Main Lane Entrance	2578.0	1: Main Lanes

Count	Cont	TimeInt	Volume	VehComp	VolType
1	<input type="checkbox"/>	0-300	3020.0	2: Entrance Ramp	Exact
2	<input checked="" type="checkbox"/>	300-36...	3020.0	2: Entrance Ramp	Exact
3	<input checked="" type="checkbox"/>	3600-...	3020.0	2: Entrance Ramp	Exact
4	<input type="checkbox"/>	0-300	2578.0	1: Main Lanes	Exact
5	<input checked="" type="checkbox"/>	300-36...	2578.0	1: Main Lanes	Exact
6	<input checked="" type="checkbox"/>	3600-...	2578.0	1: Main Lanes	Exact

Figure 6: Vehicle Input (8am)

VISSIM OUTPUTS

Simulation data output is collected from data collection data points. Simulation results (e.g., minimum speed, mean speed, maximum speed, number of vehicles, acceleration, etc.) can be collected from a single point or a single cross section. In Figure 7 and Figure 8, detectors are located at points midway between the ramp gores and shown by the red circles. And volume data was collected at the collected at the blue circles.

Both the volumes and speeds collected at these points were used in the calibration of VISSIM for this problem.

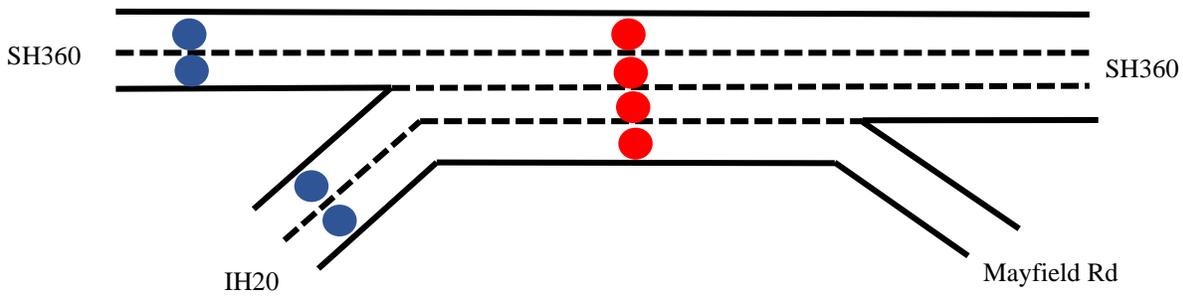


Figure 7: Data Collection Points

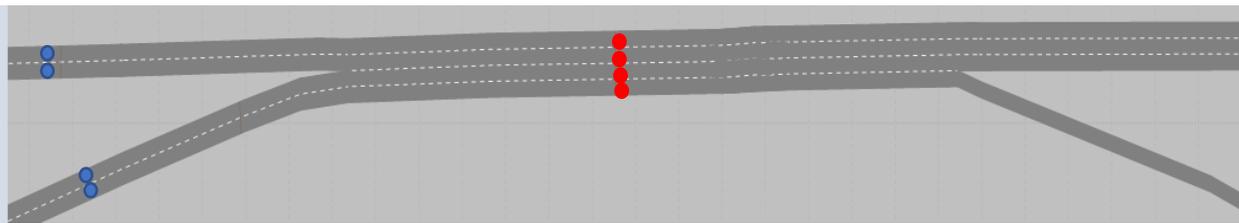


Figure 8: Data Collection Points in VISSIM Network

SIMULATION

Running Time and Resolution

The simulation running time is 4,200 seconds, which includes 300 seconds for warm-up and 300 seconds at the end. The simulation resolution, which is the number of times each vehicle's position is calculated within one simulation second, is set to 5 simulation steps per second (range 1 to 10).

Number of Runs

The number of observations (simulation runs) required to find statistically significant data for the measures of effectiveness can be computed using the following equation:

$$n = \left(\frac{Z \times \sigma}{e} \right)^2$$

Where n is the number of simulations runs required for each measure of effectiveness by location. Z is the standard normal deviation for the desired level of significance, and e is the tolerance (margin of error).

The standard deviation and mean are obtained from performing the simulation runs for 30 iterations each with a different random seed. The two major parameters, volumes for each entrance to weaving section (freeway entrance and entrance ramp) and speed for the middle freeway section were selected to calculate the required number of runs.

The number of simulation runs required for the calculation was found using the above equation, with a tolerance of (0.1) times the mean value obtained from 30 runs. The standard normal deviate for 95% confidence is 1.96. We found that three simulation runs are needed for the 7 pm dataset calibration. The average value from the three simulation runs was used to compare the results among models. However, the number of runs for validation is different from the number for calibration. The validation process using 8 am dataset is presented in the next section.

As shown in Table 1, sample size for volume on lane one of the entrance ramp (Ent.R- L1) is significantly higher than other data collection points. The high entrance ramp volume (3,509 vph) combined with 92% of the entering vehicles desiring to stay on the freeway results in a greater variability, requiring a higher number of observations. Therefore, most vehicles must weave to the left at some point. This high number of lane-changes results in more variability in the outputs for the on-ramp link.

To summarize, more traffic results in more congestion resulting, in turn, in more variability, therefore, a greater number of runs are needed to get a statistically significant result.

Table 1: Sample Size (7pm)

Data Collection Point Name	Volume			Speed			Confidence Interval	Sample Size	Sample Size
	Std Dev	Mean	e(0.1)	Std Dev	Mean	e(0.1)	95%	Volume	Speed
Freeway L4				1.09	61.64	6.16	1.96		1
Freeway L3				1.05	59.03	5.90	1.96		1
Freeway L2				0.86	58.38	5.84	1.96		1
Freeway L1				0.97	63.40	6.34	1.96		1
Entrance Ramp- L2	21.9	2,400	240				1.96	1	
Entrance Ramp- L1	68.2	814	81.4				1.96	3	
Freeway Entrance- L2	16.8	1,464	146.4				1.96	1	
Freeway Entrance- L1	14.2	1,570	157				1.96	1	
								n=3	

CALIBRATION

The model was calibrated using the data collected in the field for the 7 pm interval. For calibration, a variety of simulation runs were made over a range of values of selected parameters until the best-fit model was found. The parameter selection methodology consisted of iterated runs, visual evaluation, and volume and speed comparisons. Volume counts for each entrance lane (freeway entrance and entrance ramp) were available, and these were compared with the output values of

the VISSIM model. The locations where volumes were collected and compared are indicated in blue circles in Figure 7 and Figure 8. Similarly, time-mean speeds for each lane on the freeway midway between adjacent ramps are compared with field values (red circles in Figure 7 and Figure 8).

As shown in Table 2, field and VISSIM output speeds were found to be visually satisfactory and within a reasonable variance. Since only four travel speed samples were available, the speed comparison with a 5% tolerance interval is used to make sure that the travel speeds from the simulation output are reasonable when compared with the field values.

The accuracy of VISSIM's simulated volumes compared to the original field volumes is confirmed by the volume comparison in Table 2. The GEH measure was also calculated for each volume and evaluated using Table 2. M is the simulated volume and C is the measured volume (both are hourly volumes).

$$GEH = \sqrt{\frac{2(M - C)^2}{M + C}}$$

Calibration targets in Table 2 (coming from Wisconsin DOT VISSIM guide) show that for links that have flows less than 700 vph, 85% of model flows must be within 100 vph of the actual count.

Links with the flows between 700 and 2,700 vph, 85% of model flows must be within 15% of the actual count. And for links with flows more than 2,700 vph, 85% of model flows must be within 400 vph of the actual count.

GEH should be less than 5 for individual links in 85% of link flows. The lower the GEH, the fitter the model is.

In traffic modelling, a GEH of less than 5 is considered to be a good match between the modelled and observed hourly volumes. GEHs in the range of 5 to 10 may warrant investigation. If the GEH is greater than 10, there is a high probability that there is a problem with either the travel demand model or the data (FHA, 2019).

The Wisconsin DOT freeway model calibration target table (Table 2) leaves the acceptance of model speed to the analysts. The speed for individual link should be visually acceptable to the analyst's satisfaction and within reasonable variance from the field data.

Table 2: Freeway Model Calibration Targets (FHA, 2019)

	MOE Criteria	Calibration Acceptance Targets
Individual Link Flows	< 700 vph	Within 100 vph of field flow for > 85% of cases
	700 to 2,700 vph	Within 15% of field flow for > 85% of cases
	> 2,700 vph	Within 400 vph of field flow for > 85% of cases
	Sum of all links flows	Within 5% of sum of all link counts
GEH Statistic	For individual link flow	GEH < 5 for > 85% of cases
	For sum of link flow	GEH < 4 for sum of all link counts
	Individual link speed	Visually acceptable to analyst's satisfaction

PARAMETER ADJUSTMENT

Model calibration is the procedure where parameters are adjusted so that the model represents local driver behavior. In other words, model calibration is the process to ensure that the model behaves the same as the observed traffic.

Calibration is important because no single model is expected to have the ability to equally represent all possible traffic conditions. Every microscopic simulation software package includes a set of parameters for the purpose of calibrating the model to local conditions. The calibration process is an optimization procedure that requires an unpredictable number of iterations.

Lane Change Distance (LCD)

LCD refers to the location where a vehicle in the model will start trying to make a lane change prior to a decision point (i.e., freeway exit). The default setting for this distance is 656.2 feet. In most freeway networks, this distance is not realistic; causing vehicles to change lanes too late on freeways. It is important, however, to evaluate the network-wide impact of large LCDs, as overlapping lane change maneuvers can have adverse effects on upstream traffic. Moreover, LCD modifications greatly impact network performance within and outside the influence area and should be considered in the initial steps of the calibration process. The Emergency Stop Distance (ESD) can also be updated to more realistically match the location vehicles ultimately stop to wait for a lane change. It is important, however, to evaluate the network-wide impact of large LCDs, as overlapping lane change maneuvers can have adverse effects on upstream traffic. Moreover, LCD modifications greatly impact network performance within and outside the influence area.

In this study, field observation showed that the default lane change value of 656.2 ft was not sufficient for all lane change maneuvers, especially for the vehicles entering ramp. Therefore, the value of lane change distance for each connector was adjusted to half a mile (for most of them, almost equal to the length of its previous link).

In addition, observations of driving behavior, and as reported in (ref.), the lane change rate is much higher in the first 500 feet after a ramp merges with the freeway lanes. Therefore, the available modeling tools in VISSIM were used to model this behavior (Figure 9).



Figure 9: 500 feet High -Density Lane Change Area

Driving Behavior

Driving behavior is essential part of any model. It is one of the most important elements in a simulation a weaving segment. (PTV VISSIM 10 USER MANUAL, 2018)

VISSIM represents vehicular interactions using the Wiedemann 74 and Wiedemann 99 car-following models alongside additional proprietary lane changing models. Wiedemann 74 model is used for local/urban roads while Wiedemann 99 model is used for freeway modeling. These models are controlled by a set of parameters located in a driving behavior container. Driving behavior containers are assigned to each link in a network to dictate how vehicles traverse the link and interact with one another.

A new feature in VISSIM 2020 allows us to define these driving behaviors by individual lanes in every link. Previously, driving behavior was only applied to the entire link.

For this study calibration purpose, driving behaviors were defined in two categories, basic freeway (driving behavior 1) and weaving behavior (driving behavior 2). Weaving behavior was applied to the lanes on each side of the entrance ramp gore (freeway second and third lanes from right), and the weaving traffic was that whose origin-destination was freeway to ramp or ramp to freeway. The most right and the most left lanes of freeway are followed driving behavior 2.

Driving Behavior/ Lane Change

The lane change logic is a key element in simulating a weaving section. There are two types of lane changes in VISSIM: necessary and free lane changes. A necessary lane change occurs when a vehicle must make a lane change in order to reach the next connector of a route while a free lane change occurs when drivers have more room and time to change their lanes.

The driving behavior parameter for necessary lane changes includes the maximum acceptable deceleration for the vehicle and the trailing vehicle in the next lane, which depends on the distance to the emergency stop position of the next connector of the route. Other parameters included in the necessary lane change model include look-back distance, emergency stop distance, waiting time before diffusion, and minimum headway. (PTV VISSIM 10 USER MANUAL, 2018)

In the case of a free lane change, VISSIM checks for the desired safety distance of the trailing vehicles on the new lane, which depends on its speed and the speed of the vehicle that wants to change to that lane. Even though the user cannot change the “aggressiveness” for these lane changes, changing the parameters for the desired safety distance will affect the free lane changes as well. Those parameters that are important for the weaving simulation are described below:

Cooperative Lane Change (CLC)

parameter is a binary parameter that is deactivated by default in VISSIM. By activating this parameter, vehicles are conditioned to identify opportunities to assist other vehicles in making lane change maneuvers. This feature allows a vehicle traveling on the freeway to make an unnecessary lane change to create space for a merging vehicle to enter the freeway. Activation of CLC has greater influence on link speeds and densities compared to vehicular throughput. Activation of CLC in heavy weave and merge areas is beneficial to freeway operations and can be used to prevent unrealistic wait times as a vehicle merges into the network. The impact of activating CLC at a weave, merge, or diverge segments can be seen further upstream as the increased number of lane changes produces upstream traffic flow turbulence.

Advanced Merge

This parameter is shown to improve the fluidity of traffic flow through heavy weave segments. If this option is selected, more vehicles can change lanes earlier, increasing the operational capacity of the roadway and reduce the probability that vehicles will come to a stop waiting for a gap. These benefits are identified in the actual influence area as well as upstream segments. Advanced Merge is shown to have a greater influence on speed, density, and travel time, while limited impact on throughput.

The Emergency Stopping Distance

This parameter is the distance where a vehicle will stop to wait for an opportunity to change lanes in order to stay on its route if the vehicles cannot change lanes because of heavy traffic; default value is 16.4 ft.

The Waiting Time before Diffusion

This parameter is the maximum time a vehicle can wait at the emergency stop position for a gap to change lanes in order to stay on its route. When the time is reached, the vehicle is taken out of the network and a message will be written to the error file; default value is 60 seconds. The original purpose of this feature was to prevent unrealistic queues caused by vehicles not being able to make a lane change. Proper measures should be taken to limit the number of vehicles removed from the network to less than 5%.

Minimum Headway (front/rear)

This parameter defines the minimum distance to the vehicle in front that must be available for lane change in standstill condition, default value 1.64 s.

Safety Distance Reduction Factor (SDRF)

This parameter is applied to the lane-change algorithm as a multiplier that reduces the minimum safety distance required between the trailing and proceeding vehicles to initiate a lane change.

The lane change parameters in the calibration process are summarized in Table 3. Cooperative lane change, advanced merge, and vehicle static routing decision look ahead parameters have been activated as they have a positive effect on the traffic flow. Other lane change parameters have been kept as default except waiting time before diffusion that we reduced to 40 seconds, as opposed to the default value of 60 seconds, in order to prevent bottlenecks and queues in the network. Results show that this reduction does not have a negative effect on the network flow rate.

We made sure that not too many vehicles disappeared due to this reduction.

Driving Behavior/ Car Following Model

Car-following models provide quantitative values of the acceleration/deceleration for one vehicle following another when the leading vehicle changes its speed over time. Since this project is about freeway weaves, only the Wiedemann 99 model is used. The Wiedemann 99 model consists of ten adjustable parameters: CC0 to CC9. Those CC-parameters that are modified from the default values were described below:

Table 3: Lane Change Parameters

Parameters	Driving Behavior 1	Driving Behavior 2	Default Value
Cooperative Lane Change	Activated (with default value)	-	-
Advanced Merge	Activated	Activated	-
Vehicle Weaving Share Look Ahead	Activated	Activated	-
Emergency Stopping Distance	16.4 ft	16.4 ft	16.4 ft
Waiting Time Before Diffusion	40 s	40 s	60 s
Minimum Headway	1.64s	1.64s	1.64s
Safety Distance Reduction Factor	0.6	0.6	0.6

CC0 (Standstill Distance)

This parameter represents the minimum allowable gap between vehicles at a complete stop. This parameter is used to calculate the desired following distance. It serves as the bare minimum following distance and remains a baseline as the following distance increases with increases in speed. The default value of CC0 is 4.92 feet.

CC1 (Headway Time)

This parameter is used as an input that reflects the average time headway maintained by vehicles and is used to calculate the desired following distance of each vehicle from the leading vehicle. The CC1 parameter should remain consistent throughout the entire freeway network.

To prevent the creation of unrealistic and artificially imposed shockwaves caused by changes to this parameter in consecutive links.

Thus, changes to the car-following model between different types of freeway segments should be kept to the CC2 parameter. The CC0 and CC1 parameters should be calibrated to match average corridor-wide observed or expected headways. The higher the value, the more cautious the driver is. The default value of CC1 is 0.9 seconds.

CC0 and CC1 are used to calculate the safety distance defined as a minimum distance a driver will keep while following another car:

Safe distance= $CC0 + V * CC1$, where V is the speed of the trailing vehicle.

CC2, Following Variation

This parameter rather than directly contributing to the computation of the desired following distance as the CC0 and CC1 parameters do this parameter is used to set the boundary or range of acceptable following distances a vehicle can maintain before corrective action (i.e., acceleration or deceleration) is taken. Essentially, the CC0 and CC1 parameters define the “average desired following distance” and the CC2 parameter defines the amount of allowable oscillation around that mean. A larger CC2 value provides a wider range in allowable following distance, while a smaller CC2 value gives a narrower range.

While CC0 and CC1 values should stay consistent among continuous freeway segments, CC2 values can be updated to more realistically model differences in observed behavior. In general, the value for CC2 along freeway basic segments should be less than the CC2 value at weave, diverge, and merge segments.

CC4 and CC5

These control the speed differences during the “car following” state. Smaller values result in a more sensitive reaction of drivers to accelerations or decelerations of the preceding car. Usually, these parameters have opposite signs and equal absolute values. The default values are $CC4 = -0.35$ and $CC5 = 0.35$.

Due to the high volume entering the freeway from the entrance ramp (especially the left lane), queues occurred as the entering car could not find enough space between cars in the other lanes to perform a lane change. Adjusting CC0, CC1, and CC2 provides enough space for lane changing. CC0 is adjusting this space in the stopping situation and CC2 is for the stop and go situation.

Six models have been developed in terms of CC0, CC1, and CC2 adjustment as they were the most effective variables in terms of car following. The results have been compared to each other in terms of volume and speed in order to select the optimal model. Iterations have shown that other CC parameters do not have significant effect on the network performance.

Volume for each model is compared at 500 feet before the gore for both freeway and entrance ramps. The speed is collected on the middle of gore-to-gore distance. All models are adjusted to account for the fact that people prefer to change lane in the first 500 feet, based on field observation.

Table 4: Car Following Parameters

Parameters	Driving Behavior 1	Driving Behavior 2	Default Value
CC0	Iterative Parameters		
CC1			
CC2			
CC3	-8	-8	-8
CC4	-0.35	-0.35	-0.35
CC5	.35	.35	.35
CC6	11.44	11.44	11.44
CC7	0.82	0.82	0.82
CC8	11.48	11.48	11.48
CC9	4.92	4.92	4.92

In models presentation:

Ent. R-L1: is the rightest lane entering ramp.

Ent. R-L2: is the second lane from right entering ramp.

Main Ent- L1: is the rightest lane entering freeway.

Main Ent- L2: is the second lane from right entering freeway.

Freeway L1: is the rightest lane on freeway.

Freeway L2: is the second lane from right on freeway.

Freeway L3: is the third lane from right on freeway.

Freeway L4: is the fourth lane from right on freeway.

Model 1

Model 1 has CC0 equal to 4.92 feet for both behaviors, CC1 equal to 0.9 for both behaviors, and CC2 equal to 12 for behavior 1, and equal to 14 for behavior 2 (Table 5). CC2 is less on behavior 1 than behavior 2 as vehicles in lanes with behavior 1 require less lane changing than weaving vehicles.

Results show that overall GEH is too high and speed on lanes 1 and 4 on the freeway are too far from desired speed. However, the volume comparison is not that off. (Table 6, and Figure 10 and Figure 11)

Table 5: Car Following Parameters- Model 1

Parameters	Driving Behavior 1	Driving Behavior 2	Default Value
CC0	4.92	4.92	4.92
CC1	0.9	0.9	0.9
CC2	12	14	13.12

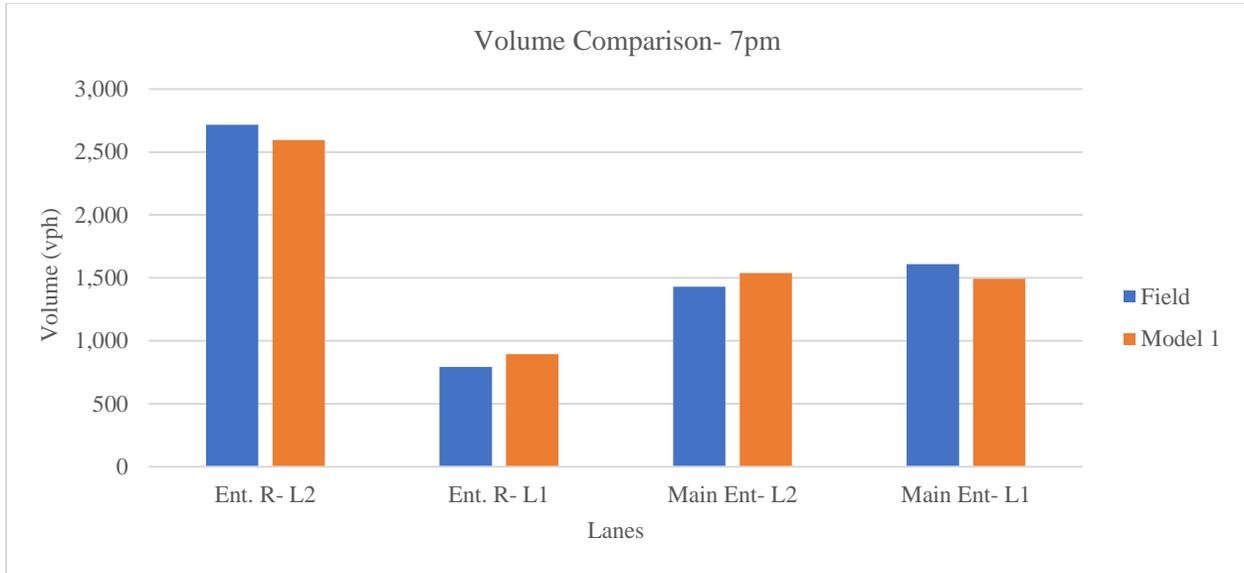


Figure 10: Model 1- 7pm- Volume

Table 6: Model 1- 7pm- GEH

Volume (vph)	Vehicle Input (vph)	Field Volume (vph)	VISSIM Volume (vph)	GEH
Ent. R- L2	3,509	2,716	2,594	2.4
Ent. R- L1		793	893	3.4
Main Ent- L2	3,040	1,430	1,538	2.8
Main Ent- L1		1,610	1,494	2.9

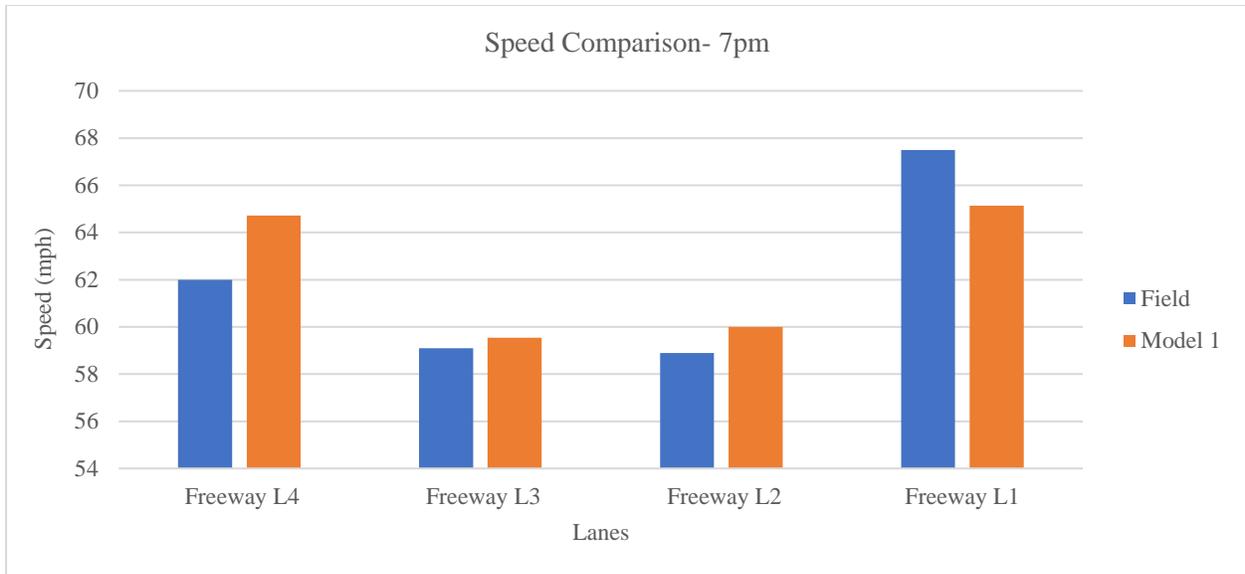


Figure 11: Model 1- 7pm- Speed

Model 2

Model 2 has CC0 equal to 9 and CC1 equal to 0.9 for both behaviors. CC2 is equal to 12 for behavior 1, and 14 for behavior 2 (Table 7). CC1 is higher in this model than the previous in order to let vehicles change lanes.

Table 8, and Figure 13 show that overall GEH and speed difference is better than Model 1.

Table 7: Car Following Parameters- Model 2

Parameters	Driving Behavior 1	Driving Behavior 2	Default Value
CC0	9	9	4.92
CC1	0.9	0.9	0.9
CC2	12	14	13.12

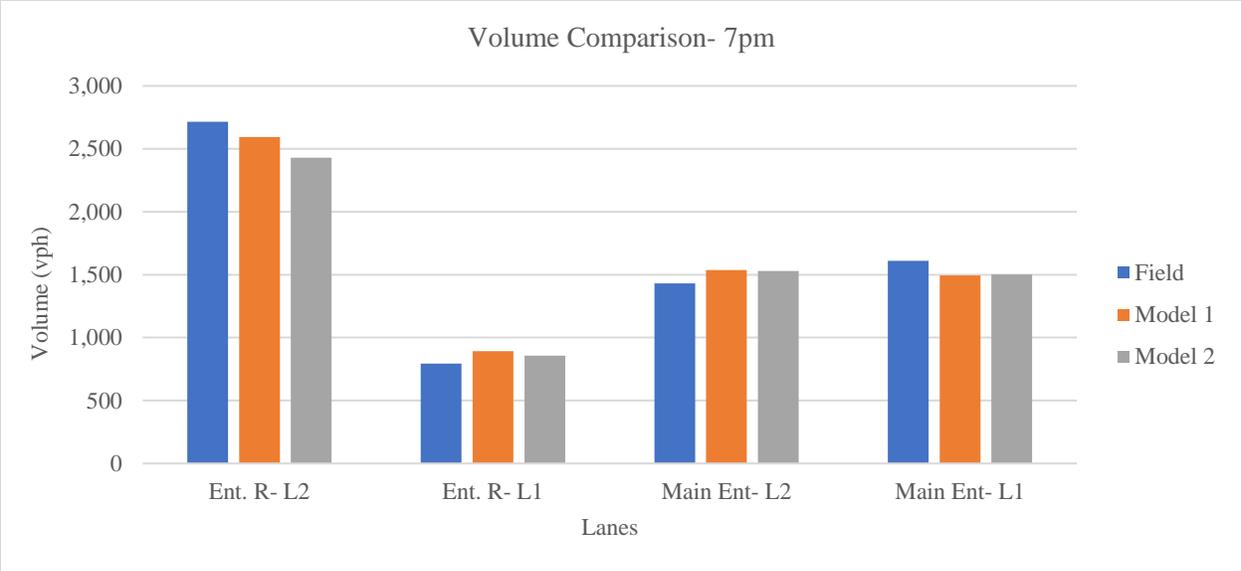


Figure 12: Model 2- 7pm- Volume

Table 8: Model 2- 7pm- GEH

Volume (vph)	Vehicle Input (vph)	Field Volume (vph)	VISSIM Volume (vph)	GEH
Ent. R- L2	3,509	2,716	2,428	5.7
Ent. R- L1		793	856	2.2
Main Ent- L2	3,040	1,430	1,530	2.6
Main Ent- L1		1,610	1,501	2.8

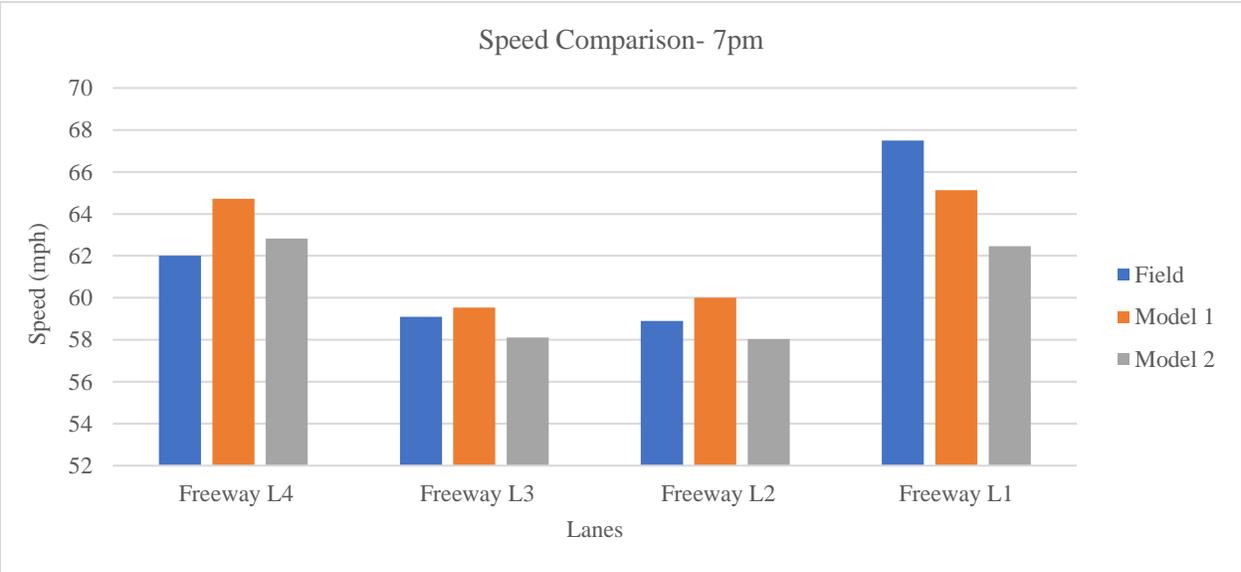


Figure 13: Model 2- 7 pm – Speed

Model 3

Model 3 has CC0 equal to 7, CC1 equal to 0.9, and CC2 is 13.12 for both behaviors (Table 9).

Results show that volume and GEH are the same as model 2, however, speed got worse (Table 10, Figure 14 and Figure 15).

Table 9: Car Following Parameters- Model 3

Parameters	Driving Behavior 1	Driving Behavior 2	Default Value
CC0	7	7	4.92
CC1	0.9	0.9	0.9
CC2	13.12	13.12	13.12

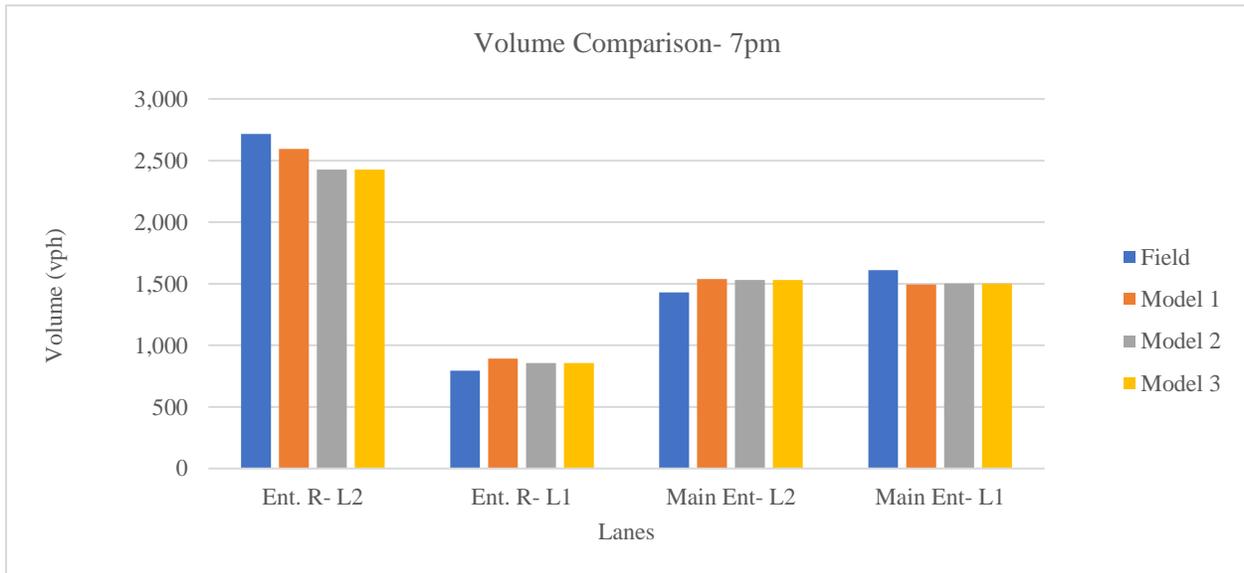


Figure 14: Model 3- 7pm- Volume

Table 10: Model 3- 7pm- GEH

Volume (vph)	Vehicle Input (vph)	Field Volume (vph)	VISSIM Volume (vph)	GEH
Ent. R- L2	3,509	2,716	2,428	5.7
Ent. R- L1		793	856	2.2
Main Ent- L2	3,040	1,430	1,530	2.6
Main Ent- L1		1,610	1,501	2.8

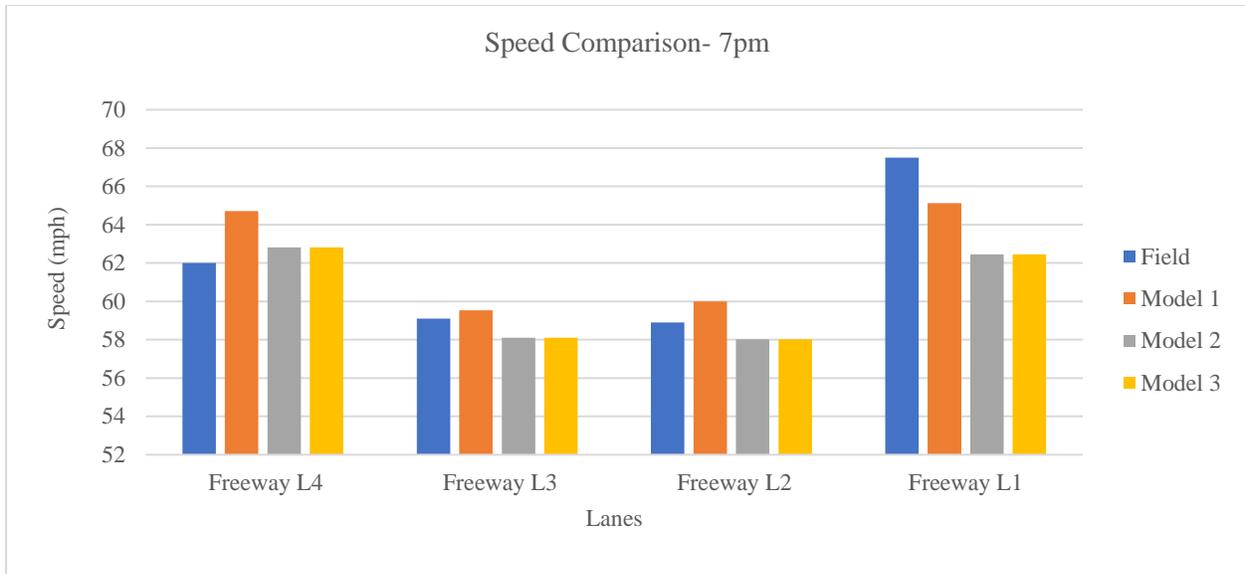


Figure 15: Model 3- 7 pm – Speed

Model 4

For model 4 CC0 is 7 and CC1 is 0.5 for both behaviors. CC2 is set to 12 for behavior 1 while it is 14 behavior 2. (Table 11)

According to Table 12, and Figure 16 and Figure 17, volume, GEH, and speed all got worse by reducing headway (CC1).

Table 11: Car Following Parameters- Model 4

Parameters	Driving Behavior 1	Driving Behavior 2	Default Value
CC0	7	7	4.92
CC1	0.5	0.5	0.9
CC2	12	14	13.12

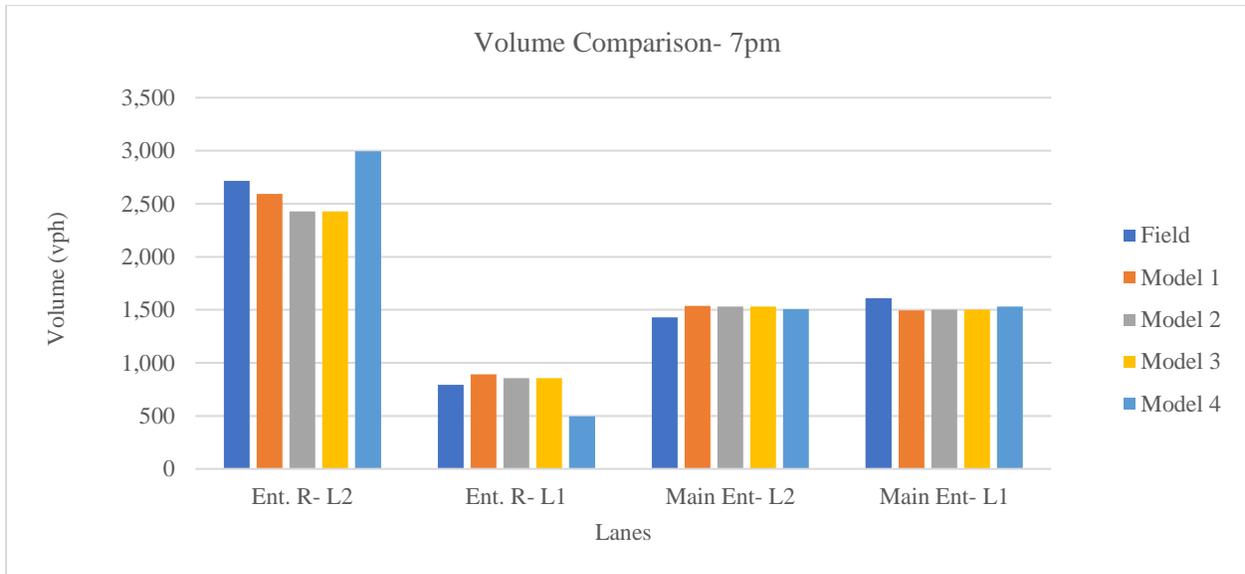


Figure 16: Model 4- 7pm- Volume

Table 12: Model 4- 7pm- GEH

Volume (vph)	Vehicle Input (vph)	Field Volume (vph)	VISSIM Volume (vph)	GEH
Ent. R- L2	3,509	2,716	2,996	5.2
Ent. R- L1		793	495	11.7
Main Ent- L2	3,040	1,430	1,506	2.0
Main Ent- L1		1,610	1,530	2.0

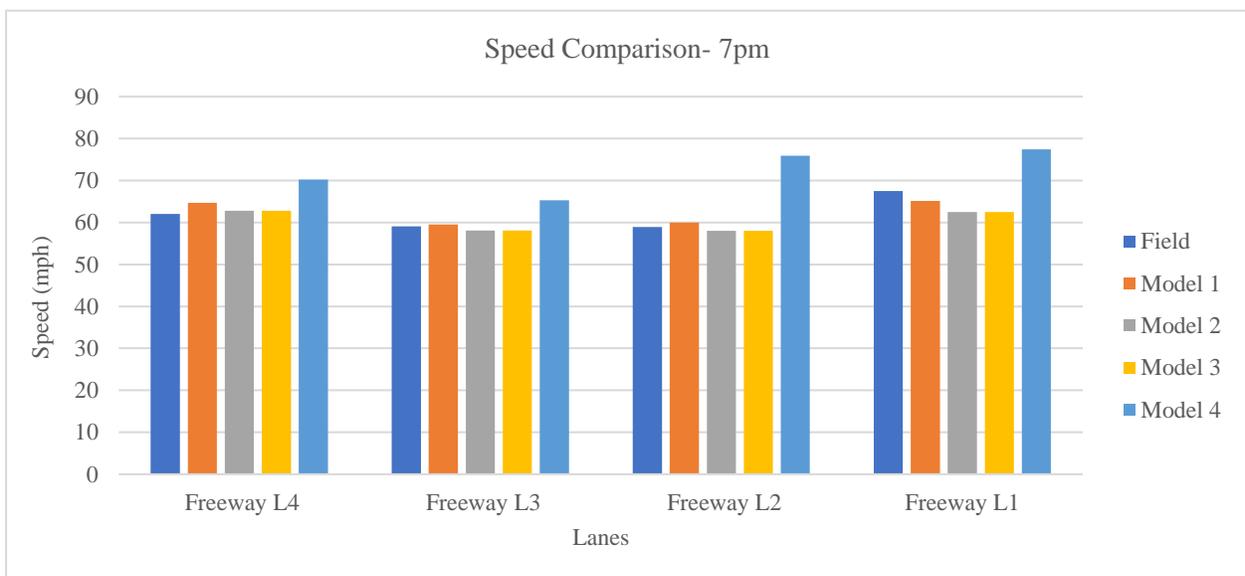


Figure 17: Model 4- 7pm- Speed

Model 5

Model 5 parameters include CC0 as 7 and CC1, 1.5 for both behaviors. CC2 is equal to 12 for behavior 1, and equal to 14 behavior 2. (Table 13)

Results claim that, volume, GEH, and speed while increasing headway (CC1) is as bad as when we decrease it (Table 12 and Table 14, and Figure 16, Figure 17, Figure 18, Figure 19).

Model 4 and 5 suggests that the optimal value for CC1 is 0.9.

Table 13: Car Following Parameters- Model 5

Parameters	Driving Behavior 1	Driving Behavior 2	Default Value
CC0	7	7	4.92
CC1	1.5	1.5	0.9
CC2	12	14	13.12

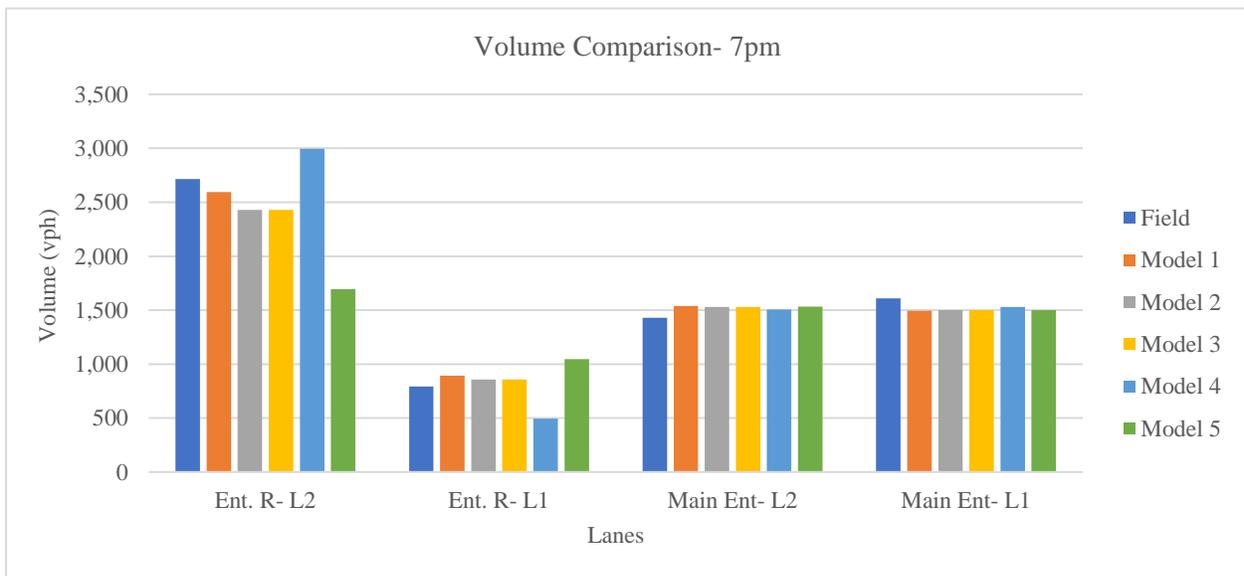


Figure 18: Model 5- 7pm- Volume

Table 14: Model 5- 7pm- GEH

Volume (vph)	Vehicle Input (vph)	Field Volume (vph)	VISSIM Volume (vph)	GEH
Ent. R- L2	3,509	2,716	1,695	21.7
Ent. R- L1		793	1,047	8.4
Main Ent- L2	3,040	1,430	1,533	2.7
Main Ent- L1		1,610	1,500	2.8

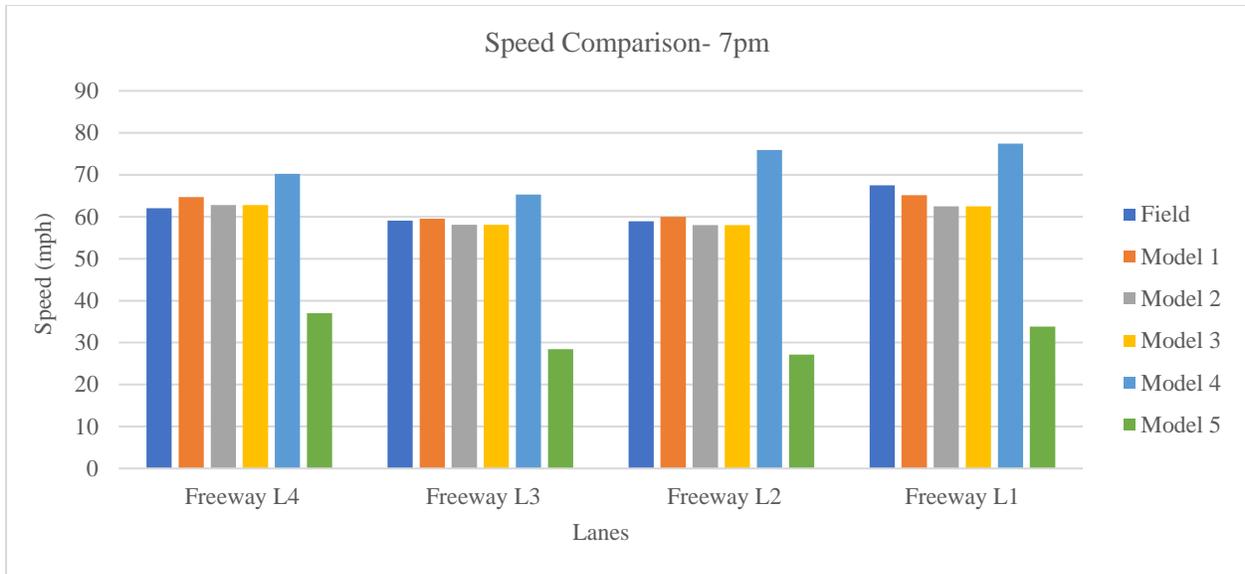


Figure 19: Model 5- 7pm- Speed

Model 6

Model 6 applied following parameters on network. CC0= 7, and CC1= 0.9 for both behaviors. CC2 equals to 12 for behavior 1 and equals to 14 for behavior 2. (Table 15)

Volume, GEH, and speed all represent their best feasible values. (Table 16, Figure 20 and Figure 21)

Table 15: Car Following Parameters- Model 6

Parameters	Driving Behavior 1	Driving Behavior 2	Default Value
CC0	7	7	4.92
CC1	0.9	0.9	0.9
CC2	12	14	13.12

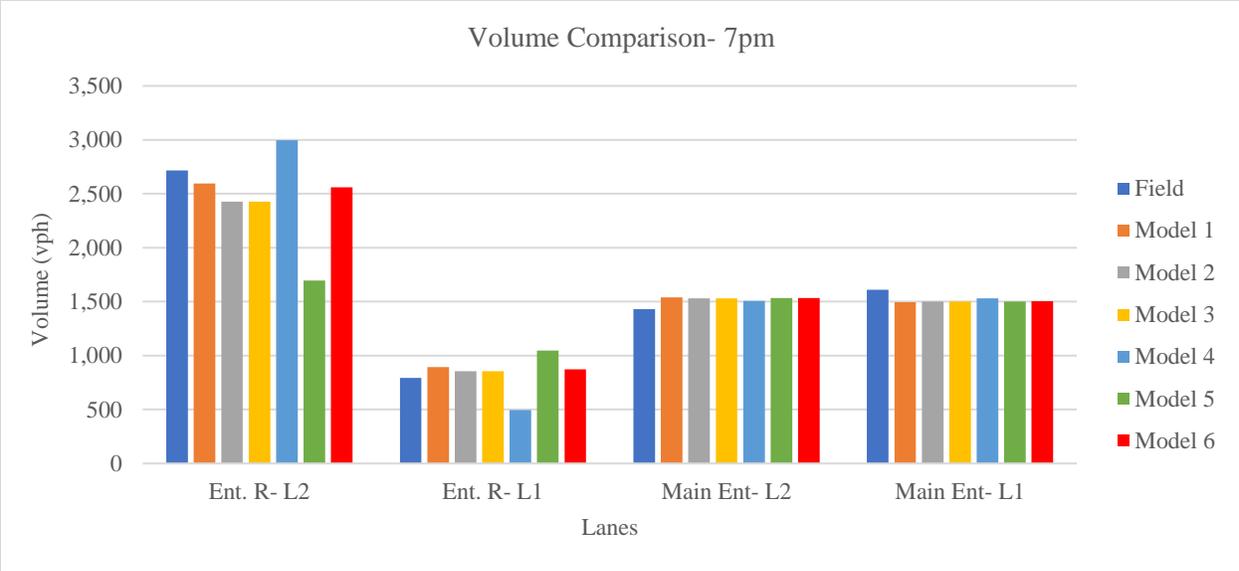


Figure 20: Model 6- 7pm- Volume

Table 16: Model 6- 7pm- GEH

Volume (vph)	Vehicle Input (vph)	Field Volume (vph)	VISSIM Volume (vph)	GEH
Ent. R- L2	3,509	2,716	2,559	3.1
Ent. R- L1		793	874	2.8
Main Ent- L2	3,040	1,430	1,533	2.7
Main Ent- L1		1,610	1,503	2.7

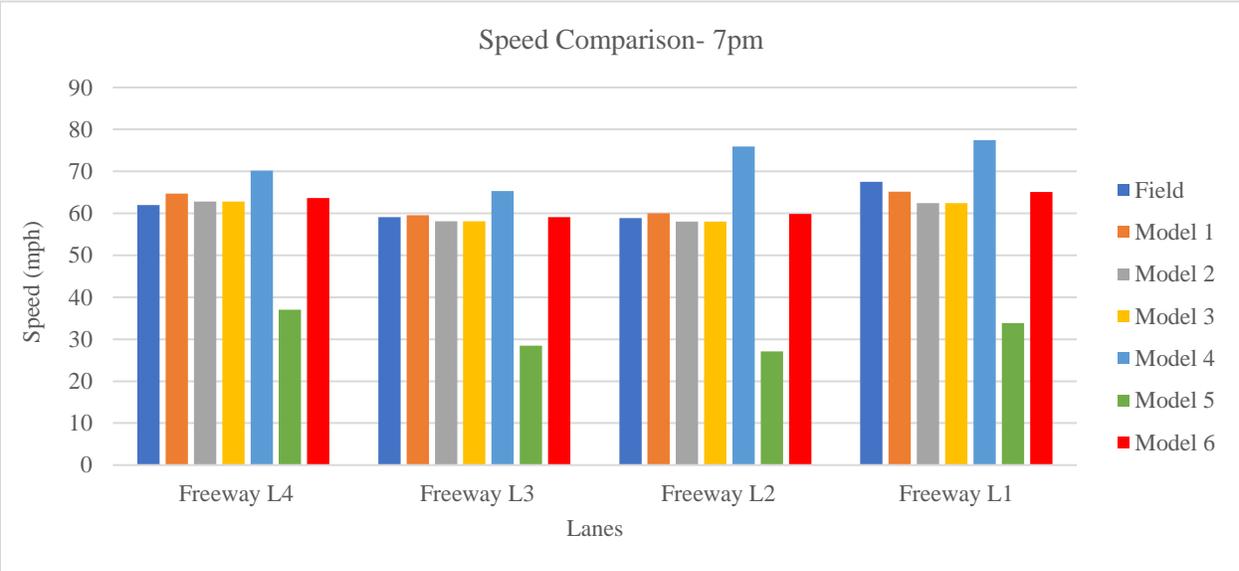


Figure 21: Model 6- 7pm- Speed

MODEL SELECTION

Six models were introduced in the previous section. Each model performs well with some measure of effectiveness (MOEs) but performs poorly with others. In order to select the best model, a multi-criteria analysis process was conducted using the Simple Additive Weighting (SAW) method. In this method, a score is obtained by adding the contributions from each of the chosen criteria. The overall weight score, V_a , for model a, using this method can be written as follows: (Vo, 2007)

$$V_a = \sum_{j=1}^{j=n} W_j r_{aj}$$

W_j = Weight for criterion j

r_{aj} = rating for model on criterion j

The model with the largest value of V_a is selected.

12 criteria are used to rate each model: Four for volume on each entrance lane, four for GEH for each entrance lane, and four speed measurements, one in each lane midway from the two ramps. For volume and GEH comparison, we had “Entrance ramp, lane 1”, “Entrance ramp, lane 2”, “Freeway entrance, lane 1”, and “Freeway entrance, lane 2”. For speed measurement, we had “Middle section, lane 1”, “Middle section, lane 2”, “Middle section, lane 3”, and “Middle section, lane 4”.

Each of the 12 criteria in this SAW model has the same weight score. The criterion with the largest difference to the field value has the rating of 0 and the field data has the rating of 1. The largest possible score for each model is 12. The raw criterion scores on each criteria option of each model are determined by the difference between the criteria value on each model and the field value.

The raw score of models is calculated using following equation:

$$Raw\ Score = 1 - \frac{difference}{max\ difference}$$

This technique can quantify the performance of each model compared to the field data. The model with the highest score out of 12 MOEs will be the best candidate for validation.

Table 17: Raw Score

Speed (mph)- 7pm			
	Lane 2- Freeway L4	Difference	Raw Score
Field	62	0	1
Model 1	64.7	2.72	0.891
Model 2	62.8	0.82	0.967
Model 3	62.8	0.82	0.967
Model 4	70.2	8.19	0.672
Model 5	37.0	24.96	0.000
Model 6	63.7	1.66	0.934
	Max	24.96	

Table 18: Scoring- 7pm

Performance Measures		Lanes	Lanes	Model 2	Model 3	Model 4	Model 5	Model 6
7:00 PM	Volume	Ent. R- L2	0.881	0.718	0.718	0.726	0.000	0.846
	Volume	Ent. R- L1	0.664	0.789	0.789	0.000	0.148	0.728
	Volume	Main Ent- L2	0.000	0.074	0.074	0.296	0.046	0.046
	Volume	Main Ent- L1	0.000	0.060	0.060	0.310	0.052	0.078
	GEH	Ent. R- L2	0.891	0.739	0.739	0.759	0.000	0.859
	GEH	Ent. R- L1	0.707	0.813	0.813	0.000	0.287	0.761
	GEH	Main Ent- L2	0.000	0.073	0.073	0.292	0.045	0.045
	GEH	Main Ent- L1	0.000	0.061	0.061	0.314	0.053	0.079
	Speed	Freeway L4	0.891	0.967	0.967	0.672	0.000	0.934
	Speed	Freeway L3	0.983	0.960	0.960	0.751	0.228	1.000
	Speed	Freeway L2	0.956	0.965	0.965	0.319	0.273	0.961
	Speed	Freeway L1	0.905	0.798	0.798	0.602	0.349	0.904
				6.877	7.018	7.018	5.041	1.481

VALIDATION

On previous section models 1, 2, 3 and 6 got the highest criterion scores and were selected to be validated using a different dataset (8 am). The number of runs is also calculated using the same equation as calibration section (Table 19). Five simulation runs conducted for 8 am data set over the four selected models. Results show that models 2 and 6 have a better performance in terms of volume, GEH, and speed than model 1 and 3. Summary of validation results are presented in Figure 22, Figure 23 and Table 20. Scoring result for validation is presented in Table 22 and Table 23. It is preferred to use the same car following model for both datasets (calibration and validation ones) unless we have significant difference in volumes, driving behaviors, or type of drivers.

Table 19: Sample Size (8am)

Data Collection Point Name	Volume			Speed			Confidence Interval 95%	Sample Size	Sample Size
	Std Dev	Mean	e(0.05)	Std Dev	Mean	e(0.05)		Volume	Speed
Freeway L4				1.07	64.92	3.25	1.96		1
Freeway L3				0.93	62.88	3.14	1.96		1
Freeway L2				1.07	62.53	3.13	1.96		1
Freeway L1				1.22	67.63	3.38	1.96		1
Ent. R- L2	30.0	2452	122.6				1.96	1	
Ent. R- L1	31.0	565	28.25				1.96	5	
Main Ent- L2	14.0	1258	62.9				1.96	1	
Main Ent- L1	13.0	1316	65.8				1.96	1	
								n=5	

Table 20: Car Following Parameters (Validation)

	Parameters	Driving Behavior 1	Driving Behavior 2	Default Value
Model 1	CC0	4.92	4.92	4.92
	CC1	0.9	0.9	0.9
	CC2	12	14	13.12
Model 2	CC0	9	9	4.92
	CC1	0.9	0.9	0.9
	CC2	12	14	13.12
Model 3	CC0	7	7	4.92
	CC1	0.9	0.9	0.9
	CC2	13.12	13.12	13.12
Model 6	CC0	7	7	4.92
	CC1	0.9	0.9	0.9
	CC2	12	14	13.12

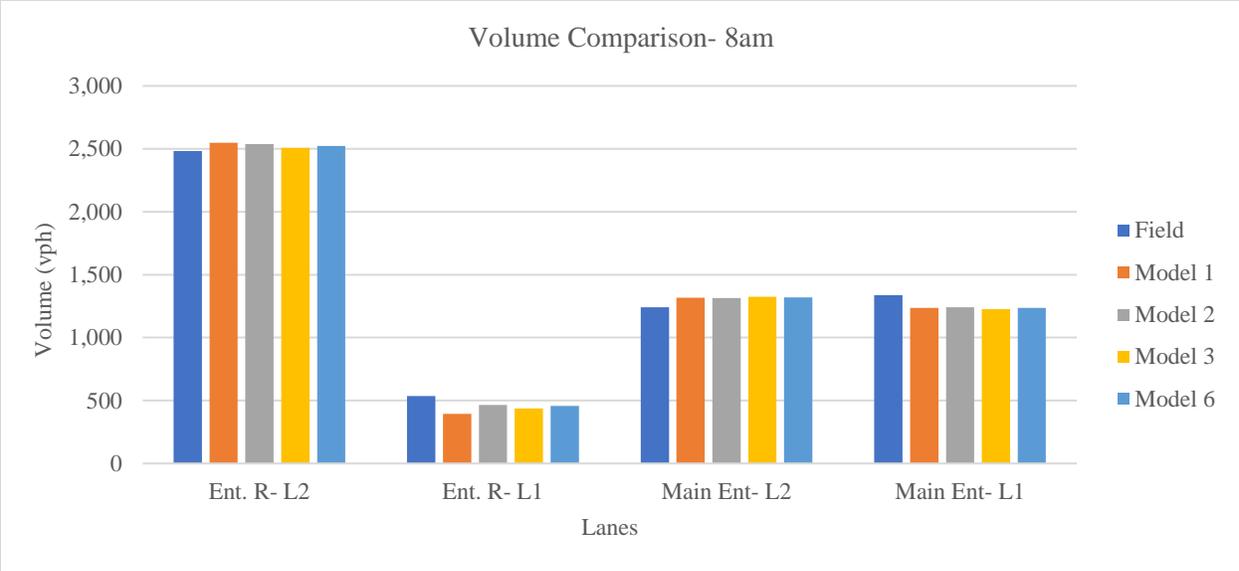


Figure 22: Volume Comparison- 8 am

Table 21: GEH Comparison- 8 am

Volume (vph)	Vehicle Input (vph)	Field Volume (vph)	Model 1	Model 2	Model 3	Model 6
			GEH	GEH	GEH	GEH
Ent. R- L2	3,020	2,483	1.3	1.1	0.5	0.8
Ent. R- L1		537	6.6	3.3	4.5	3.5
Main Ent- L2	2,578	1,241	2.2	2.0	2.3	2.2
Main Ent- L1		1,337	2.8	2.7	3.1	2.8



Figure 23: Speed Comparison- 8 am

We are looking for a model to replicate both datasets at the same time. However, model 2 has a slightly higher score in validation section, as model 6 has the better overall score (on the 7pm and 8 am datasets), therefore, the selected model is model 6. (Table 22 and Table 23)

So, the selected parameters values are $CC0 = 7$, $CC1 = 0.9$, and $CC2 = 12$ for behavior 1, and $CC2 = 14$ for behavior 2.

Table 22: Models Scoring- 8am

	Performance Measures	Lanes	Model 1	Model 2	Model 3	Model 6
8:00 AM	Volume	Ent. R- L2	0.897	0.914	0.962	0.939
	Volume	Ent. R- L1	0.684	0.839	0.781	0.826
	Volume	Main Ent- L2	0.072	0.120	0.000	0.048
	Volume	Main Ent- L1	0.091	0.127	0.000	0.073
	GEH	Ent. R- L0	0.904	0.920	0.965	0.943
	GEH	Ent. R- L1	0.596	0.801	0.727	0.784
	GEH	Main Ent- L0	0.071	0.119	0.000	0.047
	GEH	Main Ent- L1	0.093	0.130	0.000	0.074
	Speed	Freeway L4	0.933	0.961	0.998	0.917
	Speed	Freeway L3	0.495	0.448	0.475	0.597
	Speed	Freeway L2	0.664	0.585	0.629	0.620
	Speed	Freeway L1	0.868	0.953	0.937	0.934
				6.369	6.917	6.475

Table 23: Total Scoring

Data set	Performance Measures	Lanes	Model 1	Model 2	Model 3	Model 4	Model 5	Model 6	
7:00 PM	Volume	Ent. R- L2	0.881	0.718	0.718	0.726	0.000	0.846	
	Volume	Ent. R- L1	0.664	0.789	0.789	0.000	0.148	0.728	
	Volume	Main Ent- L2	0.000	0.074	0.074	0.296	0.046	0.046	
	Volume	Main Ent- L1	0.000	0.060	0.060	0.310	0.052	0.078	
	GEH	Ent. R- L0	0.891	0.739	0.739	0.759	0.000	0.859	
	GEH	Ent. R- L1	0.707	0.813	0.813	0.000	0.287	0.761	
	GEH	Main Ent- L0	0.000	0.073	0.073	0.292	0.045	0.045	
	GEH	Main Ent- L1	0.000	0.061	0.061	0.314	0.053	0.079	
	Speed	Freeway L4	0.891	0.967	0.967	0.672	0.000	0.934	
	Speed	Freeway L3	0.983	0.960	0.960	0.751	0.228	1.000	
	Speed	Freeway L2	0.956	0.965	0.965	0.319	0.273	0.961	
	Speed	Freeway L1	0.905	0.798	0.798	0.602	0.349	0.904	
				6.877	7.018	7.018	5.041	1.481	7.242
		Performance Measures	Lanes	Model 1	Model 2	Model 3			Model 6
8:00 AM	Volume	Ent. R- L2	0.897	0.914	0.962			0.939	
	Volume	Ent. R- L1	0.684	0.839	0.781			0.826	
	Volume	Main Ent- L2	0.072	0.120	0.000			0.048	
	Volume	Main Ent- L1	0.091	0.127	0.000			0.073	
	GEH	Ent. R- L0	0.904	0.920	0.965			0.943	
	GEH	Ent. R- L1	0.596	0.801	0.727			0.784	
	GEH	Main Ent- L0	0.071	0.119	0.000			0.047	
	GEH	Main Ent- L1	0.093	0.130	0.000			0.074	
	Speed	Freeway L4	0.933	0.961	0.998			0.917	
	Speed	Freeway L3	0.495	0.448	0.475			0.597	
	Speed	Freeway L2	0.664	0.585	0.629			0.620	
	Speed	Freeway L1	0.868	0.953	0.937			0.934	
				6.369	6.917	6.475			6.802
	Total Score			13.246	13.935	13.493			14.044

SENSITIVITY ANALYSIS FOR CALIBRATION PARAMETERS

During the calibration process, we found a set of parameters and the optimal model which fits the observed traffic operations. The car-following sensitivity is analyzed in this section to evaluate the network sensitivity to the selected parameter's value.

CC0, CC1, and CC2 were shown in the previous section to have most significant effect on network performance. Over a range of reasonable values, including those that provided the best fit for both

AM and PM data sets, the results showed that these parameters had a significant effect on network performance.

In this section we have examined what may happen to the calibrated network if CC0, or CC2 change by $\pm 10\%$ or $\pm 20\%$. We monitored the network to see if the network is sensitive to these changes or if they cause any unreasonable queues.

CC1 was not examined for this analysis as the value of this parameter has fixed values in VISSIM and we cannot change it up and down by desirable factors manually.

Results for sensitivity analysis are presented in Table 24 and Table 25 and Figure 24 and Figure 25. Each scenario represents by S (for example, S1 stands for scenario 1). For each scenario, only one is changed at the time to see how sensitive the network is. Not only the throughput is important, but also, we monitored the network in term of queue, bottleneck, and volume on each ramp. We looked at the driving behavior as well.

This analysis illustrated that only extreme changes in these parameters (CC0, and CC2) appeared to have a substantial effect on network.

The calibration and validation of VISSIM were detailed in this chapter. This was done with a data set from Arlington, Texas, in the Dallas/Fort Worth area. In the next chapter, various scenarios are identified on the basis of lane configuration, number of lanes, and distances between ramps. Then the capacities are estimated by raising the flows until a link output is less than its corresponding input. This condition assumes that the link in question is experiencing queueing. Then, capacity is estimated based on the HCM's definition of capacity, i.e., a density of 43 pcphpl.

Table 24: Sensitivity Analysis Scenarios

Scenario	Parameter	Optimal Value	Change by	Value	Queue/Bottleneck
1	CC0	7	+10%	7.70	No
2			-10%	6.30	No
3			+20%	8.40	No
4			-20%	5.60	No
5	CC2- Behavior 1	12	+10%	13.20	No
6			-10%	10.80	No
7			+20%	14.40	No
8			-20%	9.60	No
9	CC2-Behavior 2	14	+10%	15.40	No
10			-10%	12.60	No
11			+20%	16.80	No
12			-20%	11.20	No

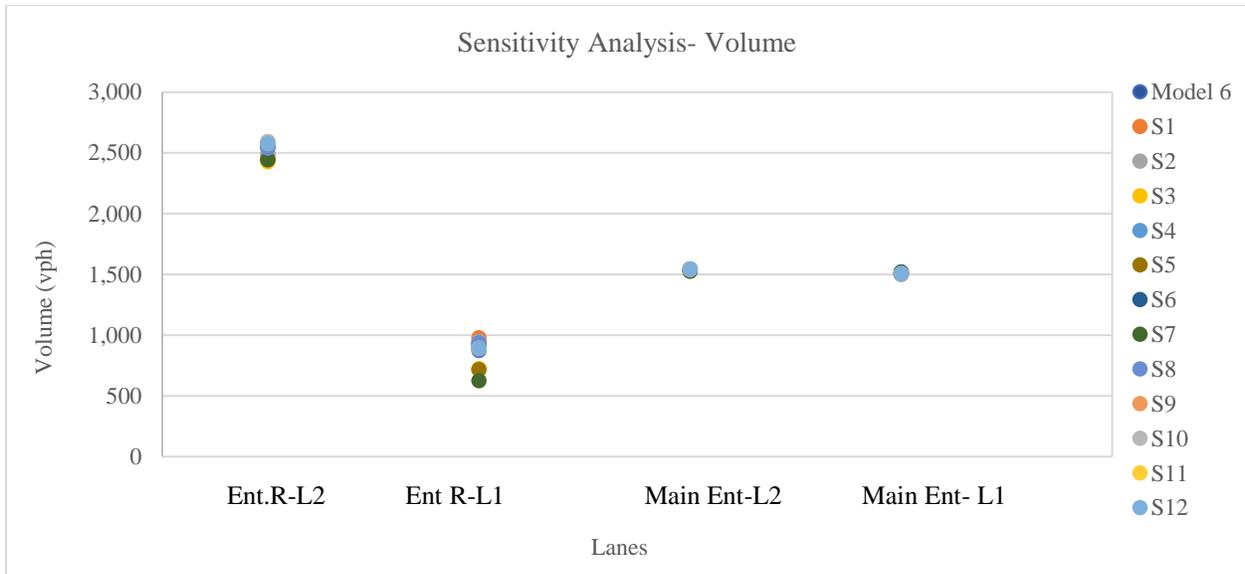


Figure 24: Sensitivity Analysis- Volume

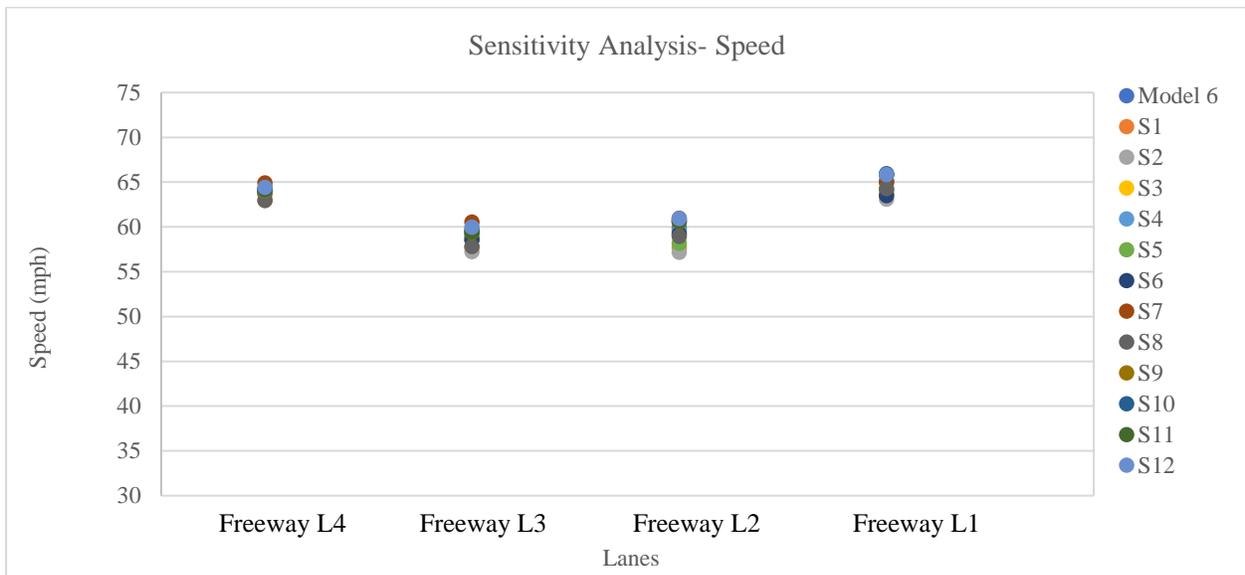


Figure 25: Sensitivity Analysis- Speed

Table 25: Sensitivity Analysis- GEH

	Lanes	Model 6	S1	S2	S3	S4	S5	S6	S7	S8	S9	S10	S11	S12
GEH	Ent. R- L2	3.1	4.7	4.3	5.7	2.6	5.4	3.3	5.3	3.4	2.4	2.4	2.6	2.6
	Ent. R- L1	2.8	6.2	5.4	2.4	3.5	2.8	4.5	6.3	4.9	3.3	3.3	3.4	3.4
	Main Ent- L2	2.7	2.9	3.0	2.8	2.8	2.6	3.0	2.5	2.8	3.0	3.0	3.0	3.0
	Main Ent- L1	2.7	2.6	2.7	2.5	2.5	2.3	2.7	2.2	2.5	2.7	2.7	2.7	2.7

CHAPTER 3: SIMULATION MODELING

In chapter 3, repeated simulations will be performed under varying number of lanes, flow range, heavy vehicle percentage, and weaving share. Simulations results will be used to estimate the capacity of the weaving area. Variables are:

- L_{S1} : Gore to gore distances for R1 to R2
- L_{S2} : Gore to gore distances for R2 to R3
- VF1: Flow for freeway entrance
- VR1: Flow for first entrance ramp
- VR2: Flow for second entrance ramp
- HVF1: Heavy vehicle percentage for freeway entrance
- HVR1: Heavy vehicle percentage for first entrance ramp
- HVR2: Heavy vehicle percentage for second entrance ramp
- WSF1-F2: Weaving share for drivers entering F1 and exiting at F2
- WSR1-F2: Weaving share for drivers entering R1 and exiting at F2
- WSR2-F2: Weaving share for drivers entering R2 and exiting at F2
- F1: Number of lanes for freeway entrance
- R1: Number of lanes for first entrance ramp
- R2: Number of lanes for second entrance ramp
- F2: Number of lanes for freeway exit
- R3: Number of lanes for third exit ramp

R1-R2 refers to the segment between R1 and R2 and R2-R3 refers to the segment between R2 and R3.

A weaving section is a common design on major highway facilities that always has been of interest to researchers. Weaving areas are characterized by frequent lane changes, which significantly reduce the capacity of the freeway. The HCM defined weaving capacity as “any combination of flows that causes the density to reach the LOS E/F boundary condition of 43 pc/m/ln for freeways” based on configuration, number of lanes in the weaving section, free-flow speed, length of the weave, and volume ratio (VR). (HCM 2016)

A multiple weaving area is one where two or more weaving areas overlap. No satisfactory means of estimating capacity have been found. Current procedures make assumptions about where weaving occurs in the individual weaving segments. A multiple weaving area is found when “a series of closely spaced merge and diverge areas create overlapping weaving movements (between different merge-diverge points).” (HCM 2016)

This study is limited to cases where there are just two overlapping weaving movements created by two entry ramps following by an exit ramp.

The study develops relations for capacity and service volume for a range of geometric and flow conditions, and traffic mix. Geometric conditions include number of lanes (n) on the freeway entry and each entrance ramp into and exit ramp from the weaving area, and distances between ramps (L_S). Flow conditions include a range of flows (V) in each of the entry and exit roadways in the multiple weaving area. The traffic mix represents the fraction of heavy vehicles in the traffic stream (P_{HV}). These variables are shown in Figure 26 for the conditions simulated in this work.

Simulation is the key element for this research and calibration ensured the model behaves in the same way as the observed traffic; the calibration process and results are discussed in Chapter 2. Calibrated values are used for simulation.

The weaving area for this research is two entrance ramps followed by an exit ramp as shown in Figure 26, and the elements are:

- F1: Freeway Lanes Entering Weaving Area
- R1: First Entrance Ramp
- R2: Second Entrance Ramp
- R3: Exit Ramp
- F2: Freeway Lanes Leaving Weaving Area

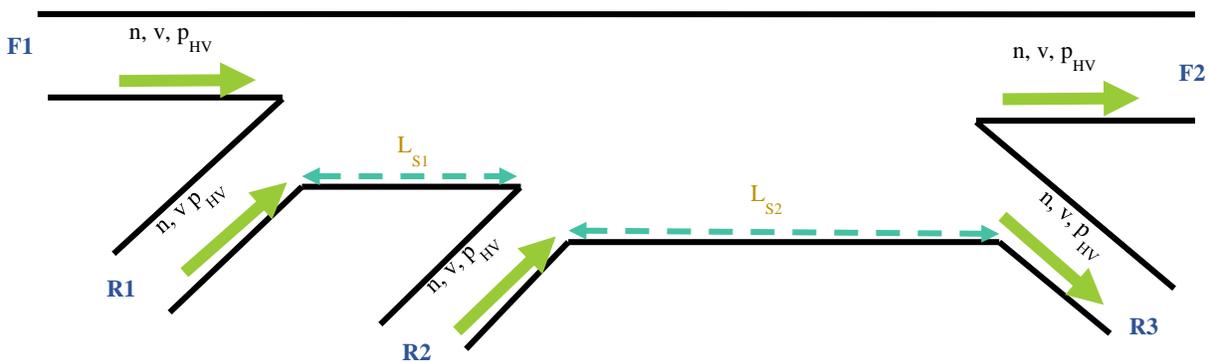


Figure 26: Multiple Weaving Area Elements

STAGES

For each geometric condition, this study simulates the range of flows in order to estimate the capacities.

Stage 1- Simulation runs, which investigate the correlation between capacity of a weaving section and each of the following variables or mix of selected factors in the multiple weaving area. (Figure 26 and Figure 27)

- Number of lanes on freeway entry and each entrance ramp into and exit ramp from the weaving area (n)
- Gore to gore distances between ramps (L_s)
- Origin-Destination flows (V)
- The traffic mix represents the fraction of heavy vehicles in the traffic stream (p_{HV})

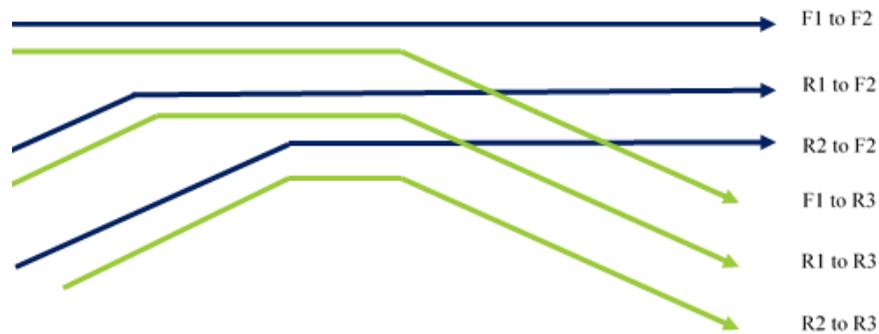


Figure 27: Flow Distribution

Stage 2 – Discuss simulations

Stage 3 – Regression model for estimating capacity/level of service for each scenario. In this model, the dependent variable are the weaving capacity and service flows. Potential independent variables include number of lanes on each entry into and exit (n), weaving length (L), freeway flow, exit ramp flow, entrance ramp flow, fraction of weaving traffic, and the fraction of heavy vehicles in the traffic stream (p_{HV}).

Stage 4 - Compares the densities obtained from the simulation with HCM values.

VISSIM INPUT

Variables

In order to estimate the capacity of the weaving area, repeated simulations are performed under varying number of lanes, flow range, heavy vehicle percentage, and weaving share. The ranges for the number of lanes and the flows are summarized in Table 26 through Table 29. In the simulation runs, capacity is going to be determined as the point where the demand starts to exceed the throughput flow as the factors are changed.

Number of Lanes (48 Scenarios)

Table 26: Number of Lanes Range

Ranges	F1 --- 2 to 4 lanes
	R1 --- 1 to 2 lanes
	R2 --- 1 to 2 lanes
	R3 --- 1 to 2 lanes

The range of the number of lanes for the freeway entry roadways and each of the ramps is shown in Table 26. Number of lanes for freeway exit (F2) will be calculated based on number of lanes for R3. Total number of lanes for F2 and R3 should be the same as number of lanes for R2-R3. If n is number of lanes, then:

$$n(R1-R2) = n(F1) + n(R1)$$

$$n(R2-R3) = n(R1-R2) + n(R2)$$

$$n(R3) + n(F2) = n(R2-R3)$$

n(R3) as the number of lanes in Ramp 3, and n(R2-R3) as the number of lanes on the freeway between Ramps 2 and 3.

A complete enumeration of the scenarios tested is shown in Table 27, where the number of lanes in each segment of the weaving area are shown. In addition, for the three ramp-freeway intersection points, whether the merge or diverge is accomplished by reducing or adding lanes (Figure 28), or the number of lanes is the same before and after the gore (Figure 29).

Table 27: Number of Lanes Scenarios

Freeway Entrance	First Entrance Ramp	Merge	First Gore to Gore	Second Entrance Ramp	Merge	Second Gore to Gore	Diverge	Freeway Exit	Exit Ramp
F1	R1		R1-R2	R2		R2-R3		F2	R3
2	1	B	3	1	B	4	B B	2 3	2 1
2	2	B	4	1	B	5	B B	3 4	2 1
3	1	B	4	1	B	5	B B	3 4	2 1
3	2	B	5	1	B	6	B B	4 5	2 1
4	1	B	5	1	B	6	B B	4 5	2 1
4	2	B	6	1	B	7	B B	5 6	2 1

Freeway Entrance	First Entrance Ramp	Me rge	First Gore to Gore	Second Entrance Ramp	Merge	Second Gore to Gore	Diverge	Freeway Exit	Exit Ramp
F1	R1		R1-R2	R2		R2-R3		F2	R3
2	1	B	3	2	B	5	B B	3 4	2 1
2	2	B	4	2	B	6	B B	4 5	2 1
3	1	B	4	2	B	6	B B	4 5	2 1
3	2	B	5	2	B	7	B B	5 6	2 1
4	1	B	5	2	B	7	B B	5 6	2 1
F1	R1		R1-R2	R2		R2-R3		F2	R3
2	1	A	2	1	B	3	B A	2 3	1 1
2	2	B	4	1	A	4	B A	3 2	1 2
3	1	A	3	1	A	3	B A	2 3	1 2
3	2	B	5	1	A	5	B B	4 3	1 2
4	1	A	4	1	A	4	B B	3 2	1 2
4	2	B	6	1	A	6	B B	5 4	1 2
F1	R1		R1-R2	R2		R2-R3		F2	R3
2	1	A	2	2	B	4	B B	3 2	1 2
2	2	B	4	2	B	6	B B	4 5	2 1
3	1	A	3	2	B	5	B B	4 3	1 2
3	2	B	5	2	B	7	B B	5 6	2 1
4	1	B	5	2	A	6	B B	5 4	1 2

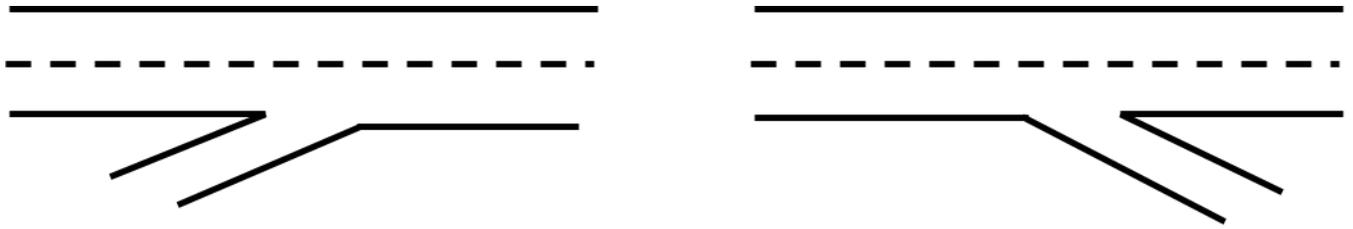


Figure 28: Type A Lane Configurations at The Merge/Diverge Points

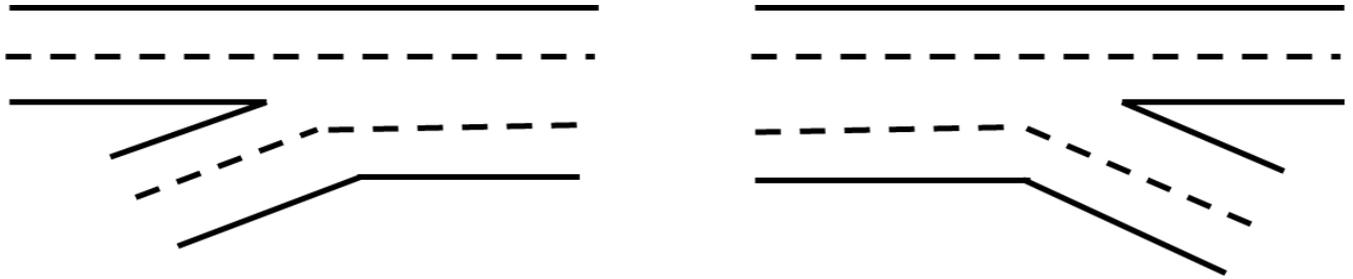


Figure 29: Type B Lane Configurations at The Merge/Diverge Points

Runs start with V_{F1} increase by 500 vph in each run. And the same for V_{R1} and V_{R2} . For each origin case, weaving shares are between 50/50 (50 for freeway exit and 50 for exit ramp) to 90/10 based on number of exit lanes for freeway exit and exit ramp.

Table 28 presents the range of flows for each of the entrances to the weaving area. Flow varies between 1,000 and 4,000 vph for the freeway entrance. First entrance ramp (R1) would get a flow of 500 to 2,000 vph for different runs and second entrance ramp flow also varies between 500 to 2,000 vph. A complete enumeration of the scenarios tested is shown in Table 29.

Table 28: Flow Range (vph)

	Freeway Entrance (V_{F1}) vph	First Entrance (V_{R1}) vph	Second Entrance (V_{R2}) vph
Flow Range	1,000	500	500
	2,000	1,000	1,000
	3,000	1,500	1,500
	4,000	2,000	2,000

Table 29: Flow Scenarios

Scenarios	Flow (vph)		
	V _{F1}	V _{R1}	V _{R2}
1	1,000	500	500
	1,000	500	1,000
	1,000	500	1,500
	1,000	500	2,000
10	1,000	500	500
	1,000	1,000	500
	1,000	1,500	500
11	1,000	2,000	500
	1,000	500	500
	1,000	1,000	1,000
	1,000	1,500	1,500
100	1,000	2,000	2,000
	1,000	500	500
	2,000	500	500
	3,000	500	500
101	4,000	500	500
	1,000	500	500
	2,000	500	1,000
	3,000	500	1,500
110	4,000	500	2,000
	1,000	500	500
	2,000	1,000	500
	3,000	1,500	500
111	4,000	2,000	500
	1,000	500	500
	2,000	1,000	1,000
	3,000	1,500	1,500
	4,000	2,000	2,000

COM PROGRAMMING

For the next steps, COM programming are involved. This VISSIM scripting tool enable the user to automate the analysis process.

This way performed more of simulation iterations. We consider all possible combination of variables to see which one will give us a higher throughput, which is the capacity.

A code in Visual Basic environment is developed in order to make changing variables more automatically and save a significant amount of time. More than 76,000 scenarios have been simulated, in order to compare capacity for multiple weave section under different conditions.

SIMULATION RUNS AND RESULTS

Simulation runs:

1. Investigate relationship between capacity and flow.
2. Compare densities obtained from the simulation with the values in the highway capacity manual (HCM).
3. Provide the data to create regression models which allow for the estimation of the capacity.
 - dependent variable is capacity.
 - potential independent variables include:
 - Flow on the freeway entering the weaving area
 - Flow on each of the three ramps
 - Heavy vehicle percentage for each entrance
 - Gore to gore distances
 - Weaving shares for all routes
 - Number of lanes per links

To determine the capacity of the weaving area, repeated simulations are performed under varying traffic flow rates, heavy vehicle percentages, gore to gore distances, weaving shares, and number of lanes on freeway and ramps. The ranges for the variables mentioned above are shown in Table 30.

- L_{S1} : Gore to gore distances for R1 to R2
- L_{S2} : Gore to gore distances for R2 to R3
- $VF1$: Flow for freeway entrance
- $VR1$: Flow for first entrance ramp
- $VR2$: Flow for second entrance ramp
- $HVF1$: Heavy vehicle percentage for freeway entrance
- $HVR1$: Heavy vehicle percentage for first entrance ramp
- $HVR2$: Heavy vehicle percentage for second entrance ramp
- $WSF1-F2$: Weaving share for drivers entering F1 and exiting at F2
- $WSR1-F2$: Weaving share for drivers entering R1 and exiting at F2
- $WSR2-F2$: Weaving share for drivers entering R2 and exiting at F2

- F1: Number of lanes for freeway entrance
- R1: Number of lanes for first entrance ramp
- R2: Number of lanes for second entrance ramp
- F2: Number of lanes for freeway exit
- R3: Number of lanes for third exit ramp

R1-R2 refers to the segment between R1 and R2 and R2-R3 refers to the segment between R2 and R3.

Weaving share for each route is the percentage of vehicle entering from at specific leg and exiting at the other specific leg. For example, WSF1-R3 is the percentages of vehicles entering from F1 leg (Freeway) and exiting at R3 (exit ramp).

Table 30: Range of Variable for Capacity Estimation

Gore to Gore Distance (ft)		Flow (vph)			Heavy Vehicle Percentage		
Ls1	Ls2	VF1	VR1	VR2	HVF1	HVR1	HVR2
1,000	1,500	1,000	500	500	5%	5%	5%
1,500	2,000	2,000	1,000	1,000	10%	10%	10%
		3,000	1,500	1,500			

Weaving Share					
WSF1_F2	WSF1_R3	WSR1_F2	WSR1_R3	WSR2_F2	WSR2_R3
70%	30%	70%	30%	70%	30%
90%	10%	90%	10%	90%	10%

Number of Lanes				
F1	R1	R2	F2	R3
2	1	1		1
3	2	2	to be calculated	2
4				

Capacity is assumed to be reached when the flows drop below the demand for the links as the demand increases. The demand for link R1-R2 is $(VF1+VR1)$, and the demand for link (R2-R3) is $(VF1+VR1+VR2)$.

VISSIM OUTPUTS

One of the VISSIM output is link evaluation. The results will be used for a capacity estimation model for the weaving area. The link evaluation feature in VISSIM allows the user to gather simulation results (link number, lane number, speed, density, volume, etc.) based on an active link in a user-defined time interval. The location of each link in the network is shown in Figure 30.



Figure 30: Multiple Weave Model Network in VISSIM

After a warm-up time of five minutes, required to fill the network with vehicles, the simulation was executed for a period of 900 seconds (15 minutes). The average output value from three runs corresponding to different random seed numbers is used for analysis. At this stage, VISSIM outputs include link evaluation (*.STR), which allow extracting all parameters, such as R-R flow, exit ramp flow, entrance ramp flow, freeway flow, density.

For all scenarios in order to convert the VISSIM Density in terms of vph to pcph, following equations have been applied. vph numbers are divided to f_{HV} to calculate pcph.

$$f_{HV} = \frac{1}{1 + P_{HV} (ET - 1)}$$

- ET=2 for Terrain = level

$$P_{HV} = \frac{(VF1 \times HVF1) + (VR1 \times HVR1) + (VR2 \times HVR2)}{(VF1 + VR1 + VR2)}$$

MODELING CAPACITY

Error! Reference source not found. shows the 44 scenarios used in the development of the capacity estimations. Scenarios are selected based on the more common multiple weaving area designs. Lane geometries for 11 possible geometries are presented in Appendix A and flow and density charts for scenarios 2 to 44 are presented in Appendix B.

Table 31: Possible Scenarios

Scenarios	L _{S1} (ft)	L _{S2} (ft)	Freeway Entrance (Lanes)	First Entrance (Lanes)	First Gore to Gore (Lanes)	Second Entrance (Lanes)	Second Gore to Gore (Lanes)	Exit (Lanes)	Freeway Exit (Lanes)
			F1	R1	R1-R2	R2	R2-R3	R3	F2
S1	1,000	1,500	2	1	3	1	4	2	2
S2	1,000	1,500	3	1	4	1	5	2	3

Scenarios	L _{S1} (ft)	L _{S2} (ft)	Freeway Entrance (Lanes)	First Entrance (Lanes)	First Gore to Gore (Lanes)	Second Entrance (Lanes)	Second Gore to Gore (Lanes)	Exit (Lanes)	Freeway Exit (Lanes)
			F1	R1	R1-R2	R2	R2-R3	R3	F2
S3	1,000	1,500	4	1	5	1	6	2	4
S4	1,000	1,500	2	1	2	1	3	1	2
S5	1,000	1,500	2	2	4	1	4	2	2
S6	1,000	1,500	3	1	3	1	3	1	3
S7	1,000	1,500	3	2	5	1	5	2	3
S8	1,000	1,500	4	2	6	1	6	2	4
S9	1,000	1,500	2	1	2	2	4	2	2
S10	1,000	1,500	3	1	3	2	5	2	3
S11	1,000	1,500	4	1	4	2	6	2	4
S12	1,000	2,000	2	1	3	1	4	2	2
S13	1,000	2,000	3	1	4	1	5	2	3
S14	1,000	2,000	4	1	5	1	6	2	4
S15	1,000	2,000	2	1	2	1	3	1	2
S16	1,000	2,000	2	2	4	1	4	2	2
S17	1,000	2,000	3	1	3	1	3	1	3
S18	1,000	2,000	3	2	5	1	5	2	3
S19	1,000	2,000	4	2	6	1	6	2	4
S20	1,000	2,000	2	1	2	2	4	2	2
S21	1,000	2,000	3	1	3	2	5	2	3
S22	1,000	2,000	4	1	4	2	6	2	4
S23	1,500	1,500	2	1	3	1	4	2	2
S24	1,500	1,500	3	1	4	1	5	2	3
S25	1,500	1,500	4	1	5	1	6	2	4
S26	1,500	1,500	2	1	2	1	3	1	2
S27	1,500	1,500	2	2	4	1	4	2	2
S28	1,500	1,500	3	1	3	1	3	1	3
S29	1,500	1,500	3	2	5	1	5	2	3

Scenarios	L _{S1} (ft)	L _{S2} (ft)	Freeway Entrance (Lanes)	First Entrance (Lanes)	First Gore to Gore (Lanes)	Second Entrance (Lanes)	Second Gore to Gore (Lanes)	Exit (Lanes)	Freeway Exit (Lanes)
			F1	R1	R1-R2	R2	R2-R3	R3	F2
S30	1,500	1,500	4	2	6	1	6	2	4
S31	1,500	1,500	2	1	2	2	4	2	2
S32	1,500	1,500	3	1	3	2	5	2	3
S33	1,500	1,500	4	1	4	2	6	2	4
S34	1,500	2,000	2	1	3	1	4	2	2
S35	1,500	2,000	3	1	4	1	5	2	3
S36	1,500	2,000	4	1	5	1	6	2	4
S37	1,500	2,000	2	1	2	1	3	1	2
S38	1,500	2,000	2	2	4	1	4	2	2
S39	1,500	2,000	3	1	3	1	3	1	3
S40	1,500	2,000	3	2	5	1	5	2	3
S41	1,500	2,000	4	2	6	1	6	2	4
S42	1,500	2,000	2	1	2	2	4	2	2
S43	1,500	2,000	3	1	3	2	5	2	3
S44	1,500	2,000	4	1	4	2	6	2	4

SCENARIO 1 (S1)

Capacity Estimation Using Link Flows

The geometric condition (number of lanes and distance between gores) in Scenario 1 is as shown in Table 32 (which is excerpted from Table 31). Capacity is checked on links R1-R2 and R2-R3, the freeway links between the ramps. Here, the demands are the volumes that were specified in the VISSIM input, while the flows are the volumes that are able to pass the end of the subject link. Capacity is assumed to be reached when the flows drop below the demand for the links as the demand increases. Estimating capacity using density is covered in the next section.

Table 32: Number of Lanes and Gore to Gore Distance for S1

Scenario	Gore to Gore Distances (ft)		Number of Lanes						
	L _{S1}	L _{S2}	F1	R1	R1-R2	R2	R2-R3	R3	F2
S1	1,000	1,500	2	1	3	1	4	2	2

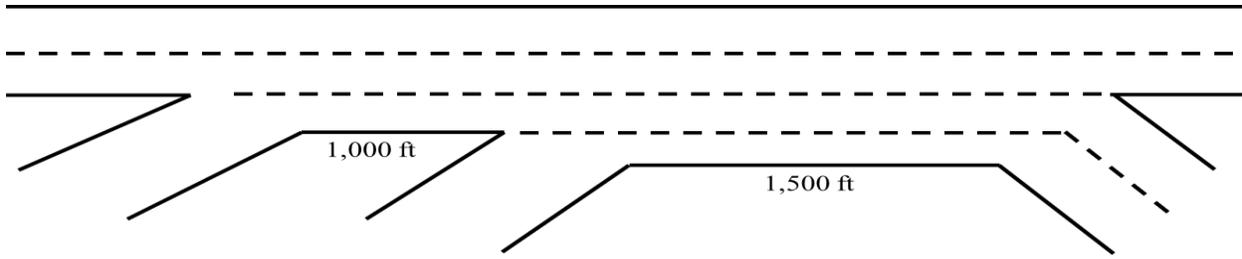


Figure 31: Scenario 1 Lane Geometry

Capacity Conditions for R1-R2

The demand for link R1-R2 is $(VF1+VR1)$, and the demand for link (R2-R3) is $(VF1+VR1+VR2)$. In this section, VF1 ranges between 1,000 and 3,000 vph, and VR1 and VR2 range from 500 to 1,500 vph (each). Given the lane geometry specified above, the freeway entry link and the two entry ramps stay below their capacities. In Figure 32, VF1 is only allowed to go up to 2,000 vph. The Figures were created through the pivot point analysis available in Excel.

The y-axis in Figure 32 is the sum $VF1+VR1$; so, for a volume of 1,500 vph, this is a VF1 of 1,000 vph and a VR1 of 500 vph. The highest volume is demand of 3,000 vph and is the condition of VF1 of 2,000 vph and VR1 of 1,000 vph.

For each volume level on the y-axis, there are 16 points, representing each run with the values for the heavy vehicle percentage for F1 (HVF1), the heavy vehicle percentage for R1 (HVR1), the weaving shares for F1 (WSF1_F2), and the weaving shares for R1 (WSR1_F2). The weaving shares are 70% or 90% of F1 traffic leaves the network at F2; similarly, for R1. Given that there are 2 options in each of these variables, there are 24 or 16 combinations of these variables for each value of the sum of VR1 and VF1.

- 1- HVF1=0.05, HVR1=0.05, WSF1_F2=0.7, WSR1_F2=0.7
- 2- HVF1=0.05, HVR1=0.05, WSF1_F2=0.7, WSR1_F2=0.9
- 3- HVF1=0.05, HVR1=0.05, WSF1_F2=0.9, WSR1_F2=0.7
- 4- HVF1=0.05, HVR1=0.05, WSF1_F2=0.9, WSR1_F2=0.9
- 5- HVF1=0.10, HVR1=0.05, WSF1_F2=0.7, WSR1_F2=0.7
- 6- HVF1=0.10, HVR1=0.05, WSF1_F2=0.7, WSR1_F2=0.9
- 7- HVF1=0.10, HVR1=0.05, WSF1_F2=0.9, WSR1_F2=0.7
- 8- HVF1=0.10, HVR1=0.05, WSF1_F2=0.9, WSR1_F2=0.9
- 9- HVF1=0.05, HVR1=0.10, WSF1_F2=0.7, WSR1_F2=0.7
- 10- HVF1=0.05, HVR1=0.10, WSF1_F2=0.7, WSR1_F2=0.9
- 11- HVF1=0.05, HVR1=0.10, WSF1_F2=0.9, WSR1_F2=0.7
- 12- HVF1=0.05, HVR1=0.10, WSF1_F2=0.9, WSR1_F2=0.9
- 13- HVF1=0.10, HVR1=0.10, WSF1_F2=0.7, WSR1_F2=0.7
- 14- HVF1=0.10, HVR1=0.10, WSF1_F2=0.7, WSR1_F2=0.9
- 15- HVF1=0.10, HVR1=0.10, WSF1_F2=0.9, WSR1_F2=0.7
- 16- HVF1=0.10, HVR1=0.10, WSF1_F2=0.9, WSR1_F2=0.9

Using the Excel format, the values of these variables are shown in the line of boxes above the graph. The values that were used in the runs are highlighted in blue boxes. The demands are shown in orange and the flows are shown in blue.

As shown in Figure 32, capacity was not reached for any of the combinations of VR1+VF1.

The higher demands for VF1 (3,000 vph) and VR1 (1,500 vph) are added in in **Error! Reference s source not found..** There are still 16 points shown for each volume level, except 2,500 vph and 3,500 vph. In these two cases there are two combinations of (VF1+VR1) that yield these to demands (1,000 vph+1,500 vph and 2,000 vph+500 vph; and 2,000 vph +1,500 vph and 3,000 vph +500 vph) and there are 32 points. By and large, the orange and blue points coincide, meaning that the demands are still below capacity. However, for the combined demand of 3,500 vph, the flow is slightly less than the demand for half the points, which represent the demand case of VR1 being 1,500 vph. A similar condition is observed for the combined demand of 4,000 vph, in this case VF1 is 3,000 vph. In both, the demand is approaching link capacity.

The interesting point is when the combined demand is 4,500 vph (VF1 is 3,000 vph and VR1 is 1,500 vph). The flows are below the demands in all these cases, but the weaving shares have a much greater impact than the truck percentages. The case of VF1 is 3,000 vph and VR1 is 1,500 vph is highlighted in Figure 34. The four cases with the largest difference between demand and flow are when the weaving share is 90% for both streams (90% of traffic from each entry leaves the network via F2), for both heavy vehicle values. The next two largest differences between demand and flow are the case where the weaving share for R1 traffic is 70% of traffic from R1 leaves the network via F2, while 90% of traffic entering by F1 leave at F2.

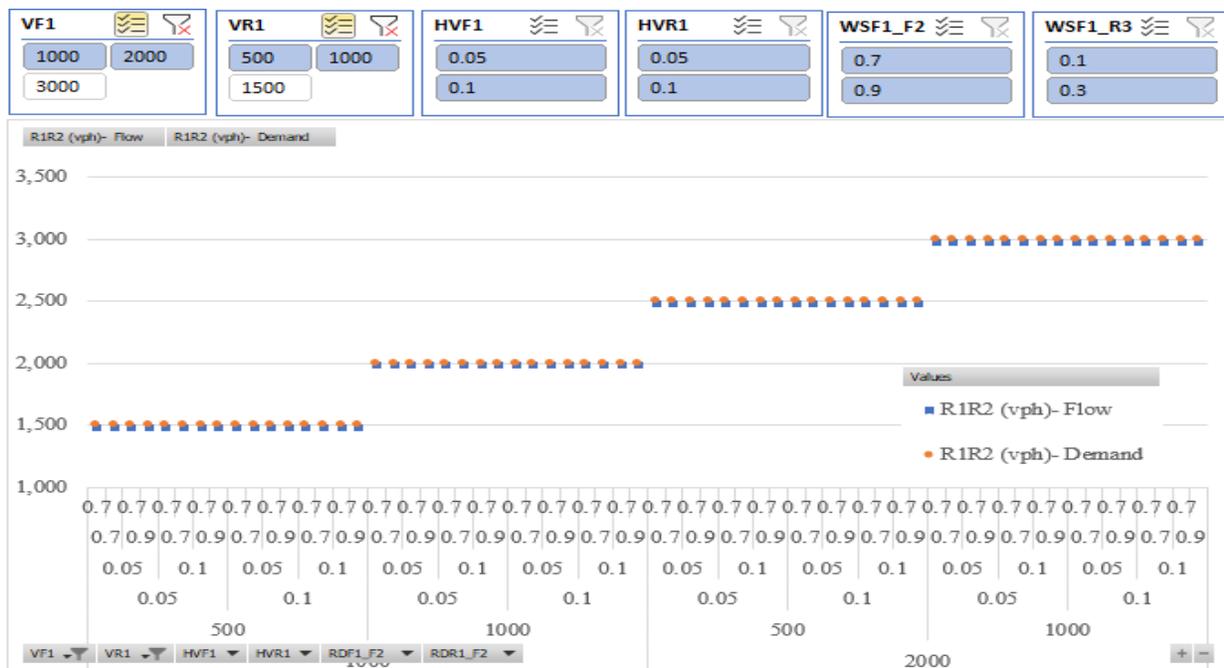


Figure 32: Demand vs. Flow for R1-R2 Segment, Excluding VR1=3,000 & 1,500 vph

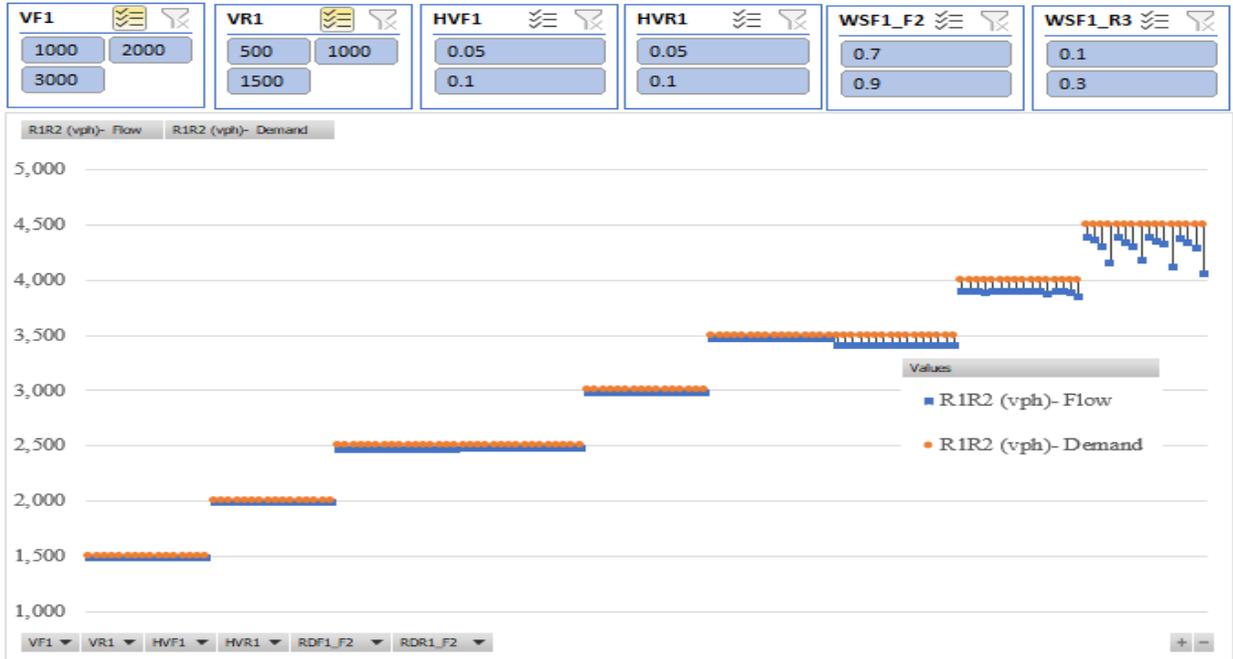


Figure 33: Demand vs. Flow for R1-R2 Segment, All Possible Variable Combinations

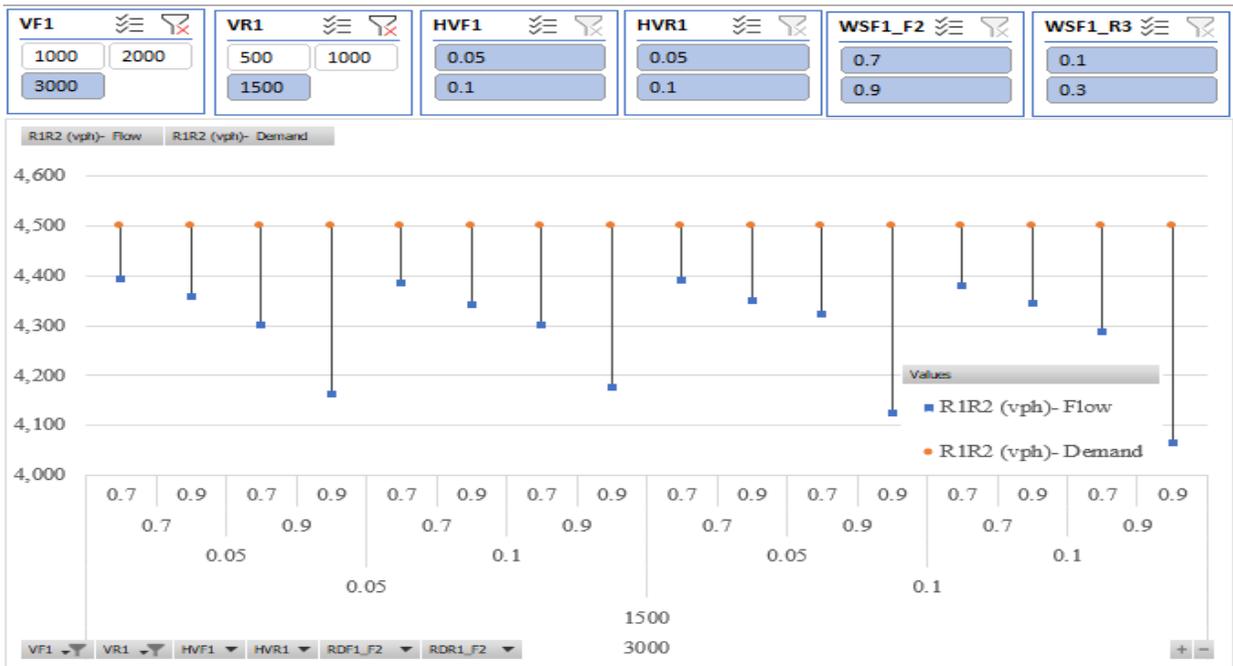


Figure 34: Demand vs. Flow for R1-R2 Segment, VF1=3,000 vph and VR1=1,500 vph

Capacity Conditions for link R2-R3

The input volumes to this link come from link R1-R2 and R2 (second entrance ramp). The range of simulation output is shown in Figure 35. The output is neatly ranked in groups of 3. The first group of 3 lines is for VR1-R2 of 1,500 vph and VR2 ranging from 500 vph to 1,000 vph to 1,500

vph. The second group is for VR1-R2 of 2,000 vph and the same range of VR2. Each short line segment has 64 points (26, as there are 6 variables with 2 possible values each).

Of course, VR1-R2 can have a value of 2,000 vph two different ways (1,000 vph/1,000 vph and 1,500 vph/500 vph), and there are two short segments at VR1-R2 of 2,000 vph and VR2 of 500 vph, each representing 64 points, for a total of 128 points. The line segments where there is a small difference between the demand and the flow (and the blue points peek out from the orange points). These points are the cases where one (or more) of the entry flows are close to capacity for that link (3,000 vph for the two-lane freeway entry (F1) and 1,500 vph for one of the two entry ramps (R1 and R2)).

From Figure 35, one can see three conditions where demand exceeds capacity; VR1-R2 is 4,000 vph and VR2 is 1,500 vph (Figure 36), VR1-R2 is 4,500 vph and VR2 is 1,000 vph (Figure 37), and VR1-R2 is 4,500 vph and VR2 is 1,500 vph (Figure 39). In Figure 38, the most severe reduction in capacity is when 90% of the vehicles entering at R2 that leave the network at F2 is 90%. These maximums occur for 90% vehicles leaving at F2 from both F1 and R1.

In Figure 37, there is a similar pattern in that the cases with the largest difference between the demands and flows are those where 90% the traffic that enters by any of the three entry points must leave the network at F2. However, the cases where R1 is only 70% and where R1 and R2 are both 70% are also similarly large.

In Figure 39, the volume case with the highest flows, the cases where 90% percent of all traffic must leave the network at F2, regardless of their network entry location, are still the situation that experience the largest reduction in capacity. However, many of the other combinations (including fraction of heavy vehicles) also produce sizeable reductions in capacity.

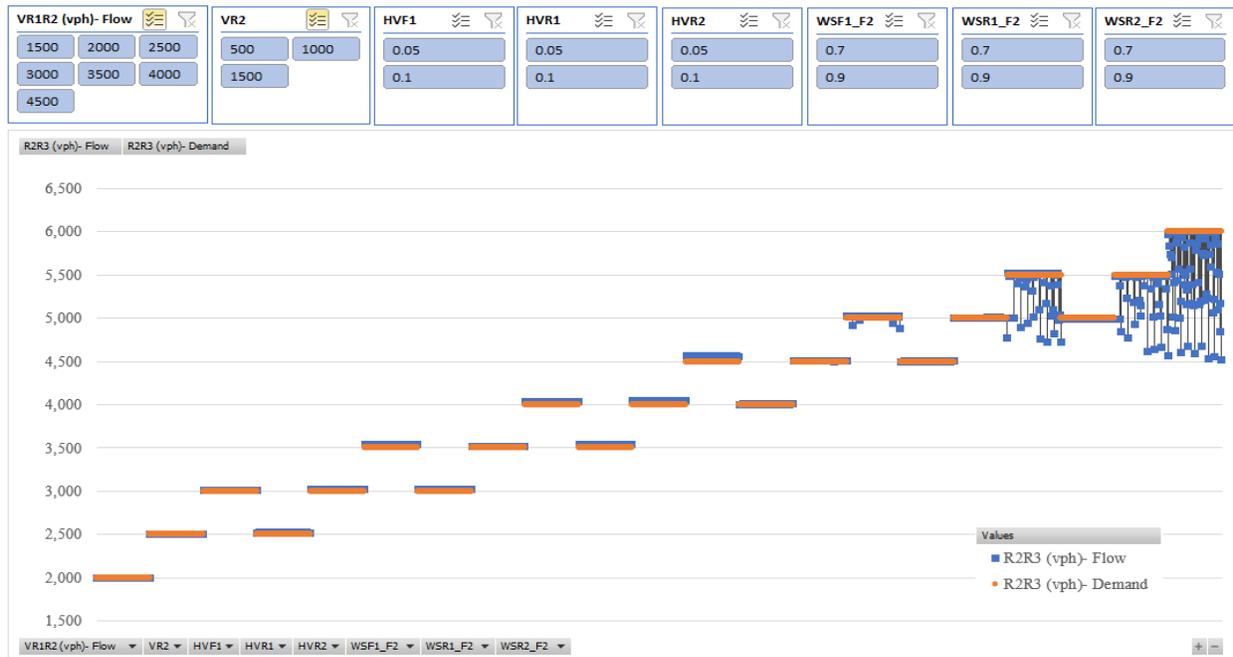


Figure 35: Demand vs. Flow for R2-R3 Segment, All Possible Variable Combinations

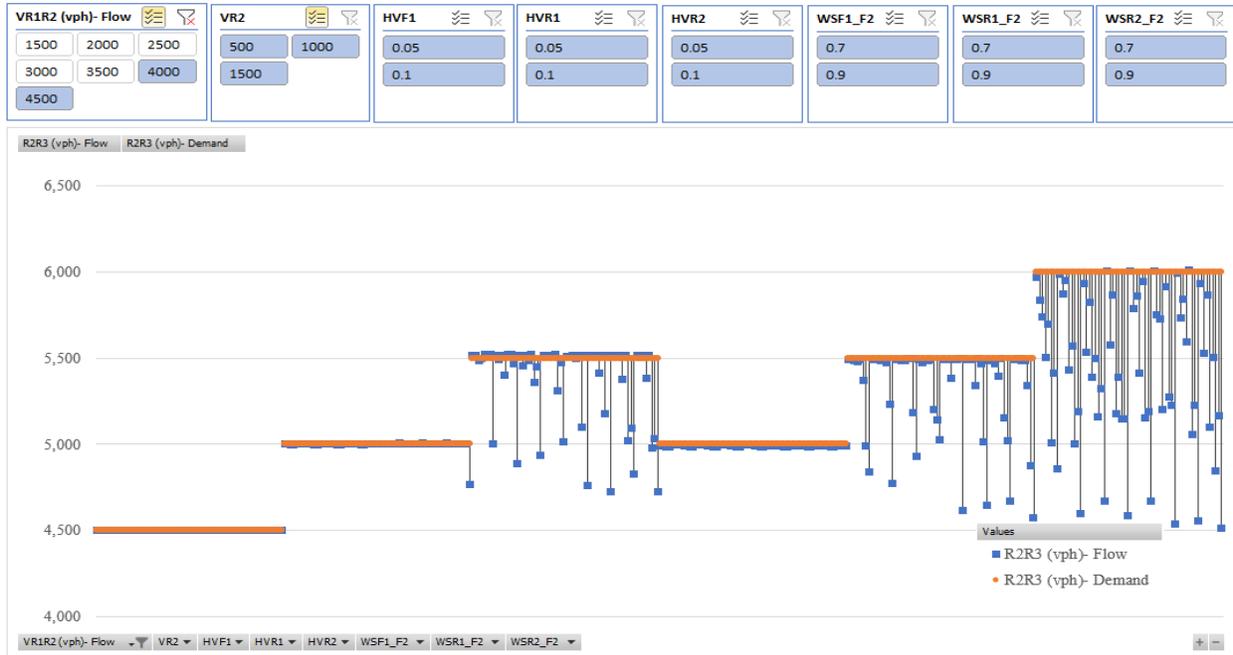


Figure 36: Demand vs. Flow for R2-R3 Segment, VR1-R2= 4,000/4,500 vph

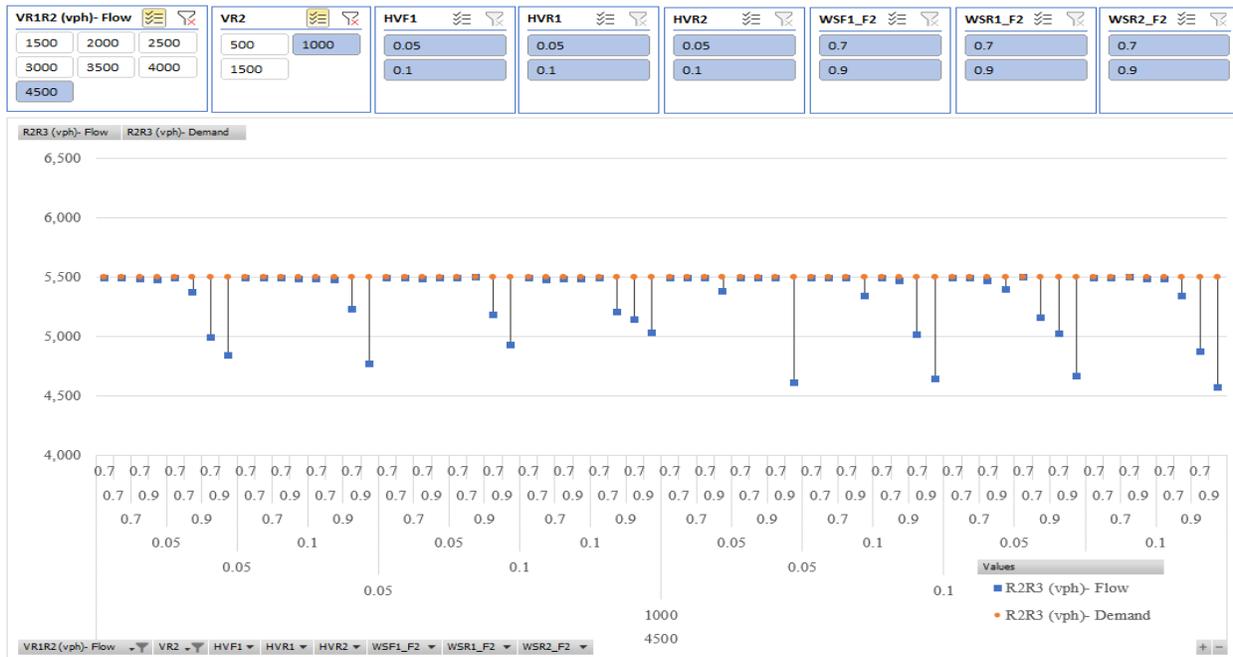


Figure 37: Demand vs. Flow for R2-R3 Segment, VR1-R2= 4,500 vph and VR2= 1,000 vph

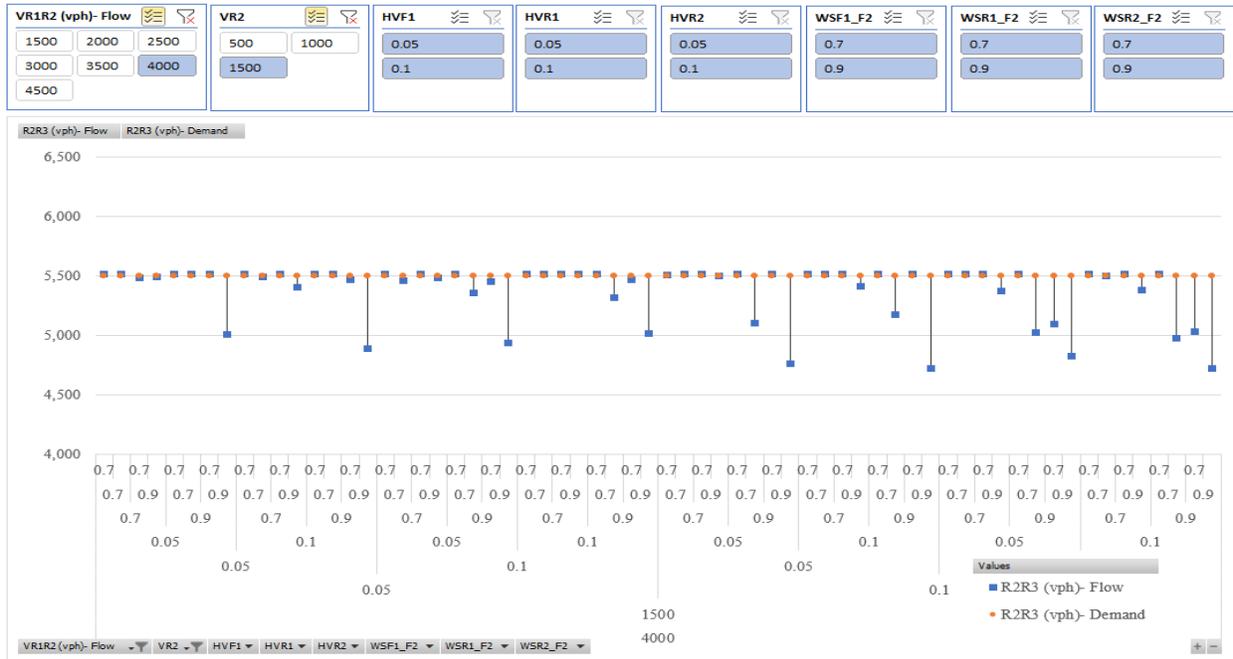


Figure 38: Demand vs. Flow for R2-R3 Segment, VR1-R2= 4,000 vph and VR2=1,500 vph

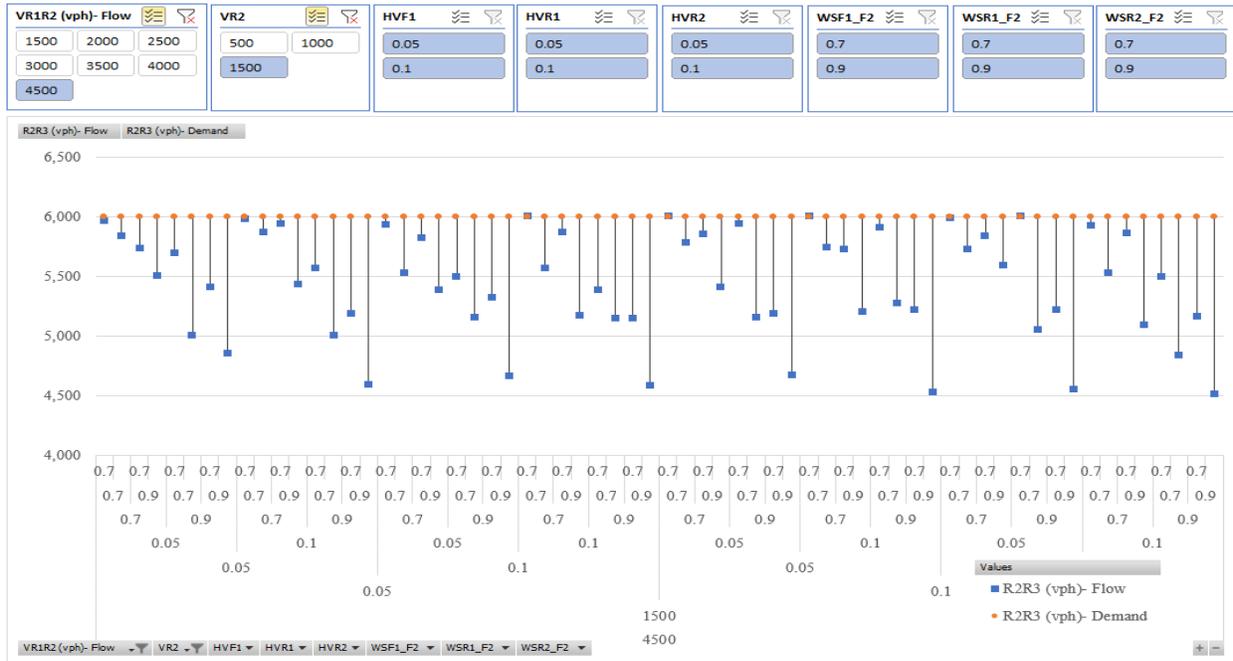


Figure 39: Demand vs. Flow for R2-R3 Segment, VR1-R2= 4,500 vph and VR2=1,500 vph

Capacity by Density

Density is used to define capacity in the HCM 2016. In this section we compare the density from the VISSIM runs to the density that defines capacity. The density at capacity is 43 pcphpl. VISSIM calculates density by averaging the number of vehicles on a link during the simulation time (in our case, over 15 minutes, ignoring the 5-minute warm-up time). VISSIM reports this information as the average number of vehicles on the link, we then calculate the density by dividing the number reported by VISSIM by the length of the link and dividing by the number of lanes on the link, resulting in the density in vpmppl. This is further corrected for the percentage trucks by multiplying the density (in vpmppl) by the f_{HV} factor, adjusted for the percentage of trucks in the traffic stream resulting in density in pcphpl.

Density values for links R1-R2 and R2-R3 are shown in Figure 40, the density at capacity (43 pcphpl) is the grey horizontal line across the Figure. Densities for link R1-R2 are shown as blue dots, and orange dots are used for link R2-R3. The only conditions which result in capacity are towards the right in the Figure. The volume combinations omitting 1,000 vph for VF1, and 500 vph for VR1 and VR2 are shown in Figure 41.

The bulk of the capacity runs are those with 2,000 or 3,000 vph from VF1, and 1,000 and 1,500 vph from the two entrance ramps. Virtually all the capacity runs occurred when 90% of the vehicles entering from the freeway or from one of the ramps. Similarly, capacity conditions occur when the 10% of the entering flows are heavy vehicles. Both conditions are expected, since the truck percentages increase the flows (converting vph to pcphpl) and the higher percentage of traffic leaving the network at F2 induces more weaving from the entrance ramp traffic, since that traffic must weave to the left.

Density is used to define levels of service in the weaving chapter of the Highway Capacity Manual (HCM). The objective of this section is to present the density associated with the simulation runs summarized above and to compare these values with the values in the HCM.

We see more significant gap between HCM recommended density and our model density by moving toward the right side on Figures 40 and 41 where the flows increase. At the time that VF1 exceeds 2,000 vph and each of the entrance ramp flows exceed 1,000 vph, more orange and blue dots (model density at R1-R2 and R2-R3 segment) will be noticed above 43 pcphpl.

Illustrating in Figure 40 and 41, density neither for R1-R2 nor for R2-R3 segments exceed the 43 pcphpl (HCM density cap) if:

- a) F1 flow is less than 3,000 vph or 1,500 vphpl.
- b) R1 and R2 flows are less than 1,500 vph.
- c) Weaving share for one of the routes heading to F2 is less than 0.9.

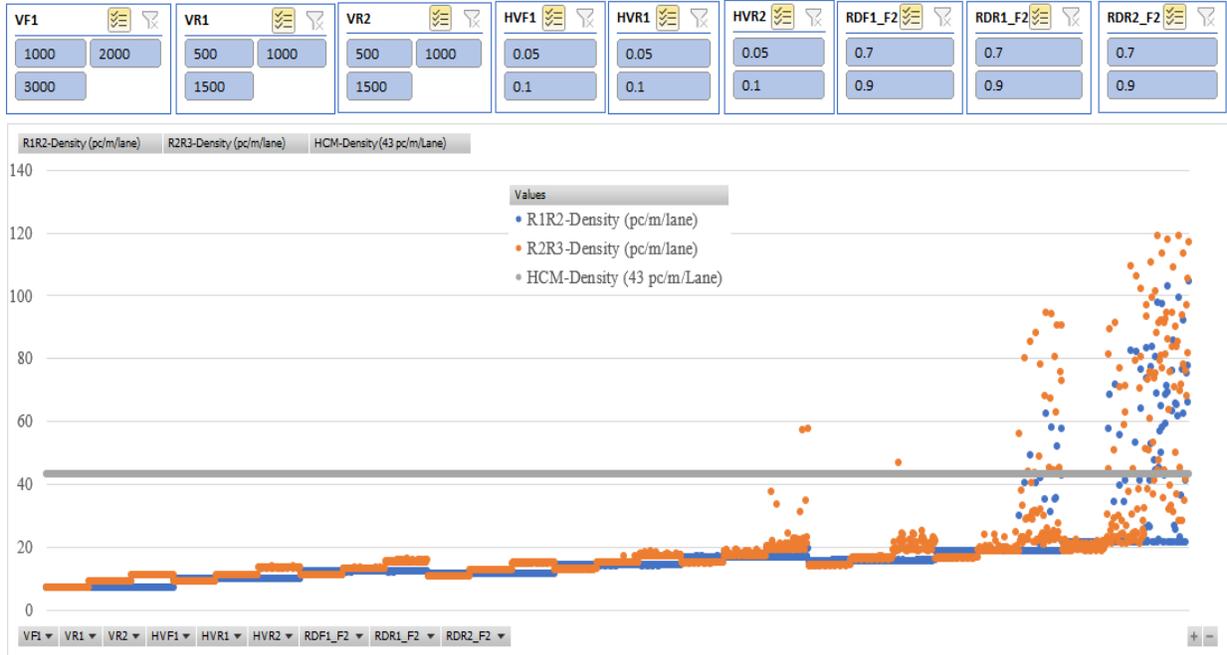


Figure 40: Density Presentation

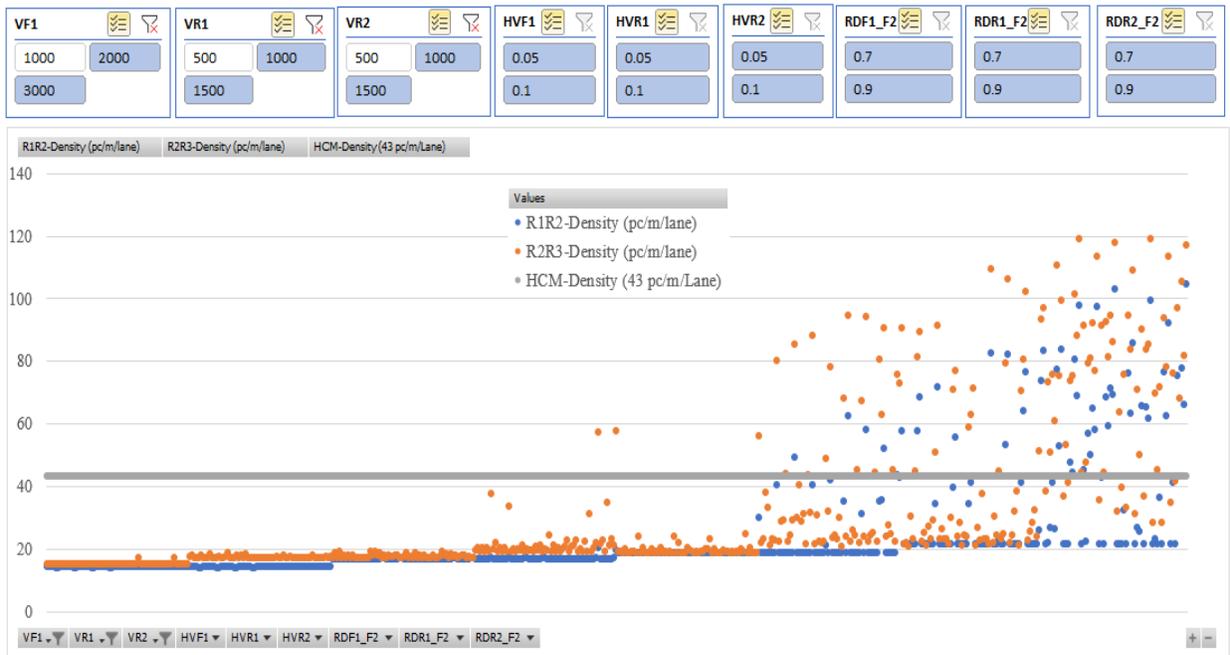


Figure 41: Density Presentation (Saturated)

Regression Analysis

A stepwise regression model is developed. Density is the dependent variable in the developed model and the independent variables are flow for each entrance leg, weaving share for each route, and heavy vehicle percentages for each entry legs.

Stepwise regression first selects the independent variable that has the highest correlation with the dependent variable, then checks the significance of the model. This process is followed for each independent variable. At each step, an additional variable is considered, if it fails to improve the model by a preset level, the variable is not added to the model. Also, at each step, variables in the model are checked to see if they still provide a significant improvement to the model. A once important variable may be dropped if other variables are correlated with the dropped variable but, in combination, improve the model to a greater extent. Once each independent variable is tested, the procedure stops. The confidence interval for the regression analysis was 95%, and there are 1,728 data points.

R1-R2 Analysis

Applying stepwise regression, using simulated results, VF1 has the most significant effect on density. Higher density will result congestion.

Coefficient table (**Error! Reference source not found.**) shows that flow for mainline entry to the network has the most significant impact on R1-R2 density followed by the R1 and R2 flows. As we expected weaving shares to F3 destination have the lowest impact.

$$\text{Capacity (based on density)} = (0.525 \times VF1) + (0.367 \times VR1) + (0.142 \times VR2) + (0.116 \times WSF1_F2) + (0.077 \times WSR1_F2) + (0.075 \times WSR2_F2)$$

R² is increasing across models as well as Adjusted R². Standard Error Estimate is decreasing as the percentage of variances accounted for dependent variable is increasing. We see that R and R² values are statistically significant in model 6 (selected model) as well as Adjusted R² which is a more accurate estimate.

R2 value for this model is 0.455 which means that 45% of the variation in weaving area density can be explained by this model. Moreover, the value of standard error of the estimate in Table 33(positive square root of variance of the errors), which typically measures the difference between predicted density with the “true” density, is relatively small. The model is more reliable as the standard error decreases.

Table 33: Model Summary, R1-R2 Segment

Model	R	R ²	Adj R ²	Std. Error
1 (a. Predictors: (Constant), VF1)	0.525 ^a	0.275	0.275	27.534
2 (b. Predictors: (Constant), VF1, VR1)	0.640 ^b	0.410	0.409	24.853
3 (c. Predictors: (Constant), VF1, VR1, VR2)	0.656 ^c	0.430	0.429	24.431
4 (d. Predictors: (Constant), VF1, VR1, VR2, WSF1_F2)	0.666 ^d	0.443	0.442	24.150
5 (e. Predictors: (Constant), VF1, VR1, VR2, WSF1_F2, WSR1_F2)	0.670 ^e	0.449	0.448	24.028
6 (f. Predictors: (Constant), VF1, VR1, VR2, WSF1_F2, WSR1_F2, WSR2_F2)	0.675 ^f	0.455	0.453	23.912

R2-R3 Analysis

For the R2-R3 segment, VF1, VR2, VR1, WSR2_F2, WSF1_F2, WSR1_F2 have the most significant impact on capacity.

$$\text{Capacity (based on density)} = (0.460 \times VF1) + (0.321 \times VR2) + (0.320 \times VR1) + (0.103 \times WSR2_F2) + (0.099 \times WSF1_F2) + (0.069 \times WSR1_F2)$$

Scenario 1 Conclusion

The feasible range of variable combinations was used as input in order to determine the capacity for various scenarios. A capacity density model for a multiple weaving area was developed as a function of freeway, and two entrance ramp flows, heavy vehicle percentages, and weaving shares. The following conclusions were drawn for scenario 1:

- When there are only two freeway lanes entering the multiple weaving area, the freeway entrance (F1) flow should always be less than 3,000 vph, even when the entering ramp flows are small, to prevent congestion on the immediate downstream segment.
- R1 and R2 ramps capacity are each less than 1,500 vph if F1 demand exceeds 2,000 vph.
- Entrance legs should have the heavy vehicle percentage of less than 10% to prevent congestion on the immediate downstream segment.
- If the weaving share for any one of the three routes heading to F2 is 90% or higher, there is congestion on the R2-R3 link.

SCENARIO 2 through 44

Order of scenarios in this section is based on which scenario reaches its capacity sooner (with lower number of iterations).

For scenario 4, when there are only two freeway lanes entering the multiple weaving area, to prevent congestion, the freeway entrance flow (VF1) should always be less than 3,000 vph, and at least one of the ramp flows (VR1 or VR2) should stay less than 1,000 vph.

In addition, for all legs, keeping the heavy vehicle percentage less than 10%, and weaving shares exiting at F2, less than 90%, allows network to obtain up to 3,000 vph for VF1, and up to 1,500 vph for R1 and R2.

Table 34: Number of Lanes and Gore to Gore Distance for S4

Scenario	Gore to Gore Distances (ft)		Number of Lanes						
	LS1	LS2	F1	R1	R1-R2	R2	R2-R3	R3	F2
S4	1,000	1,500	2	1	2	1	3	1	2

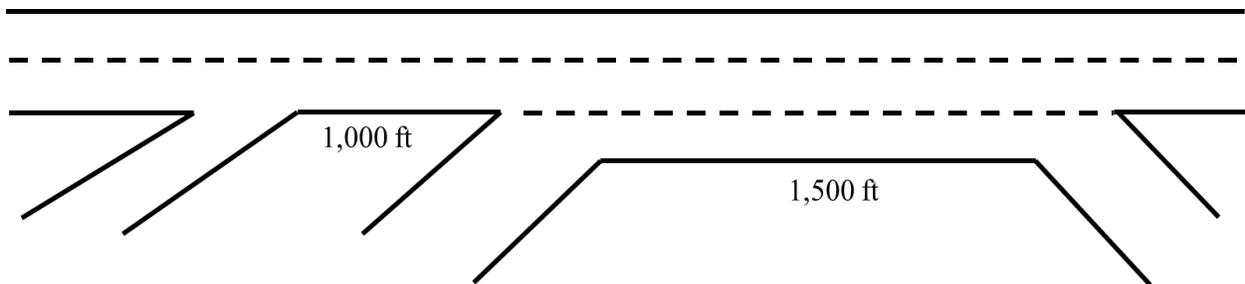


Figure 42: Scenario 4 Lane Geometry

R1-R2 segment regression formulation:

$$\begin{aligned} \text{Capacity (based on density)} &= (1.271 \times VF1) + (0.274 \times VR1) + (0.117 \times VR2) - (0.033 \times HVF1) \\ &- (0.080 \times HVR1) - (0.053 \times HVR2) - (0.099 \times WSF1_F2) - (0.254 \times WSR1_F2) - (0.129 \times WSR2_F2) \\ R^2 &= 94.8\% \end{aligned}$$

R2-R3 segment regression formulation:

$$\begin{aligned} \text{Capacity (based on density)} &= (0.752 \times VF1) - (0.113 \times VR1) + (0.873 \times VR2) - (0.115 \times HVF1) \\ &- (0.069 \times HVR1) - (0.042 \times HVR2) - (0.100 \times WSF1_F2) - (0.312 \times WSR1_F2) - (0.052 \times WSR2_F2) \\ R^2 &= 88.5\% \end{aligned}$$

For scenario 5, R1-R2 segment reaches its capacity if either VF1 reaches 3,000 vph or both VR1 and VR2 reach 1,500 vph. Also, if simultaneously, HVF1 is 10% and WSF1_F2 is 90%.

R2-R3 touches capacity point if either of the following conditions happen:

- VF1 reaches 3,000 vph.
- VR1 and VR2 hit 1,500 vph.
- F1 weaving share exiting at F2 hit 90%, and heavy vehicle percentage for R1 and R2 is 10%.

Table 35: Number of Lanes and Gore to Gore Distance for S5

Scenario	Gore to Gore Distances (ft)		Number of Lanes						
	LS1	LS2	F1	R1	R1-R2	R2	R2-R3	R3	F2
S5	1,000	1,500	4	1	5	1	6	2	4

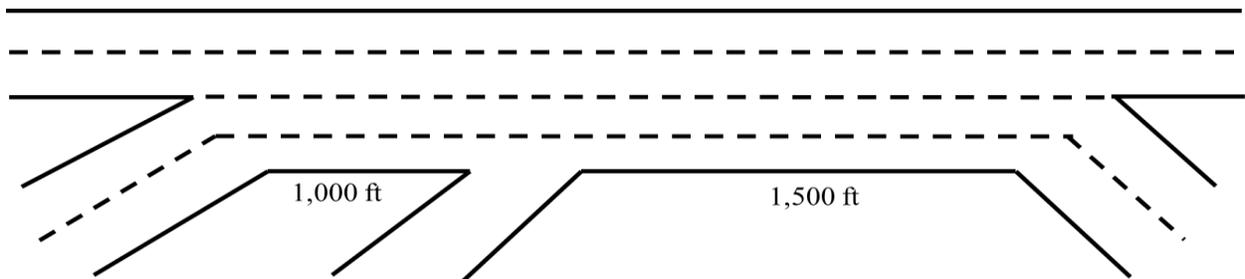


Figure 43: Scenario 5 Lane Geometry

R1-R2 segment regression formulation:

$$\begin{aligned} \text{Capacity (based on density)} &= (1.145 \times VF1) + (0.320 \times VR1) + (0.310 \times VR2) - (0.137 \times HVF1) \\ &- (0.150 \times HVR1) - (0.064 \times HVR2) + (0.431 \times WSF1_F2) - (0.700 \times WSR1_F2) \\ &- (0.374 \times WSR2_F2) \\ R^2 &= 66.7\% \end{aligned}$$

R2-R3 segment regression formulation:

$$\begin{aligned} \text{Capacity (based on density)} &= (1.252 \times VF1) + (0.238 \times VR1) + (0.573 \times VR2) - (0.128 \times HVF1) \\ &- (0.170 \times HVR1) - (0.099 \times HVR2) + (0.216 \times WSF1_F2) - (0.689 \times WSR1_F2) \\ &- (0.380 \times WSR2_F2) \\ R^2 &= 73.2\% \end{aligned}$$

Scenario 9 faces congestion (reaches capacity) on both R1-R2 segment and R2-R3 segment if VF1 passes 3,000 vph or either VR1 or VR2 passes 1,500 vph.

Table 36: Number of Lanes and Gore to Gore Distance for S9

Scenario	Gore to Gore Distances (ft)		Number of Lanes						
	LS1	LS2	F1	R1	R1-R2	R2	R2-R3	R3	F2
S9	1,000	1,500	2	1	2	2	4	2	2

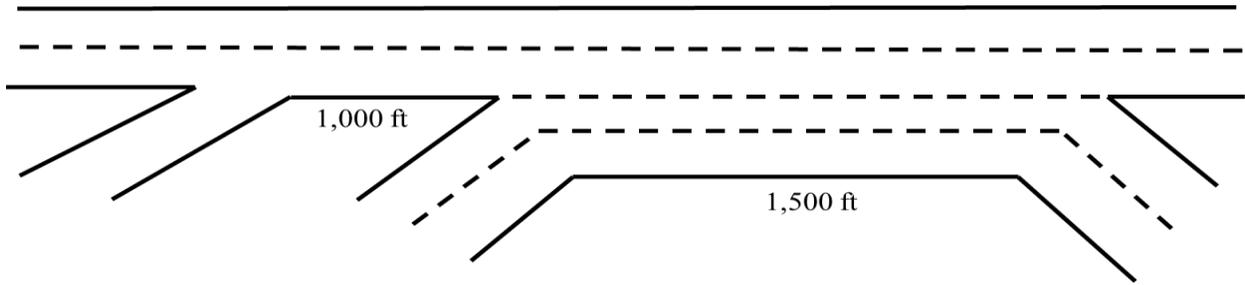


Figure 44: Scenario 9 Lane Geometry

R1-R2 segment regression formulation:

$$\text{Capacity (based on density)} = (1.247 \times VF1) + (0.111 \times VR1) + (0.283 \times VR2) - (0.072 \times HVF1) - (0.062 \times HVR1) - (0.023 \times HVR2) - (0.171 \times WSF1_F2) - (0.348 \times WSR1_F2) - (0.029 \times WSR2_F2)$$

$$R^2 = 90.6\%$$

R2-R3 segment regression formulation:

$$\text{Capacity (based on density)} = (0.777 \times VF1) - (0.226 \times VR1) + (0.651 \times VR2) - (0.091 \times HVF1) - (0.106 \times HVR1) - (0.073 \times HVR2) + (0.740 \times WSF1_F2) - (0.557 \times WSR1_F2) - (0.253 \times WSR2_F2)$$

$$R^2 = 78.3\%$$

For scenario 12, no congestion is observed if VF1 is less than 3,000 vph or either of the ramps (R1 or R2) obtain demand of less than 1,500 vph. The other situation which will prevent congestion (even with VF1 of 3,000 vph and VRs of 1,500 vph) is when weaving shares for all entrances exiting at F2 is less than 90%.

Table 40: Number of Lanes and Gore to Gore Distance for S12

Scenario	Gore to Gore Distances (ft)		Number of Lanes						
	LS1	LS2	F1	R1	R1-R2	R2	R2-R3	R3	F2
S12	1,000	2,000	2	1	3	1	4	2	2

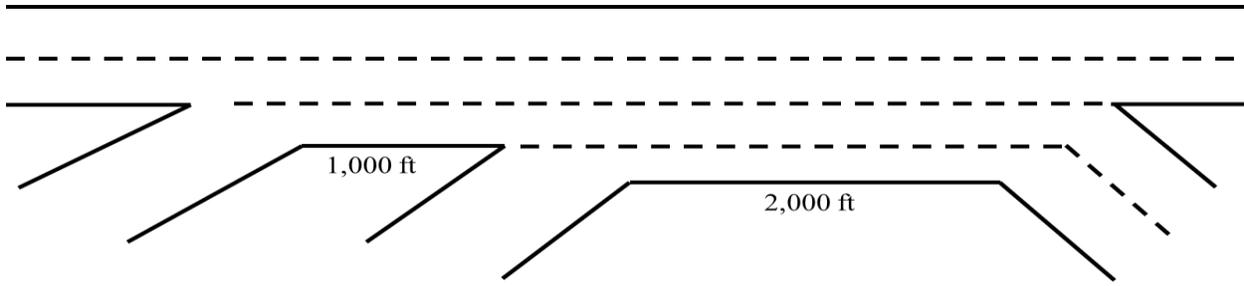


Figure 45: Scenario 12 Lane Geometry

R1-R2 segment regression formulation:

$$\begin{aligned} \text{Capacity (based on density)} = & (0.946 \times VF1) + (0.091 \times VR1) + (0.309 \times VR2) - (0.058 \times HVF1) \\ & - (0.154 \times HVR1) - (0.070 \times HVR2) + (0.332 \times WSF1_F2) - (0.339 \times WSR1_F2) \\ & - (0.211 \times WSR2_F2) \end{aligned}$$

$$R^2 = 74.4\%$$

R2-R3 segment regression formulation:

$$\begin{aligned} \text{Capacity (based on density)} = & (1.054 \times VF1) - (0.007 \times VR1) + (0.657 \times VR2) - (0.065 \times HVF1) \\ & - (0.173 \times HVR1) - (0.093 \times HVR2) + (0.236 \times WSF1_F2) - (0.478 \times WSR1_F2) \\ & - (0.324 \times WSR2_F2) \end{aligned}$$

$$R^2 = 70.4\%$$

Scenario number 15 network experiences congestion only if VF1 increases up to 3,000 vph.

Table 37: Number of Lanes and Gore to Gore Distance for S15

Scenario	Gore to Gore Distances (ft)		Number of Lanes						
	L _{S1}	L _{S2}	F1	R1	R1-R2	R2	R2-R3	R3	F2
S15	1,000	2,000	2	1	2	1	3	1	2

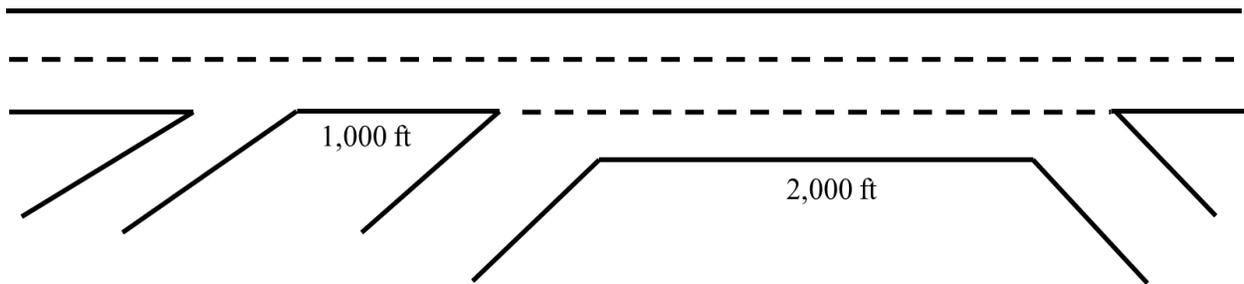


Figure 46: Scenario 15 Lane Geometry

R1-R2 segment regression formulation:

$$\begin{aligned} \text{Capacity (based on density)} = & (1.155 \times VF1) + (0.350 \times VR1) - (0.018 \times VR2) - (0.018 \times HVF1) \\ & - (0.039 \times HVR1) - (0.030 \times HVR2) - (0.032 \times WSF1_F2) - (0.186 \times WSR1_F2) - (0.208 \times WSR2_F2) \end{aligned}$$

$$R^2 = 96.3\%$$

R2-R3 segment regression formulation:

$$\begin{aligned} \text{Capacity (based on density)} = & (0.571 \times VF1) - (0.115 \times VR1) + (0.618 \times VR2) - (0.099 \times HVF1) \\ & + (0.013 \times HVR1) - (0.006 \times HVR2) - (0.038 \times WSF1_F2) - (0.073 \times WSR1_F2) \\ & + (0.081 \times WSR2_F2) \end{aligned}$$

$$R^2 = 90.4\%$$

In scenario 16, congestion is observed for VF1 higher than 3,000 vph or either VR1 or VR2 demands of more than 1,500 vph.

If weaving shares for all entrances exiting at F2 is less than 90%, no congestion is observed.

Table 38: Number of Lanes and Gore to Gore Distance for S16

Scenario	Gore to Gore Distances (ft)		Number of Lanes						
	LS1	LS2	F1	R1	R1-R2	R2	R2-R3	R3	F2
S16	1,000	2,000	2	2	4	1	4	2	2

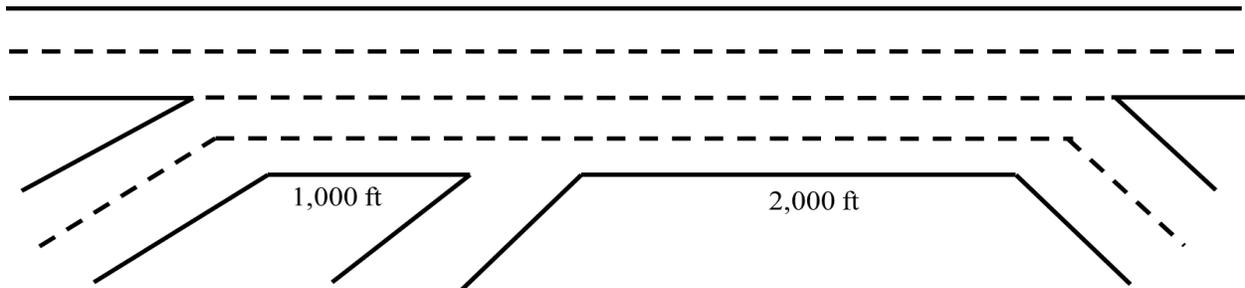


Figure 47: Scenario 16 Lane Geometry

R1-R2 segment regression formulation:

$$\begin{aligned} \text{Capacity (based on density)} = & (0.888 \times VF1) + (0.262 \times VR1) + (0.300 \times VR2) - (0.100 \times HVF1) \\ & - (0.153 \times HVR1) - (0.054 \times HVR2) + (0.271 \times WSF1_F2) - (0.203 \times WSR1_F2) \\ & - (0.410 \times WSR2_F2) \end{aligned}$$

$$R^2 = 67.1\%$$

R2-R3 segment regression formulation:

$$\begin{aligned} \text{Capacity (based on density)} = & (0.963 \times VF1) + (0.109 \times VR1) + (0.521 \times VR2) - (0.116 \times HVF1) \\ & - (0.169 \times HVR1) - (0.056 \times HVR2) + (0.303 \times WSF1_F2) - (0.358 \times WSR1_F2) \\ & - (0.358 \times WSR2_F2) \end{aligned}$$

$$R^2 = 69.5\%$$

In scenario 17, R1-R2 segment faces congestion when VF1 is more than 3,000 vph or VR1 and VR2 is higher than 1,500 vph. No congestion occurs on R2-R3 segment.

Table 39: Number of Lanes and Gore to Gore Distance for S17

Scenario	Gore to Gore Distances (ft)		Number of Lanes						
	LS1	LS2	F1	R1	R1-R2	R2	R2-R3	R3	F2
S17	1,000	2,000	3	1	3	1	3	1	3

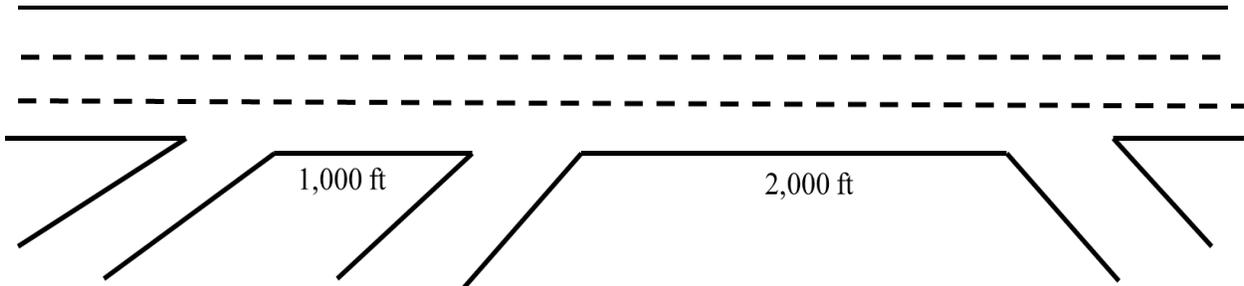


Figure 48: Scenario 17 Lane Geometry

R1-R2 segment regression formulation:

$$\begin{aligned} \text{Capacity (based on density)} = & (1.318 \times VF1) + (0.857 \times VR1) + (1.148 \times VR2) + (0.032 \times HVF1) \\ & + (0.005 \times HVR1) + (0.009 \times HVR2) - (1.450 \times WSF1_F2) - (0.781 \times WSR1_F2) \\ & - (0.258 \times WSR2_F2) \end{aligned}$$

$$R^2 = 88.1\%$$

R2-R3 segment regression formulation:

$$\begin{aligned} \text{Capacity (based on density)} = & (0.589 \times VF1) + (0.382 \times VR1) + (0.492 \times VR2) + (0.006 \times HVF1) \\ & - (0.008 \times HVR1) - (0.001 \times HVR2) - (0.247 \times WSF1_F2) - (0.100 \times WSR1_F2) - (0.106 \times WSR2_F2) \end{aligned}$$

$$R^2 = 99.6\%$$

Scenario 20; VF1 of 3,000 vph and VR1 and VR2 of 1,500 vph are the traffic congestion border.

Table 40: Number of Lanes and Gore to Gore Distance for S20

Scenario	Gore to Gore Distances (ft)		Number of Lanes						
	LS1	LS2	F1	R1	R1-R2	R2	R2-R3	R3	F2
S20	1,000	2,000	2	1	2	2	4	2	2

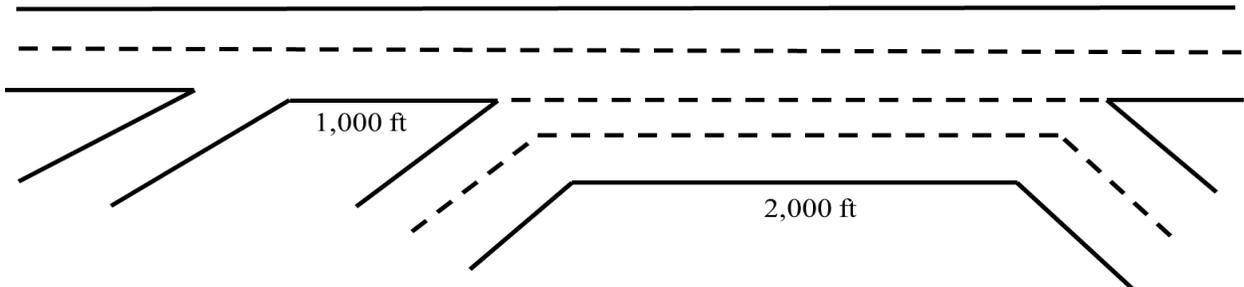


Figure 49: Scenario 20 Lane Geometry

R1-R2 segment regression formulation:

$$\begin{aligned} \text{Capacity (based on density)} &= (1.206 \times VF1) + (0.258 \times VR1) + (0.145 \times VR2) - (0.069 \times HVF1) \\ &- (0.031 \times HVR1) - (0.026 \times HVR2) - (0.372 \times WSF1_F2) - (0.153 \times WSR1_F2) - (0.002 \times WSR2_F2) \\ R^2 &= 94.7\% \end{aligned}$$

R2-R3 segment regression formulation:

$$\begin{aligned} \text{Capacity (based on density)} &= (0.617 \times VF1) - (0.063 \times VR1) + (0.523 \times VR2) - (0.078 \times HVF1) \\ &- (0.092 \times HVR1) - (0.073 \times HVR2) + (0.567 \times WSF1_F2) - (0.379 \times WSR1_F2) \\ &- (0.123 \times WSR2_F2) \\ R^2 &= 82.8\% \end{aligned}$$

Scenario 23; congestion is observed for VF1 higher than 3,000 vph or at least one of the ramp demands, VR1 or VR2, is more than 1,500 vph.

If weaving shares for all entrances exiting at F2 is less than 90%, no congestion is observed.

Table 41: Number of Lanes and Gore to Gore Distance for S23

Scenario	Gore to Gore Distances (ft)		Number of Lanes						
	L _{S1}	L _{S2}	F1	R1	R1-R2	R2	R2-R3	R3	F2
S23	1,500	1,500	2	1	3	1	4	2	2

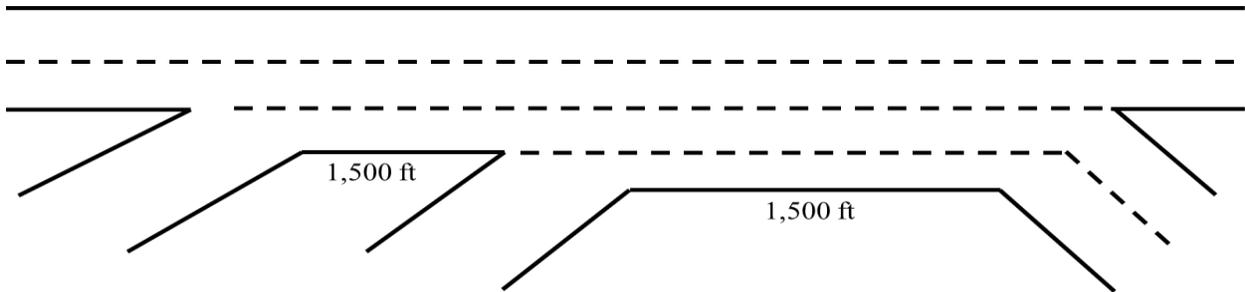


Figure 50: Scenario 23 Lane Geometry

R1-R2 segment regression formulation:

$$\begin{aligned} \text{Capacity (based on density)} &= (0.986 \times VF1) + (0.242 \times VR1) + (0.393 \times VR2) - (0.117 \times HVF1) \\ &- (0.139 \times HVR1) - (0.131 \times HVR2) + (0.169 \times WSF1_F2) - (0.363 \times WSR1_F2) \\ &- (0.273 \times WSR2_F2) \\ R^2 &= 68.5\% \end{aligned}$$

R2-R3 segment regression formulation:

$$\begin{aligned} \text{Capacity (based on density)} &= (1.075 \times VF1) + (0.257 \times VR1) + (0.687 \times VR2) - (0.178 \times HVF1) \\ &- (0.148 \times HVR1) - (0.146 \times HVR2) - (0.030 \times WSF1_F2) - (0.609 \times WSR1_F2) - (0.133 \times WSR2_F2) \\ R^2 &= 66.5\% \end{aligned}$$

Scenario 26; congestion is observed for VF1 higher than 3,000 vph or either VR1 or VR2 demands are more than 1,500 vph.

Table 42: Number of Lanes and Gore to Gore Distance for S26

Scenario	Gore to Gore Distances (ft)		Number of Lanes						
	LS1	LS2	F1	R1	R1-R2	R2	R2-R3	R3	F2
S26	1,500	1,500	2	1	2	1	3	1	2

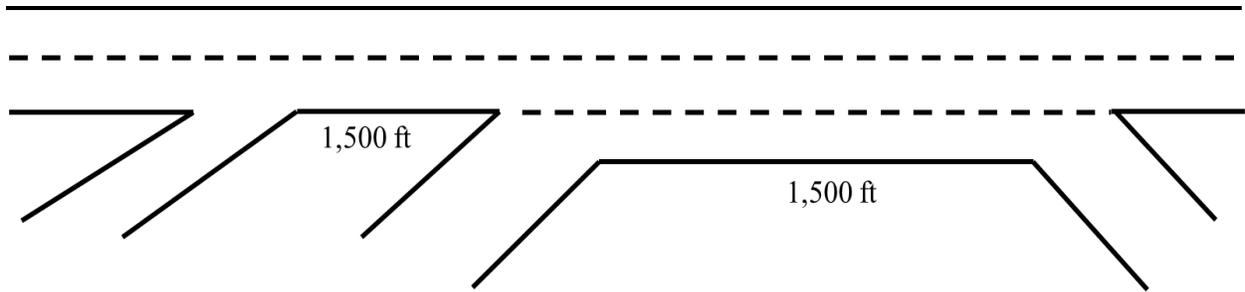


Figure 51: Scenario 26 Lane Geometry

R1-R2 segment regression formulation:

$$\begin{aligned} \text{Capacity (based on density)} = & (0.738 \times VF1) + (0.388 \times VR1) + (0.088 \times VR2) + (0.002 \times HVF1) \\ & + (0.002 \times HVR1) + (0.010 \times HVR2) - (0.192 \times WSF1_F2) - (0.101 \times WSR1_F2) \\ & + (0.508 \times WSR2_F2) \end{aligned}$$

$$R^2 = 98.1\%$$

R2-R3 segment regression formulation:

$$\begin{aligned} \text{Capacity (based on density)} = & (0.950 \times VF1) - (0.300 \times VR1) + (0.820 \times VR2) - (0.044 \times HVF1) \\ & - (0.113 \times HVR1) - (0.044 \times HVR2) - (0.124 \times WSF1_F2) - (0.234 \times WSR1_F2) - (0.008 \times WSR2_F2) \end{aligned}$$

$$R^2 = 88.2\%$$

In scenario 27, the most significant factors in creating congestion are VF1 to be more than 3,000 vph and weaving share entering F1 and exiting at F2 to be more than 90%.

Table 43: Number of Lanes and Gore to Gore Distance for S27

Scenario	Gore to Gore Distances (ft)		Number of Lanes						
	LS1	LS2	F1	R1	R1-R2	R2	R2-R3	R3	F2
S27	1,500	1,500	2	2	4	1	4	2	2

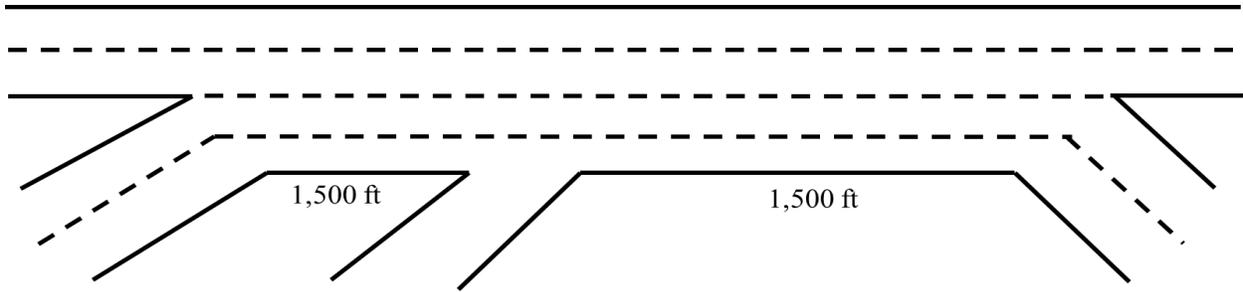


Figure 52: Scenario 27 Lane Geometry

R1-R2 segment regression formulation:

$$\begin{aligned} \text{Capacity (based on density)} &= (1.074 \times VF1) + (0.127 \times VR1) + (0.198 \times VR2) - (0.044 \times HVF1) \\ &- (0.071 \times HVR1) - (0.065 \times HVR2) - (0.023 \times WSF1_F2) - (0.159 \times WSR1_F2) - (0.082 \times WSR2_F2) \\ R^2 &= 93.1\% \end{aligned}$$

R2-R3 segment regression formulation:

$$\begin{aligned} \text{Capacity (based on density)} &= (1.039 \times VF1) + (0.159 \times VR1) + (0.333 \times VR2) - (0.181 \times HVF1) \\ &- (0.189 \times HVR1) - (0.115 \times HVR2) + (0.455 \times WSF1_F2) - (0.264 \times WSR1_F2) \\ &- (0.456 \times WSR2_F2) \end{aligned}$$

$$R^2 = 66.6\%$$

Scenario 28; R1-R2 segment may face congestion if either VF1 exceeds 3,000 vph or VR1 and VR2 exceed 1,500 vph.

Table 44: Number of Lanes and Gore to Gore Distance for S28

Scenario	Gore to Gore Distances (ft)		Number of Lanes						
	L _{S1}	L _{S2}	F1	R1	R1-R2	R2	R2-R3	R3	F2
S28	1,500	1,500	3	1	3	1	3	1	3

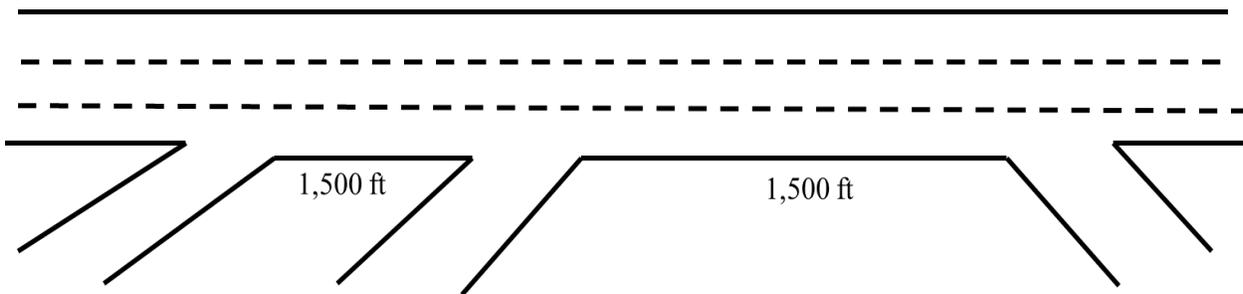


Figure 53: Scenario 28 Lane Geometry

R1-R2 segment regression formulation:

$$\begin{aligned} \text{Capacity (based on density)} &= (1.037 \times VF1) + (0.326 \times VR1) + (0.029 \times VR2) - (0.135 \times HVF1) \\ &- (0.171 \times HVR1) - (0.113 \times HVR2) + (0.445 \times WSF1_F2) - (0.219 \times WSR1_F2) \\ &- (0.409 \times WSR2_F2) \end{aligned}$$

$$R^2 = 67.3\%$$

R2-R3 segment regression formulation:

$$\begin{aligned} \text{Capacity (based on density)} = & (0.656 \times VF1) + (0.417 \times VR1) + (0.532 \times VR2) + (0.018 \times HVF1) \\ & - (0.001 \times HVR1) + (0.013 \times HVR2) - (0.306 \times WSF1_F2) - (0.151 \times WSR1_F2) \\ & - (0.172 \times WSR2_F2) \end{aligned}$$

$$R^2 = 99.3\%$$

In scenario 31, congestion is occurred if VF1=3,000 vph or VR1=1,500vph and VR2=1,500vph, and one of the weaving shares exiting at F2 is 90% or higher.

Table 45: Number of Lanes and Gore to Gore Distance for S31

Scenario	Gore to Gore Distances (ft)		Number of Lanes						
	LS1	LS2	F1	R1	R1-R2	R2	R2-R3	R3	F2
S31	1,500	1,500	2	1	2	2	4	2	2

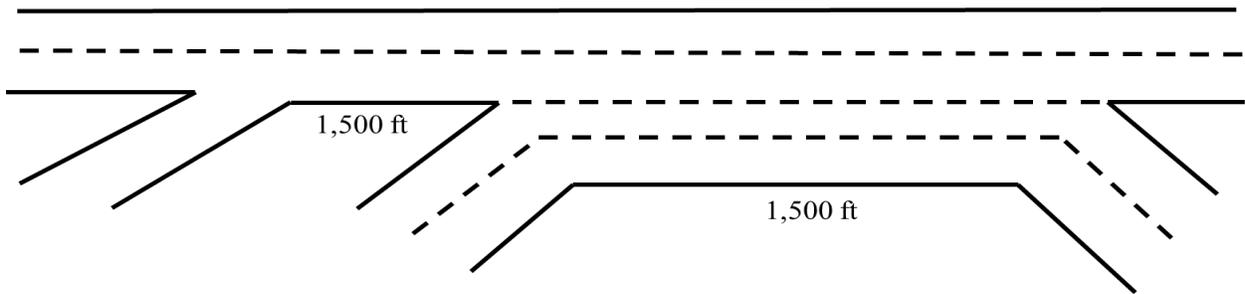


Figure 54: Scenario 31 Lane Geometry

R1-R2 segment regression formulation:

$$\begin{aligned} \text{Capacity (based on density)} = & (1.099 \times VF1) + (0.208 \times VR1) + (0.279 \times VR2) - (0.109 \times HVF1) \\ & - (0.066 \times HVR1) - (0.066 \times HVR2) + (0.022 \times WSF1_F2) - (0.346 \times WSR1_F2) \\ & - (0.091 \times WSR2_F2) \end{aligned}$$

$$R^2 = 89\%$$

R2-R3 segment regression formulation:

$$\begin{aligned} \text{Capacity (based on density)} = & (0.693 \times VF1) - (0.055 \times VR1) + (0.571 \times VR2) - (0.130 \times HVF1) \\ & - (0.164 \times HVR1) - (0.090 \times HVR2) + (0.621 \times WSF1_F2) - (0.413 \times WSR1_F2) \\ & - (0.176 \times WSR2_F2) \end{aligned}$$

$$R^2 = 77.4\%$$

In scenario 34, congestion is observed if VF1 passes 3,000 vph, VR1 and VR2 passes 1,500 vph, and one of the weaving shares entering F1 or R1 and exiting at F2 is 90% or higher.

Table 50: Number of Lanes and Gore to Gore Distance for S34

Scenario	Gore to Gore Distances (ft)		Number of Lanes						
	LS1	LS2	F1	R1	R1-R2	R2	R2-R3	R3	F2
S34	1,500	2,000	2	1	3	1	4	2	2

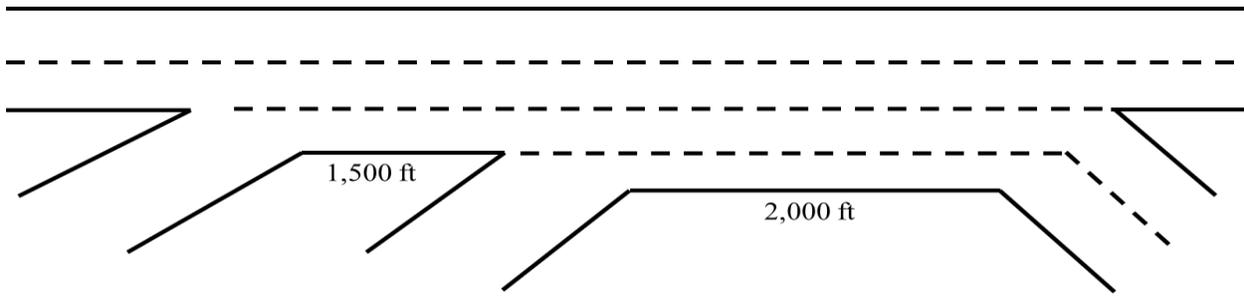


Figure 55: Scenario 34 Lane Geometry

R1-R2 segment regression formulation:

$$\begin{aligned} \text{Capacity (based on density)} = & (0.940 \times VF1) + (0.443 \times VR1) + (0.288 \times VR2) - (0.075 \times HVF1) \\ & - (0.117 \times HVR1) - (0.106 \times HVR2) + (0.429 \times WSF1_F2) - (0.710 \times WSR1_F2) \\ & - (0.264 \times WSR2_F2) \end{aligned}$$

$$R^2 = 72.4\%$$

R2-R3 segment regression formulation:

$$\begin{aligned} \text{Capacity (based on density)} = & (0.982 \times VF1) + (0.337 \times VR1) + (0.467 \times VR2) - (0.106 \times HVF1) \\ & - (0.131 \times HVR1) - (0.145 \times HVR2) + (0.485 \times WSF1_F2) - (0.882 \times WSR1_F2) \\ & - (0.204 \times WSR2_F2) \end{aligned}$$

$$R^2 = 70.1\%$$

Scenario 37 touches capacity limit if VF1 reaches 3,000 vph, VR1 and VR2 passes 1,500 vph, and the weaving share entering F1 exiting at F2 is 90% or higher.

Table 46: Number of Lanes and Gore to Gore Distance for S37

Scenario	Gore to Gore Distances (ft)		Number of Lanes						
	LS1	LS2	F1	R1	R1-R2	R2	R2-R3	R3	F2
S37	1,500	2,000	2	1	2	1	3	1	2

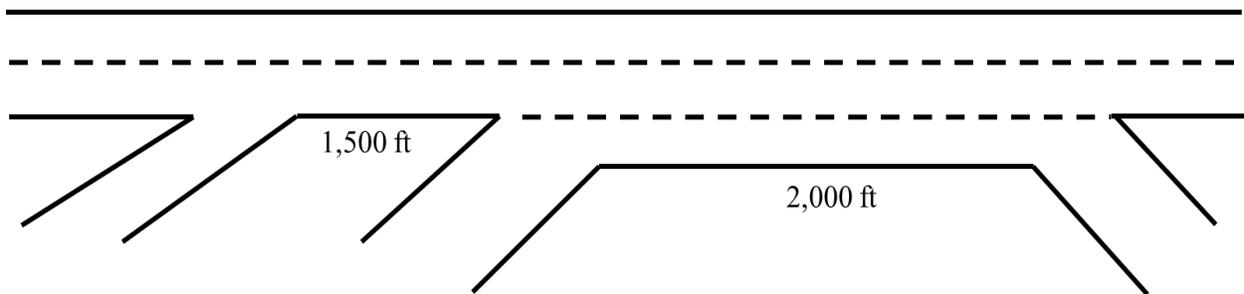


Figure 56: Scenario 37 Lane Geometry

R1-R2 segment regression formulation:

$$\begin{aligned} \text{Capacity (based on density)} &= (1.010 \times VF1) + (0.258 \times VR1) + (0.110 \times VR2) + (0.007 \times HVF1) \\ &- (0.051 \times HVR1) - (0.034 \times HVR2) - (0.139 \times WSF1_F2) - (0.163 \times WSR1_F2) - (0.024 \times WSR2_F2) \\ R^2 &= 95.2\% \end{aligned}$$

R2-R3 segment regression formulation:

$$\begin{aligned} \text{Capacity (based on density)} &= (0.622 \times VF1) - (0.075 \times VR1) + (0.623 \times VR2) - (0.058 \times HVF1) \\ &- (0.074 \times HVR1) - (0.034 \times HVR2) + (0.368 \times WSF1_F2) - (0.331 \times WSR1_F2) - \\ &\quad (0.108 \times WSR2_F2) \\ R^2 &= 88\% \end{aligned}$$

In scenario 38, congestion is experienced if simultaneously, VF1 exceeds 3,000 vph, or VR1 and VR2 exceeds 1,500 vph.

Table 47: Number of Lanes and Gore to Gore Distance for S38

Scenario	Gore to Gore Distances (ft)		Number of Lanes						
	L _{S1}	L _{S2}	F1	R1	R1-R2	R2	R2-R3	R3	F2
S38	1,500	2,000	2	2	4	1	4	2	2

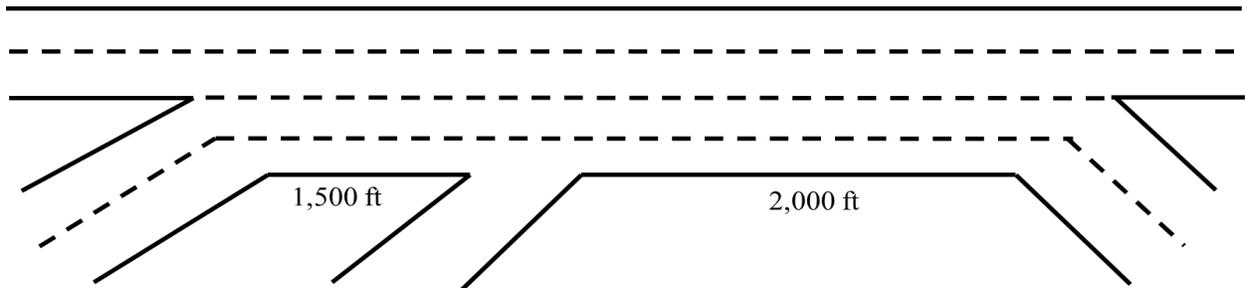


Figure 57: Scenario 38 Lane Geometry

R1-R2 segment regression formulation:

$$\begin{aligned} \text{Capacity (based on density)} &= (0.868 \times VF1) + (0.331 \times VR1) + (0.331 \times VR2) - (0.112 \times HVF1) \\ &- (0.099 \times HVR1) - (0.144 \times HVR2) + (0.135 \times WSF1_F2) - (0.360 \times WSR1_F2) \\ &\quad - (0.112 \times WSR2_F2) \\ R^2 &= 73.1\% \end{aligned}$$

R2-R3 segment regression formulation:

$$\begin{aligned} \text{Capacity (based on density)} &= (0.938 \times VF1) + (0.194 \times VR1) + (0.608 \times VR2) - (0.132 \times HVF1) \\ &- (0.113 \times HVR1) - (0.179 \times HVR2) + (0.077 \times WSF1_F2) - (0.408 \times WSR1_F2) \\ &\quad - (0.158 \times WSR2_F2) \\ R^2 &= 72.9\% \end{aligned}$$

Scenario 39 faces congestion in R1-R2 segment for VF1 more than 3,000 vph or VR2 more than 1,500vph.

Table 48: Number of Lanes and Gore to Gore Distance for S39

Scenario	Gore to Gore Distances (ft)		Number of Lanes						
	L _{S1}	L _{S2}	F1	R1	R1-R2	R2	R2-R3	R3	F2
S39	1,500	2,000	3	1	3	1	3	1	3

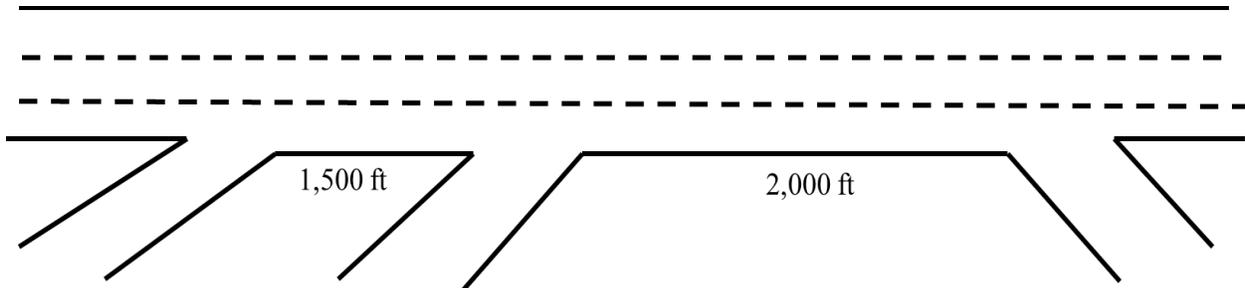


Figure 58: Scenario 39 Lane Geometry

R1-R2 segment regression formulation:

$$\begin{aligned} \text{Capacity (based on density)} = & (1.330 \times VF1) + (0.819 \times VR1) + (0.889 \times VR2) + (0.092 \times HVF1) \\ & + (0.008 \times HVR1) + (0.026 \times HVR2) - (1.247 \times WSF1_F2) - (0.803 \times WSR1_F2) \\ & - (0.228 \times WSR2_F2) \end{aligned}$$

$$R^2 = 86.2\%$$

R2-R3 segment regression formulation:

$$\begin{aligned} \text{Capacity (based on density)} = & (0.602 \times VF1) + (0.353 \times VR1) + (0.521 \times VR2) + (0.012 \times HVF1) \\ & + (0.001 \times HVR1) + (0.003 \times HVR2) - (0.259 \times WSF1_F2) - (0.078 \times WSR1_F2) \\ & - (0.147 \times WSR2_F2) \end{aligned}$$

$$R^2 = 99.6\%$$

Scenario 42 congestion is occurred if VF1 goes beyond 3,000 vph, VR1 and VR2 passes 1,500 vph, or if the weaving share entering F1 exiting at F2 is 90% or higher.

Table 49: Number of Lanes and Gore to Gore Distance for S42

Scenario	Gore to Gore Distances (ft)		Number of Lanes						
	L _{S1}	L _{S2}	F1	R1	R1-R2	R2	R2-R3	R3	F2
S42	1,500	2,000	2	1	2	2	4	2	2

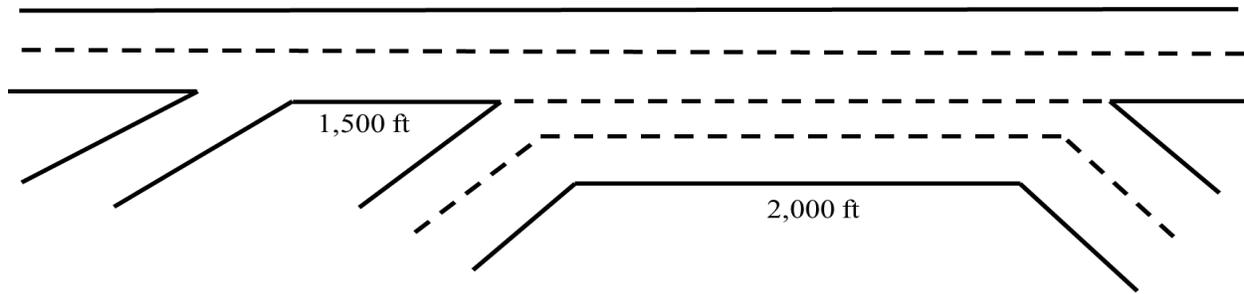


Figure 59: Scenario 42 Lane Geometry

R1-R2 segment regression formulation:

$$\begin{aligned} \text{Capacity (based on density)} = & (1.117 \times VF1) + (0.285 \times VR1) + (0.101 \times VR2) - (0.014 \times HVF1) \\ & - (0.053 \times HVR1) - (0.056 \times HVR2) - (0.082 \times WSF1_F2) - (0.209 \times WSR1_F2) - (0.129 \times WSR2_F2) \\ R^2 = & 93.8\% \end{aligned}$$

R2-R3 segment regression formulation:

$$\begin{aligned} \text{Capacity (based on density)} = & (0.557 \times VF1) + (0.167 \times VR1) + (0.550 \times VR2) - (0.153 \times HVF1) \\ & - (0.074 \times HVR1) - (0.081 \times HVR2) + (0.401 \times WSF1_F2) - (0.325 \times WSR1_F2) \\ & - (0.145 \times WSR2_F2) \\ R^2 = & 82.3\% \end{aligned}$$

Model Extension

In previous section, some scenarios did not experience congestion on either of gore-to-gore segments (R1-R2 and R2-R3) for selected variables ranges. Therefore, we have extended variable ranges up to 2,400 vphpl for freeway lanes and up to 2,000 vphpl for ramp lanes (Table 50). Heavy vehicle percentage and weaving shares are as before.

Table 50: Range of Flow for Model Extension

Flow		
VF1	VR1	VR2
Up to 2,400 vphpl	Up to 2,000 vphpl	Up to 2,000 vphpl

Scenario 2; neither the R1-R2 segment nor the R2-R3 segment touches capacity point while VF1 is less than 4,000 vph and VR1 and VR2 are less than 2,000 vph.

Table 51: Number of Lanes and Gore to Gore Distance for S2

Scenario	Gore to Gore Distances (ft)		Number of Lanes						
	Ls1	Ls2	F1	R1	R1-R2	R2	R2-R3	R3	F2
S2	1,000	1,500	3	1	4	1	5	2	3

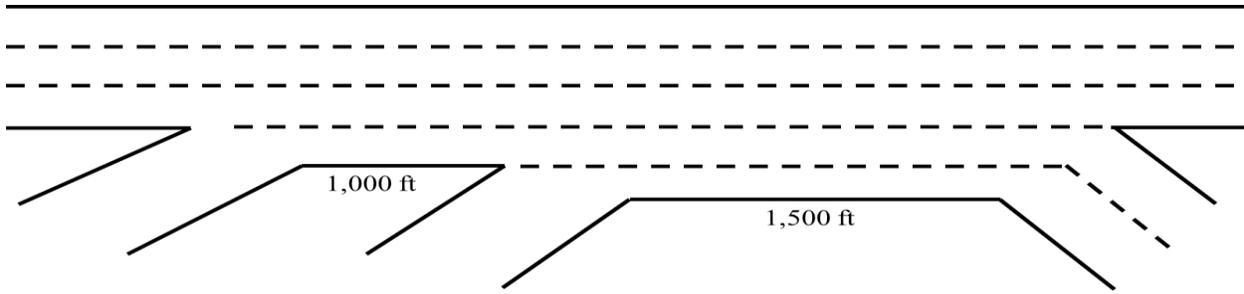


Figure 60: Scenario 2 Lane Geometry

The regression formulation for R1-R2 segment is:

$$\begin{aligned} \text{Capacity (based on density)} = & (0.551 \times VF1) + (0.535 \times VR1) + (0.213 \times VR2) + (0.021 \times HVF1) \\ & - (0.032 \times HVR1) - (0.042 \times HVR2) - (0.148 \times WSF1_F2) - (0.045 \times WSR1_F2) - (0.096 \times WSR2_F2) \\ R^2 = & 90.6\% \end{aligned}$$

And for R2-R3 segment is:

$$\begin{aligned} \text{Capacity (based on density)} = & (0.444 \times VF1) + (0.769 \times VR1) + (0.879 \times VR2) - (0.016 \times HVF1) \\ & - (0.098 \times HVR1) - (0.082 \times HVR2) - (0.747 \times WSF1_F2) - (0.252 \times WSR1_F2) - (0.023 \times WSR2_F2) \\ R^2 = & 83\% \end{aligned}$$

Scenario 3; neither R1-R2 segment nor R2-R3 segment face congestion while F1 demand is less than 4,000 vph and R1 and R2 demands are less than 2,000 vph.

Table 52: Number of Lanes and Gore to Gore Distance for S3

Scenario	Gore to Gore Distances (ft)		Number of Lanes						
	Ls1	Ls2	F1	R1	R1-R2	R2	R2-R3	R3	F2
S3	1,000	1,500	4	1	5	1	6	2	4

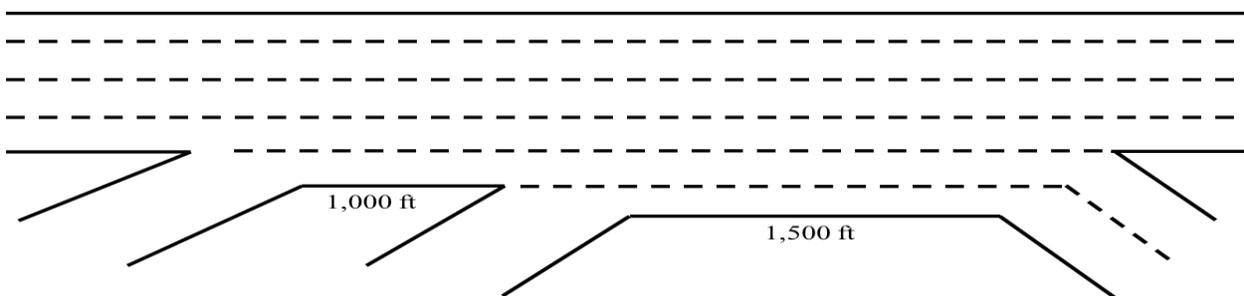


Figure 61: Scenario 3 Lane Geometry

The regression formulation for R1-R2 segment is:

$$\begin{aligned} \text{Capacity (based on density)} = & (0.676 \times VF1) + (0.336 \times VR1) + (0.006 \times VR2) + (0.003 \times HVF1) \\ & + (0.003 \times HVR1) + (0.000 \times HVR2) - (0.025 \times WSF1_F2) + (0.00-00 \times WSR1_F2) \\ & + (0.012 \times WSR2_F2) \end{aligned}$$

$$R^2 = 100\%$$

And for R2-R3 segment is:

$$\begin{aligned} \text{Capacity (based on density)} = & (0.578 \times VF1) + (0.428 \times VR1) + (0.500 \times VR2) + (0.019 \times HVF1) \\ & + (0.013 \times HVR1) + (0.024 \times HVR2) - (0.509 \times WSF1_F2) - (0.209 \times WSR1_F2) \\ & + (0.151 \times WSR2_F2) \end{aligned}$$

$$R^2 = 97.9\%$$

Scenario 6; to prevent congestion, either the F1 flow should stay under 3,500 vhp, or VR1 and VR2 stay under 1,500 vph. Also, all weaving shares to be less than 90% and heavy vehicle percentages are 0.05.

Table 53: Number of Lanes and Gore to Gore Distance for S6

Scenario	Gore to Gore Distances (ft)		Number of Lanes						
	L _{S1}	L _{S2}	F1	R1	R1-R2	R2	R2-R3	R3	F2
S6	1,000	1,500	3	1	3	1	3	1	3

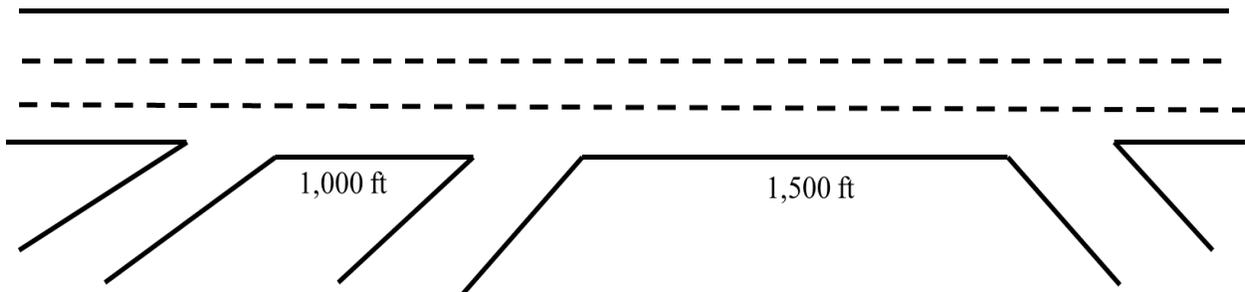


Figure 62: Scenario 6 Lane Geometry

R1-R2 segment regression formulation:

$$\begin{aligned} \text{Capacity (based on density)} = & (1.605 \times VF1) + (0.627 \times VR1) + (0.993 \times VR2) - (0.043 \times HVF1) \\ & - (0.078 \times HVR1) - (0.028 \times HVR2) - (1.145 \times WSF1_F2) - (0.403 \times WSR1_F2) - (0.595 \times WSR2_F2) \end{aligned}$$

$$R^2 = 94.3\%$$

R2-R3 segment regression formulation:

$$\begin{aligned} \text{Capacity (based on density)} = & (0.585 \times VF1) + (0.164 \times VR1) + (0.264 \times VR2) + (0.011 \times HVF1) \\ & - (0.002 \times HVR1) + (0.008 \times HVR2) + (0.005 \times WSF1_F2) + (0.041 \times WSR1_F2) \\ & - (0.071 \times WSR2_F2) \end{aligned}$$

$$R^2 = 99.5\%$$

In scenario 7 congestion occurs if at the same time VF1 exceeds 4,000 vph, VR1 and VR2 exceed 2,000 vph, and all weaving shares pass 90%.

Table 54: Number of Lanes and Gore to Gore Distance for S7

Scenario	Gore to Gore Distances (ft)		Number of Lanes						
	LS1	LS2	F1	R1	R1-R2	R2	R2-R3	R3	F2
S7	1,000	1,500	3	2	5	1	5	2	3

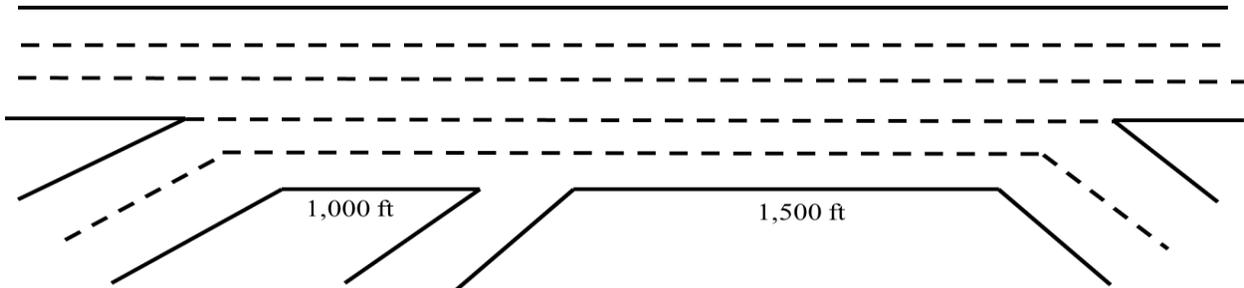


Figure 63: Scenario 7 Lane Geometry

R1-R2 segment regression formulation:

$$\begin{aligned} \text{Capacity (based on density)} = & - (0.283 \times VF1) + (0.414 \times VR1) + (0.137 \times VR2) - (0.004 \times HVF1) \\ & + (0.043 \times HVR1) + (0.029 \times HVR2) + (0.218 \times WSF1_F2) + (0.247 \times WSR1_F2) \\ & + (0.200 \times WSR2_F2) \end{aligned}$$

$$R^2 = 96.9\%$$

R2-R3 segment regression formulation:

$$\begin{aligned} \text{Capacity (based on density)} = & - (1.939 \times VF1) + (0.736 \times VR1) + (0.828 \times VR2) + (0.107 \times HVF1) \\ & + (0.091 \times HVR1) + (0.010 \times HVR2) - (0.133 \times WSF1_F2) + (0.508 \times WSR1_F2) \\ & + (0.735 \times WSR2_F2) \end{aligned}$$

$$R^2 = 90.4\%$$

Scenario 10; congestion is observed when VF1 goes beyond 4,000 vph, and VR1 and VR2 pass 2,000 vph.

Table 60: Number of Lanes and Gore to Gore Distance for S10

Scenario	Gore to Gore Distances (ft)		Number of Lanes						
	LS1	LS2	F1	R1	R1-R2	R2	R2-R3	R3	F2
S10	1,000	1,500	3	1	3	2	5	2	3

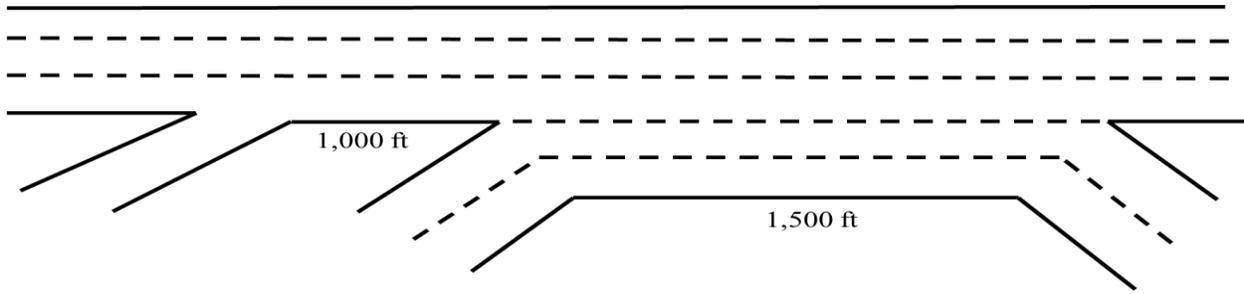


Figure 64: Scenario 10 Lane Geometry

R1-R2 segment regression formulation:

$$\begin{aligned} \text{Capacity (based on density)} = & (0.910 \times VF1) + (0.582 \times VR1) + (0.062 \times VR2) + (0.002 \times HVF1) \\ & + (0.005 \times HVR1) - (0.013 \times HVR2) - (0.358 \times WSF1_F2) - (0.112 \times WSR1_F2) \\ & - (0.088 \times WSR2_F2) \end{aligned}$$

$$R^2 = 98.8\%$$

R2-R3 segment regression formulation:

$$\begin{aligned} \text{Capacity (based on density)} = & (0.549 \times VF1) + (0.201 \times VR1) + (0.281 \times VR2) + (0.000 \times HVF1) \\ & - (0.011 \times HVR1) + (0.005 \times HVR2) + (0.010 \times WSF1_F2) - (0.035 \times WSR1_F2) \\ & + (0.011 \times WSR2_F2) \end{aligned}$$

$$R^2 = 99.5\%$$

Scenario 13; R2-R3 segment may experience congestion if simultaneously F1 leg demand reaches 4,000 vph, VR1 and VR2 demands hit 2,000 vph, all weaving shares exiting F2 with the probability of 90%, and all entrance legs obtain 10% heavy vehicle in their traffic mix.

Table 55: Number of Lanes and Gore to Gore Distance for S13

Scenario	Gore to Gore Distances (ft)		Number of Lanes						
	L _{S1}	L _{S2}	F1	R1	R1-R2	R2	R2-R3	R3	F2
S13	1,000	2,000	3	1	4	1	5	2	3

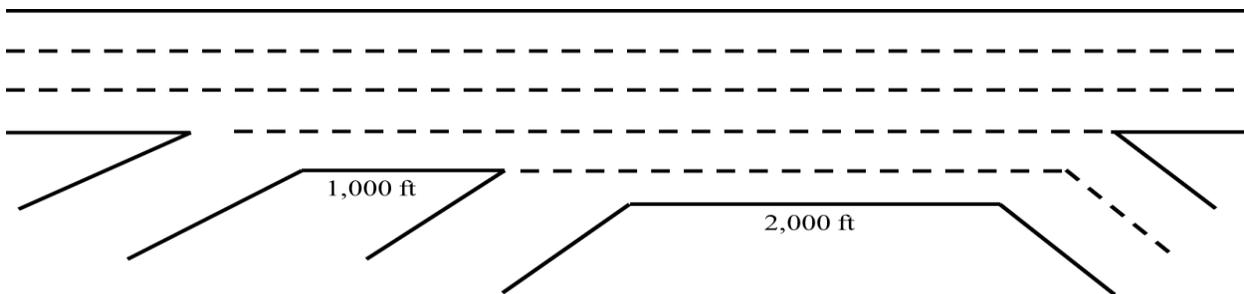


Figure 65: Scenario 13 Lane Geometry

R1-R2 segment regression formulation:

$$\begin{aligned} \text{Capacity (based on density)} = & (0.669 \times VF1) + (0.376 \times VR1) + (0.063 \times VR2) + (0.015 \times HVF1) \\ & - (0.006 \times HVR1) + (0.000 \times HVR2) - (0.073 \times WSF1_F2) - (0.019 \times WSR1_F2) \\ & - (0.024 \times WSR2_F2) \end{aligned}$$

$$R^2 = 97.8\%$$

R2-R3 segment regression formulation:

$$\begin{aligned} \text{Capacity (based on density)} = & (0.529 \times VF1) + (0.452 \times VR1) + (0.504 \times VR2) + (0.009 \times HVF1) \\ & - (0.014 \times HVR1) - (0.004 \times HVR2) - (0.328 \times WSF1_F2) - (0.155 \times WSR1_F2) - (0.026 \times WSR2_F2) \end{aligned}$$

$$R^2 = 92.7\%$$

In scenario 18, R2-R3 segment may touch capacity limit if VF1 passes 4,000 vph, VR1 and VR2 go beyond 2,000 vph, and at least one of the weaving shares exiting at F2 is 90%, or one of the heavy vehicle percentages is 10%.

Table 56: Number of Lanes and Gore to Gore Distance for S18

Scenario	Gore to Gore Distances (ft)		Number of Lanes						
	L _{S1}	L _{S2}	F1	R1	R1-R2	R2	R2-R3	R3	F2
S18	1,000	2,000	3	2	5	1	5	2	3

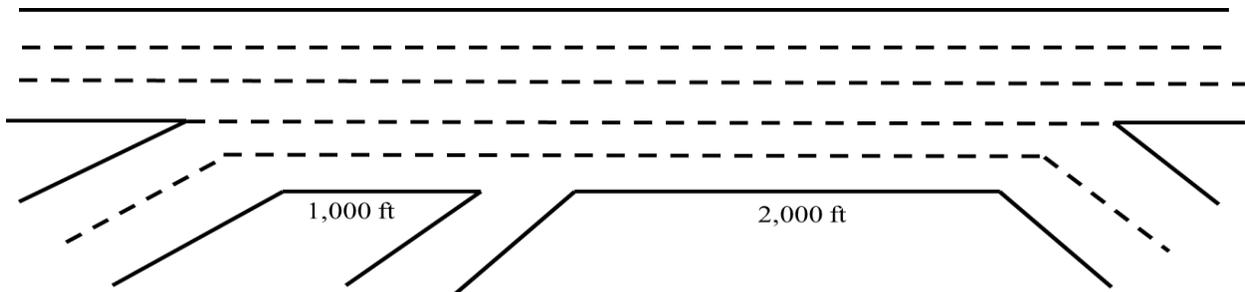


Figure 66: Scenario 18 Lane Geometry

R1-R2 segment regression formulation:

$$\begin{aligned} \text{Capacity (based on density)} = & (0.677 \times VF1) + (0.354 \times VR1) + (0.034 \times VR2) - (0.023 \times HVF1) \\ & + (0.005 \times HVR1) - (0.007 \times HVR2) - (0.025 \times WSF1_F2) + (0.007 \times WSR1_F2) \\ & - (0.017 \times WSR2_F2) \end{aligned}$$

$$R^2 = 99.2\%$$

R2-R3 segment regression formulation:

$$\begin{aligned} \text{Capacity (based on density)} = & (0.541 \times VF1) + (0.402 \times VR1) + (0.446 \times VR2) - (0.037 \times HVF1) \\ & - (0.014 \times HVR1) - (0.025 \times HVR2) - (0.196 \times WSF1_F2) - (0.062 \times WSR1_F2) - (0.071 \times WSR2_F2) \end{aligned}$$

$$R^2 = 95.9\%$$

Scenario 21; R1-R2 segment faces congestion if VF1 passes 4,000 vph, VR1 and VR2 pass 2,000 vph, and the weaving shares entering F1 and exiting at F2 is 90%.

Table 57: Number of Lanes and Gore to Gore Distance for S21

Scenario	Gore to Gore Distances (ft)		Number of Lanes						
	LS1	LS2	F1	R1	R1-R2	R2	R2-R3	R3	F2
S21	1,000	2,000	3	1	3	2	5	2	3

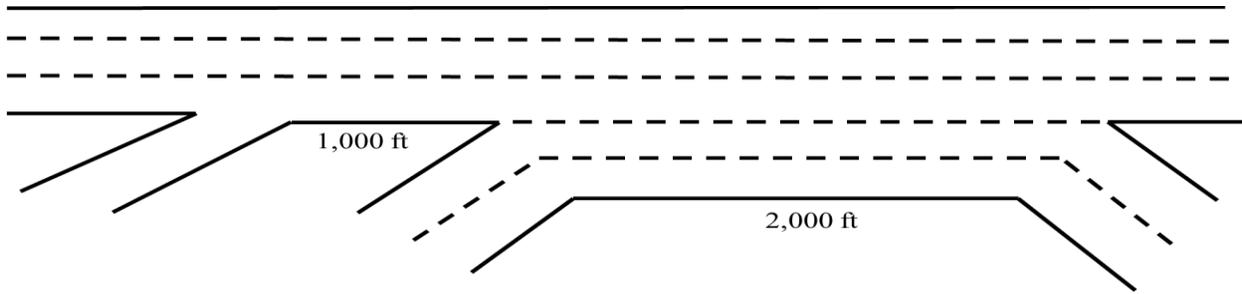


Figure 67: Scenario 21 Lane Geometry

R1-R2 segment regression formulation:

$$\begin{aligned} \text{Capacity (based on density)} = & (0.910 \times VF1) + (0.582 \times VR1) + (0.061 \times VR2) + (0.002 \times HVF1) \\ & + (0.005 \times HVR1) - (0.013 \times HVR2) - (0.358 \times WSF1_F2) - (0.112 \times WSR1_F2) \\ & - (0.088 \times WSR2_F2) \end{aligned}$$

$$R^2 = 98.8\%$$

R2-R3 segment regression formulation:

$$\begin{aligned} \text{Capacity (based on density)} = & (0.527 \times VF1) + (0.194 \times VR1) + (0.244 \times VR2) + (0.006 \times HVF1) \\ & - (0.005 \times HVR1) - (0.004 \times HVR2) + (0.066 \times WSF1_F2) - (0.016 \times WSR1_F2) \\ & + (0.001 \times WSR2_F2) \end{aligned}$$

$$R^2 = 99.9\%$$

Scenario 24 experiences congestion when VF1 reaches 4,000 vph, VR1 and VR2 hit 2,000 vph, and all entrance legs obtain 10% heavy vehicle in their traffic mix.

Table 58: Number of Lanes and Gore to Gore Distance for S24

Scenario	Gore to Gore Distances (ft)		Number of Lanes						
	LS1	LS2	F1	R1	R1-R2	R2	R2-R3	R3	F2
S24	1,500	1,500	3	1	4	1	5	2	3

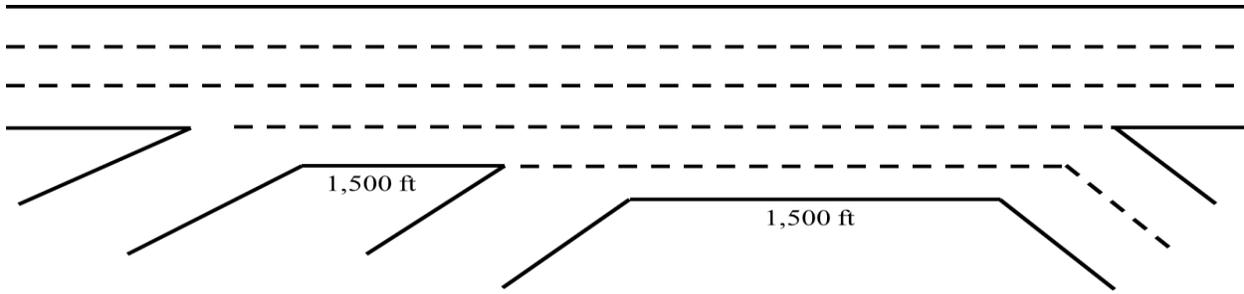


Figure 68: Scenario 24 Lane Geometry

R1-R2 segment regression formulation:

$$\begin{aligned} \text{Capacity (based on density)} = & (0.664 \times VF1) + (0.452 \times VR1) + (0.154 \times VR2) - (0.005 \times HVF1) \\ & - (0.057 \times HVR1) - (0.026 \times HVR2) - (0.127 \times WSF1_F2) - (0.081 \times WSR1_F2) \\ & + (0.004 \times WSR2_F2) \end{aligned}$$

$$R^2 = 95\%$$

R2-R3 segment regression formulation:

$$\begin{aligned} \text{Capacity (based on density)} = & (0.588 \times VF1) + (0.758 \times VR1) + (0.843 \times VR2) - (0.030 \times HVF1) \\ & - (0.089 \times HVR1) - (0.053 \times HVR2) - (0.693 \times WSF1_F2) - (0.411 \times WSR1_F2) - (0.018 \times WSR2_F2) \end{aligned}$$

$$R^2 = 87.6\%$$

Scenario 29; R2-R3 segment faces congestion if VF1 passes 4,000 vph, VR1 and VR2 exceed 2,000 vph, and all the weaving shares exiting at F2 is 90%.

Table 59: Number of Lanes and Gore to Gore Distance for S29

Scenario	Gore to Gore Distances (ft)		Number of Lanes						
	L _{S1}	L _{S2}	F1	R1	R1-R2	R2	R2-R3	R3	F2
S29	1,500	1,500	3	2	5	1	5	2	3

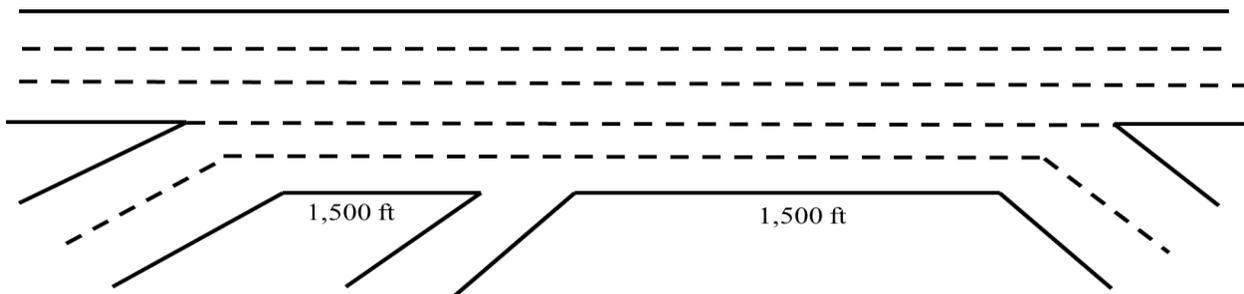


Figure 69: Scenario 29 Lane Geometry

R1-R2 segment regression formulation:

$$\begin{aligned} \text{Capacity (based on density)} = & (1.427 \times VF1) + (0.938 \times VR1) + (0.734 \times VR2) + (0.095 \times HVF1) \\ & + (0.039 \times HVR1) + (0.057 \times HVR2) - (1.368 \times WSF1_F2) - (0.755 \times WSR1_F2) \\ & - (0.270 \times WSR2_F2) \end{aligned}$$

$$R^2 = 88.9\%$$

R2-R3 segment regression formulation:

$$\begin{aligned} \text{Capacity (based on density)} = & (0.421 \times VF1) + (0.276 \times VR1) + (0.398 \times VR2) - (0.101 \times HVF1) \\ & - (0.063 \times HVR1) - (0.108 \times HVR2) - (0.678 \times WSF1_F2) + (0.607 \times WSR1_F2) \\ & + (0.281 \times WSR2_F2) \end{aligned}$$

$$R^2 = 87.2\%$$

Scenario 35 gets in congestion as soon as VF1 goes beyond 4,000 vph, VR1 and VR2 exceed 2,000 vph, and either the weaving shares entering R2 and exiting at F2 is 90%, or the heavy vehicle percentages entering F1 leg is 10%.

Table 60: Number of Lanes and Gore to Gore Distance for S35

Scenario	Gore to Gore Distances (ft)		Number of Lanes						
	LS1	LS2	F1	R1	R1-R2	R2	R2-R3	R3	F2
S35	1,500	2,000	3	1	4	1	5	2	3

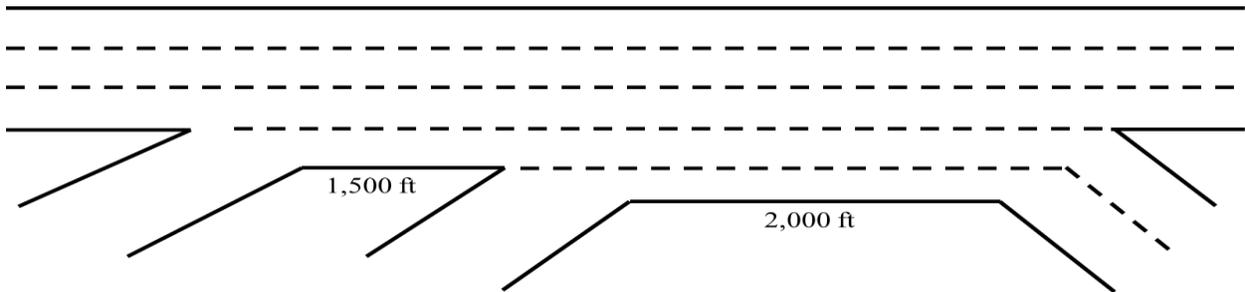


Figure 70: Scenario 35 Lane Geometry

R1-R2 segment regression formulation:

$$\begin{aligned} \text{Capacity (based on density)} = & (0.663 \times VF1) + (0.386 \times VR1) + (0.077 \times VR2) + (0.005 \times HVF1) \\ & - (0.009 \times HVR1) - (0.033 \times HVR2) - (0.048 \times WSF1_F2) - (0.021 \times WSR1_F2) - (0.028 \times WSR2_F2) \end{aligned}$$

$$R^2 = 96.7\%$$

R2-R3 segment regression formulation:

$$\begin{aligned} \text{Capacity (based on density)} = & (0.522 \times VF1) + (0.501 \times VR1) + (0.565 \times VR2) - (0.021 \times HVF1) \\ & - (0.037 \times HVR1) - (0.037 \times HVR2) - (0.323 \times WSF1_F2) - (0.213 \times WSR1_F2) - (0.007 \times WSR2_F2) \end{aligned}$$

$$R^2 = 91.0\%$$

Scenario 40 faces congestion if VF1 passes 4,000 vph, VR1 and VR2 touches 2,000 vph, and two of weaving shares exiting at F2 is simultaneously 90%.

Table 61: Number of Lanes and Gore to Gore Distance for S40

Scenario	Gore to Gore Distances (ft)		Number of Lanes						
	LS1	LS2	F1	R1	R1-R2	R2	R2-R3	R3	F2
S40	1,500	2,000	3	2	5	1	5	2	3

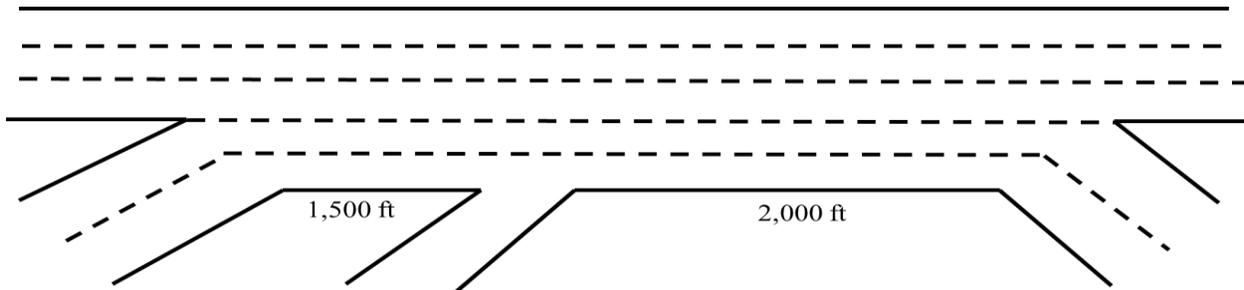


Figure 71: Scenario 40 Lane Geometry

R1-R2 segment regression formulation:

$$\begin{aligned} \text{Capacity (based on density)} = & (0.663 \times VF1) + (0.375 \times VR1) + (0.070 \times VR2) - (0.038 \times HVF1) \\ & - (0.009 \times HVR1) - (0.008 \times HVR2) - (0.024 \times WSF1_F2) - (0.009 \times WSR1_F2) - (0.025 \times WSR2_F2) \\ R^2 = & 97.5\% \end{aligned}$$

R2-R3 segment regression formulation:

$$\begin{aligned} \text{Capacity (based on density)} = & (0.528 \times VF1) + (0.484 \times VR1) + (0.517 \times VR2) - (0.114 \times HVF1) \\ & - (0.028 \times HVR1) - (0.035 \times HVR2) - (0.257 \times WSF1_F2) - (0.049 \times WSR1_F2) - (0.096 \times WSR2_F2) \\ R^2 = & 91.3\% \end{aligned}$$

Scenario 8, R2-R3 segment gets in congestion as soon as VF1 passes 5,000 vph, VR1 and VR2 hit 2,000 vph, and either the weaving shares entering R1 or R2 and exiting F2 is 90%, or all heavy vehicle percentages are 10%.

Table 62: Number of Lanes and Gore to Gore Distance for S8

Scenario	Gore to Gore Distances (ft)		Number of Lanes						
	LS1	LS2	F1	R1	R1-R2	R2	R2-R3	R3	F2
S8	1,000	1,500	4	2	6	1	6	2	4

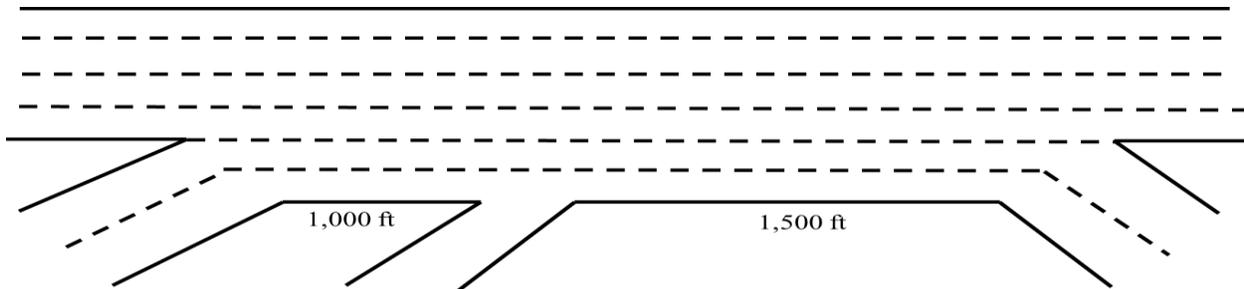


Figure 72: Scenario 8 Lane Geometry

R1-R2 segment regression formulation:

$$\begin{aligned} \text{Capacity (based on density)} = & (0.680 \times VF1) + (0.330 \times VR1) + (0.012 \times VR2) - (0.001 \times HVF1) \\ & + (0.001 \times HVR1) + (0.000 \times HVR2) - (0.025 \times WSF1_F2) + (0.012 \times WSR1_F2) - \\ & (0.001 \times WSR2_F2) \end{aligned}$$

$$R^2 = 100\%$$

R2-R3 segment regression formulation:

$$\begin{aligned} \text{Capacity (based on density)} = & (0.673 \times VF1) + (0.413 \times VR1) + (0.486 \times VR2) - (0.024 \times HVF1) \\ & - (0.008 \times HVR1) + (0.005 \times HVR2) - (0.528 \times WSF1_F2) - (0.083 \times WSR1_F2) \\ & + (0.038 \times WSR2_F2) \end{aligned}$$

$$R^2 = 96.3\%$$

In scenario 11, R1-R2 segment faces congestion when VF1 reaches 7,000 vph, VR1 and VR2 hit 2,000 vph, and the weaving shares entering F1 and exiting at F2 is 90%.

Table 63: Number of Lanes and Gore to Gore Distance for S11

Scenario	Gore to Gore Distances (ft)		Number of Lanes						
	L _{S1}	L _{S2}	F1	R1	R1-R2	R2	R2-R3	R3	F2
S11	1,000	1,500	4	1	4	2	6	2	4

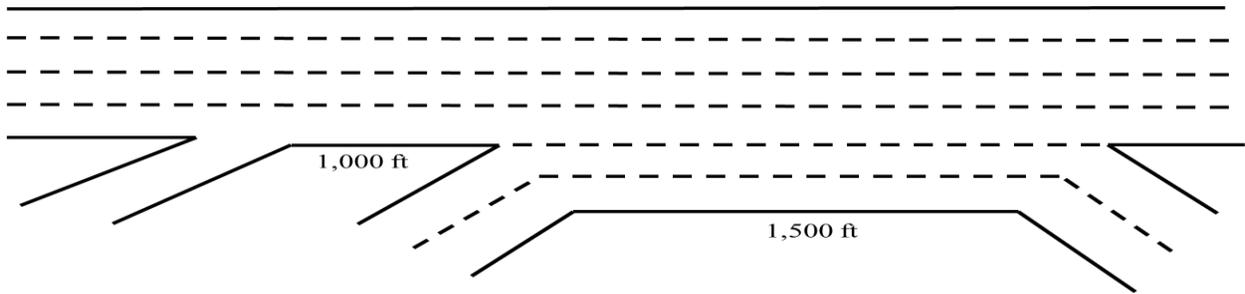


Figure 73: Scenario 11 Lane Geometry

R1-R2 segment regression formulation:

$$\begin{aligned} \text{Capacity (based on density)} = & (0.902 \times VF1) + (0.413 \times VR1) + (0.136 \times VR2) - (0.008 \times HVF1) \\ & - (0.017 \times HVR1) - (0.018 \times HVR2) - (0.192 \times WSF1_F2) - (0.128 \times WSR1_F2) - (0.116 \times WSR2_F2) \end{aligned}$$

$$R^2 = 99.2\%$$

R2-R3 segment regression formulation:

$$\begin{aligned} \text{Capacity (based on density)} = & (0.599 \times VF1) + (0.193 \times VR1) + (0.240 \times VR2) + (0.022 \times HVF1) \\ & - (0.014 \times HVR1) - (0.009 \times HVR2) - (0.002 \times WSF1_F2) - (0.053 \times WSR1_F2) \\ & + (0.029 \times WSR2_F2) \end{aligned}$$

$$R^2 = 99.2\%$$

In scenario 14, congestion is observed for R2-R3 segment if VF1 exceeds 6,000 vph, and VR1 and VR2 go beyond 2,000 vph.

Table 70: Number of Lanes and Gore to Gore Distance for S14

Scenario	Gore to Gore Distances (ft)		Number of Lanes						
	LS1	LS2	F1	R1	R1-R2	R2	R2-R3	R3	F2
S14	1,000	2,000	4	1	5	1	6	2	4

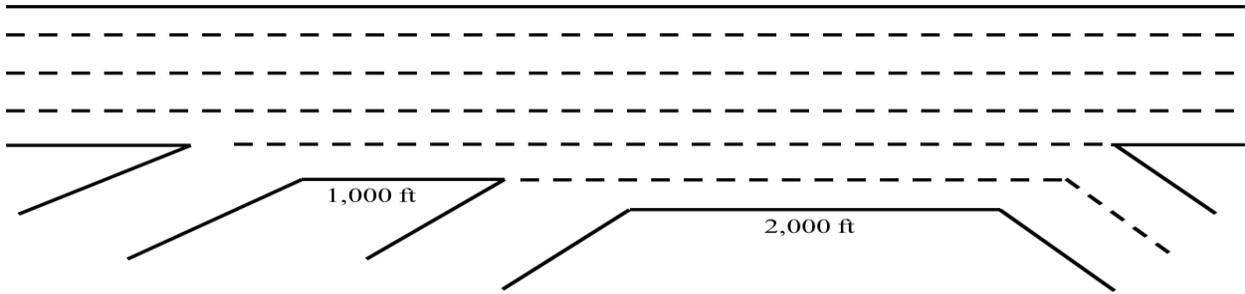


Figure 74: Scenario 14 Lane Geometry

R1-R2 segment regression formulation:

$$\begin{aligned} \text{Capacity (based on density)} = & (0.732 \times VF1) + (0.320 \times VR1) + (0.018 \times VR2) + (0.000 \times HVF1) \\ & + (0.002 \times HVR1) + (0.000 \times HVR2) - (0.062 \times WSF1_F2) - (0.028 \times WSR1_F2) \\ & + (0.022 \times WSR2_F2) \end{aligned}$$

$$R^2 = 99.4\%$$

R2-R3 segment regression formulation:

$$\begin{aligned} \text{Capacity (based on density)} = & (0.855 \times VF1) + (0.329 \times VR1) + (0.365 \times VR2) - (0.018 \times HVF1) \\ & - (0.020 \times HVR1) - (0.012 \times HVR2) - (0.485 \times WSF1_F2) - (0.128 \times WSR1_F2) \\ & + (0.050 \times WSR2_F2) \end{aligned}$$

$$R^2 = 92.6\%$$

Scenario 19; R2-R3 segment experiences congestion when VF1 reaches 6,000 vph, VR1 and VR2 obtain 2,000 vph, and the weaving shares entering R2 and exiting at F2 is 90%.

Table 64: Number of Lanes and Gore to Gore Distance for S19

Scenario	Gore to Gore Distances (ft)		Number of Lanes						
	LS1	LS2	F1	R1	R1-R2	R2	R2-R3	R3	F2
S19	1,000	2,000	4	2	6	1	6	2	4

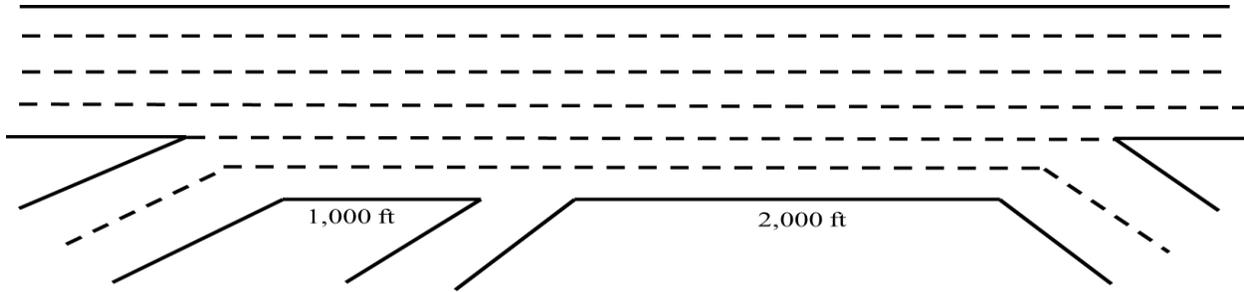


Figure 75: Scenario 19 Lane Geometry

R1-R2 segment regression formulation:

$$\begin{aligned} \text{Capacity (based on density)} = & (0.700 \times VF1) + (0.321 \times VR1) + (0.013 \times VR2) - (0.004 \times HVF1) \\ & - (0.003 \times HVR1) - (0.004 \times HVR2) - (0.026 \times WSF1_F2) + (0.012 \times WSR1_F2) \\ & - (0.003 \times WSR2_F2) \end{aligned}$$

$$R^2 = 99.9\%$$

R2-R3 segment regression formulation:

$$\begin{aligned} \text{Capacity (based on density)} = & (0.786 \times VF1) + (0.294 \times VR1) + (0.333 \times VR2) - (0.041 \times HVF1) \\ & - (0.039 \times HVR1) - (0.030 \times HVR2) - (0.306 \times WSF1_F2) - (0.021 \times WSR1_F2) - (0.014 \times WSR2_F2) \end{aligned}$$

$$R^2 = 95.6\%$$

In scenario 22, R1-R2 segment may experience congestion when F1 leg demand reaches 7,000 vph, VR1 and VR2 demands pass 2,000 vph, and all weaving shares exiting at F2 have the probability of 90%.

Table 65: Number of Lanes and Gore to Gore Distance for S22

Scenario	Gore to Gore Distances (ft)		Number of Lanes						
	LS1	LS2	F1	R1	R1-R2	R2	R2-R3	R3	F2
S22	1,000	2,000	4	1	4	2	6	2	4

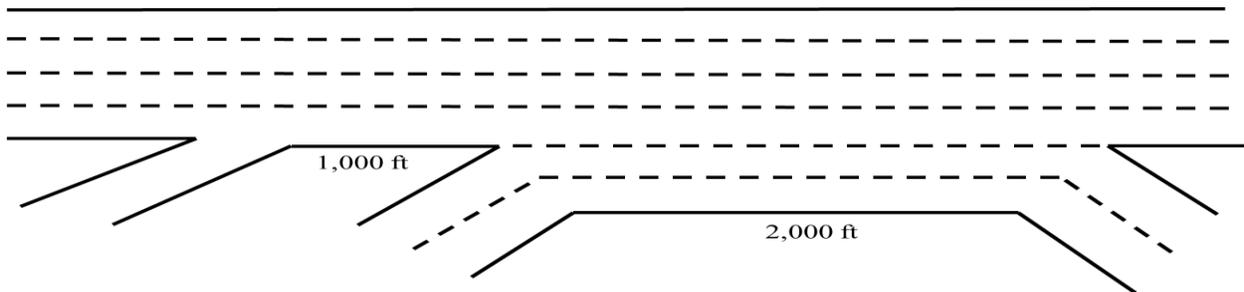


Figure 76: Scenario 22 Lane Geometry

R1-R2 segment regression formulation:

$$\begin{aligned} \text{Capacity (based on density)} = & (0.901 \times VF1) + (0.414 \times VR1) + (0.136 \times VR2) - (0.008 \times HVF1) \\ & - (0.017 \times HVR1) - (0.017 \times HVR2) - (0.192 \times WSF1_F2) - (0.128 \times WSR1_F2) - (0.116 \times WSR2_F2) \end{aligned}$$

$$R^2 = 99.2\%$$

R2-R3 segment regression formulation:

$$\begin{aligned} \text{Capacity (based on density)} = & (0.521 \times VF1) + (0.194 \times VR1) + (0.236 \times VR2) + (0.013 \times HVF1) \\ & - (0.003 \times HVR1) + (0.000 \times HVR2) + (0.060 \times WSF1_F2) - (0.020 \times WSR1_F2) + \\ & (0.012 \times WSR2_F2) \end{aligned}$$

$$R^2 = 99.7\%$$

In scenario 25, R2-R3 segment faces congestion if VF1 passes 5,000 vph, and VR1 and VR2 exceed 2,000 vph.

Table 66: Number of Lanes and Gore to Gore Distance for S25

Scenario	Gore to Gore Distances (ft)		Number of Lanes						
	Ls1	Ls2	F1	R1	R1-R2	R2	R2-R3	R3	F2
S25	1,500	1,500	4	1	5	1	6	2	4

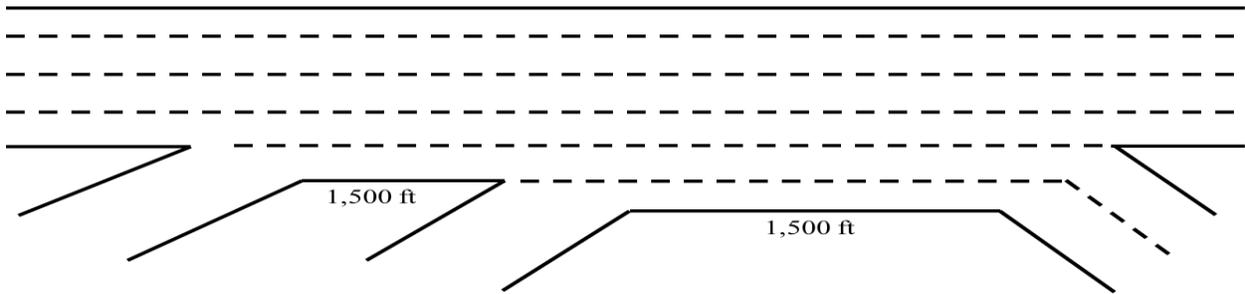


Figure 77: Scenario 25 Lane Geometry

R1-R2 segment regression formulation:

$$\begin{aligned} \text{Capacity (based on density)} = & (0.738 \times VF1) + (0.388 \times VR1) + (0.088 \times VR2) + (0.002 \times HVF1) \\ & + (0.002 \times HVR1) + (0.010 \times HVR2) - (0.192 \times WSF1_F2) \\ & - (0.101 \times WSR1_F2) + (0.508 \times WSR2_F2) \end{aligned}$$

$$R^2 = 98.1\%$$

0.35R2-R3 segment regression formulation:

$$\begin{aligned} \text{Capacity (based on density)} = & (0.727 \times VF1) + (0.605 \times VR1) + (0.644 \times VR2) - (0.011 \times HVF1) \\ & - (0.008 \times HVR1) + (0.003 \times HVR2) - (0.814 \times WSF1_F2) - (0.321 \times WSR1_F2) \\ & + (0.086 \times WSR2_F2) \end{aligned}$$

$$R^2 = 90.8\%$$

Scenario 30; R2-R3 segment touches capacity point for VF1 of more than 6,000 vph, and VR1 and VR2 of more than 2,000 vph.

Table 67: Number of Lanes and Gore to Gore Distance for S30

Scenario	Gore to Gore Distances (ft)		Number of Lanes						
	LS1	LS2	F1	R1	R1-R2	R2	R2-R3	R3	F2
S30	1,500	1,500	4	2	6	1	6	2	4

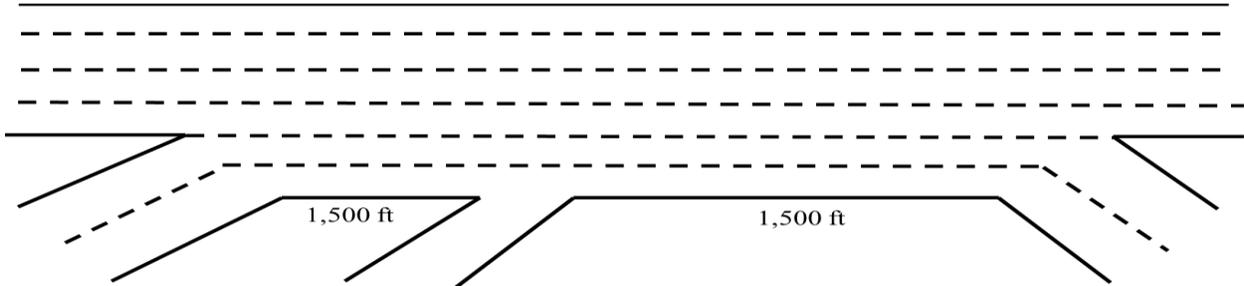


Figure 78: Scenario 30 Lane Geometry

R1-R2 segment regression formulation:

$$\begin{aligned} \text{Capacity (based on density)} = & (0.741 \times VF1) + (0.325 \times VR1) + (0.021 \times VR2) + (0.001 \times HVF1) \\ & - (0.016 \times HVR1) - (0.003 \times HVR2) - (0.053 \times WSF1_F2) - (0.008 \times WSR1_F2) - (0.011 \times WSR2_F2) \\ R^2 = & 98.8\% \end{aligned}$$

R2-R3 segment regression formulation:

$$\begin{aligned} \text{Capacity (based on density)} = & (0.863 \times VF1) + (0.357 \times VR1) + (0.403 \times VR2) - (0.040 \times HVF1) \\ & - (0.047 \times HVR1) - (0.021 \times HVR2) - (0.502 \times WSF1_F2) - (0.118 \times WSR1_F2) \\ & + (0.025 \times WSR2_F2) \\ R^2 = & 91.3\% \end{aligned}$$

Scenario 32 gets in congestion when VF1 passes 5,000 vph, R1 and R2 demands obtain 2,000 vph, and at least one of the weaving shares exiting at F2 is 90%, or one of the heavy vehicle percentages is 10%.

Table 68: Number of Lanes and Gore to Gore Distance for S32

Scenario	Gore to Gore Distances (ft)		Number of Lanes						
	LS1	LS2	F1	R1	R1-R2	R2	R2-R3	R3	F2
S32	1,500	1,500	3	1	3	2	5	2	3

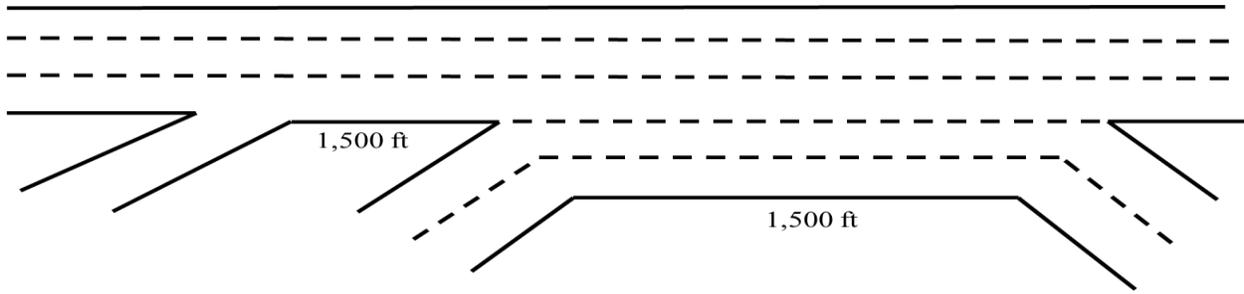


Figure 79: Scenario 32 Lane Geometry

R1-R2 segment regression formulation:

$$\begin{aligned} \text{Capacity (based on density)} = & (0.800 \times VF1) + (0.508 \times VR1) + (0.058 \times VR2) - (0.003 \times HVF1) \\ & - (0.007 \times HVR1) - (0.005 \times HVR2) - (0.254 \times WSF1_F2) - (0.062 \times WSR1_F2) - (0.040 \times WSR2_F2) \\ R^2 = & 99.4\% \end{aligned}$$

R2-R3 segment regression formulation:

$$\begin{aligned} \text{Capacity (based on density)} = & (0.509 \times VF1) + (0.175 \times VR1) + (0.245 \times VR2) + (0.002 \times HVF1) \\ & - (0.002 \times HVR1) + (0.008 \times HVR2) + (0.053 \times WSF1_F2) - (0.018 \times WSR1_F2) \\ & + (0.037 \times WSR2_F2) \end{aligned}$$

$$R^2 = 98.8\%$$

Scenario 33; congestion occurs if F1 demand goes beyond 7,000 vph, VR1 and VR2 hit 2,000 vph, and either all the weaving shares exiting at F2 is 90%, or all the heavy vehicle percentages is 10%.

Table 69: Number of Lanes and Gore to Gore Distance for S33

Scenario	Gore to Gore Distances (ft)		Number of Lanes						
	L _{S1}	L _{S2}	F1	R1	R1-R2	R2	R2-R3	R3	F2
S33	1,500	1,500	4	1	4	2	6	2	4

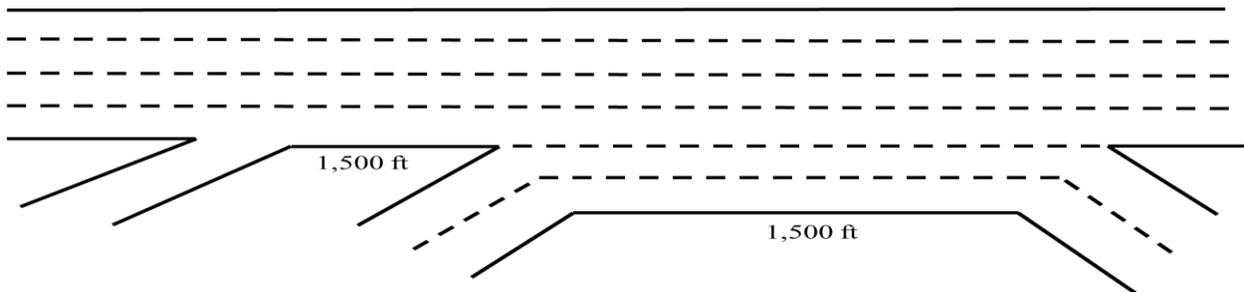


Figure 80: Scenario 33 Lane Geometry

R1-R2 segment regression formulation:

$$\begin{aligned} \text{Capacity (based on density)} = & (0.849 \times VF1) + (0.387 \times VR1) + (0.084 \times VR2) - (0.001 \times HVF1) \\ & - (0.015 \times HVR1) - (0.011 \times HVR2) - (0.128 \times WSF1_F2) - (0.102 \times WSR1_F2) - (0.076 \times WSR2_F2) \\ R^2 = & 99.6\% \end{aligned}$$

R2-R3 segment regression formulation:

$$\begin{aligned} \text{Capacity (based on density)} = & (0.536 \times VF1) + (0.193 \times VR1) + (0.241 \times VR2) + (0.014 \times HVF1) \\ & - (0.001 \times HVR1) + (0.005 \times HVR2) + (0.044 \times WSF1_F2) - (0.029 \times WSR1_F2) \\ & + (0.008 \times WSR2_F2) \end{aligned}$$

$$R^2 = 99.7\%$$

For scenario 36, congestion may be observed on R2-R3 segment if VF1 passes 6,000 vph, VR1 and VR2 exceed 2,000 vph, and all the heavy vehicle percentages are 10%.

Table 70: Number of Lanes and Gore to Gore Distance for S36

Scenario	Gore to Gore Distances (ft)		Number of Lanes						
	LS1	LS2	F1	R1	R1-R2	R2	R2-R3	R3	F2
S36	1,500	2,000	4	1	5	1	6	2	4

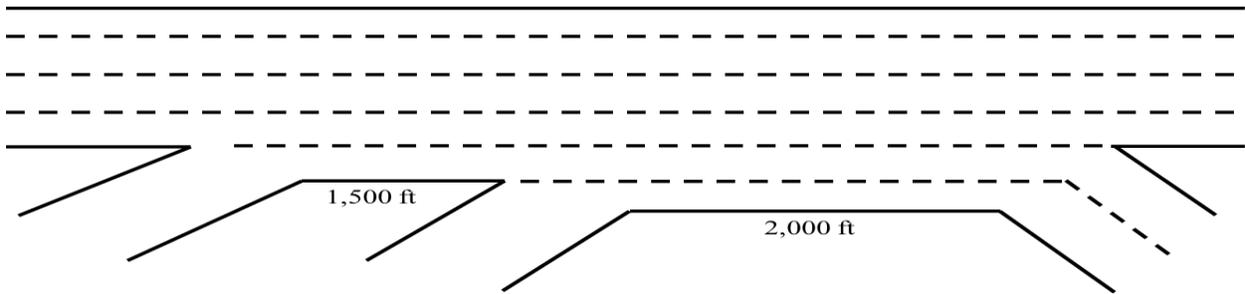


Figure 81: Scenario 36 Lane Geometry

R1-R2 segment regression formulation:

$$\begin{aligned} \text{Capacity (based on density)} = & (0.717 \times VF1) + (0.316 \times VR1) + (0.014 \times VR2) + (0.004 \times HVF1) \\ & - (0.016 \times HVR1) + (0.000 \times HVR2) - (0.034 \times WSF1_F2) - (0.002 \times WSR1_F2) \\ & + (0.003 \times WSR2_F2) \end{aligned}$$

$$R^2 = 99.3\%$$

R2-R3 segment regression formulation:

$$\begin{aligned} \text{Capacity (based on density)} = & (0.832 \times VF1) + (0.351 \times VR1) + (0.381 \times VR2) + (0.000 \times HVF1) \\ & - (0.036 \times HVR1) - (0.017 \times HVR2) - (0.390 \times WSF1_F2) - (0.207 \times WSR1_F2) \\ & + (0.030 \times WSR2_F2) \end{aligned}$$

$$R^2 = 93.8\%$$

Scenario 41; R2-R3 segment gets in congestion when VF1 is more than 6,000 vph, R1 and R2 demands are more than 2,000 vph, at least one of the weaving shares exiting at F2 is 90%, and the heavy vehicle percentages is 10%.

Table 71: Number of Lanes and Gore to Gore Distance for S41

Scenario	Gore to Gore Distances (ft)		Number of Lanes						
	LS1	LS2	F1	R1	R1-R2	R2	R2-R3	R3	F2
S41	1,500	2,000	4	2	6	1	6	2	4

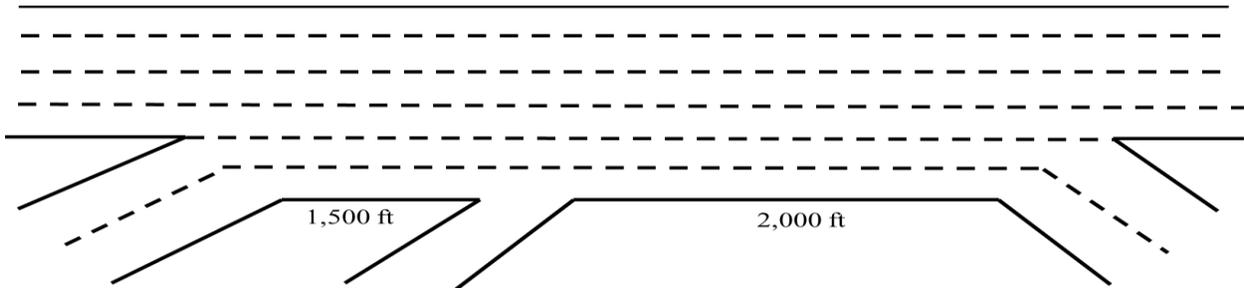


Figure 82: Scenario 41 Lane Geometry

R1-R2 segment regression formulation:

$$\begin{aligned} \text{Capacity (based on density)} = & (0.720 \times VF1) + (0.321 \times VR1) + (0.015 \times VR2) + (0.002 \times HVF1) \\ & - (0.001 \times HVR1) - (0.009 \times HVR2) - (0.035 \times WSF1_F2) + (0.005 \times WSR1_F2) \\ & - (0.014 \times WSR2_F2) \end{aligned}$$

$$R^2 = 99.5\%$$

R2-R3 segment regression formulation:

$$\begin{aligned} \text{Capacity (based on density)} = & (0.758 \times VF1) + (0.286 \times VR1) + (0.329 \times VR2) - (0.029 \times HVF1) \\ & - (0.021 \times HVR1) - (0.041 \times HVR2) - (0.256 \times WSF1_F2) - (0.039 \times WSR1_F2) - (0.027 \times WSR2_F2) \end{aligned}$$

$$R^2 = 94.5\%$$

Scenario 43 faces congestion if VF1 exceeds 6,000 vph, VR1 and VR2 hit 2,000 vph, and all weaving shares exiting F2 is 90%.

Table 72: Number of Lanes and Gore to Gore Distance for S43

Scenario	Gore to Gore Distances (ft)		Number of Lanes						
	LS1	LS2	F1	R1	R1-R2	R2	R2-R3	R3	F2
S43	1,500	2,000	3	1	3	2	5	2	3

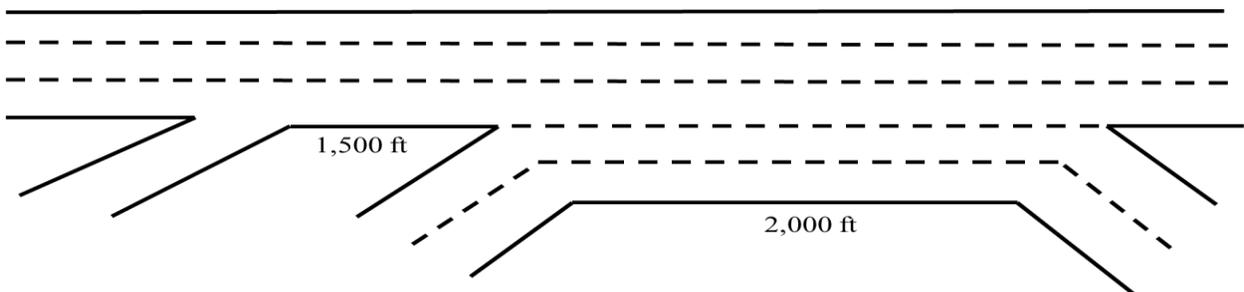


Figure 83: Scenario 43 Lane Geometry

R1-R2 segment regression formulation:

$$\begin{aligned} \text{Capacity (based on density)} = & (0.658 \times VF1) + (0.409 \times VR1) + (0.143 \times VR2) - (0.002 \times HVF1) \\ & - (0.009 \times HVR1) - (0.016 \times HVR2) - (0.076 \times WSF1_F2) - (0.133 \times WSR1_F2) \\ & + (0.011 \times WSR2_F2) \end{aligned}$$

$$R^2 = 97.4\%$$

R2-R3 segment regression formulation:

$$\begin{aligned} \text{Capacity (based on density)} = & (0.389 \times VF1) - (0.053 \times VR1) + (0.568 \times VR2) - (0.021 \times HVF1) \\ & - (0.012 \times HVR1) - (0.021 \times HVR2) + (0.199 \times WSF1_F2) - (0.135 \times WSR1_F2) \\ & + (0.061 \times WSR2_F2) \end{aligned}$$

$$R^2 = 93.2\%$$

Congestion for network 44 will be observed when VF1 is 7,000 vph, and VR1 and VR2 are 2,000 vph.

Table 73: Number of Lanes and Gore to Gore Distance for S44

Scenario	Gore to Gore Distances (ft)		Number of Lanes						
	L _{S1}	L _{S2}	F1	R1	R1-R2	R2	R2-R3	R3	F2
S44	1,500	2,000	4	1	4	2	6	2	4

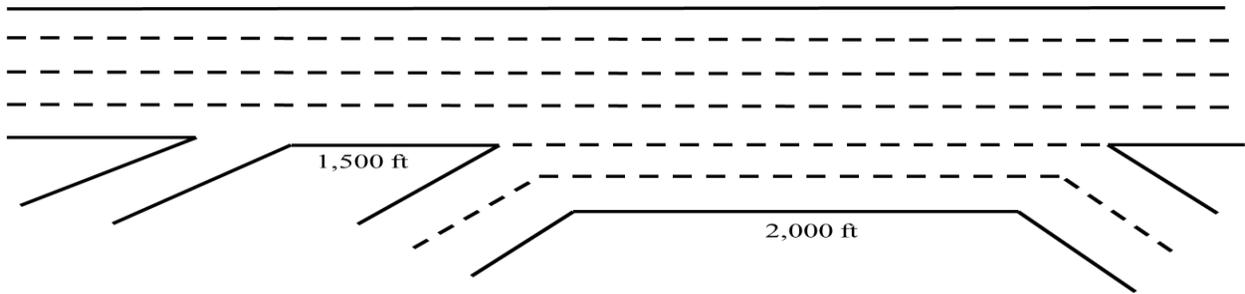


Figure 84: Scenario 44 Lane Geometry

R1-R2 segment regression formulation:

$$\begin{aligned} \text{Capacity (based on density)} = & (0.857 \times VF1) + (0.385 \times VR1) + (0.111 \times VR2) - (0.006 \times HVF1) \\ & - (0.007 \times HVR1) - (0.012 \times HVR2) - (0.163 \times WSF1_F2) - (0.103 \times WSR1_F2) - (0.079 \times WSR2_F2) \end{aligned}$$

$$R^2 = 99.5\%$$

R2-R3 segment regression formulation:

$$\begin{aligned} \text{Capacity (based on density)} = & (0.493 \times VF1) + (0.218 \times VR1) + (0.259 \times VR2) + (0.011 \times HVF1) \\ & - (0.003 \times HVR1) - (0.002 \times HVR2) + (0.029 \times WSF1_F2) + (0.000 \times WSR1_F2) + \\ & (0.008 \times WSR2_F2) \end{aligned}$$

$$R^2 = 99.9\%$$

Significant Factors for Capacity Evaluation: Multiple Weaving Networks

To conclude this chapter, for each segment the most significant factors based on their frequencies is as shown Table 73:

- For R1-R2 segment: (1) VF1 > (2) VR1 > (3) WSR1-F2 & WSF1_F2 > (4) VR2 > (5) WSR2_F2
- For R2-R3 segment: (1) VF1 > (2) VR2 > (3) WSF1-F2 > (4) VR1 > (5) WSR1_F2 > (6) WSR2_F2

Table 73: Significant Factors for Capacity Evaluation

Scenario	Segment	Coefficient									Significant Variables for Capacity
		VF1	VR1	VR2	HVF1	HVR1	HVR2	WSF1_F2	WSR1_F2	WSR2_F2	
S2	R1-R2	0.551	0.535	0.213	0.021	-0.032	-0.042	-0.148	-0.045	-0.096	VF1, VR1
	R2-R3	0.444	0.769	0.879	-0.016	-0.098	-0.082	-0.747	-0.252	-0.023	VF1, VR1, VR2, WSF1_F2
S3	R1-R2	0.676	0.336	0.006	0.003	0.003	0.000	-0.025	0.000	0.012	VF1, VR1
	R2-R3	0.578	0.428	0.500	0.019	0.013	0.024	-0.509	-0.209	-0.151	VF1, VR2, VR1, WSF1_F2
S4	R1-R2	1.271	0.274	0.117	-0.033	-0.080	-0.053	-0.099	-0.254	-0.129	VF1
	R2-R3	0.752	-0.113	0.873	-0.115	-0.069	-0.042	-0.100	-0.321	-0.052	VR2, VF1
S5	R1-R2	1.145	0.320	0.310	-0.137	-0.150	-0.064	0.431	-0.700	-0.374	VF1, WSR1_F2
	R2-R3	1.252	0.238	0.573	-0.128	-0.170	-0.099	0.216	-0.689	-0.380	VF1, VR2, WSR1_F2
S6	R1-R2	1.605	0.627	0.993	-0.043	-0.078	-0.028	-1.145	-0.403	-0.595	VR2, VF1, WSF1_F2
	R2-R3	0.585	0.164	0.264	0.011	-0.002	0.008	0.005	0.041	-0.071	VF1
S7	R1-R2	-0.283	0.414	0.137	-0.004	0.043	0.029	0.218	0.247	0.200	VF1, VR1, WSF1_F2, WSR1_F2, WSR2_F2
	R2-R3	-1.939	0.736	0.828	0.107	0.091	0.010	-0.133	0.508	0.735	VR2, VF1
S8	R1-R2	0.680	0.330	0.012	-0.001	0.001	0.000	-0.025	0.012	0.001	VF1, VR1
	R2-R3	0.673	0.413	0.486	-0.024	-0.008	0.005	-0.528	-0.083	0.038	VF1, VR2, VR1, WSF1_F2
S9	R1-R2	1.247	0.111	0.283	-0.072	-0.062	-0.023	-0.171	-0.348	-0.029	VF1
	R2-R3	0.777	-0.226	0.651	-0.091	-0.106	-0.073	0.740	-0.557	-0.253	VF1, VR2, WSF1_F2, WSR1_F2
S10	R1-R2	0.910	0.582	0.062	0.002	0.005	-0.013	-0.358	-0.112	-0.088	VF1, VR1
	R2-R3	0.549	0.201	0.281	0.000	-0.011	0.005	0.010	-0.035	0.011	VF1
S11	R1-R2	0.902	0.413	0.136	-0.008	-0.017	-0.018	-0.192	-0.128	-0.116	VF1, VR1
	R2-R3	0.599	0.193	0.240	0.022	-0.014	-0.009	-0.002	-0.053	0.029	VF1
S12	R1-R2	0.946	0.091	0.309	-0.058	-0.154	-0.070	0.332	-0.339	-0.211	VF1
	R2-R3	1.054	-0.007	0.657	-0.065	-0.173	-0.093	0.236	-0.478	-0.324	VF1, VR2
S13	R1-R2	0.669	0.376	0.063	0.015	-0.006	0.000	-0.073	-0.019	-0.024	VF1, VR1
	R2-R3	0.529	0.452	0.504	0.009	-0.014	-0.004	-0.328	-0.155	-0.026	VR2, VR1, VF1
S14	R1-R2	0.732	0.320	0.018	0.000	0.002	0.000	-0.062	-0.028	0.022	VF1

	Segment	Coefficient									Significant Variables for Capacity
		VF1	VR1	VR2	HVF1	HVR1	HVR2	WSF1_F2	WSR1_F2	WSR2_F2	
	R2-R3	0.855	0.329	0.365	-0.018	-0.020	-0.012	-0.485	-0.128	0.050	VF1, WSR1_F2
S15	R1-R2	1.155	0.350	0.018	-0.018	-0.039	-0.030	-0.032	-0.186	-0.208	VF1
	R2-R3	0.571	-0.115	0.618	-0.099	0.013	-0.006	-0.038	-0.073	0.081	VR2, VF1
S16	R1-R2	0.888	0.262	0.300	-0.100	-0.153	-0.054	0.271	-0.203	-0.410	VF1
	R2-R3	0.963	0.109	0.521	-0.116	-0.169	-0.056	0.303	-0.358	-0.358	VF1, VR2
S17	R1-R2	1.318	0.857	1.148	0.032	0.005	0.009	-1.450	-0.781	-0.258	VF1, VR2, VR1, WSR1_F2, WSR2_F2
	R2-R3	0.589	0.382	0.492	0.006	-0.008	-0.001	-0.247	-0.100	-0.106	VF1, VR2
S18	R1-R2	0.667	0.354	0.034	-0.023	0.005	-0.007	-0.025	0.007	-0.017	VF1, VR1
	R2-R3	0.541	0.402	0.446	-0.037	-0.014	-0.025	-0.196	-0.062	-0.071	VF1, VR2, VR1
S19	R1-R2	0.700	0.321	0.013	-0.004	-0.003	-0.004	-0.026	0.012	-0.003	VF1
	R2-R3	0.786	0.294	0.333	-0.041	-0.039	-0.030	-0.031	-0.021	-0.014	VF1
S20	R1-R2	1.206	0.258	0.145	-0.069	-0.031	-0.026	-0.372	-0.153	-0.002	VF1
	R2-R3	0.617	-0.063	0.523	-0.078	-0.092	-0.073	0.567	-0.379	-0.123	VF1, VR2, WSR1_F2
S21	R1-R2	0.910	0.582	0.061	0.002	0.005	-0.013	-0.358	-0.112	-0.088	VF1, VR1
	R2-R3	0.527	0.194	0.244	0.006	-0.005	-0.004	0.066	-0.016	0.001	VF1
S22	R1-R2	0.901	0.414	0.136	-0.008	-0.017	-0.017	-0.192	-0.128	-0.116	VF1
	R2-R3	0.521	0.194	0.236	0.013	-0.003	0.000	0.060	-0.020	0.012	VF1, VR2
S23	R1-R2	0.986	0.242	0.393	-0.117	-0.139	-0.131	0.169	-0.363	-0.273	VF1
	R2-R3	1.075	0.257	0.687	-0.178	-0.148	-0.146	-0.030	-0.069	-0.133	VF1, VR2, WSR1_F2
S24	R1-R2	0.664	0.452	0.154	-0.005	-0.507	-0.026	-0.127	-0.081	0.004	VF1, VR1
	R2-R3	0.588	0.758	0.843	-0.030	-0.089	-0.053	-0.693	-0.411	-0.018	VR2, VR1, VF1, WSR1_F2, WSR2_F2
S25	R1-R2	0.738	0.388	0.088	0.002	0.002	0.010	-0.192	-0.101	0.508	VF1, WSR2_F2
	R2-R3	0.727	0.605	0.644	-0.011	-0.008	0.003	-0.814	-0.321	0.086	VF1, VR2, VR1, WSR1_F2
S26	R1-R2	0.738	0.388	0.088	0.002	0.002	0.010	-0.192	-0.101	0.508	VF1
	R2-R3	0.950	-0.300	0.820	-0.044	-0.113	-0.044	-0.124	-0.234	-0.008	VF1, VR2
S27	R1-R2	1.074	0.127	0.198	-0.044	-0.071	-0.065	-0.023	-0.159	-0.082	VF1
	R2-R3	1.039	0.159	0.333	-0.181	-0.189	-0.115	0.455	-0.264	-0.456	VF1, WSR1_F2, WSR2_F2
S28	R1-R2	1.037	0.326	0.029	-0.135	-0.171	-0.113	0.445	-0.219	-0.409	VF1, WSR1_F2, WSR2_F2
	R2-R3	0.656	0.417	0.532	0.018	-0.001	0.013	-0.306	-0.151	-0.172	VF1, VR2, VR1
S29	R1-R2	1.427	0.938	0.734	0.095	0.039	0.057	-1.368	-0.755	-0.270	VF1, VR1, VR2, WSR1_F2, WSR2_F2
	R2-R3	0.421	0.276	0.398	-0.101	-0.063	-0.108	-0.678	0.607	0.281	VF1, VR2, WSR1_F2, WSR2_F2
S30	R1-R2	0.741	0.325	0.021	0.001	-0.016	-0.003	-0.053	-0.008	-0.011	VF1
	R2-R3	0.863	0.357	0.403	-0.040	-0.047	-0.021	-0.502	-0.118	0.025	VF1, VR2, WSR1_F2

Scenario	Segment	Coefficient									Significant Variables for Capacity
		VF1	VR1	VR2	HVF1	HVR1	HVR2	WSF1_F2	WSR1_F2	WSR2_F2	
S31	R1-R2	1.099	0.208	0.279	-0.109	-0.066	-0.066	0.022	-0.346	-0.091	VF1
	R2-R3	0.693	-0.055	0.571	-0.130	-0.164	-0.090	0.621	-0.413	-0.176	VF1, WSF1_F2, VR2, WSR1_F2
S32	R1-R2	0.800	0.508	0.058	-0.003	-0.007	-0.005	-0.254	-0.062	-0.040	VF1, VR1
	R2-R3	0.509	0.175	0.245	0.002	-0.002	0.008	0.053	-0.018	0.037	VF1
S33	R1-R2	0.849	0.387	0.084	-0.001	-0.015	-0.011	-0.128	-0.102	-0.076	VF1
	R2-R3	0.536	0.193	0.241	0.014	-0.001	0.005	0.044	-0.029	0.008	VF1
S34	R1-R2	0.940	0.443	0.288	-0.075	-0.117	-0.106	0.429	-0.710	-0.264	VF1, WSF1_F2, VR1, WSR1_F2
	R2-R3	0.982	0.337	0.467	-0.106	-0.131	-0.145	0.485	-0.882	-0.204	VF1, WSF1_F2, VR2, WSR1_F2
S35	R1-R2	0.663	0.386	0.077	0.005	-0.009	-0.033	-0.048	-0.021	-0.028	VF1, VR1
	R2-R3	0.522	0.501	0.565	-0.021	-0.037	-0.037	-0.323	-0.213	-0.007	VF1, VR2, VR1, WSF1_F2
S36	R1-R2	0.717	0.316	0.014	0.004	-0.016	0.000	-0.034	-0.002	0.003	VF1, VR1
	R2-R3	0.832	0.351	0.381	0.000	-0.036	-0.017	-0.390	-0.207	0.030	VF1
S37	R1-R2	1.010	0.258	0.110	0.007	-0.051	-0.034	-0.139	-0.163	-0.024	VF1
	R2-R3	0.622	-0.075	0.623	-0.058	-0.074	-0.034	0.368	-0.331	-0.108	VR2, VF1
S38	R1-R2	0.868	0.331	0.331	-0.112	-0.099	-0.144	0.135	-0.360	-0.112	VF1, VR1, VR2, WSR1_F2
	R2-R3	0.938	0.194	0.608	-0.132	-0.113	-0.179	0.077	-0.4080	-0.158	VF1, VR2, WSR1_F2
S39	R1-R2	1.330	0.819	0.889	0.092	0.008	0.026	-1.247	-0.803	-0.228	VF1, VR1, VR2, WSF1_F2, WSR1_F2
	R2-R3	0.602	0.353	0.521	0.012	0.001	0.003	-0.259	-0.078	-0.147	VF1, VR, VR1
S40	R1-R2	0.663	0.375	0.070	-0.038	-0.009	-0.008	-0.024	-0.009	-0.025	VF1, VR1
	R2-R3	0.528	0.484	0.517	-0.114	-0.028	-0.035	-0.257	-0.049	-0.096	VF1, VR2, VR1
S41	R1-R2	0.720	0.321	0.015	0.002	-0.001	-0.009	-0.035	0.005	-0.014	VF1
	R2-R3	0.758	0.286	0.329	-0.029	-0.021	-0.041	-0.256	-0.039	-0.027	VF1
S42	R1-R2	1.117	0.285	0.101	-0.014	-0.053	-0.056	-0.082	-0.209	-0.129	VF1
	R2-R3	0.557	0.167	0.550	-0.153	-0.074	-0.081	0.041	-0.325	-0.145	VF1, VR2, WSF1_F2, WSR1_F2
S43	R1-R2	0.658	0.409	0.143	-0.002	-0.009	-0.016	-0.076	-0.133	0.011	VF1, VR1
	R2-R3	0.389	-0.053	0.568	-0.021	-0.012	-0.021	0.199	-0.135	0.061	VR2, VF1
S44	R1-R2	0.857	0.385	0.111	-0.006	-0.007	-0.012	-0.163	-0.103	-0.079	VF1
	R2-R3	0.493	0.218	0.259	0.011	-0.003	-0.002	0.029	0.000	0.008	VF1, VR1, VR2

CHAPTER 4: ANALYTICAL MODELING

Capacity modelling is done in Chapter 4, using the simulation results from Chapter 3. Macroscopic models are created for each scenario. A sensitivity analysis is performed for each model (scenario).

Having the simulation results on hand from chapter 3, in chapter 4, we are analytically modeled the capacity. We use the HCM formulation as guidance and work to present our own equation for capacity at each segment. The same as chapter 3, to determine the capacity, variables are:

- L_{S1} : Gore to gore distances for R1 to R2
- L_{S2} : Gore to gore distances for R2 to R3
- $VF1$: Flow for freeway entrance
- $VR1$: Flow for first entrance ramp
- $VR2$: Flow for second entrance ramp
- $HVF1$: Heavy vehicle percentage for freeway entrance
- $HVR1$: Heavy vehicle percentage for first entrance ramp
- $HVR2$: Heavy vehicle percentage for second entrance ramp
- $WSF1-F2$: Weaving share for drivers entering F1 and exiting at F2
- $WSR1-F2$: Weaving share for drivers entering R1 and exiting at F2
- $WSR2-F2$: Weaving share for drivers entering R2 and exiting at F2
- $F1$: Number of lanes for freeway entrance
- $R1$: Number of lanes for first entrance ramp
- $R2$: Number of lanes for second entrance ramp
- $F2$: Number of lanes for freeway exit
- $R3$: Number of lanes for third exit ramp

R1-R2 refers to the segment between R1 and R2 and R2-R3 refers to the segment between R2 and R3.

The procedure to design, analyze, and evaluate of weaving segments in HCM 2000 consisted of five steps. Space mean speed (SMS) prediction model was developed of weaving and non-weaving segments for different configuration type as well as constrained/unconstrained operations. It developed the model to describe the weaving proportional use of lanes to determine constrained/unconstrained operations. An algorithm was developed to convert predicted speed to an average density. The Level of service criteria were defined based on density. And capacity model was presented (HCM 2000).

HCM 2016 Chapter 13, Freeway Weaving Segments, described a methodology for analyzing freeway weaving segments to estimate their capacity, speed, and density as a function of traffic demand and geometric configuration (HCM 2016).

Recently the Highway Capacity Manual has published chapter 27 as the supplemental chapter for Chapter 13. In terms of operational analysis, chapter 27 (HCM 2016) illustrates various applications of the freeway weaving segments. The procedure for all applications includes (1) convert the demand volumes to flow rates, (2) determine configuration characteristics, (3) determine maximum weaving length, (4) **determine weaving segment capacity** to determine whether LOS F exists, (5) determine lane-changing rates, (6) determine average speeds of weaving and non-weaving vehicles, (7) determine LOS.

The comprehensive analysis has been performed including all the 44 scenarios result. Almost 33,000 data rows are analyzed. Using the following HCM formulas³, capacity equation and effective factors are obtained.

- 1- Convert the four component demand volumes to flow rates under equivalent ideal conditions.
- 2- We assume PHF as 0.9 for all movements.

$$f_{HV} = \frac{1}{1 + P_{HV} (ET - 1)}$$

$$v_i = \frac{V_i}{PHF \times f_{HV}}$$

For example:

$$v_{F1-F2} = \frac{(VF1 \times (WSF1 - F2))(1 + HVF1)}{P_{HV}}$$

We need to calculate v for (F1- F2, R1- F2, R2- F2, R1- R3, R2- R3, and F1- R3).

Weaving Multiplier

We have 11 different lane geometries which repeat for 4 different sets of gore-to-gore distances (total of 44 networks). Lane change behavior is different for R1-R2 and R2-R3 segments for each network. Table 75 shows in which section drivers change lane based on the network geometry. Scenarios on this table are the same as ones in Table 31: Possible Scenarios.

³ Using HCM chapter 27

Table 75: Weaving Multipliers

Scenarios	R1-R2 Segment Weave						R2-R3 Segment Weave					
	V (F1- F2)	V (F1- R3)	V (R1- F2)	V (R1- R3)	V (R2- F2)	V (R2- R3)	V (F1- F2)	V (F1- R3)	V (R1- F2)	V (R1- R3)	V (R2- F2)	V (R2- R3)
S1			*					*	*	*	*	
S2			*					*	*	*	*	
S3			*					*	*	*	*	
S4			*					*	*	*	*	
S5			*	*				*	*	*	*	
S6			*	*				*	*	*	*	
S7			*	*				*	*	*	*	
S8			*	*				*	*	*	*	
S9			*					*	*	*	*	
S10			*					*	*	*	*	
S11			*					*	*	*	*	

For R1-R2 segment:

$$v_W = v_{R1-F2} + v_{R1-R3} \text{ (in some cases)}$$

$$v_{NW} = v_{F1-F2} + v_{F1-R3}$$

For R2-R3 segment:

$$v_W = v_{F1-R3} + v_{R1-F2} + v_{R2-F2} + v_{R1-R3}$$

$$v_{NW} = v_{F1-F2} + v_{R2-R3}$$

v_W and v_{NW} are calculating by considering L_{S1} and L_{S2} . For example, v_{R1-F2} for R1-R2 segment

$$v_{R1-F2} = \frac{L_{S1} * v_{R1-F2}}{(L_{S1} + L_{S2})}$$

$$v = v_W + v_{NW}$$

$$VR = \frac{v_W}{v}$$

Determine Weaving Segment Capacity (C)

Capacity is controlled by density of 43 pcphpl. Using HCM formulation, stepwise regression is utilized to model new equation.

$$C_{IWL}(\text{pcphpl}) = C_{IFL} - [\mathbf{a} (1 + VR)^{\mathbf{b}}] + (\mathbf{c}L_S) + (\mathbf{d}N_{WL})$$

HCM Coefficients:

$$C_{IWL}(\text{pcphpl}) = C_{IFL} - [\mathbf{438.2} (1 + VR)^{\mathbf{1.6}}] + (\mathbf{0.0765} L_S) + (\mathbf{119.8} N_{WL})$$

- C_{IFL} (Ideal freeway capacity per lane): the capacity of a basic freeway segment
 $C_{IFL} = 2,350$ pchpl (for FFS = 65 mph)
- L_S : Gore to gore distance (ft)

Regression model Coefficients:

- ✓ R1-R2 segment:

$$C(\text{pchpl}) = C_{IFL} - [887.330 (1 + VR)^{1.2}] + (0.235 L_S) + (149.491 N_M)$$

- N_M : Sum of minimum number of lane changes from R1 to F2 and R3 and from right most lane from F1.

-

- R2-R3 segment:

$$C(\text{pchpl}) = C_{IFL} - [840.192 (1 + VR)^{1.2}] + (0.053 L_S) + (245.950 N_{WL})$$

- N_{WL} : Number of lanes which weaving movements can be accomplished with one or no lane changes from both entering ramp lanes and from the rightmost freeway lane. (Optional lane changes are considered)

LINEAR REGRESSION ANALYSIS

SPSS Statistics generate quite a few tables of output for a linear regression. In case of obtaining equation using SPSS result, there are three main tables to interpret results from the linear regression procedure.

- 1- The first table of interest is the Model Summary table.

Table 74: Model Summaries

R1-R2 Segment Model Summary

Model	R	R ²	Adj R ²	Std. Error
1	.955 ^a	.912	.911	185.526155149675840

a. Predictors: N_M , L_S , $(1+VR)^{1.2}$

R2-R3 Segment Model Summary

Model	R	R ²	Adj R ²	Std. Error
1	.977 ^a	.955	.954	159.667376644515400

a. Predictors: N_{WL} , L_S , $(1+VR)^{1.2}$

This table provides the R and R^2 values. The R value represents the simple correlation and is 0.955 for R1-R2 segment and 0.977 for R2-R3 segment (the "R" Column), which indicate a high degree of correlation. The R^2 value (the " R^2 " column) indicates how much of the total variation in the dependent variable, Capacity, can be explained by the independent variables, predictors. In this

case, 91.2% for R1-R2 segment and 95.5% for R2-R3 segment can be explained, which are very high.

- 2- The second table is the ANOVA table, which reports how well the regression equation fits the data (i.e., predicts the dependent variable).

Table 75: ANOVA Tables

R1-R2 segment ANOVA^a

Model		Sum of Squares	df	Mean Square	F	Sig.
1	Regression	161116794.675	3	53705598.225	1560.304	.000 ^b
	Residual	15626659.227	454	34419.954		
	Total	176743453.902 ^d	457			

a. Dependent Variable: flow-CIFL

b. Predictors: N_M , L_S , $(1+VR)^{1.2}$

R2-R3 segment ANOVA^a

Model		Sum of Squares	df	Mean Square	F	Sig.
1	Regression	82293818.545	3	27431272.848	1076.003	.000 ^b
	Residual	3849544.346	151	25493.671		
	Total	86143362.891	154			

a. Dependent Variable: flow-CIFL

b. Predictors: N_{WL} , L_S , $(1+VR)^{1.2}$

ANOVA table indicates that the regression model predicts the dependent variable significantly well, in "Regression" row the "Sig." column. This indicates the statistical significance of the regression model that was run. For our modeling, $p < 0.0005$, which is less than 0.05, and indicates that, overall, the regression model statistically significantly predicts the outcome variable (i.e., it is a good fit for the data).

- 3- The Coefficients table provides us with the necessary information to predict Capacity from predictors, as well as determine whether predictors contribute statistically significantly to the model (by looking at the "Sig." column). Furthermore, we can use the values in the "B" column under the "Unstandardized Coefficients" column, as shown below:

Table 76: Coefficient Tables

R1-R2 segment Coefficients

Model		Unstandardized Coefficients		Standardized Coefficients	t	Sig.
		B	Std. Error	Beta		
1	(1+VR)^1.2	-887.330	44.028	-1.801	-20.154	.000
	L _S	.235	.040	.426	5.830	.000
	N _M	149.491	15.512	.460	9.637	.000

R2-R3 segment Coefficients

Model		Unstandardized Coefficients		Standardized Coefficients	t	Sig.
		B	Std. Error	Beta		
1	(1+VR)^1.2	-840.192	69.438	-1.806	-12.100	.000
	L _S	.053	.050	.122	1.063	.290
	N _{WL}	245.950	30.724	.731	8.005	.000

SENSITIVITY ANALYSIS

Sensitivity analysis is the study of how the uncertainty in the output of a mathematical model or system can be divided and allocated to different sources of uncertainty in its inputs.

As, the model we have obtained did not cover all the ranges for VR, we had to show that the predicted model reasonably works for other ranges too. Therefore, we ran the sensitivity analysis. We also wanted to compare against the HCM formulation for a typical weaving segment.

In this research, sensitivity (what-if) analysis has been performed for both segments to determine how capacity is affected based on changes in VR (volume ratio), L_S, and N_{WL}/N_M.

Obtaining from analytical modeling process, the model data is mainly for a 0.2<VR<0.6. Therefore, the sensitivity analysis is done to check the model results for VR values outside that range, 0.1<VR<1.0. Sensitivity analysis results are presented in Figure 88 to 86.

$$VR = \frac{v_W}{v_W + v_{NW}}$$

It is to predict the capacity (pcphpl) given range of variables as below:

- ✚ For all networks, lane drops end in R3.
- ✚ Minimum N_{WL} for R2-R3 segment is 2. It cannot be 1 because we have a minimum of one lane with one or no lane change from entering ramp lanes plus one lane with one or no lane changes from the rightmost freeway lane.
- ✚ N_M range for R1-R2 segment is 0-2
- ✚ L_{S1} range either 1,000ft or 1,500ft while L_{S2} obtains 1,500ft or 2,000ft.
- ✚ L_{S1} in all networks is less than L_{S2}.

For R1-R2 segment, as shown in Figures 85 and 86, N_M is varied 0 to 2. For $N_M=0$, the model capacity is 1,600 to 1,900 pcphpl, for $N_M=1$ is 1,700 to 2,100 pcphpl, and for $N_M=2$, it is 1,800 to 2,200 pcphpl. HCM capacity is around 2,000 pcphpl for $VR < 0.7$.

For R2-R3 segment, for $N_{WL}=2$, model capacity is around 2,100 and for $N_{WL}=3$, model capacity fluctuates around 2,200 pcphpl. HCM capacity is around 2,200 pcphpl for $VR < 0.7$.

As we see for both capacity drops for VR higher than 0.7. In the next section, we present VISSIM result for VR higher than 0.7 which shows the same result as sensitivity analysis result.

R1-R2 Segment Sensitivity Analysis

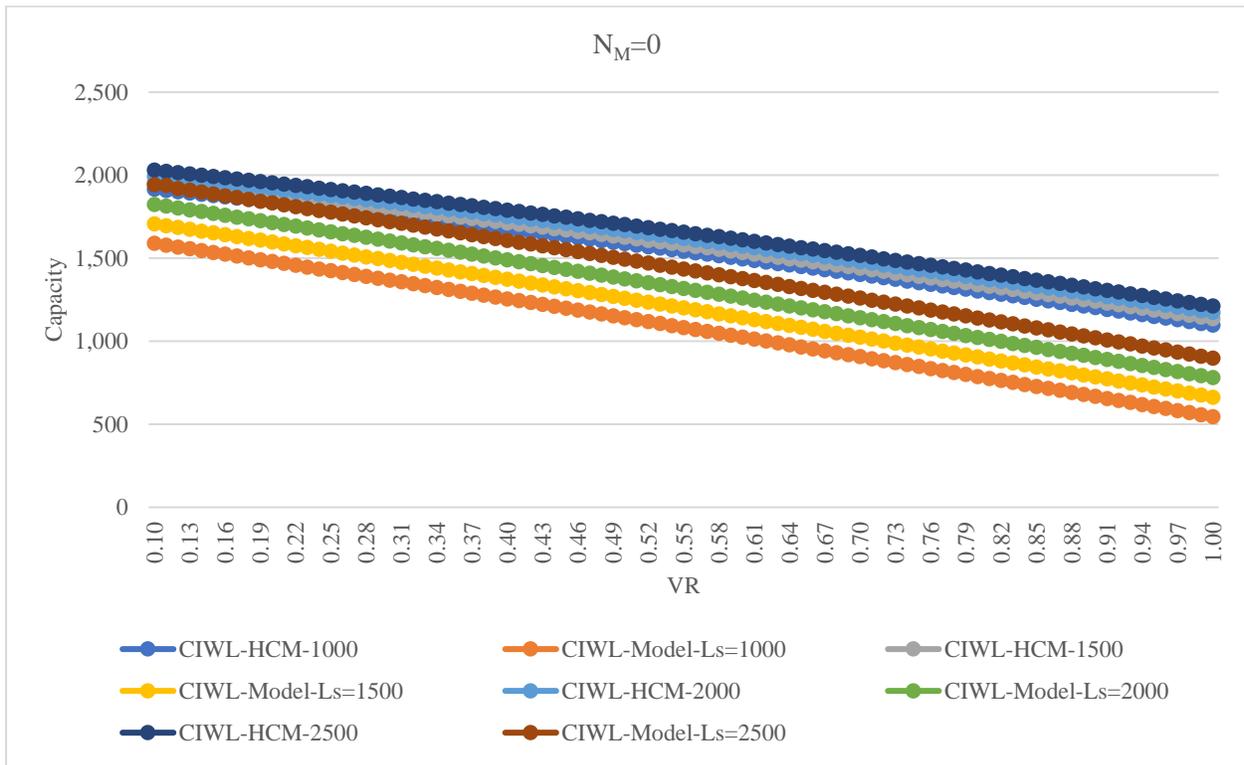


Figure 85: R1-R2 Segment- Sensitivity Analysis for $N_M=0$

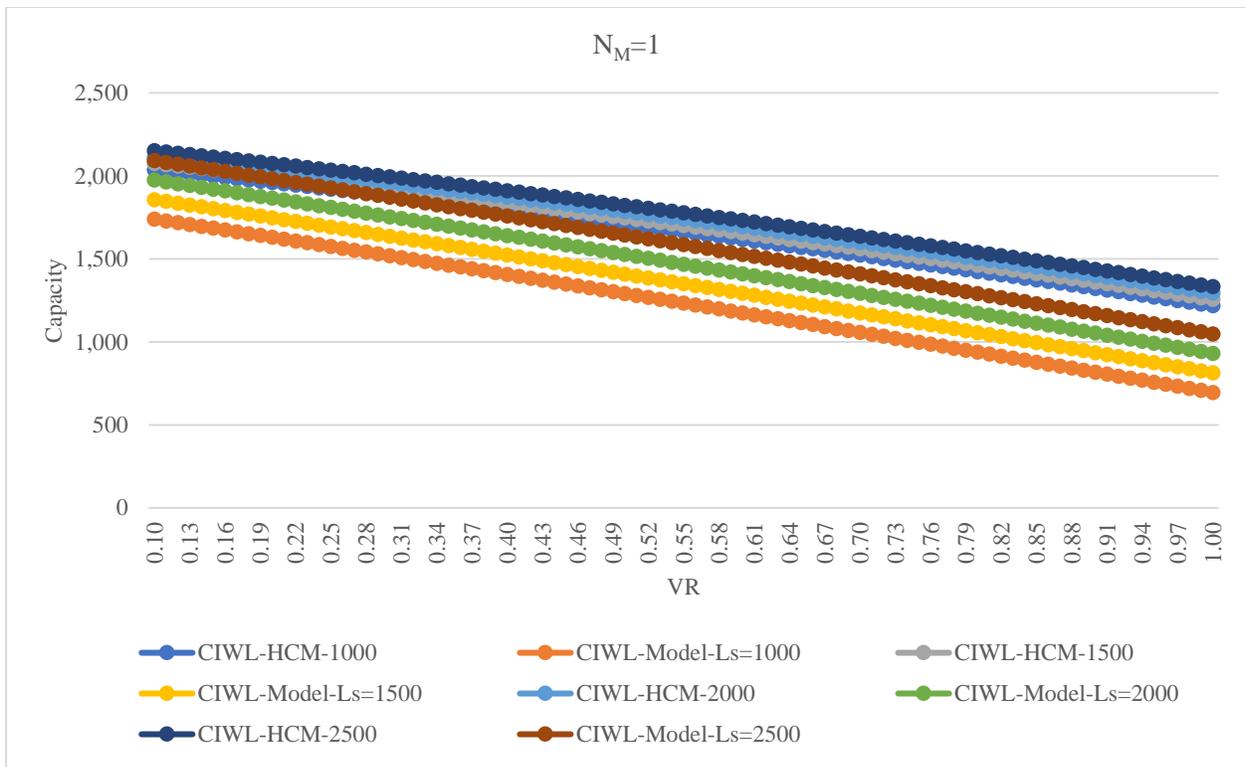


Figure 86: R1-R2 Segment- Sensitivity Analysis for $N_M=1$

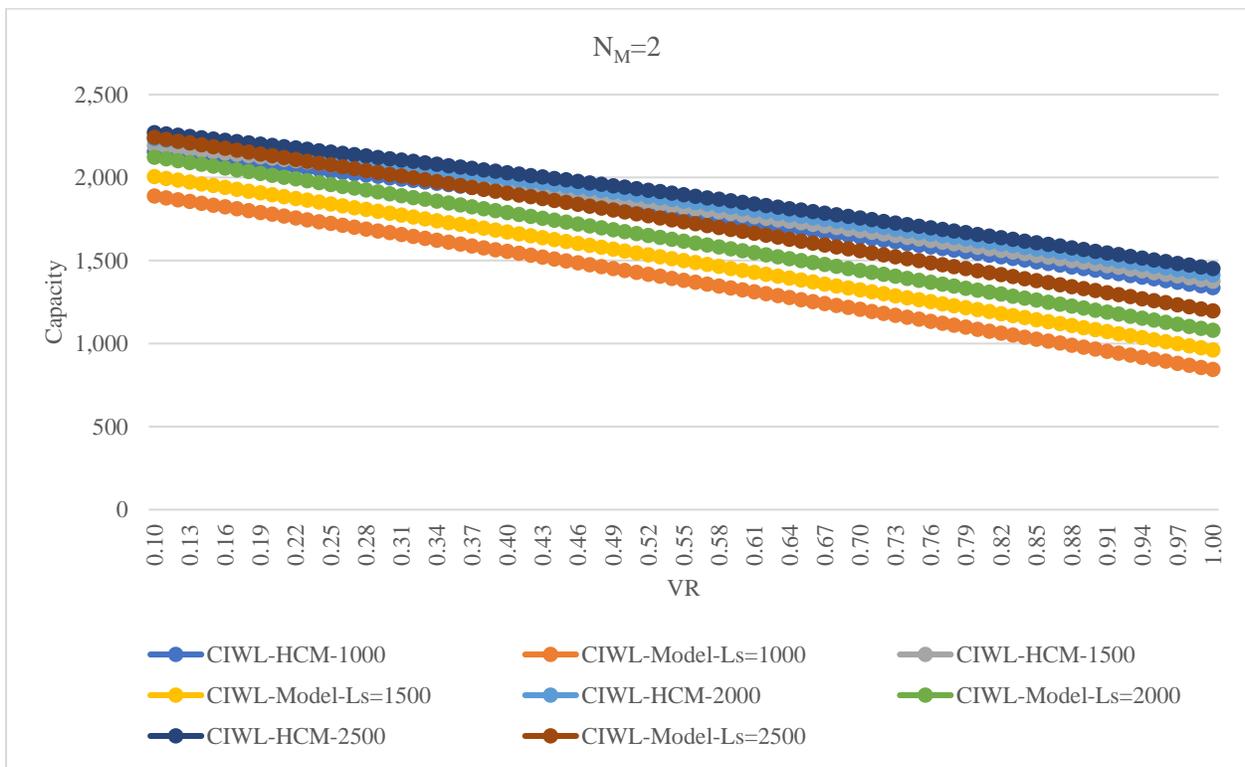


Figure 87: R1-R2 Segment- Sensitivity Analysis for $N_M=2$

R2-R3 Segment Sensitivity Analysis

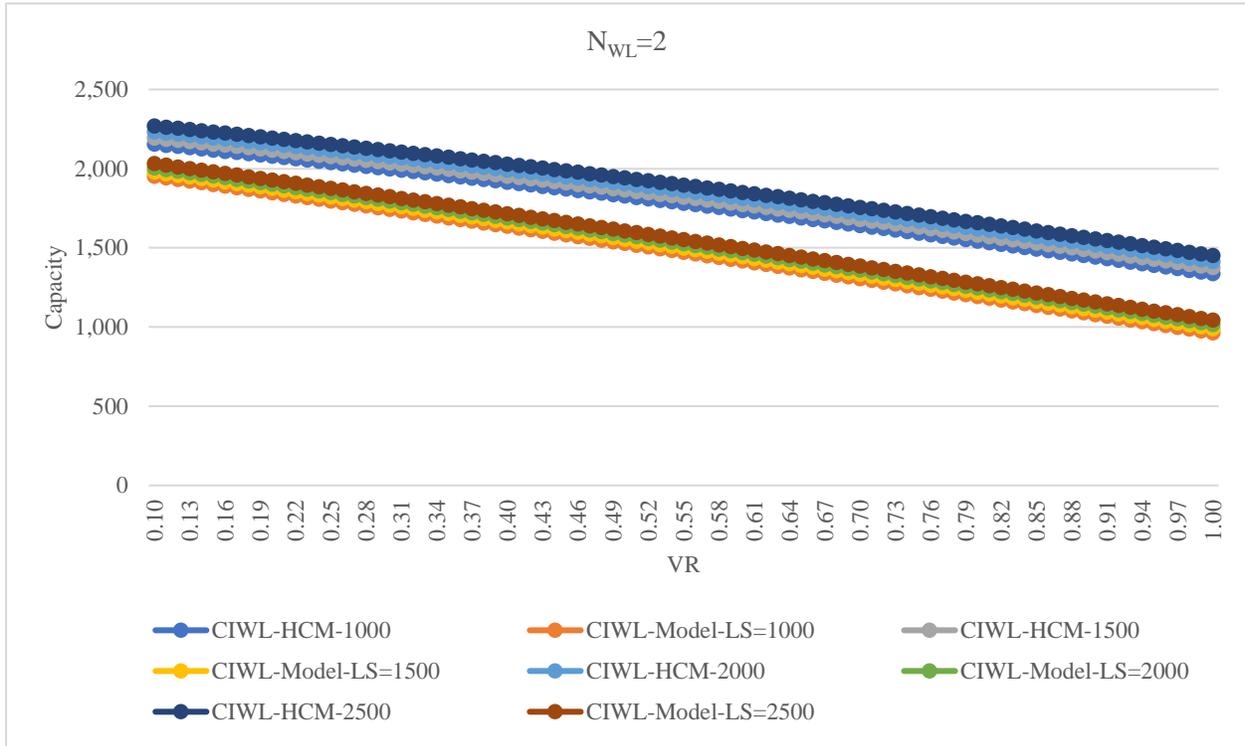


Figure 88: R2-R3 Segment- Sensitivity Analysis for $N_{WL}=2$

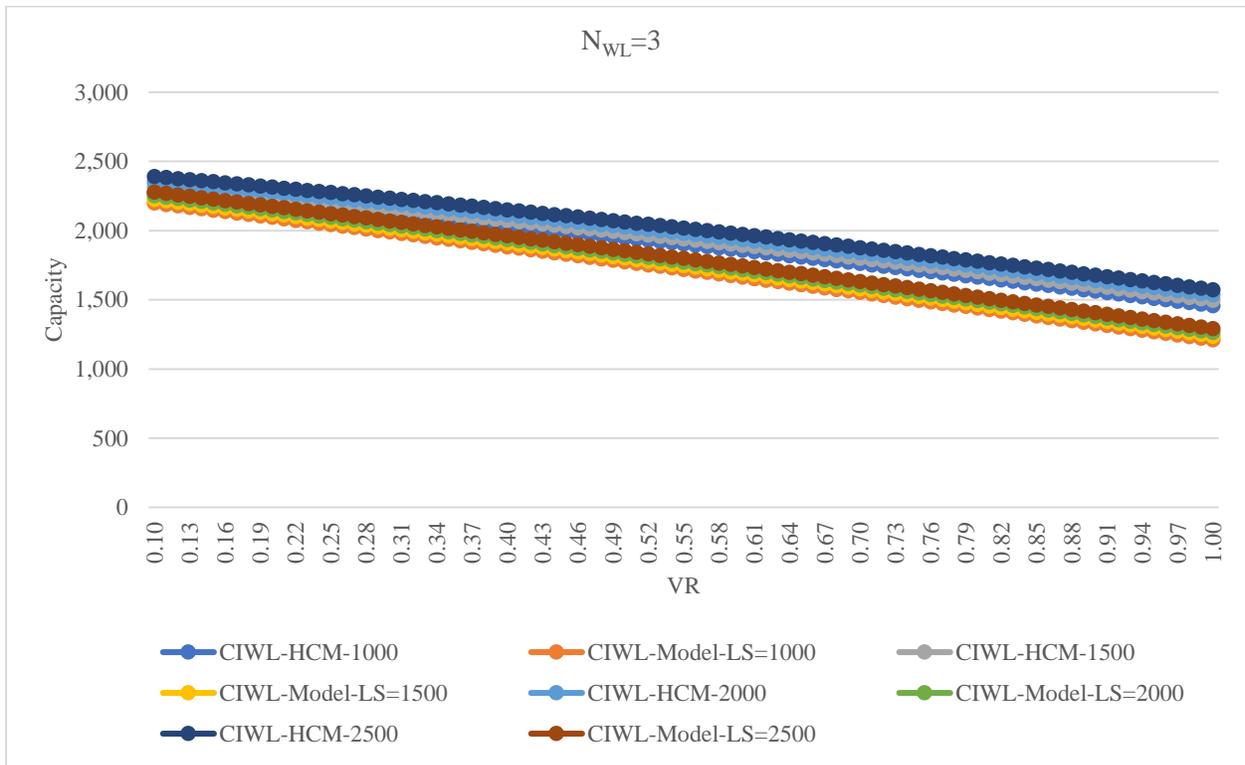


Figure 89: R2-R3 Segment- Sensitivity Analysis for $N_{WL}=3$

EXTENDED VR

Based on sensitivity analysis result, for VR higher than 0.7, capacity drops to 500 pcphpl for R1-R2 segment and to 1,000 pcphpl for R2-R3 segment. Therefore, more simulation has been run with high VR to see if we get the same capacity in VISSIM as we expect through sensitivity analysis. VISSIM results turned out to be the same as sensitivity analysis results. For R1-R2 segment, capacity drops to around 500 pcphpl if we increase VR up to 95% (Table). For R2-R3 segment, capacity drops to around 1,000 pcphpl if we increase VR more than 0.7, up to 95% (Table).

Table 79: R1-R2 Segment, VR Higher Than 0.7

VW	VNW	VR	(1+VR) ^1.2	R1-R2 Flow (pcphpl)	Model Capacity
4,644	244	0.95	2.23	946	608
4,644	244	0.95	2.23	920	608
5,133	367	0.93	2.21	1,057	628
5,133	367	0.93	2.21	977	628
6,233	489	0.93	2.20	865	635
6,233	489	0.93	2.20	839	635
9,044	733	0.93	2.19	846	638
9,044	733	0.93	2.19	716	638
7,333	611	0.92	2.19	986	640
7,333	611	0.92	2.19	830	640
5,561	550	0.91	2.17	1,039	656
5,561	550	0.91	2.17	893	656
6,356	978	0.87	2.11	911	709
6,356	978	0.87	2.11	833	709
7,333	1,222	0.86	2.10	893	720
7,333	1,222	0.86	2.10	725	720
6,294	1,650	0.79	2.01	1,017	798
6,294	1,650	0.79	2.01	938	798
4,828	1,283	0.79	2.01	1,160	801
4,828	1,283	0.79	2.01	1,149	801
5,256	1,467	0.78	2.00	1,199	810
5,256	1,467	0.78	2.00	1,102	810

Table 80: R2-R3 Segment, VR Higher Than 0.7

VW	VNW	VR	(1+VR) ^1.2	R2-R3 Flow (pcphpl)	Model Capacity
6,844	489	0.93	2.21	720	1,042
6,844	489	0.93	2.21	866	1,042
6,844	489	0.93	2.21	871	1,042
6,844	489	0.93	2.21	870	1,042
6,844	489	0.93	2.21	818	1,042
7,883	672	0.92	2.19	865	1,055
7,883	672	0.92	2.19	982	1,055

VW	VNW	VR	(1+VR) ^1.2	R2-R3 Flow (pcphpl)	Model Capacity
7,883	672	0.92	2.19	1,179	1,055
7,883	672	0.92	2.19	821	1,055
7,883	672	0.92	2.19	950	1,055
7,883	672	0.92	2.19	597	1,055
7,639	917	0.89	2.15	899	1,088
7,639	917	0.89	2.15	1,080	1,088
7,639	917	0.89	2.15	774	1,088
7,639	917	0.89	2.15	1,027	1,088
7,639	917	0.89	2.15	706	1,088

MOST SIGNIFICANT FLOWS

To find the most effective flows among V(F1-F2), V(F1-R3), V(R1-F2), V(R1-R3), V(R2-F2), and V(R2-R3), each of them has been removed and sensitivity analysis is performed to see the effect. Results show that V(F1-F2) is the most significant flow factor for capacity evaluation.

Results have been presented in detail in Appendix C.

OUTCOMES

Significant Factors Affecting Capacity: Multiple Weaving Networks (VR<0.7)

1- VF1: Flow for freeway entrance

2(tie)- VR1: Flow for first entrance ramp

2(tie)- VR2: Flow for second entrance ramp

3(tie)- WSF1-F2: Weaving share for drivers entering F1 and exiting at F2

3(tie)- WSR1-F2: Weaving share for drivers entering R1 and exiting at F2

4- WSR2-F2: Weaving share for drivers entering R2 and exiting at F2

Weaving Segment Capacity

✓ R1-R2 segment:

$$C(\text{pcphpl}) = C_{IFL} - [887.330 (1 + VR)^{1.2}] + (0.235 L_S) + (149.491 N_M)$$

N_M : Sum of minimum number of lane changes from R1 to F2 and R3 and from right most lane from F1.

✓ R2-R3 segment:

$$C(\text{pcphpl}) = C_{IFL} - [840.192 (1 + VR)^{1.2}] + (0.053 L_S) + (245.950 N_{WL})$$

N_{WL} : Number of lanes which weaving movements can be accomplished with one or no lane changes from both entering ramp lanes and from the rightmost freeway lane. (Optional lane changes are considered)

In this chapter, the capacity was modelled for each scenario, using the simulation results from Chapter 3. Macroscopic models were created for each scenario. A sensitivity analysis was performed for each model (scenario).

CHAPTER 5: SUMMARY

Systematic, well-designed research provides the most effective approach to the solution of many problems facing highway administrators and engineers. Traffic congestion on freeway systems is one significant concern in urban areas throughout the U.S.A. In this era, building new freeways to reduce congestion is less feasible due to the high capital and social costs. Thus, the effective management and operation of existing freeway facilities has become a preferred approach to reduce traffic congestion.

On the other hand, A weaving section is a common design on major highway facilities that always has been an interest to researchers. Weaving areas are characterized by frequent lane changes, which significantly reduce the capacity of the freeway system. These common design elements are located between merge and diverge points, near ramps where a lane is added or dropped, and at multilane ramps.

Traffic demands exceeding segment capacity at weaving areas cause congestion, which affects the operation of the entire freeway section. Traffic operation problems often exist at weaving areas even when traffic demands are less than capacity and may be experienced at lower traffic flows because of the complexity of vehicle interactions, that is, increased lane changing, resulting in a degradation in level of service (LOS) and potential safety problems [1].

A significant amount of research has been done to estimate capacity in weaving sections. However, little has been done to address multiple weaves. This work examines capacity for a specific example of a multiple weave. Capacity is evaluated through micro-simulation by gradually raising flows for a range of geometric and fraction of weaving-traffic conditions. Models are developed to express capacity in terms of lane configuration, flow ratios, traffic mix (heavy traffic percentages), and overall flow rate.

This work has examined capacity for a specific example of a multiple weave. Capacity is evaluated through micro-simulation (VISSIM) by gradually increasing flows for a range of geometric and fraction of weaving-traffic conditions. The simulation model is first calibrated, using a data set for a freeway weave section in Arlington, Texas. Models are developed to express capacity in terms of lane configuration, flow ratios, traffic mix (heavy traffic percentages), and overall flow rate.

This study is limited to cases where there are two overlapping weaving movements created by two entry ramps following by an exit ramp.

The study developed relations for capacity and service volume for a range of geometric, flow conditions, and traffic mix. Geometric conditions will include number of lanes on the main lane entry and each entrance ramp into and exit ramp from the weaving area (n), and distances (LS) between ramps. Flow conditions will include a range of flows from each of the entry and exit roadways (V) in the multiple weaving area. The traffic mix represents the fraction of heavy vehicles in the traffic stream (PHV).

Results show that most significant factors affecting capacity of multiple weaving networks while $VR < 0.7$ (VR : Volume Ratio) are going to be $VF1$: Flow for freeway entrance, $VR1$: Flow for first entrance ramp, $VR2$: Flow for second entrance ramp, $WSF1-F2$: Weaving share for drivers

entering F1 and exiting at F2, WSR1-F2: Weaving share for drivers entering R1 and exiting at F2, and WSR2-F2: Weaving share for drivers entering R2 and exiting at F2, respectively.

Also using this research result, unique equations have been developed for multiple weaving areas, having VR (Volume Ratio), and L_S (gore to gore length).

Weaving Segment Capacity

✓ R1-R2 segment:

$$C(\text{pcphpl}) = C_{IFL} - [887.330 (1 + VR)^{1.2}] + (0.235 L_S) + (149.491 N_M)$$

N_M : Sum of minimum number of lane changes from R1 to F2 and R3 and from right most lane from F1.

✓ R2-R3 segment:

$$C(\text{pcphpl}) = C_{IFL} - [840.192 (1 + VR)^{1.2}] + (0.053 L_S) + (245.950 N_{WL})$$

N_{WL} : Number of lanes which weaving movements can be accomplished with one or no lane changes from both entering ramp lanes and from the rightmost freeway lane. (Optional lane changes are considered)

This work's result will be presented to DOTs and MPOs. The file would be highly useful and money-saving for these agencies as they prefer to obtain higher capacity by managing existing freeways rather than buying right of ways.

REFERENCES

- Ahmed, Ishtiak, Dezhong Xu, Nagui Roupail, and Alan Karr. 2019. “Lane Change Rates at Freeway Weaving Sites: Trends in HCM6 and from NGSIM Trajectories.” *Transportation Research Record* 2673 (5): 627–36. <https://doi.org/10.1177/0361198119841281>.
- Al-jameel, Hamid A E. n.d. “Empirical Features of Weaving Sections,” 12.
- Department of Transportation Engineering Technology, Faculty of Engineering Technology, Universiti Tun Hussein Onn Malaysia, Johor, Malaysia, Joewono Prasetijo, Ishak Baba, Department of Transportation Engineering Technology, Faculty of Engineering Technology, Universiti Tun Hussein Onn Malaysia, Johor, Malaysia, Narain s/o Muthukrisnan, Department of Infrastructure and Geomatic Engineering, Faculty of Civil and Environmental Engineering, Universiti Tun Hussein Onn Malaysia, Johor, Malaysia, Nurul Elena Atasha Arifin, et al. 2018. “Analysis of Maximum Weaving Length and Lane-Changing Rate for 2-Sided Weaving Section for Federal Road FT050 Based on HCM 2010.” *International Journal of Integrated Engineering* 10 (2). <https://doi.org/10.30880/ijie.2018.10.02.011>.
- Eads, Brian S., Nagui M. Roupail, Adolf D. May, and Fred Hall. 2000. “Freeway Facility Methodology in Highway Capacity Manual 2000.” *Transportation Research Record* 1710 (1): 171–80. <https://doi.org/10.3141/1710-20>.
- FHA. (2019). Guidelines for Applying Traffic Microsimulation Modeling Software. U.S. Department of Transportation. Retrieved from https://ops.fhwa.dot.gov/trafficanalysistools/tat_vol3/sect5.htm
- Fitzpatrick, Kay, Richard J. Porter, Geza Pesti, Chi-Leung Chu, Eun Sug Park, and Thanh Le. 2011. “Guidelines for Spacing between Freeway Ramps.” *Transportation Research Record* 2262 (1): 3–12. <https://doi.org/10.3141/2262-01>.
- Guo, Yi, Changju Lee, Jiaqi Ma, David K. Hale, and Joe Bared. 2020. “Evaluating Operational Efficiency of Split Merge, Diverge, and Weaving Solutions for Reducing Freeway Bottleneck Congestion.” *Transportation Letters*, February, 1–13. <https://doi.org/10.1080/19427867.2020.1725260>.
- Hidas, Peter. 2005. “Modelling Vehicle Interactions in Microscopic Simulation of Merging and Weaving.” *Transportation Research Part C: Emerging Technologies* 13 (1): 37–62. <https://doi.org/10.1016/j.trc.2004.12.003>.
- Jolovic, Dusan, Aleksandar Stevanovic, Soheil Sajjadi, and Peter T. Martin. 2016. “Assessment of Level-Of-Service for Freeway Segments Using HCM and Microsimulation Methods.” *Transportation Research Procedia* 15: 403–16. <https://doi.org/10.1016/j.trpro.2016.06.034>.

- Kwon, Eil, Rich Lau, and James Aswegan. 2000. "Maximum Possible Weaving Volume for Effective Operations of Ramp-Weave Areas: Online Estimation." *Transportation Research Record* 1727 (1): 132–41. <https://doi.org/10.3141/1727-17>.
- Leclercq, Ludovic, Florian Marczak, Victor L. Knoop, and Serge P. Hoogendoorn. 2016. "Capacity Drops at Merges: Analytical Expressions for Multilane Freeways." *Transportation Research Record: Journal of the Transportation Research Board* 2560 (1): 1–9. <https://doi.org/10.3141/2560-01>.
- Ler2rawanich, Ponlathap, and Lily Elefteriadou. 2003. "A Methodology for Estimating Capacity at Ramp Weaves Based on Gap Acceptance and Linear Optimization." *Transportation Research Part B: Methodological* 37 (5): 459–83. [https://doi.org/10.1016/S0191-2615\(02\)00024-3](https://doi.org/10.1016/S0191-2615(02)00024-3).
- Leyn, Ulrike, and Peter Vortisch. 2015. "Calibrating VISSIM for the German Highway Capacity Manual." *Transportation Research Record* 2483 (1): 74–79. <https://doi.org/10.3141/2483-09>.
- Liu, Xiaoyue Cathy, Yin Hai Wang, Bastian J. Schroeder, and Nagui M. Roupail. 2012. "Quantifying Cross-Weave Impact on Capacity Reduction for Freeway Facilities with Managed Lanes." *Transportation Research Record* 2278 (1): 171–79. <https://doi.org/10.3141/2278-19>.
- Marczak, Florian, Ludovic Leclercq*, and Christine Buisson. 2015. "A Macroscopic Model for Freeway Weaving Sections." *Computer-Aided Civil and Infrastructure Engineering* 30 (6): 464–77. <https://doi.org/10.1111/mice.12119>.
- Minderhoud, M. M., and L. Elefteriadou Elefteriadou. 2003. "Freeway Weaving: Comparison of Highway Capacity Manual 2000 and Dutch Guidelines." *Transportation Research Record* 1852 (1): 10–18. <https://doi.org/10.3141/1852-02>.
- Pignataro, Louis J., American Association of State Highway and Transportation Officials, and United States, eds. 1975. *Weaving Areas: Design and Analysis*. Report - National Cooperative Highway Research Program; 159. Washington: Transportation Research Board, National Research Council.
- Qi, Yi, Yubian Wang, Xiaoming Sammy Chen, Ruey Long Cheu, Lei Yu, and Hualiang Teng. 2018. "Methods of Dropping Auxiliary Lanes at Freeway Weaving Segments." *Transportation Planning and Technology* 41 (4): 389–401. <https://doi.org/10.1080/03081060.2018.1453462>.
- Rakha, Hesham, and Yihua Zhang. 2006. "Analytical Procedures for Estimating Capacity of Freeway Weaving, Merge, and Diverge Sections." *Journal of Transportation Engineering* 132 (8): 618–28. [https://doi.org/10.1061/\(ASCE\)0733-947X\(2006\)132:8\(618\)](https://doi.org/10.1061/(ASCE)0733-947X(2006)132:8(618)).

- Roess, Roger P., and Jose M. Ulerio. 2000. "Weaving Area Analysis in Year 2000 Highway Capacity Manual." *Transportation Research Record* 1710 (1): 145–53. <https://doi.org/10.3141/1710-17>.
- 2009a. "Capacity of Freeway Weaving Segments." *Transportation Research Record* 2130 (1): 34–41. <https://doi.org/10.3141/2130-05>.
- 2009b. "Level of Service Analysis of Freeway Weaving Segments." *Transportation Research Record* 2130 (1): 25–33. <https://doi.org/10.3141/2130-04>.
- Sajjadi, Soheil, Bastian Schroeder, and Nagui M. Roupail. 2013. "Enhancements to the Freeway Facilities Method in the Highway Capacity Manual to Enable Reliability Analysis." *Transportation Research Record* 2395 (1): 21–30. <https://doi.org/10.3141/2395-03>.
- Shi, Liang, and Panos Prevedouros. 2016. "Autonomous and Connected Cars: HCM Estimates for Freeways with Various Market Penetration Rates." *Transportation Research Procedia* 15: 389–402. <https://doi.org/10.1016/j.trpro.2016.06.033>.
- Skabardonis, Alexander. 2002. "Simulation of Freeway Weaving Areas." *Transportation Research Record* 1802 (1): 115–24. <https://doi.org/10.3141/1802-14>.
- Skabardonis, Alexander, and Eleni Christofa. 2012. "EVALUATION OF METHODOLOGIES FOR THE DESIGN AND ANALYSIS OF FREEWAY WEAVING SECTIONS," 9.
- Skabardonis, Alexander, and Michael Mauch. 2015. "Evaluation of Methodologies for Analyzing Freeway Ramp Weaving." *Transportation Research Record* 2483 (1): 130–39. <https://doi.org/10.3141/2483-15>.
- Tilg, Gabriel, Kaidi Yang, and Monica Menendez. 2018. "Evaluating the Effects of Automated Vehicle Technology on the Capacity of Freeway Weaving Sections." *Transportation Research Part C: Emerging Technologies* 96 (November): 3–21. <https://doi.org/10.1016/j.trc.2018.09.014>.
- PTV VISSIM 10 USER MANUAL. (2018). Germany: PTV Group. Retrieved from <https://usermanual.wiki/Document/Vissim20102020Manual.1098038624.pdf>.
- Vo, Phong Thanh. 2007. "CAPACITY ESTIMATION OF 2-SIDED TYPE C WEAVES ON FREEWAYS," 266.
- Xu, Dezhong, Nagui M. Roupail, Behzad Aghdashi, Ishtiaq Ahmed, and Lily Elefteriadou. 2020. "Modeling Framework for Capacity Analysis of Freeway Segments: Application to Ramp Weaves." *Transportation Research Record* 2674 (1): 148–59. <https://doi.org/10.1177/0361198119900157>.

- Yang, Chao, Changqiao Shao, and Liqin Liu. 2012. “Study on Capacity of Urban Expressway Weaving Segments.” *Procedia - Social and Behavioral Sciences* 43: 148–56. <https://doi.org/10.1016/j.sbspro.2012.04.087>.
- Yang, Chulsu, Stephen P. Mattingly, James C. Williams, and Hyunwoong Kim. 2011. “Development of Managed-Lane Access Guidelines Based on Gap Acceptance Theory.” *Transportation Research Record* 2257 (1): 95–102. <https://doi.org/10.3141/2257-11>.
- Zhang, Yihua, and Hesham Rakha. 2004. *Systematic Analysis of Weaving Section Capacity*.

APPENDIX A; POSSIBLE LANE GEOMETRIES

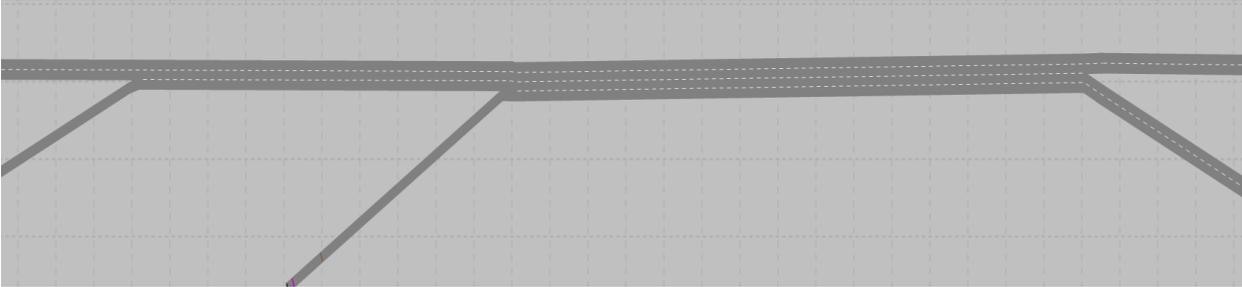


Figure 90: Lane Geometry Schematic Number 1

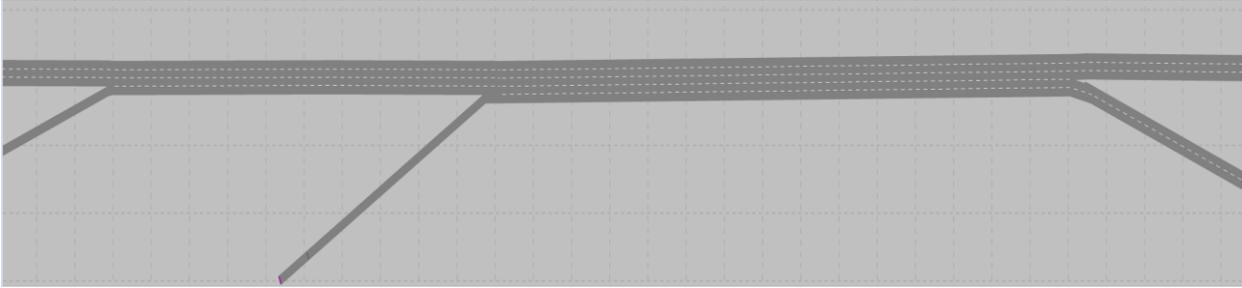


Figure 91: Lane Geometry Schematic Number 2

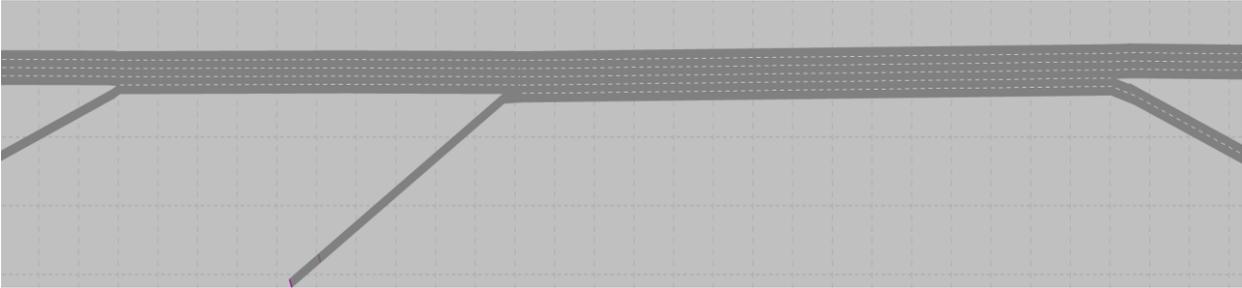


Figure 92: Lane Geometry Schematic Number 3

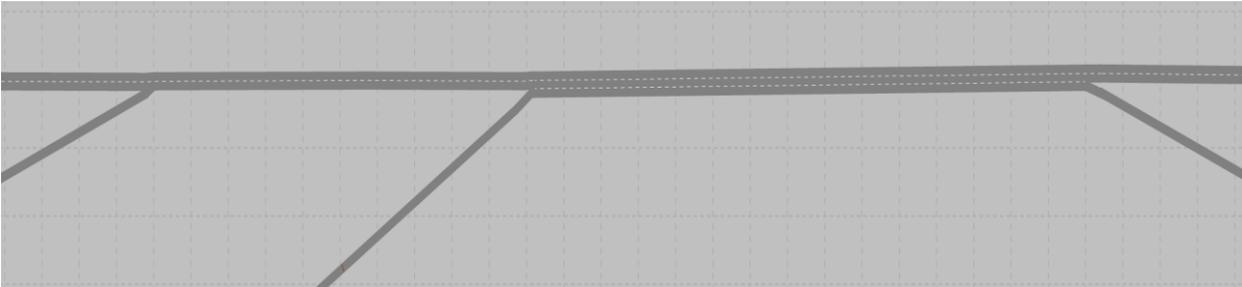


Figure 93: Lane Geometry Schematic Number 4

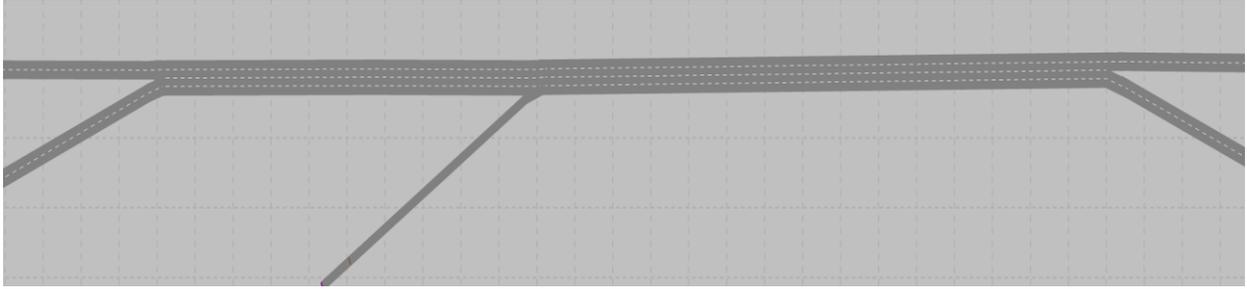


Figure 94: Lane Geometry Schematic Number 5

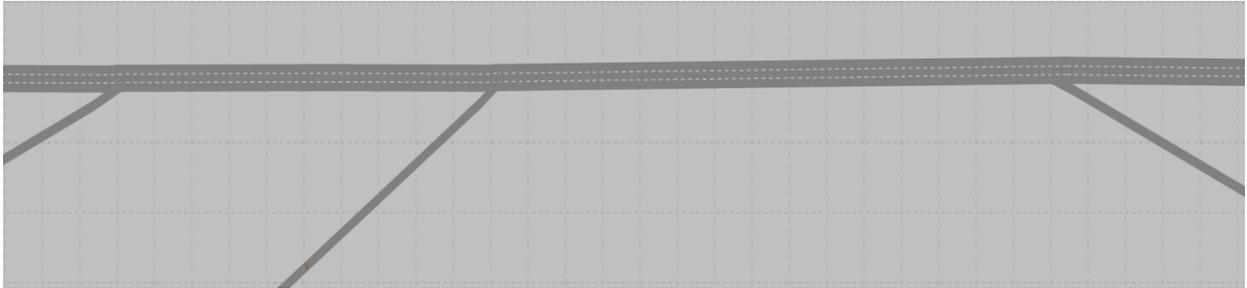


Figure 95: Lane Geometry Schematic Number 6

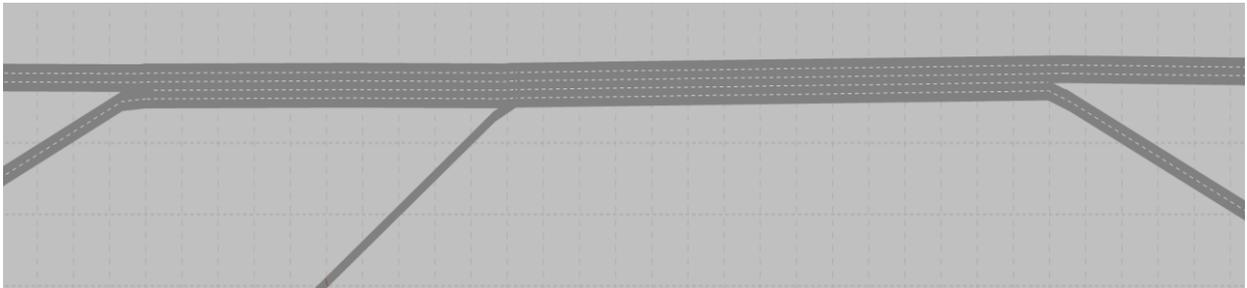


Figure 96: Lane Geometry Schematic Number 7

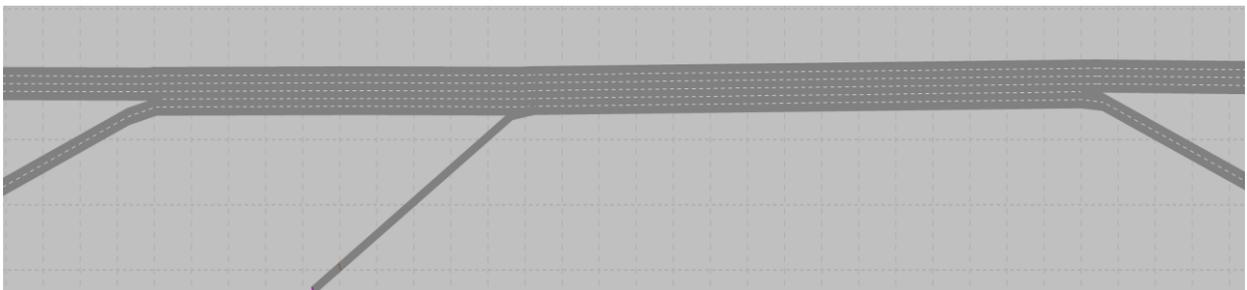


Figure 97: Lane Geometry Schematic Number 8

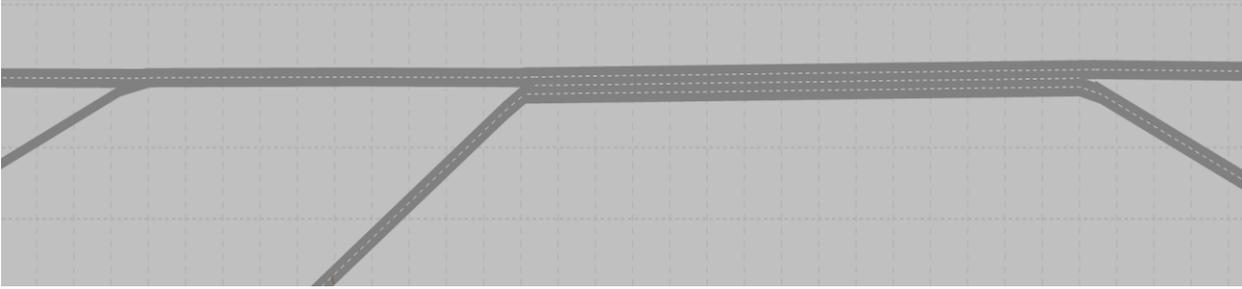


Figure 98: Lane Geometry Schematic Number 9

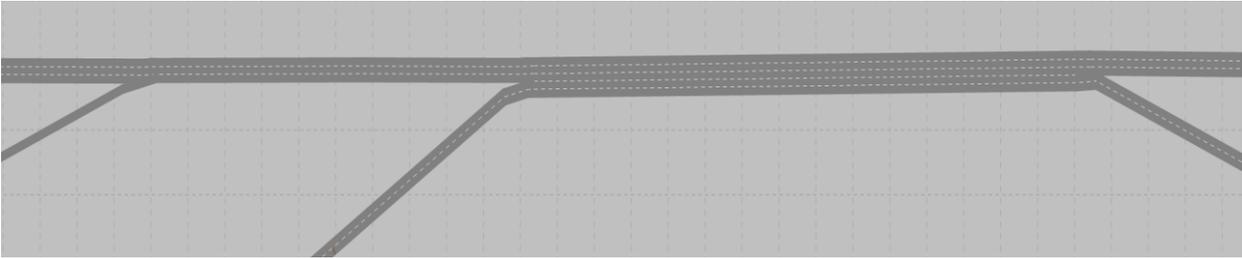


Figure 99: Lane Geometry Schematic Number 10

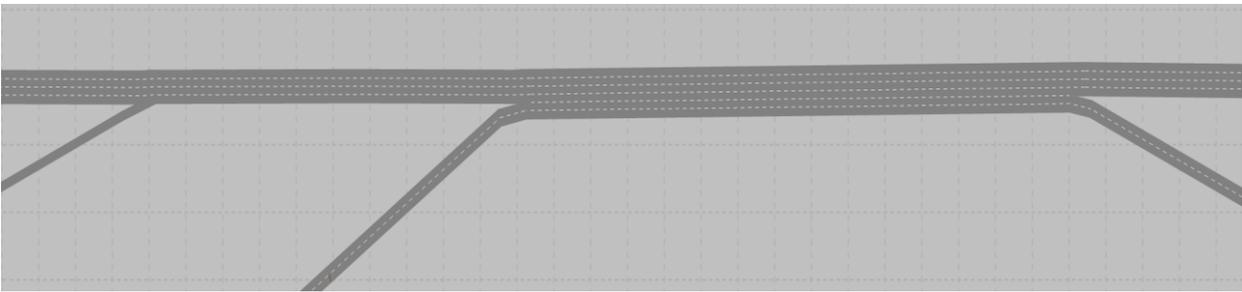


Figure 100: Lane Geometry Schematic Number 11

APPENDIX B; CHARTS

Scenario Number 2

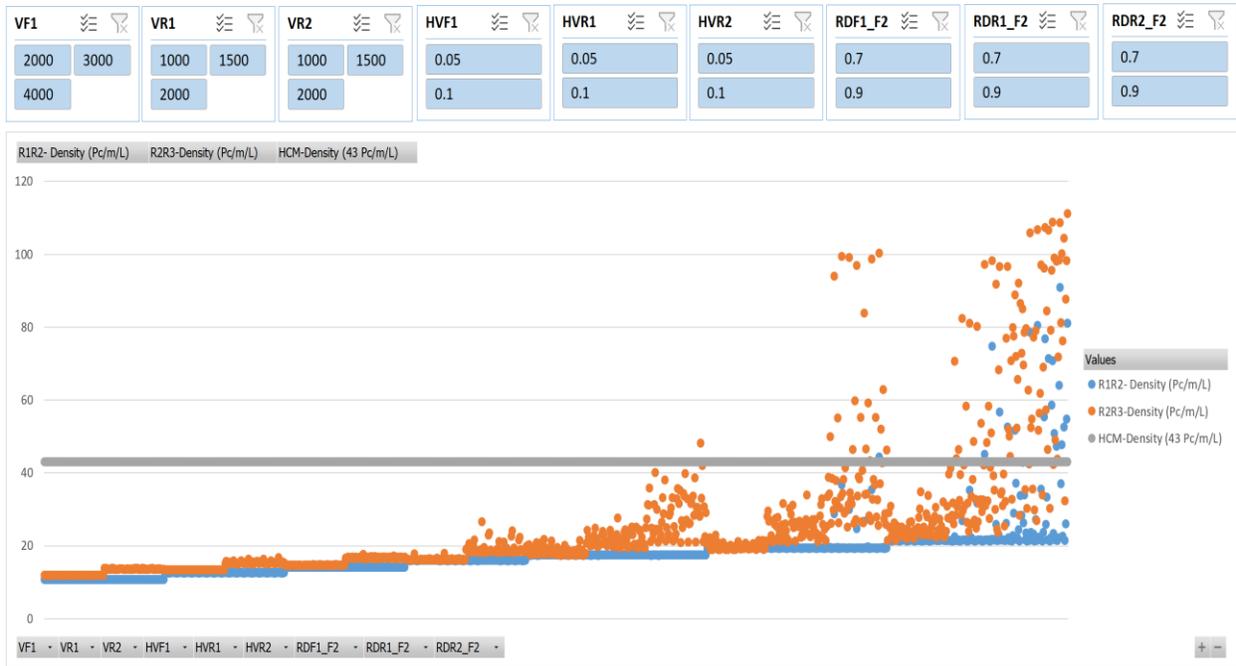


Figure 101: Scenario 2, Density

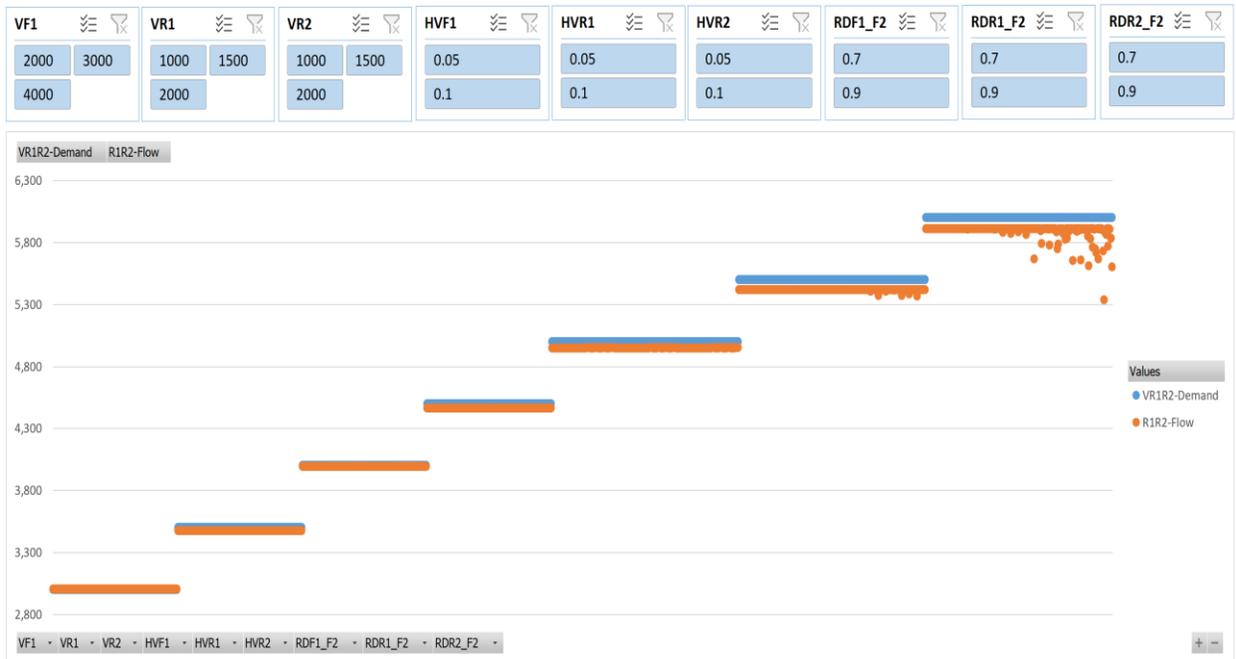


Figure 102: Scenario 2, R1R2 Flow vs. Demand

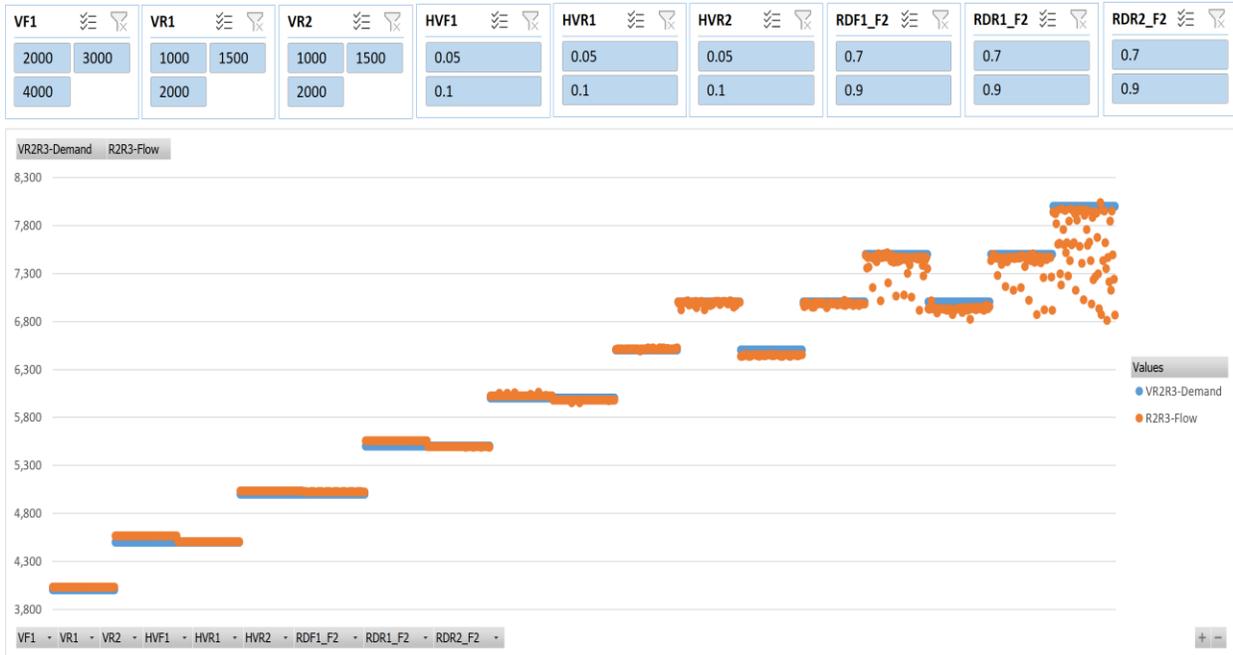


Figure 103: Scenario 2, R2R3 Flow vs. Demand

Scenario Number 3

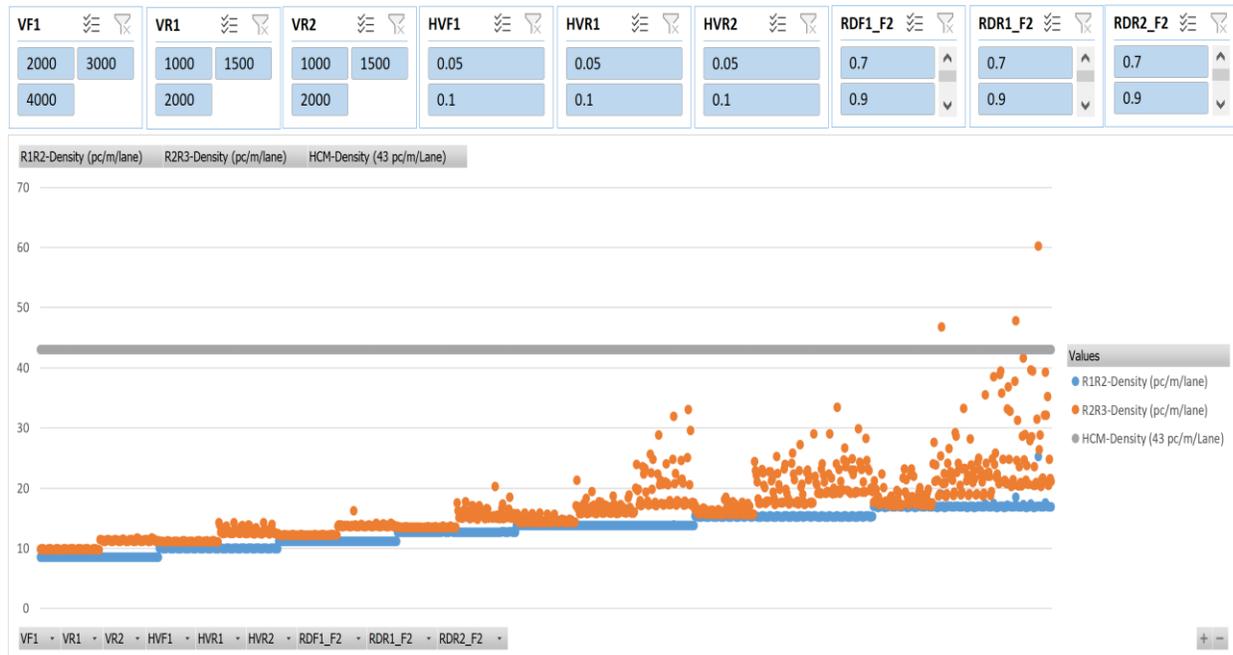


Figure 104: Scenario 3, Density

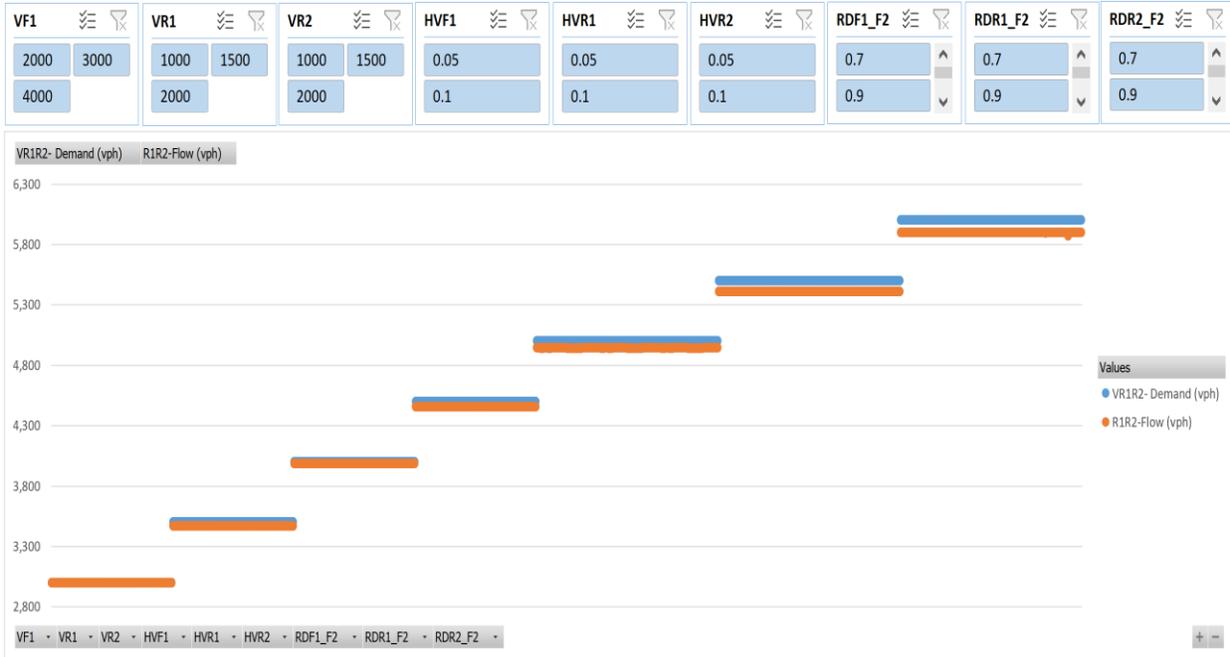


Figure 105: Scenario 3, R1R2 Flow vs. Demand

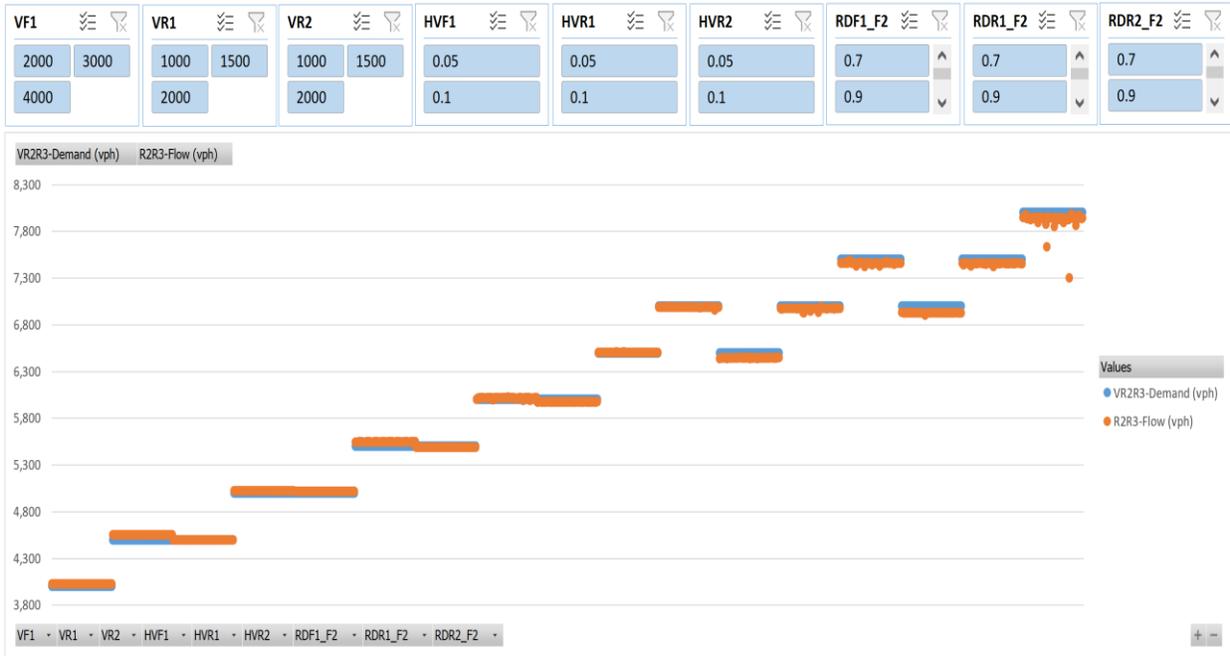


Figure 106: Scenario 3, R2R3 Flow vs. Demand

Scenario Number 4

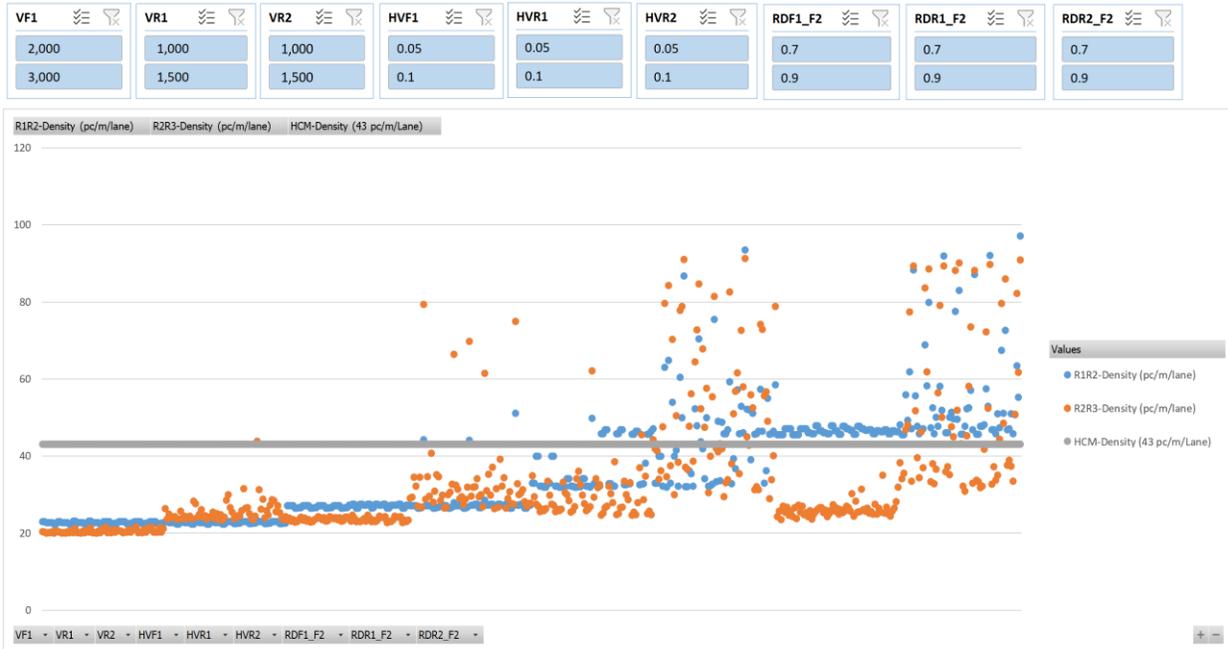


Figure 107: Scenario 4, Density

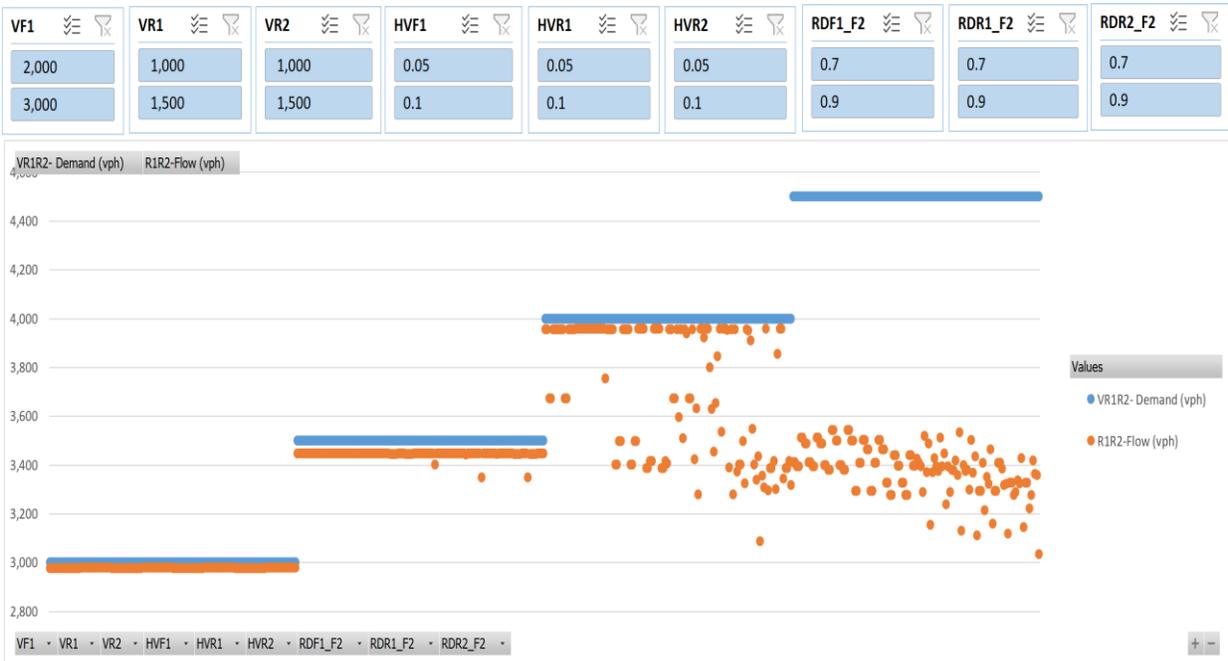


Figure 108: Scenario 4, R1R2 Flow vs. Demand

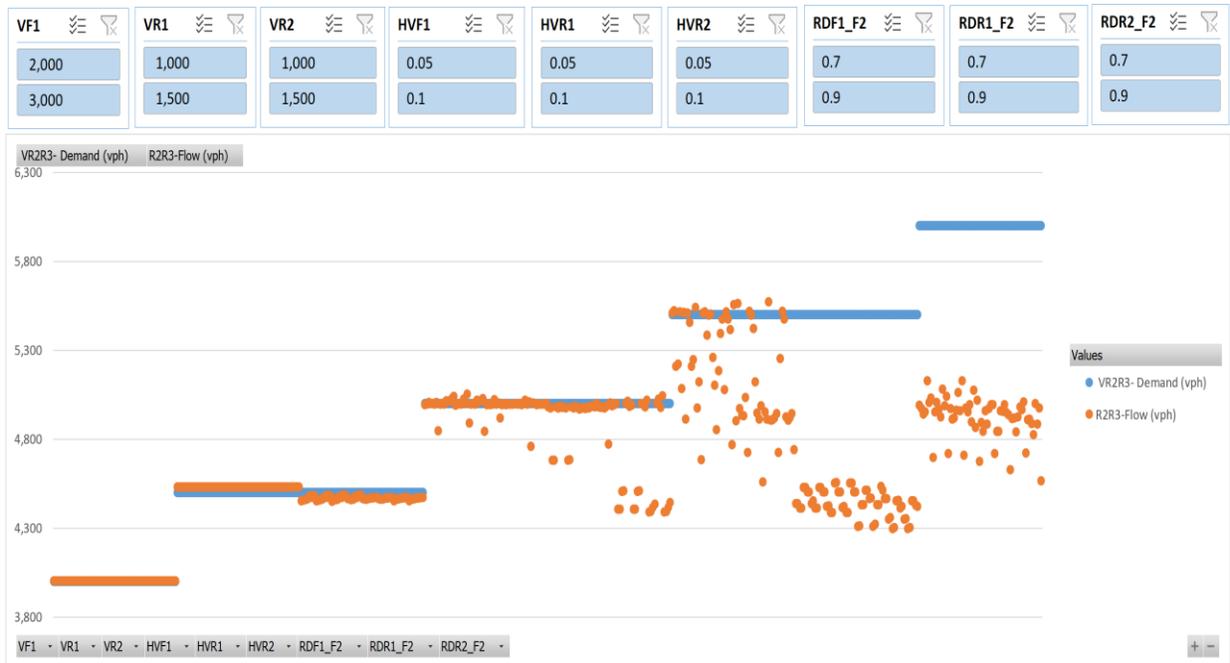


Figure 109: Scenario 4, R2R3 Flow vs. Demand

Scenario Number 5

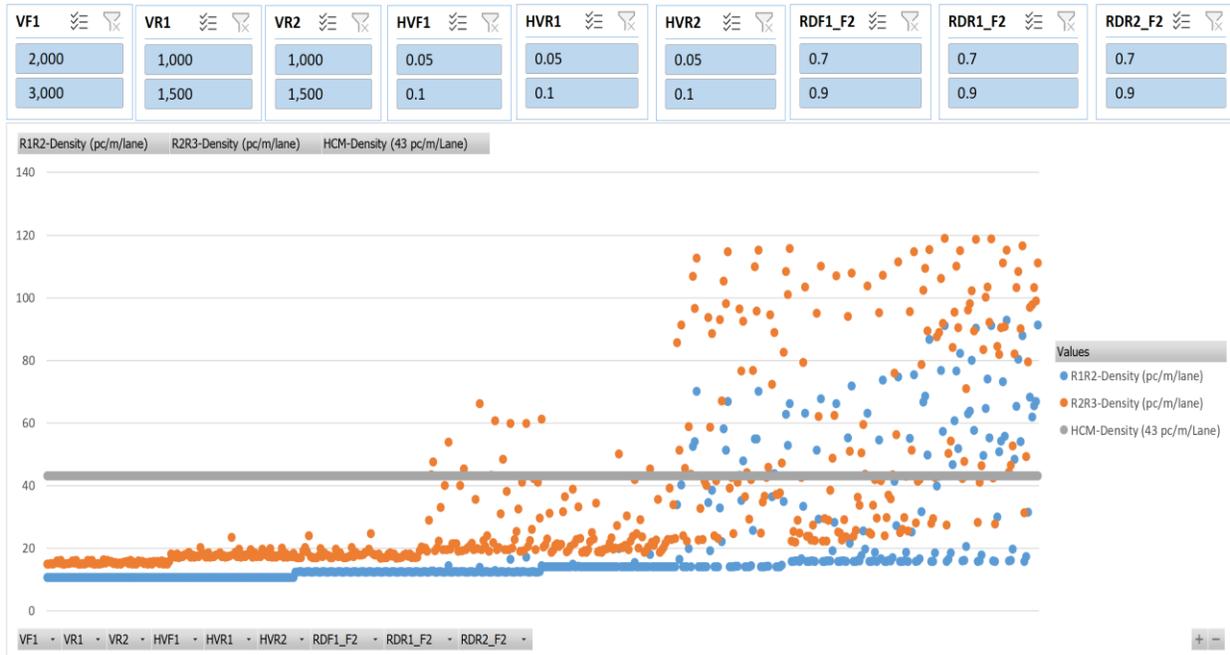


Figure 110: Scenario 5, Density

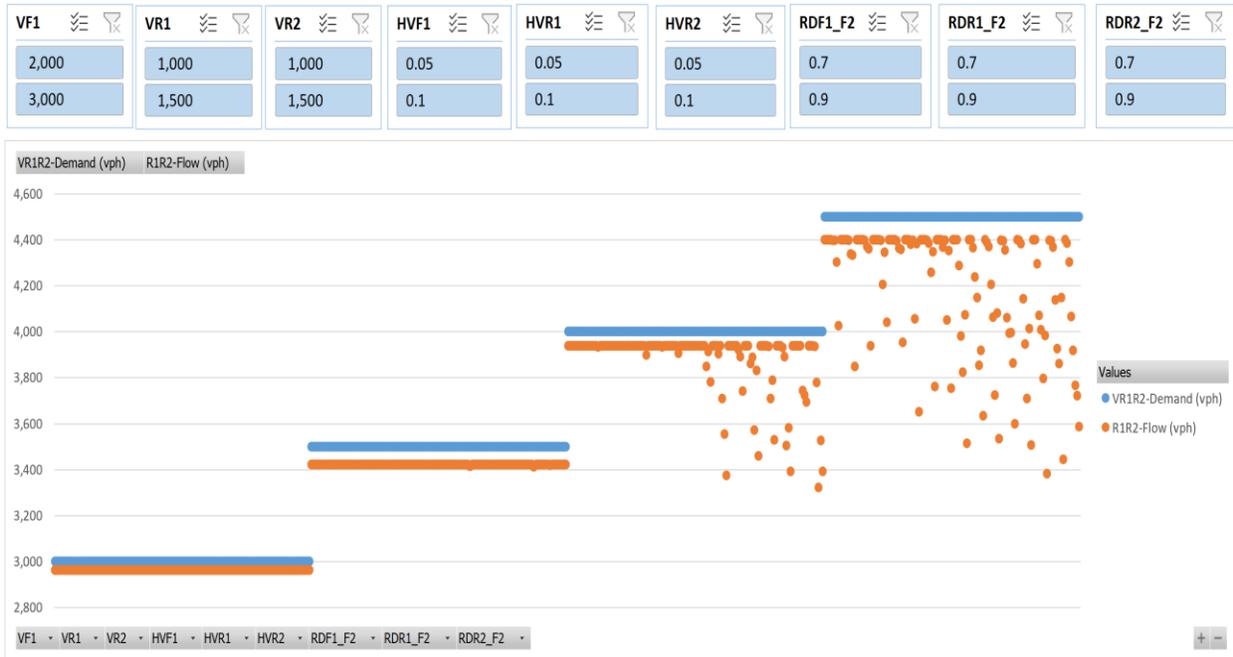


Figure 111: Scenario 5, R1R2 Flow vs. Demand

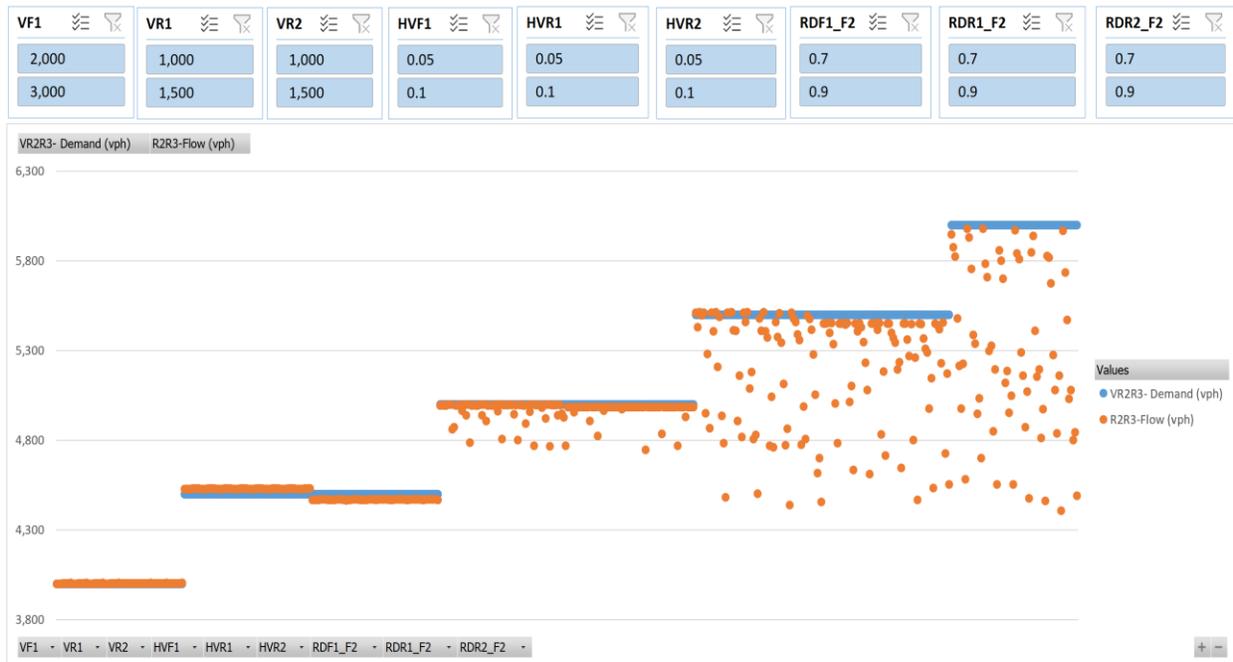


Figure 112: Scenario 5, R2R3 Flow vs. Demand

Scenario Number 6

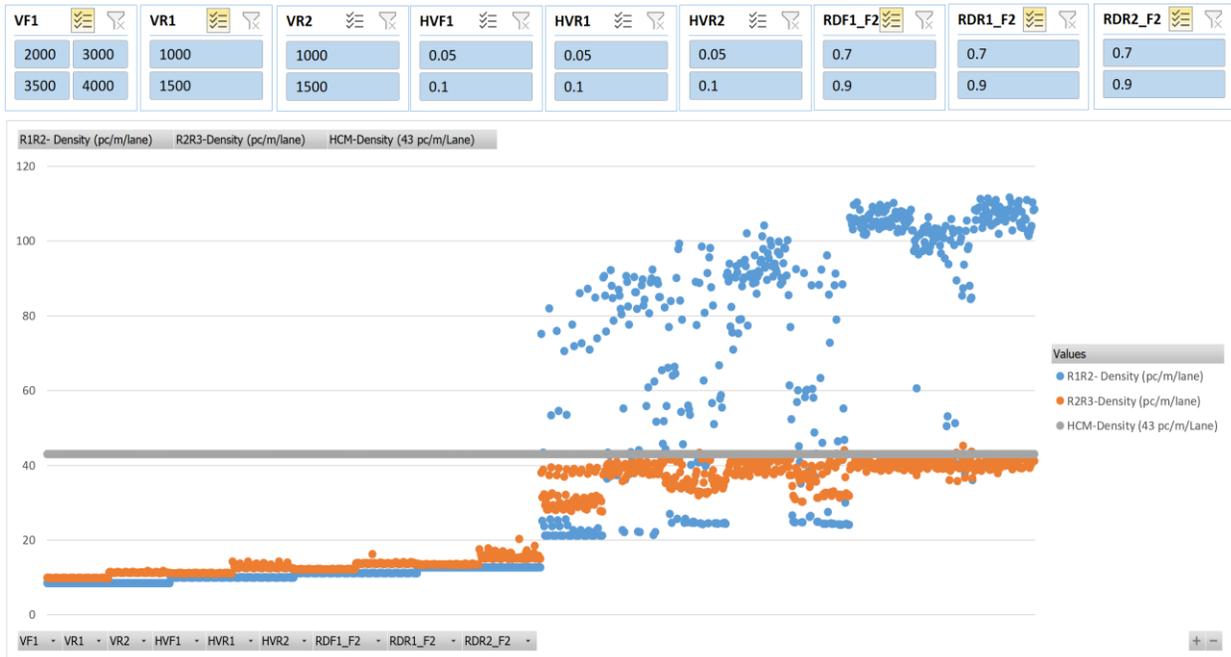


Figure 113: Scenario 6, Density

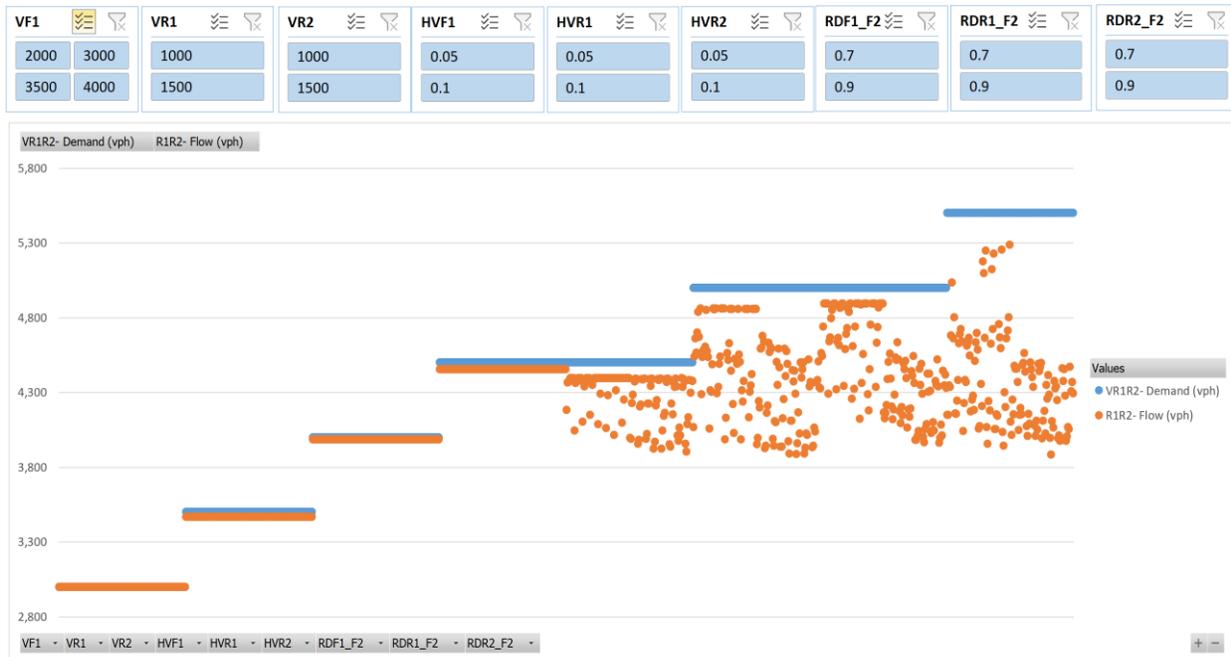


Figure 114: Scenario 6, R1R2 Flow vs. Demand



Figure 115: Scenario 6, R2R3 Flow vs. Demand

Scenario Number 7

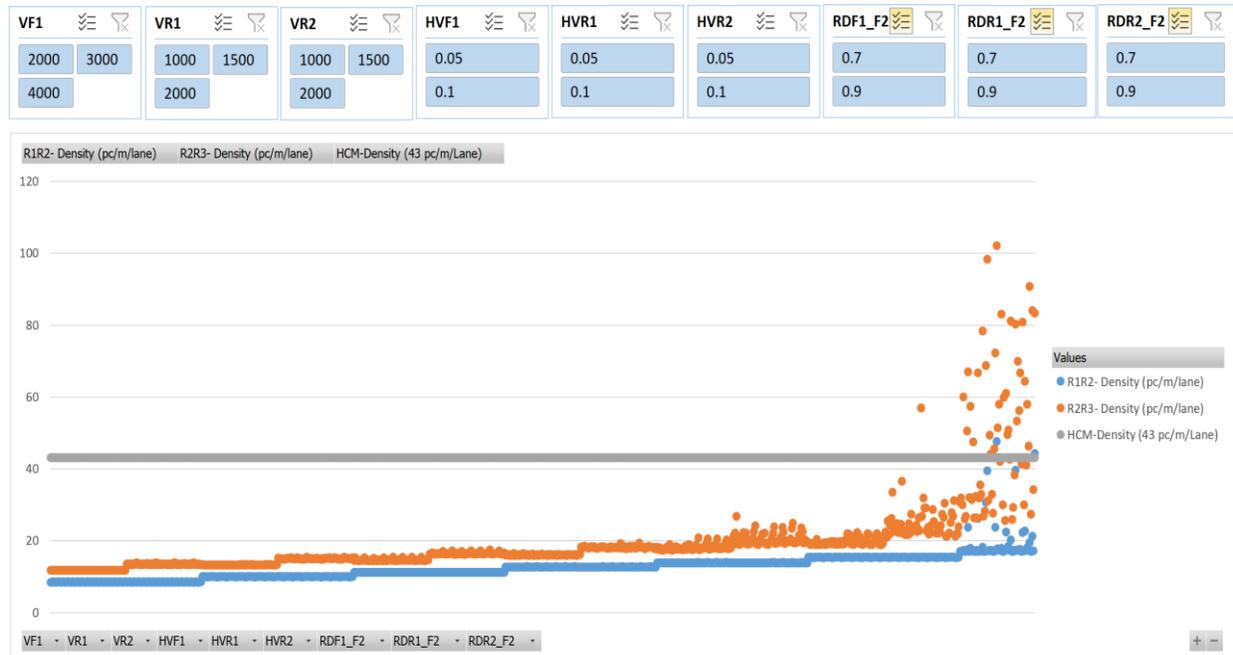


Figure 116: Scenario 7, Density

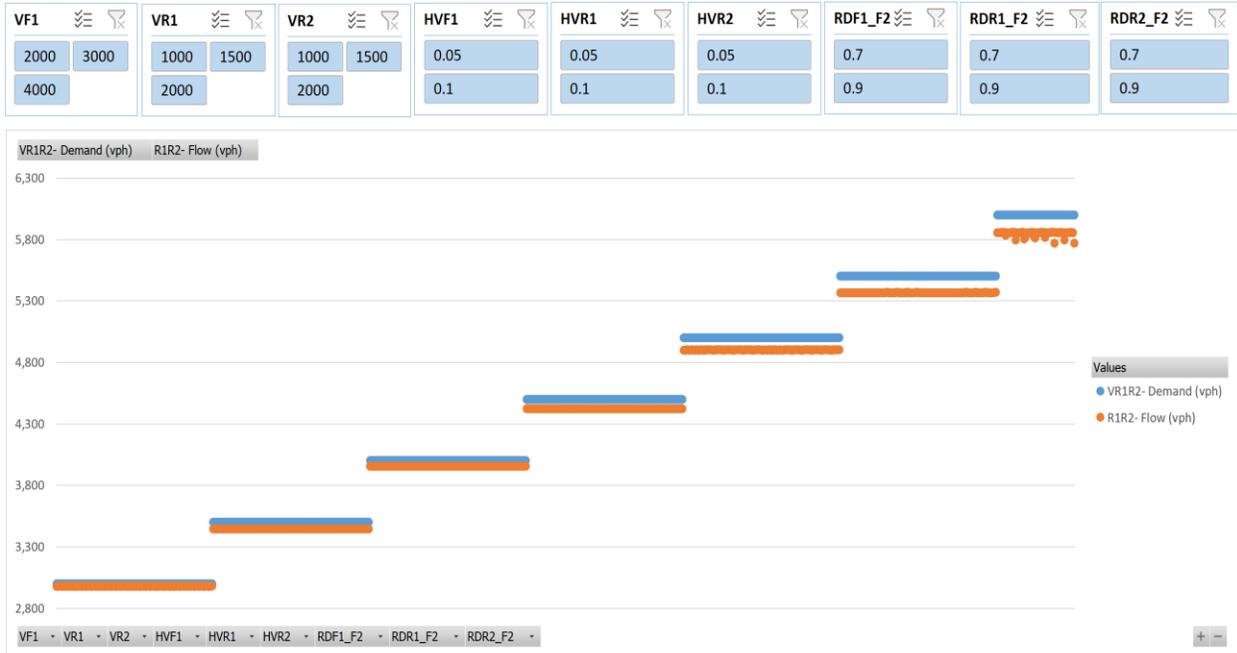


Figure 117: Scenario 7, R1R2 Flow vs. Demand

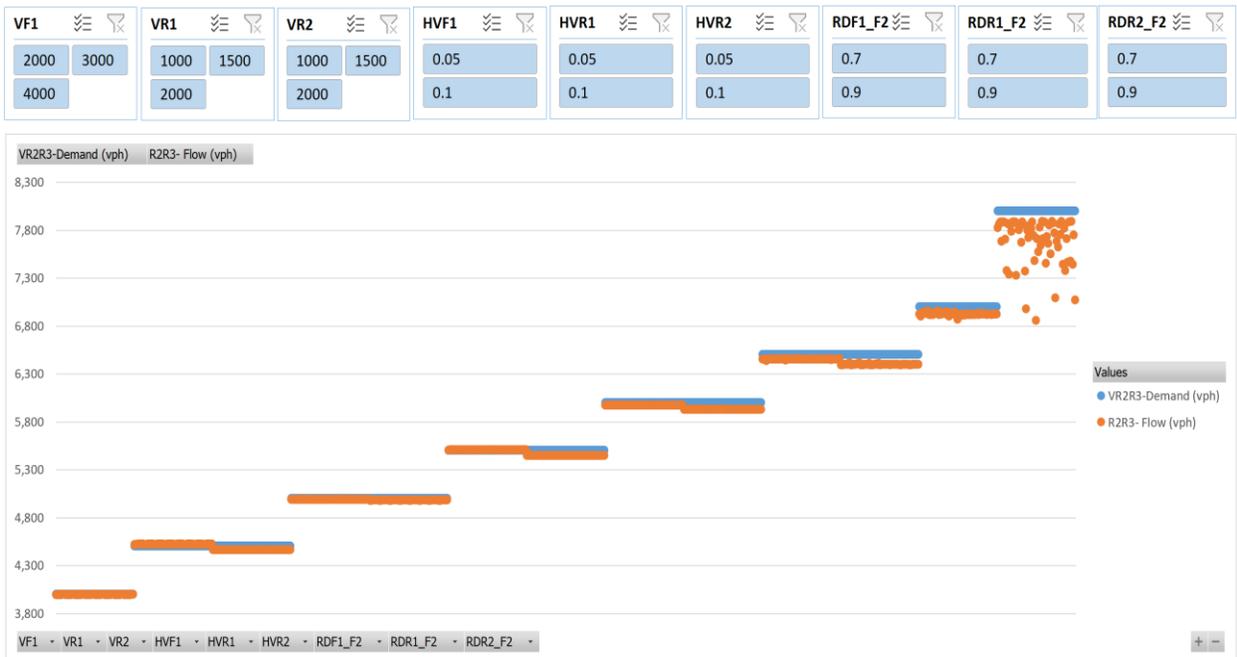


Figure 118: Scenario 7, R2R3 Flow vs. Demand

Scenario Number 8

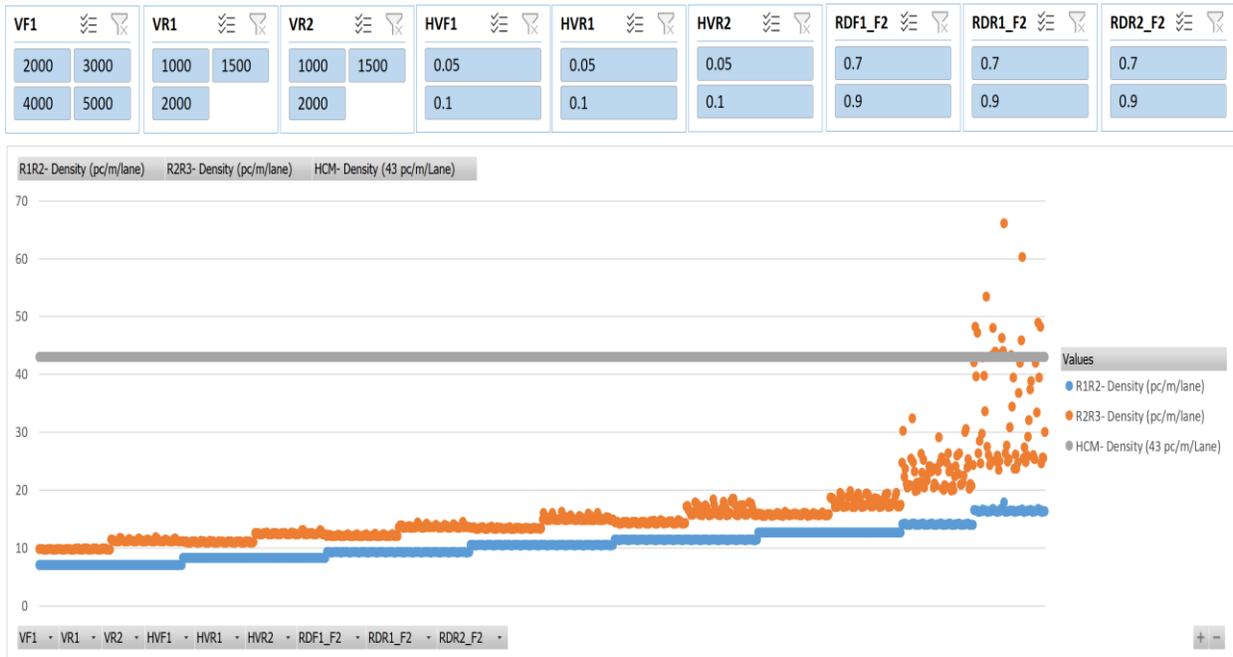


Figure 119: Scenario 8, Density

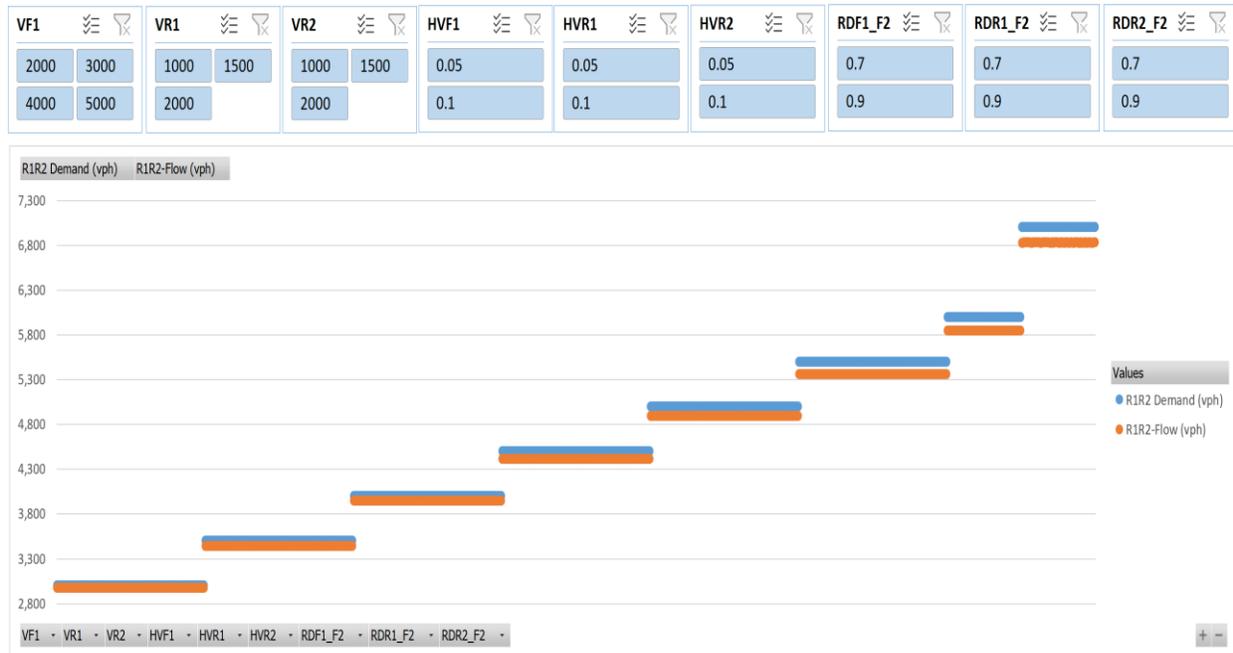


Figure 120: Scenario 8, R1R2 Flow vs. Demand

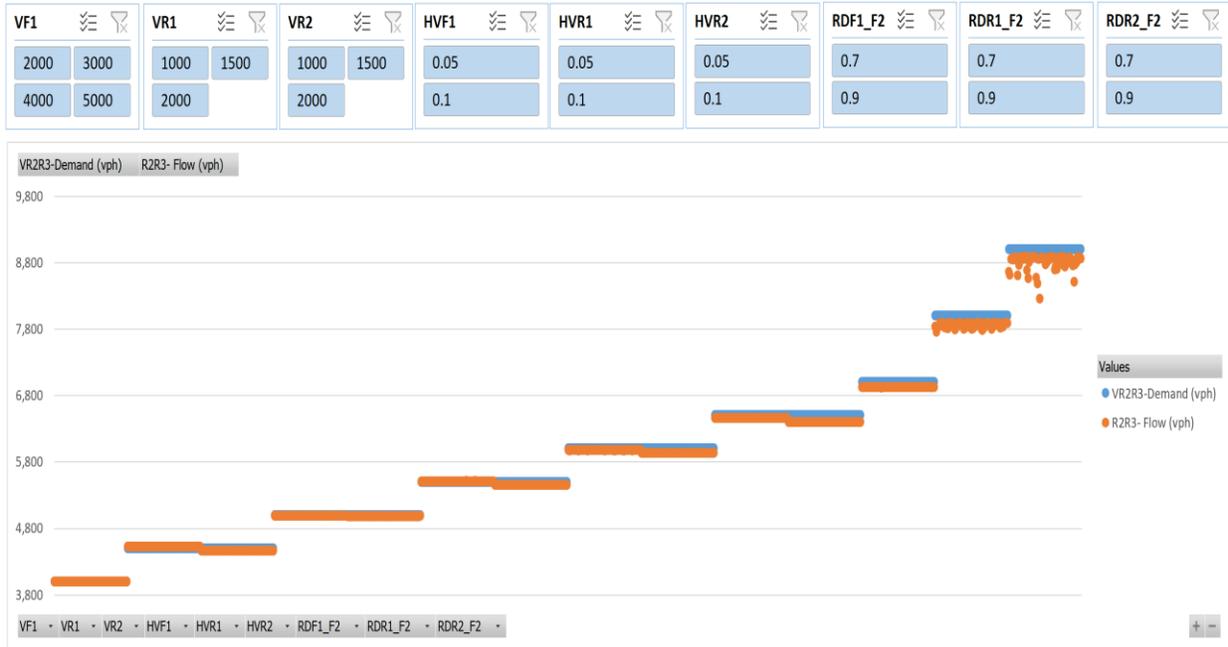


Figure 121: Scenario 8, R2R3 Flow vs. Demand

Scenario Number 9

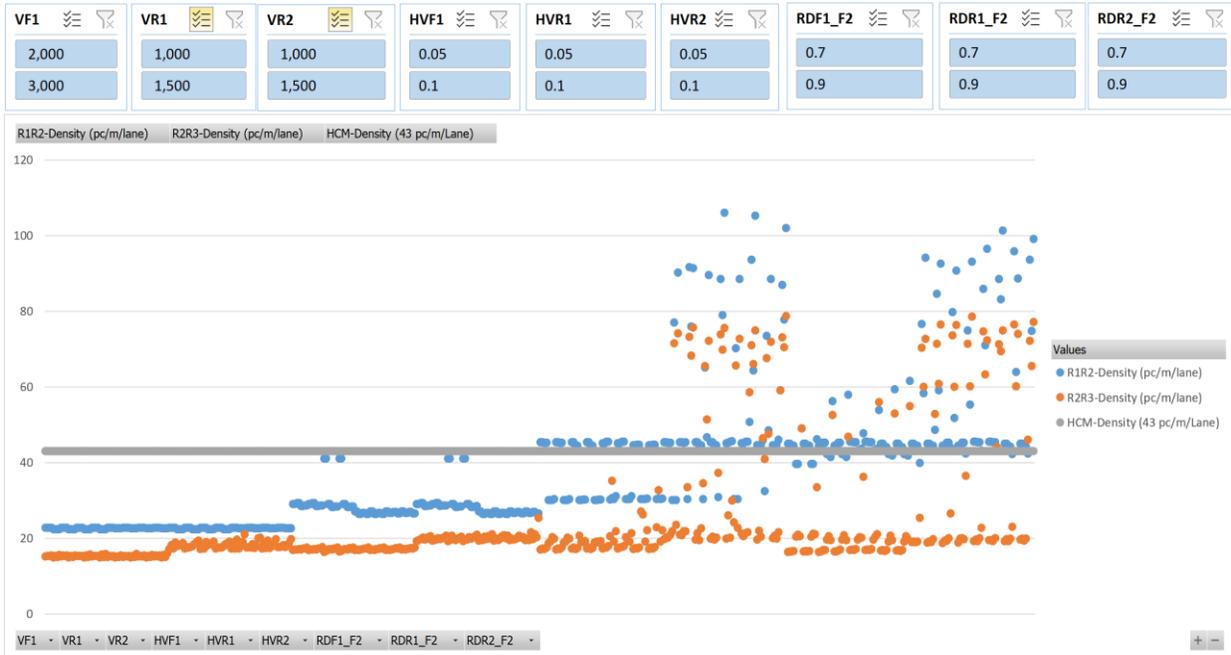


Figure 122: Scenario 9, Density

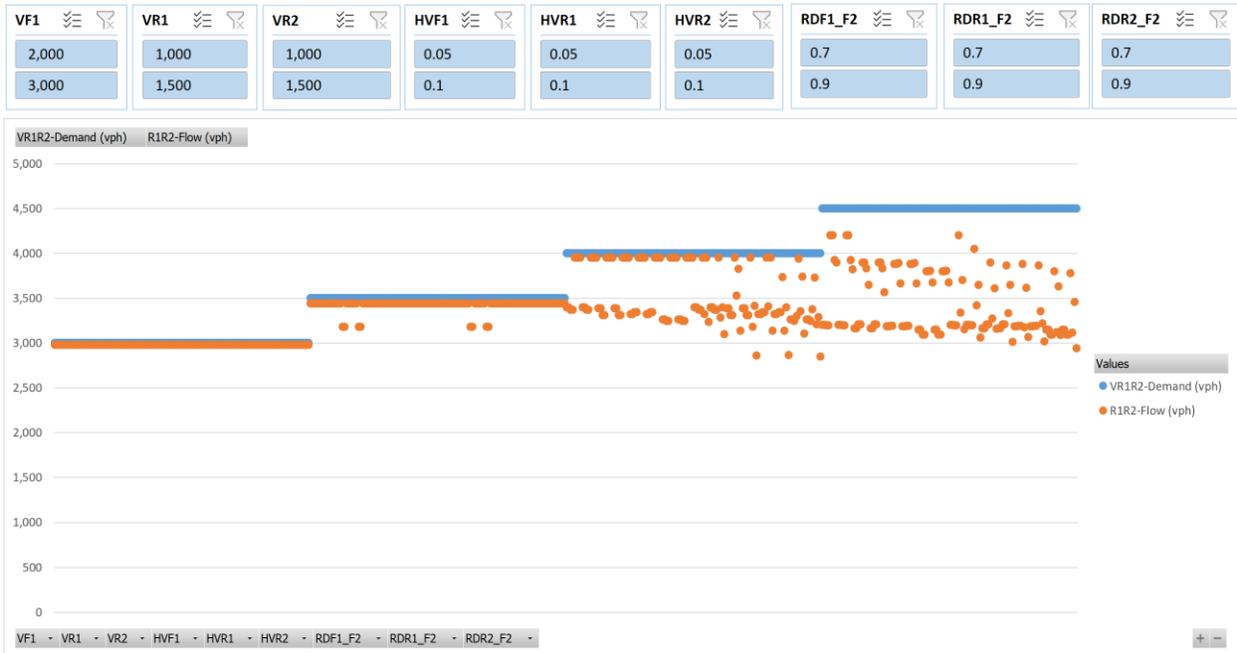


Figure 123: Scenario 9, R1R2 Flow vs. Demand



Figure 124: Scenario 9, R2R3 Flow vs. Demand

Scenario Number 10

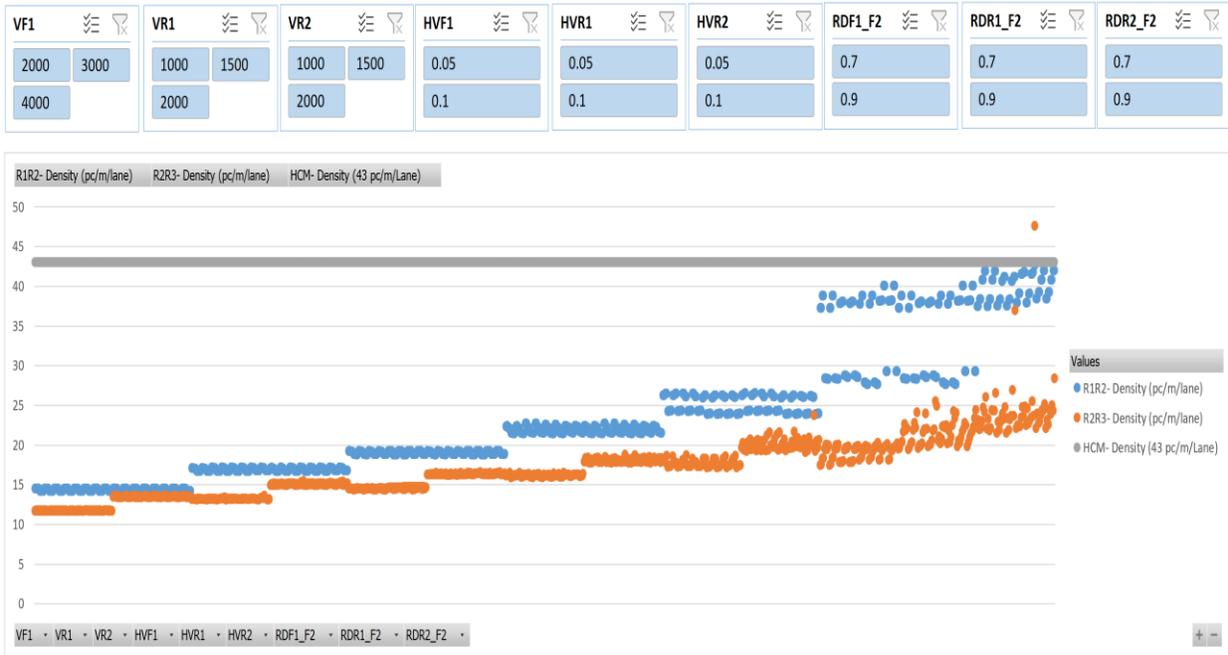


Figure 125: Scenario 10, Density

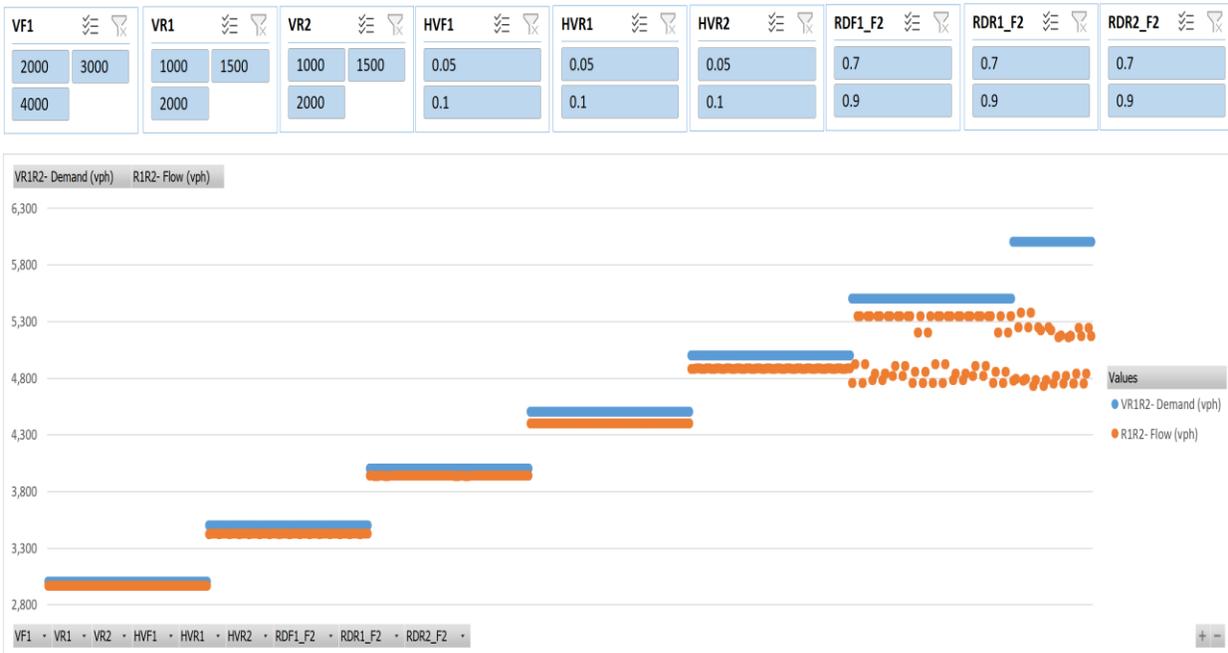


Figure 126: Scenario 10, R1R2 Flow vs. Demand

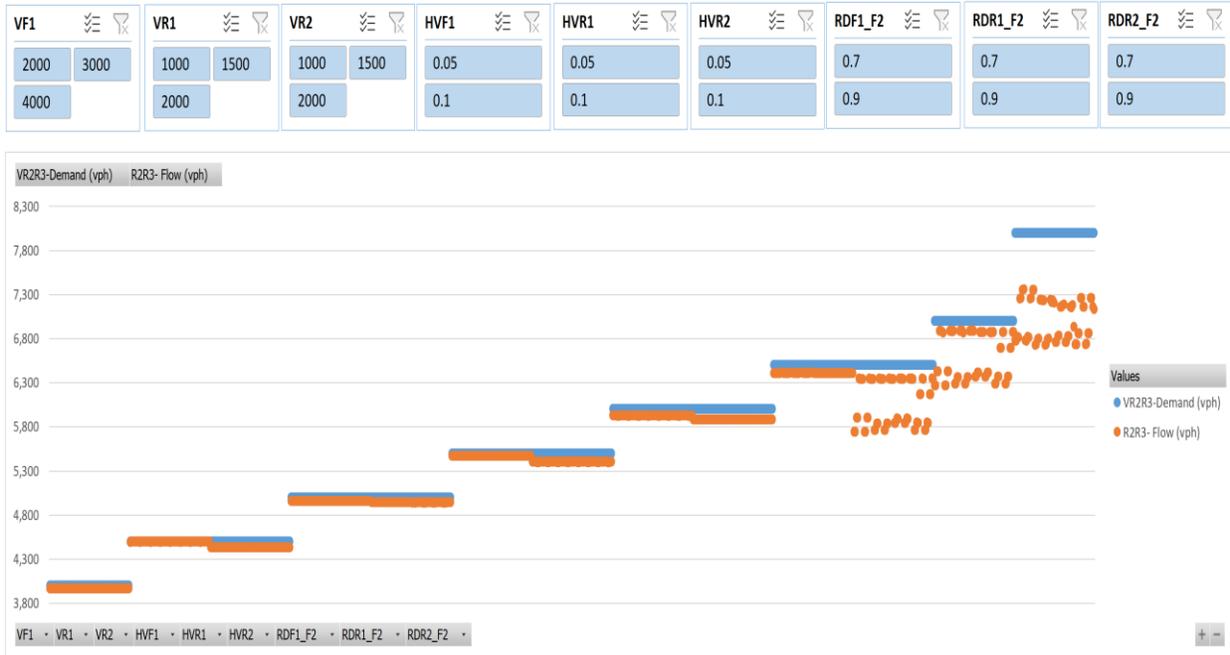


Figure 127: Scenario 10, R2R3 Flow vs. Demand

Scenario Number 11

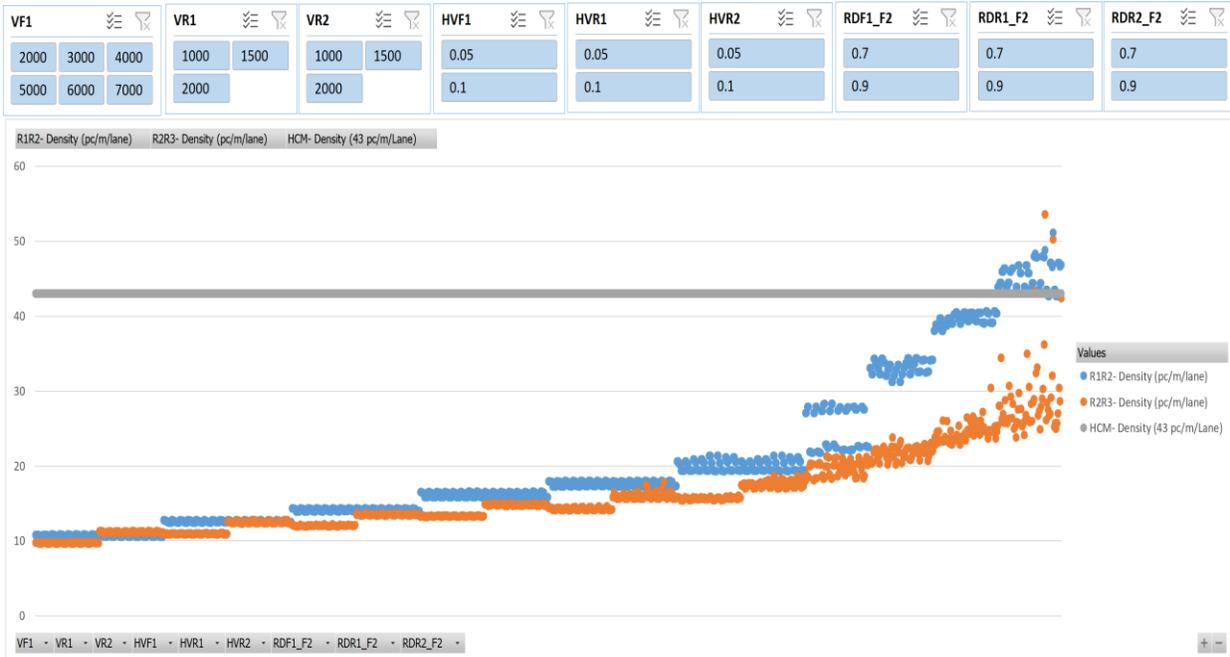


Figure 128: Scenario 11, Density

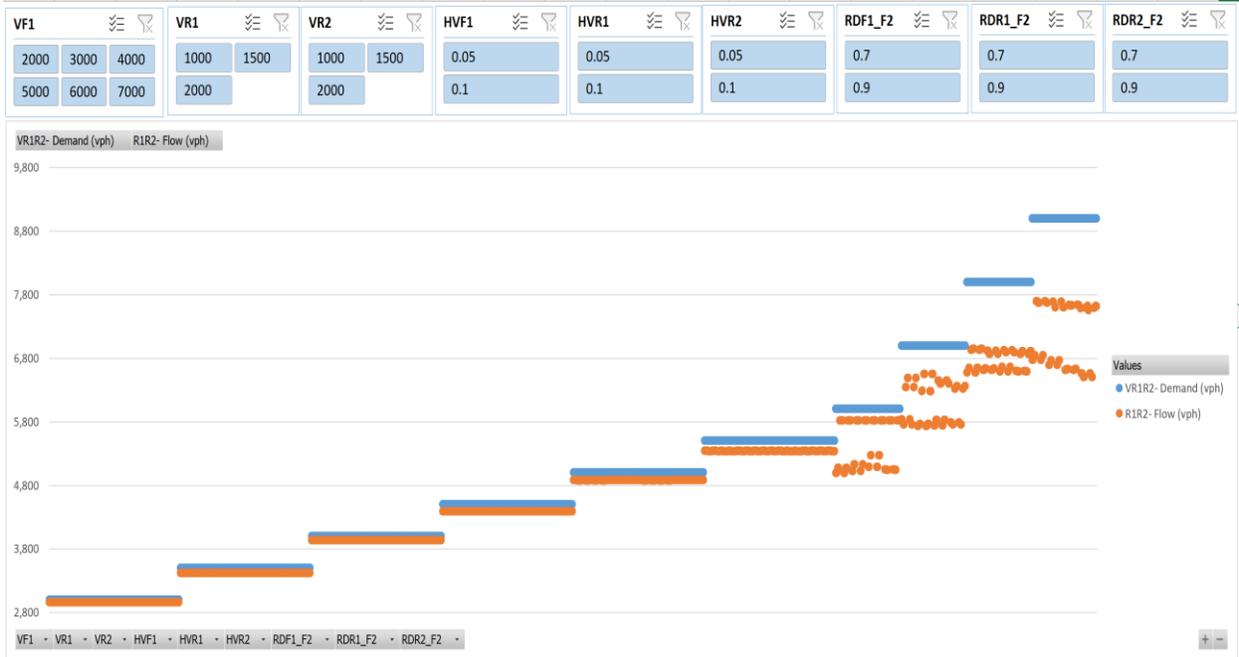


Figure 129: Scenario 11, R1R2 Flow vs. Demand

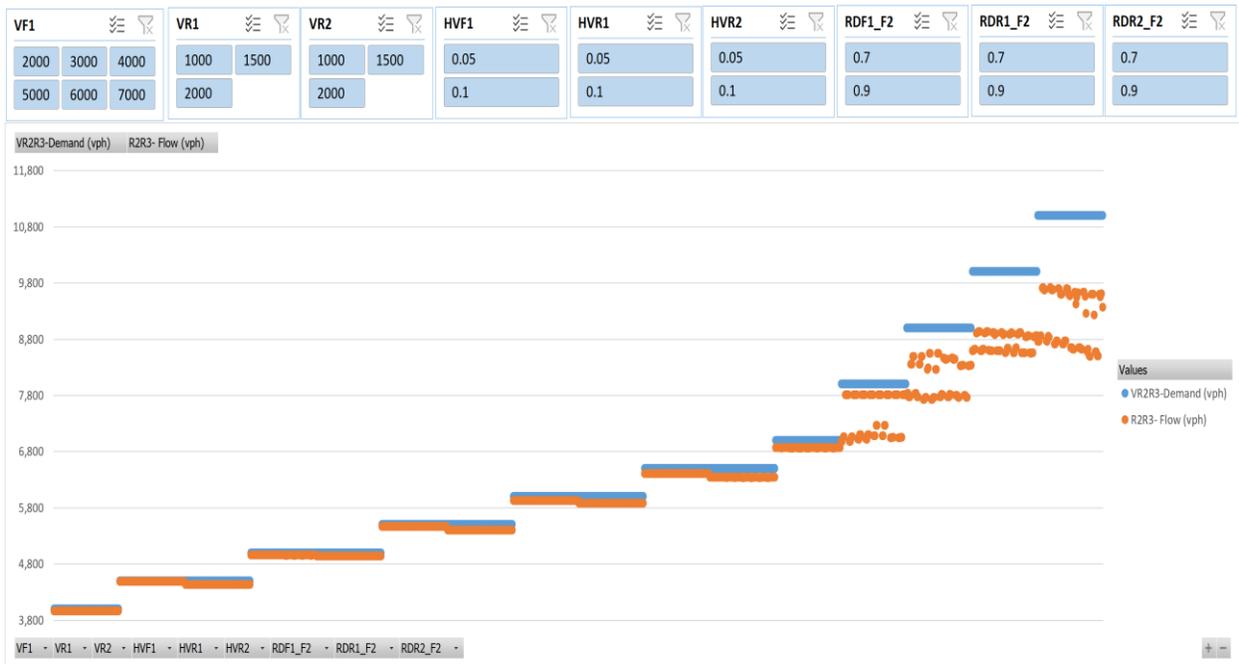


Figure 130: Scenario 11, R2R3 Flow vs. Demand

Scenario Number 12

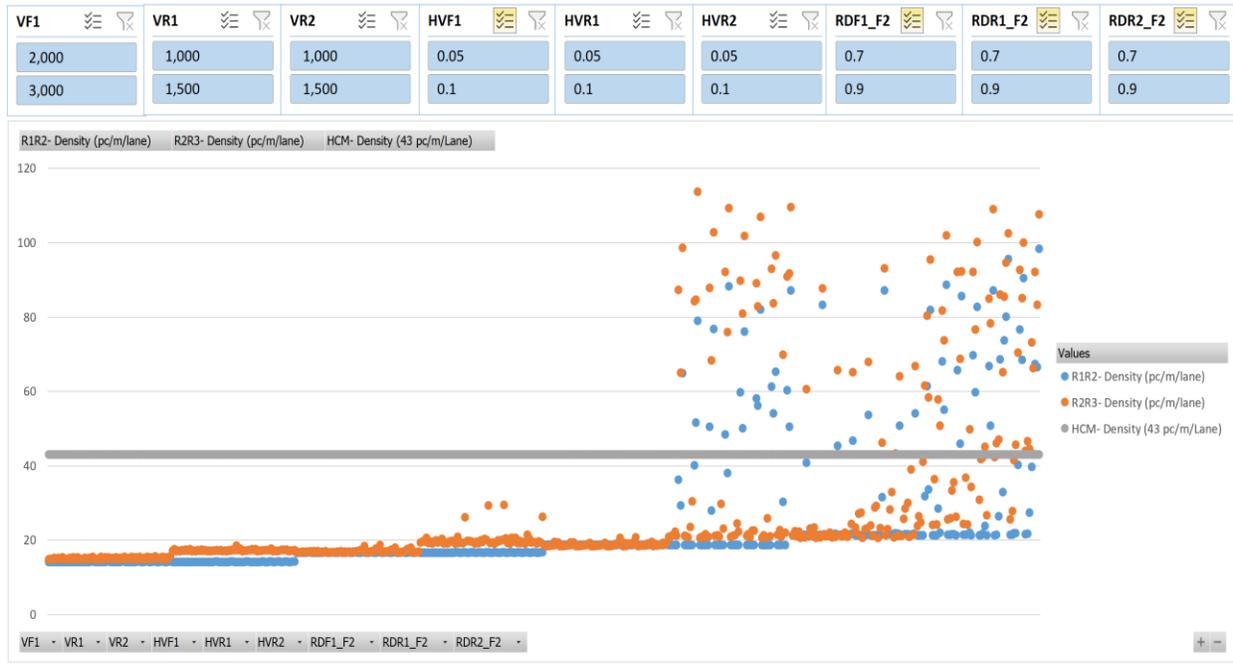


Figure 131: Scenario 12, Density

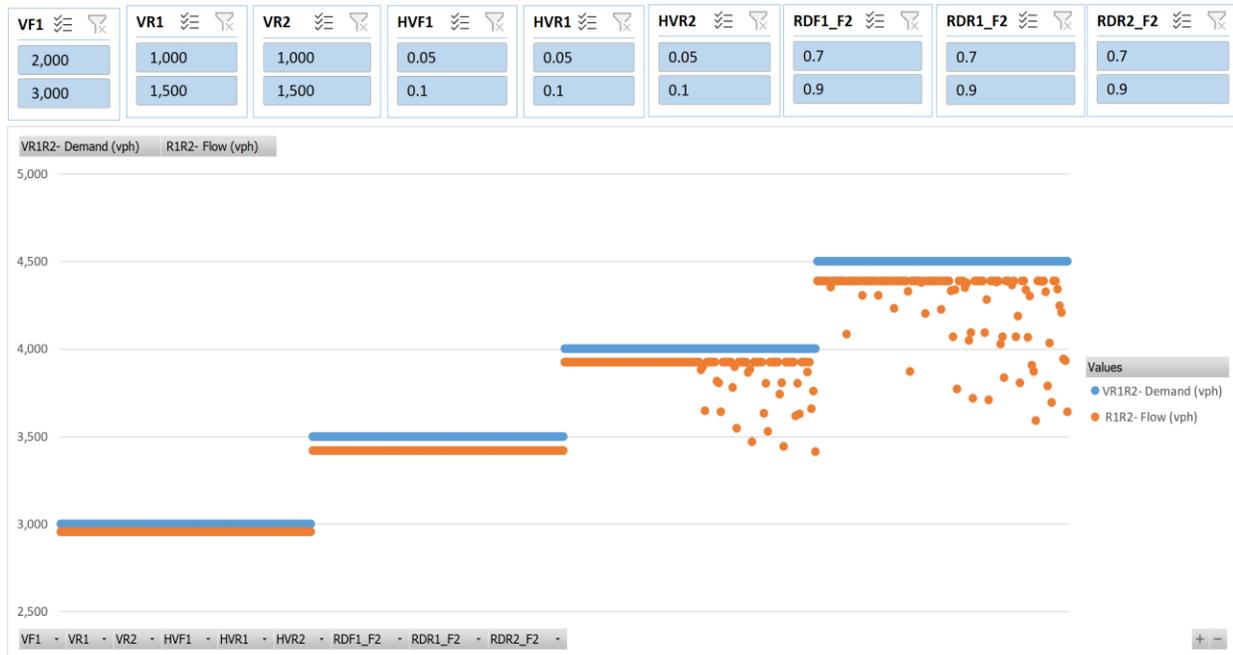


Figure 132: Scenario 12, R1R2 Flow vs. Demand

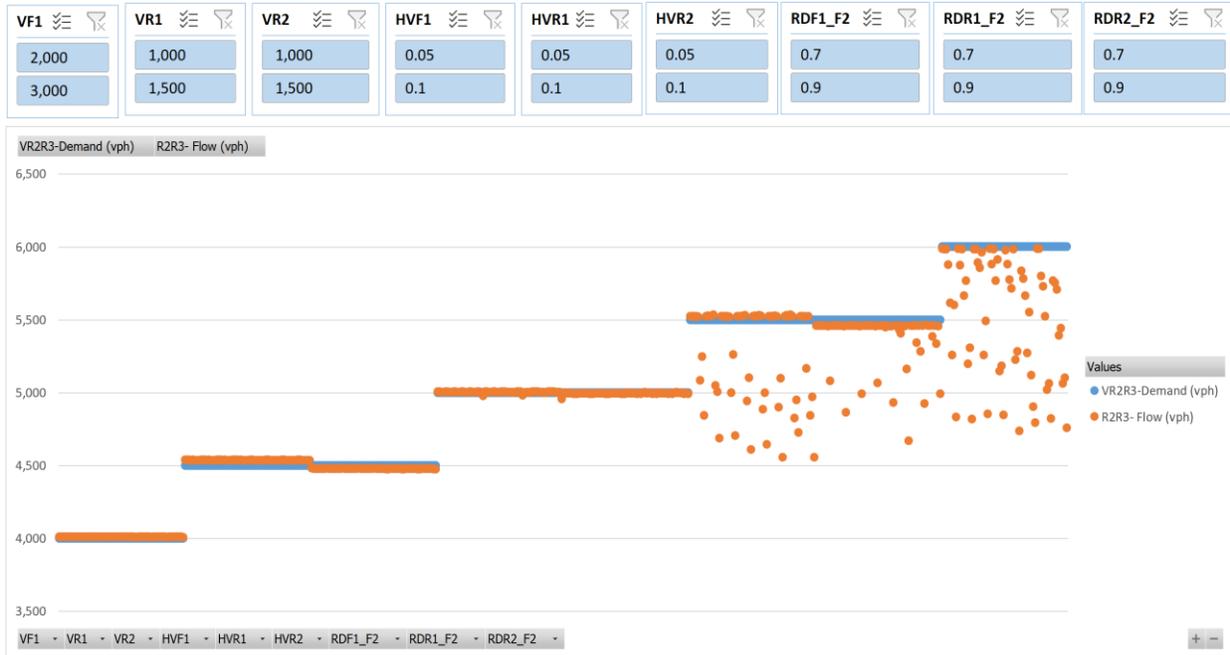


Figure 133: Scenario 12, R2R3 Flow vs. Demand

Scenario Number 13

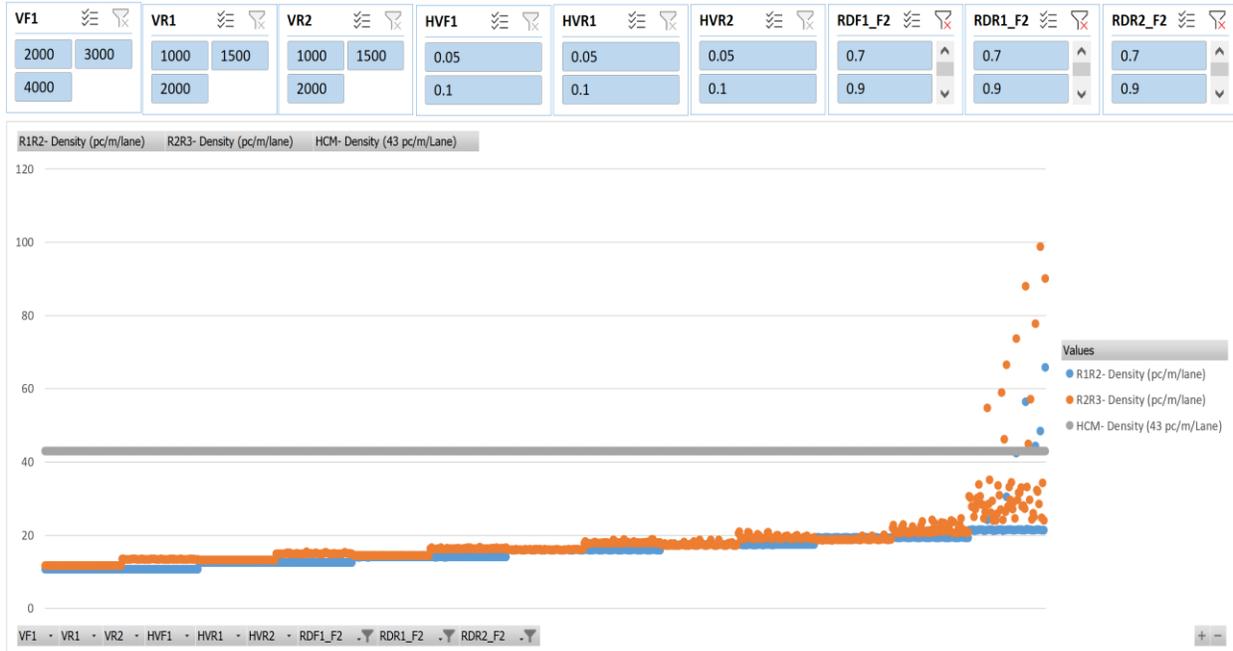


Figure 134: Scenario 13, Density

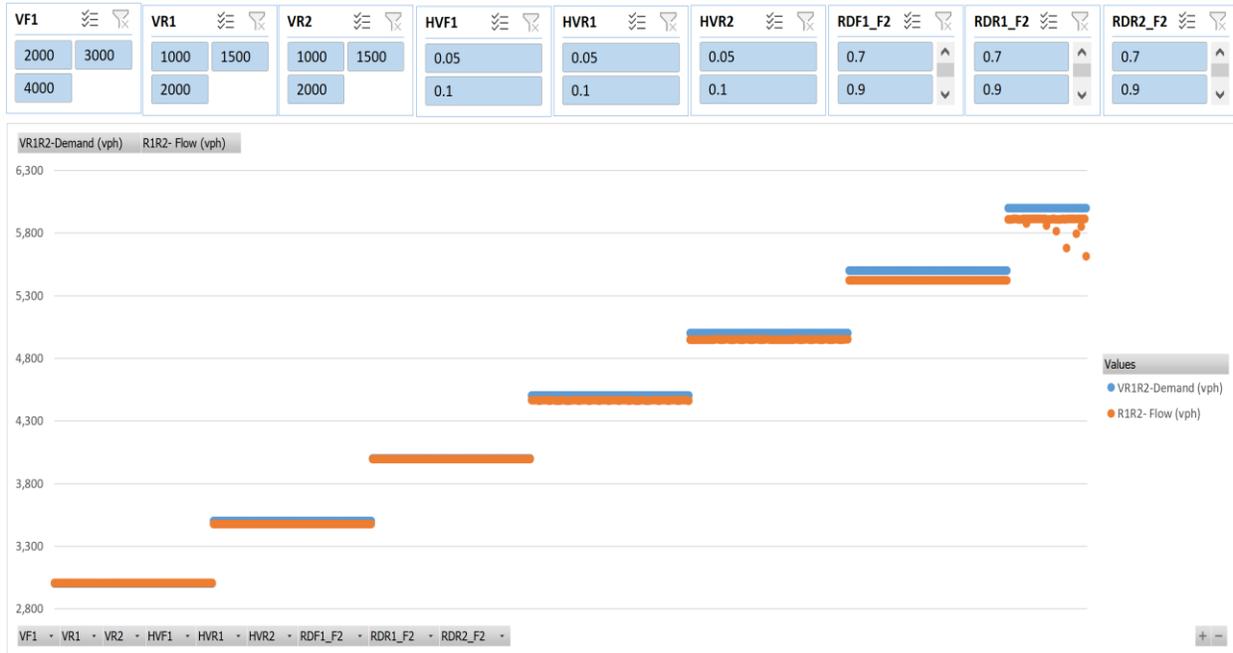


Figure 135: Scenario 13, R1R2 Flow vs. Demand

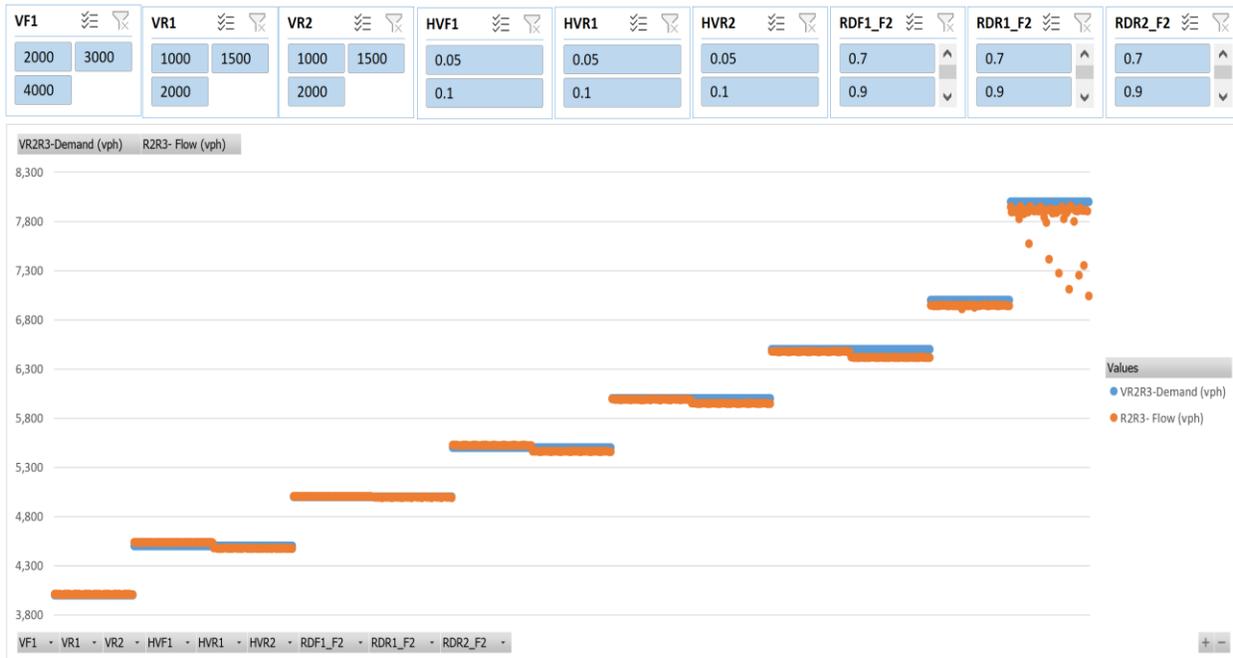


Figure 136: Scenario 13, R2R3 Flow vs. Demand

Scenario Number 14

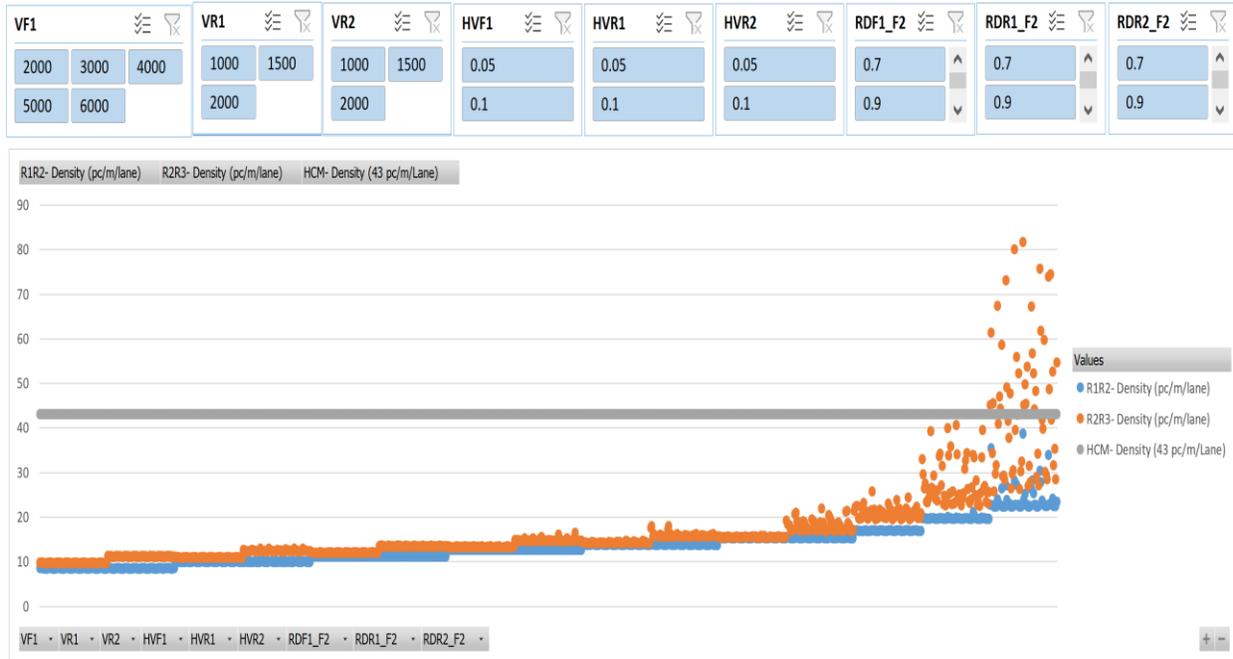


Figure 137: Scenario 14, Density

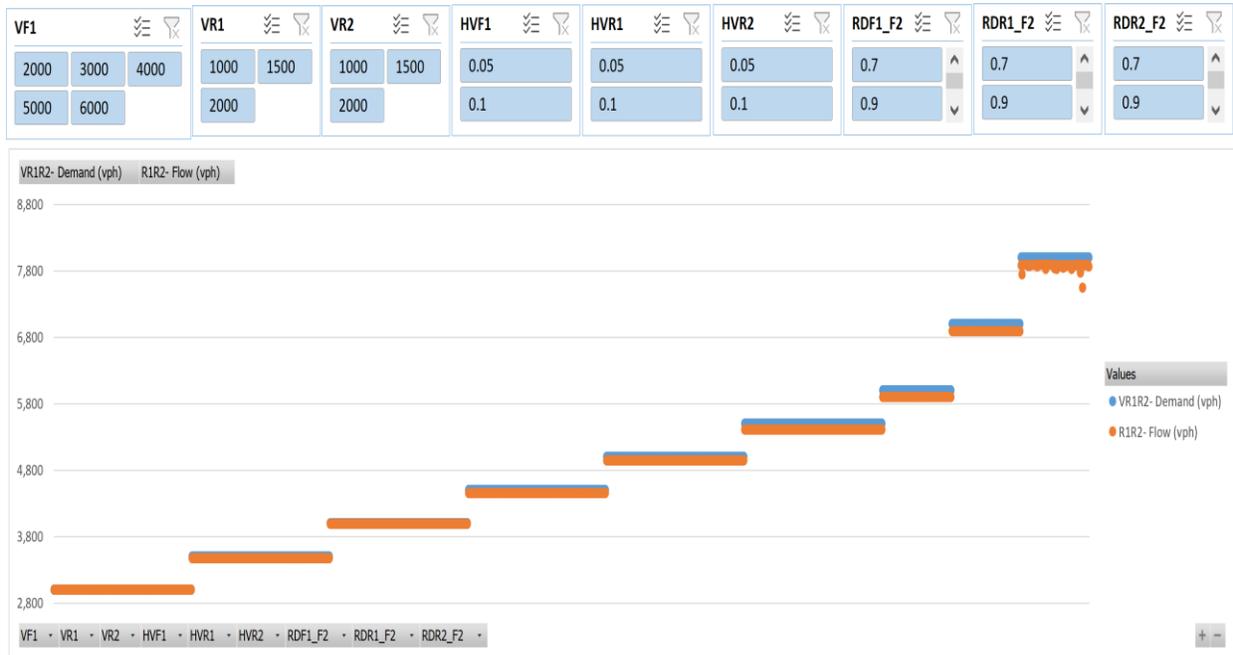


Figure 138: Scenario 14, R1R2 Flow vs. Demand

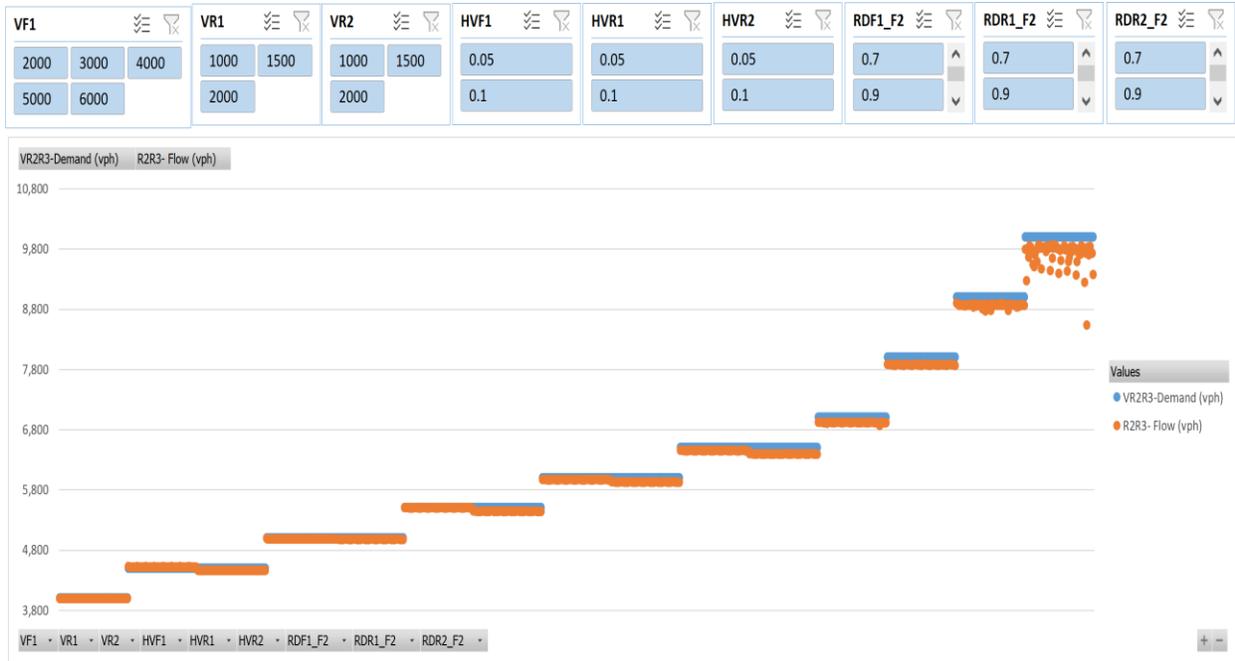


Figure 139: Scenario 14, R2R3 Flow vs. Demand

Scenario Number 15

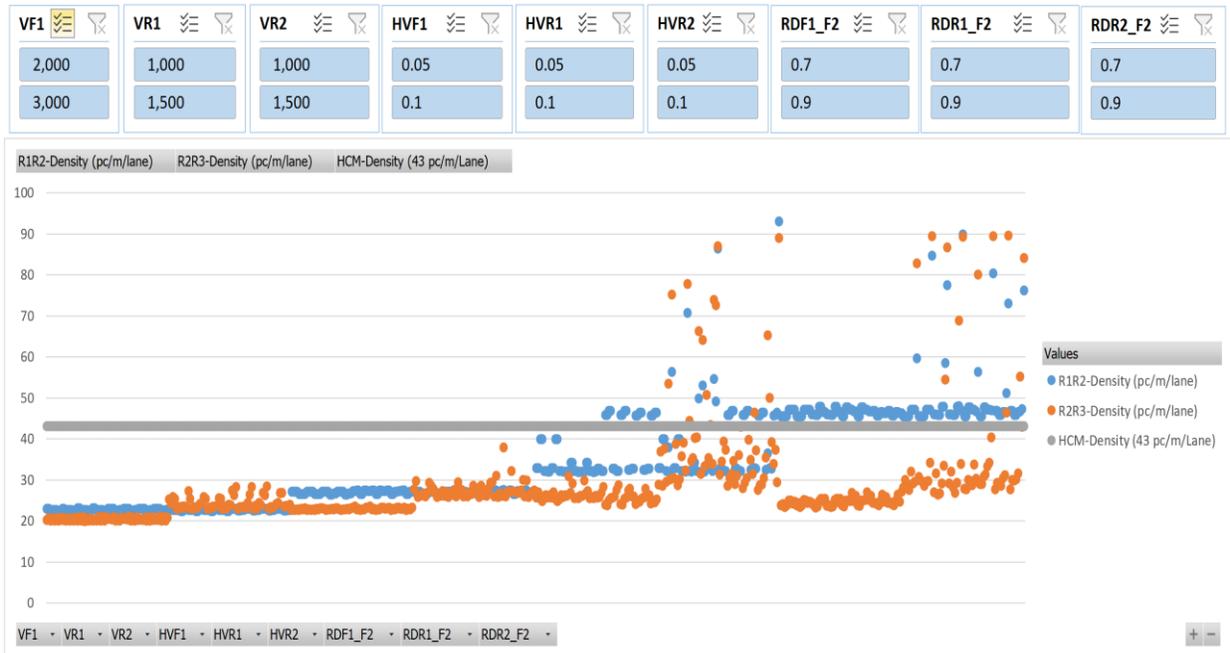


Figure 140: Scenario 15, Density

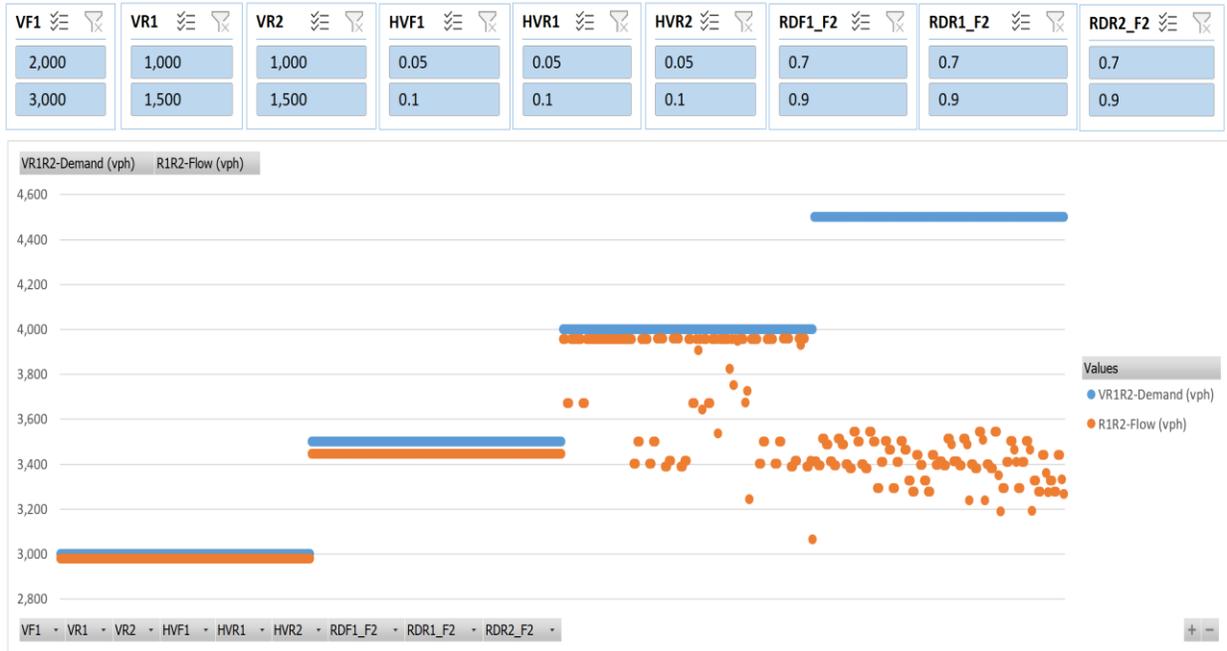


Figure 141: Scenario 15, R1R2 Flow vs. Demand

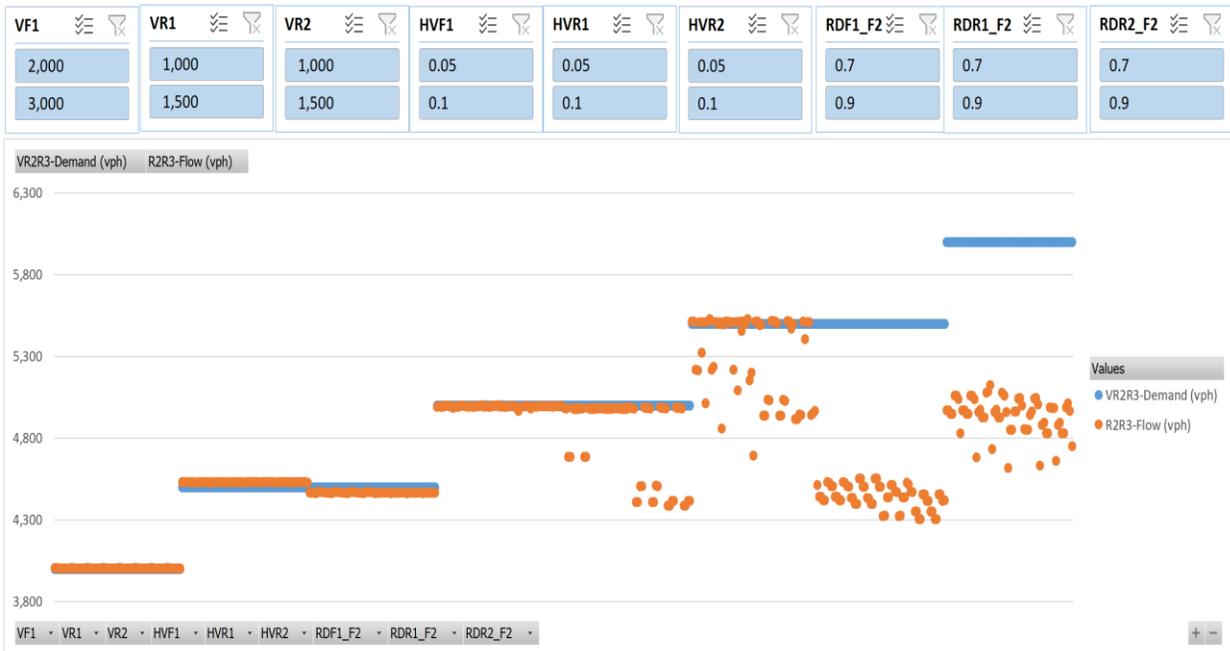


Figure 142: Scenario 15, R2R3 Flow vs. Demand

Scenario Number 16

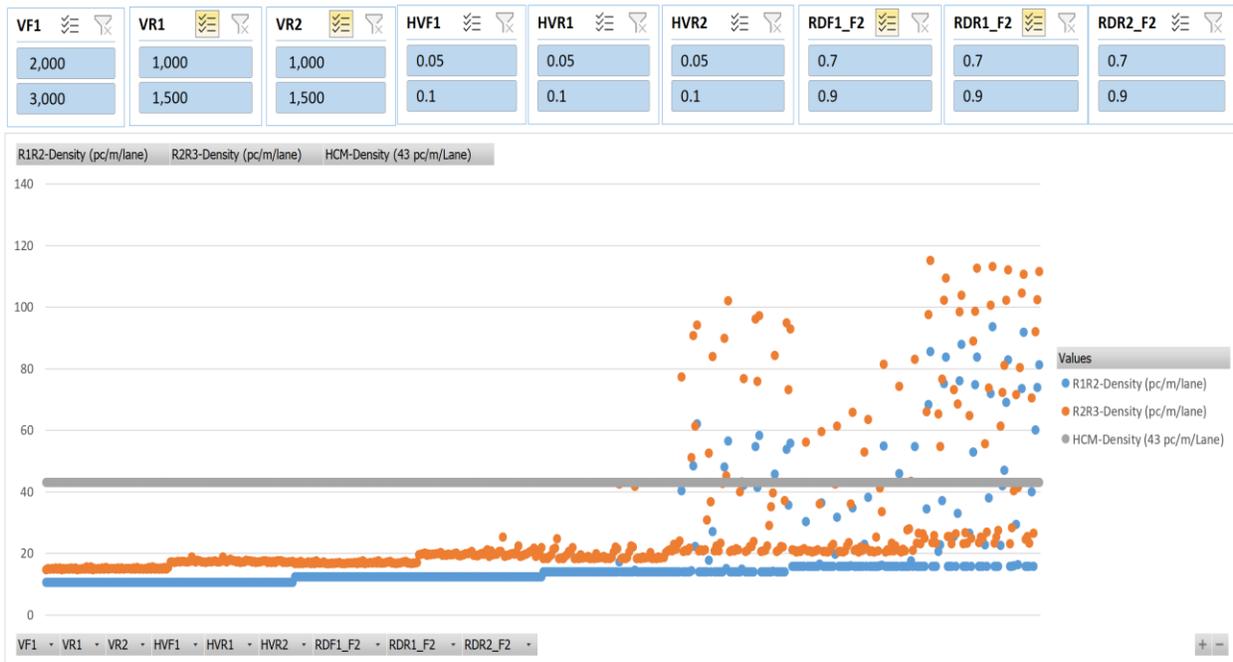


Figure 143: Scenario 16, Density

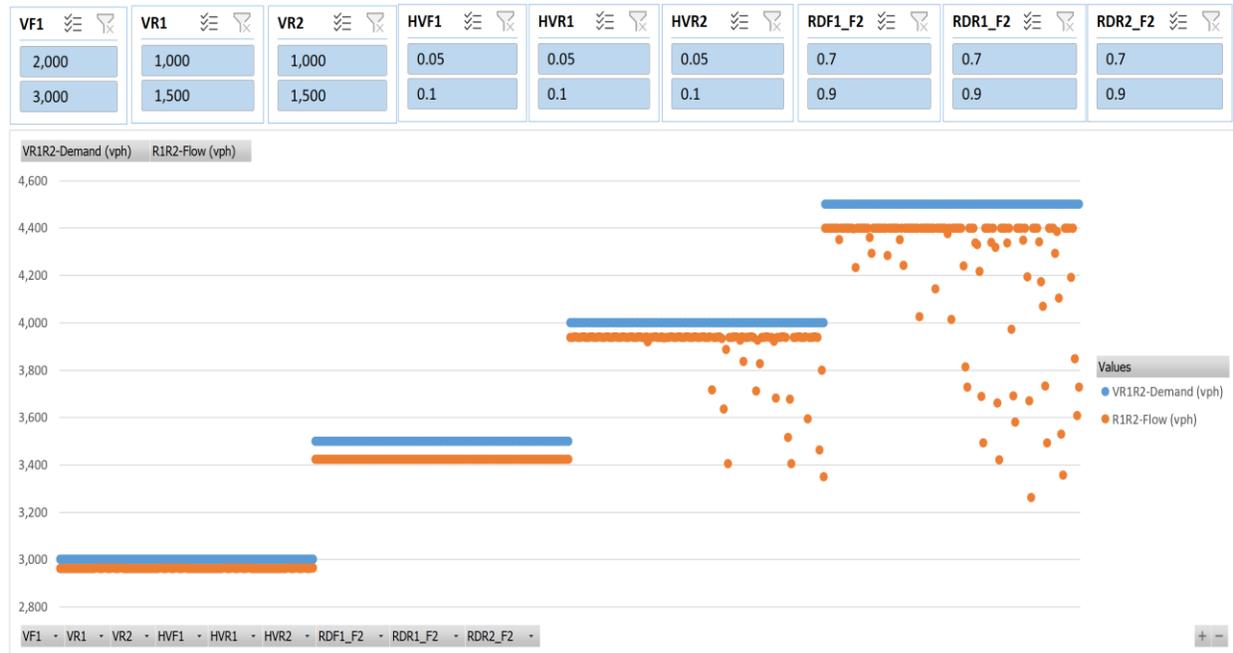


Figure 144: Scenario 16, R1R2 Flow vs. Demand

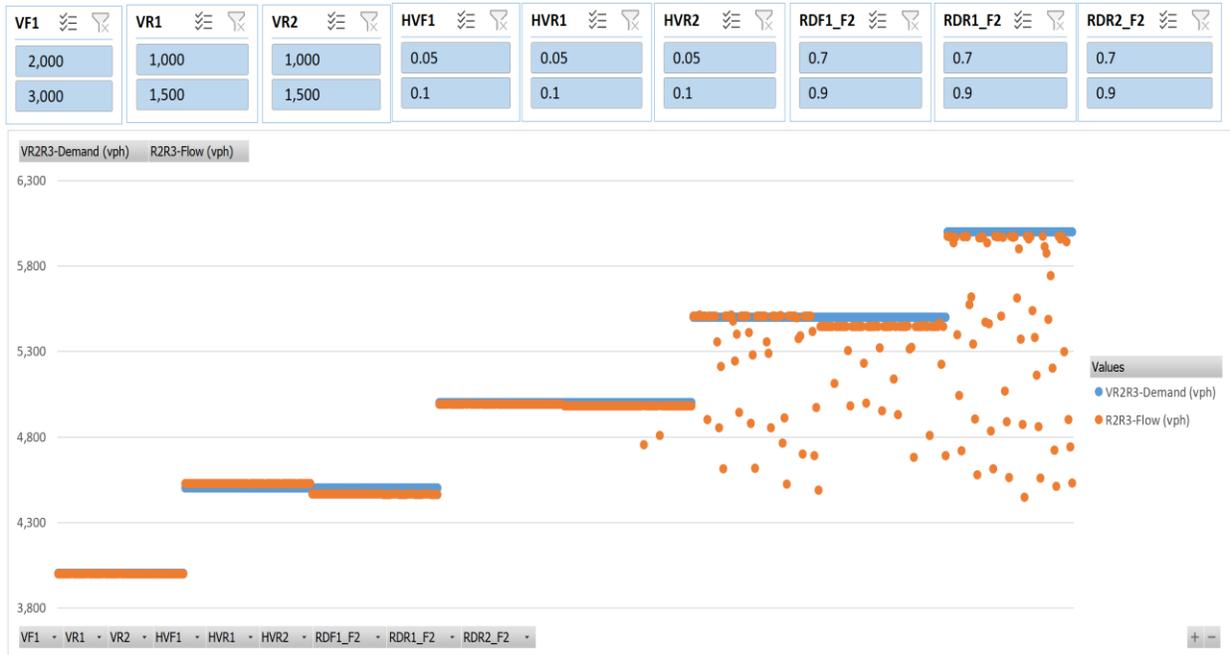


Figure 145: Scenario 16, R2R3 Flow vs. Demand

Scenario Number 17

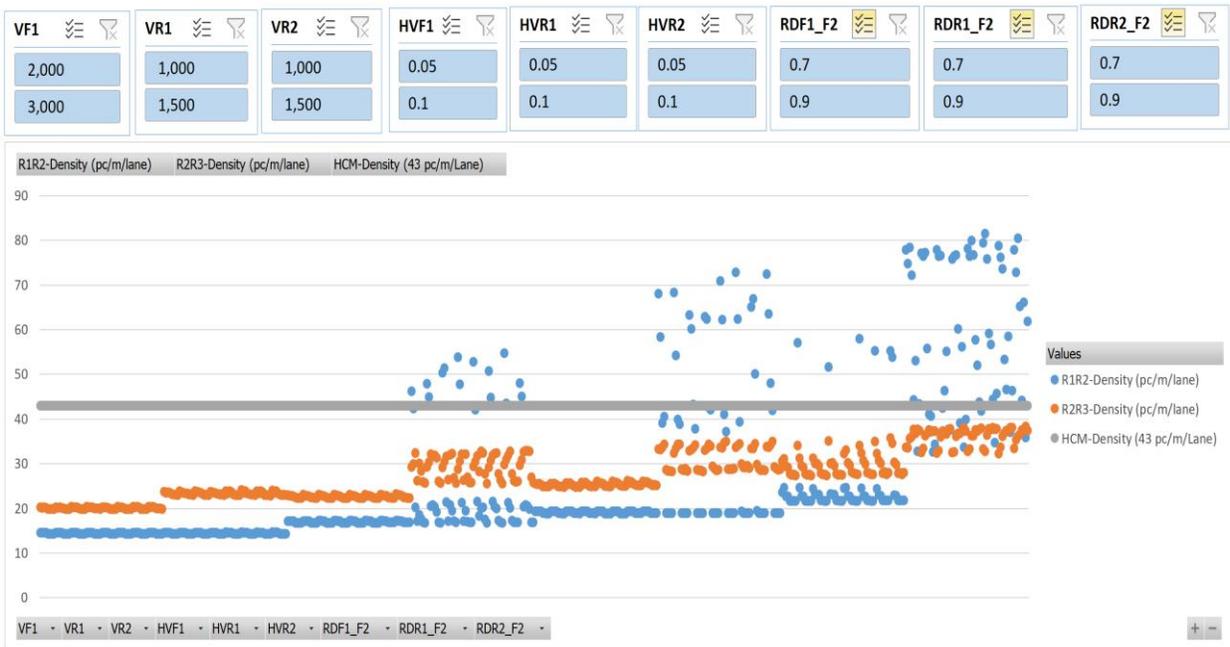


Figure 146: Scenario 17, Density

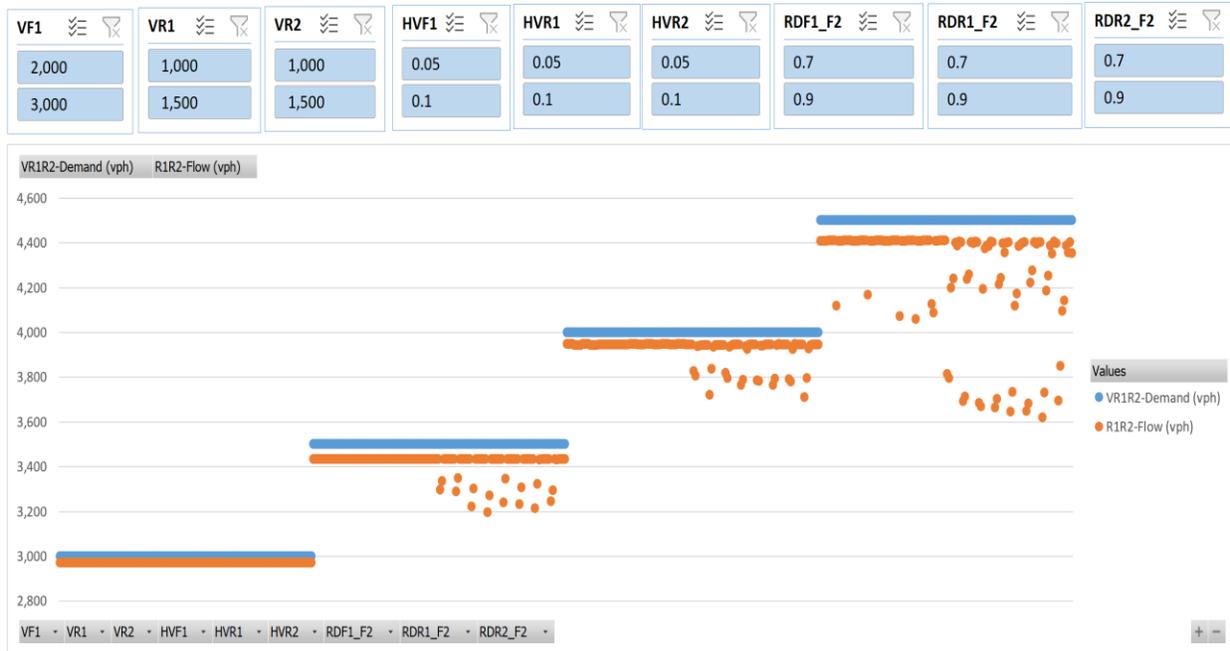


Figure 147: Scenario 17, Flow vs. Demand

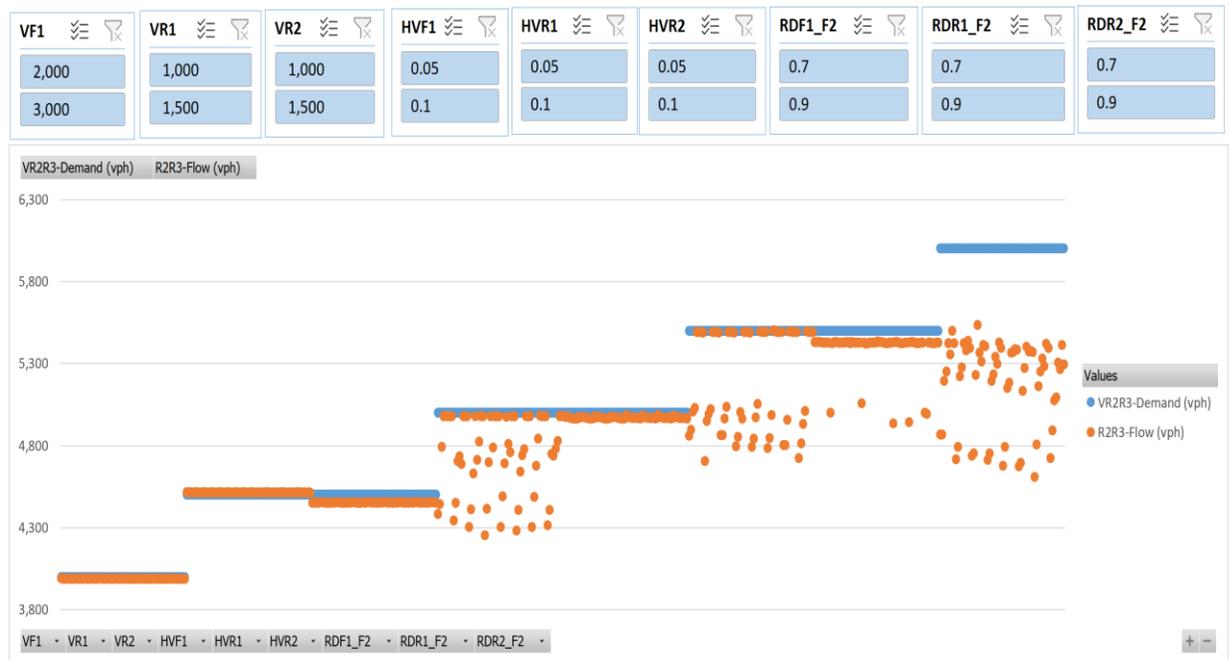


Figure 148: Scenario 17, R2R3 Flow vs. Demand

Scenario Number 18

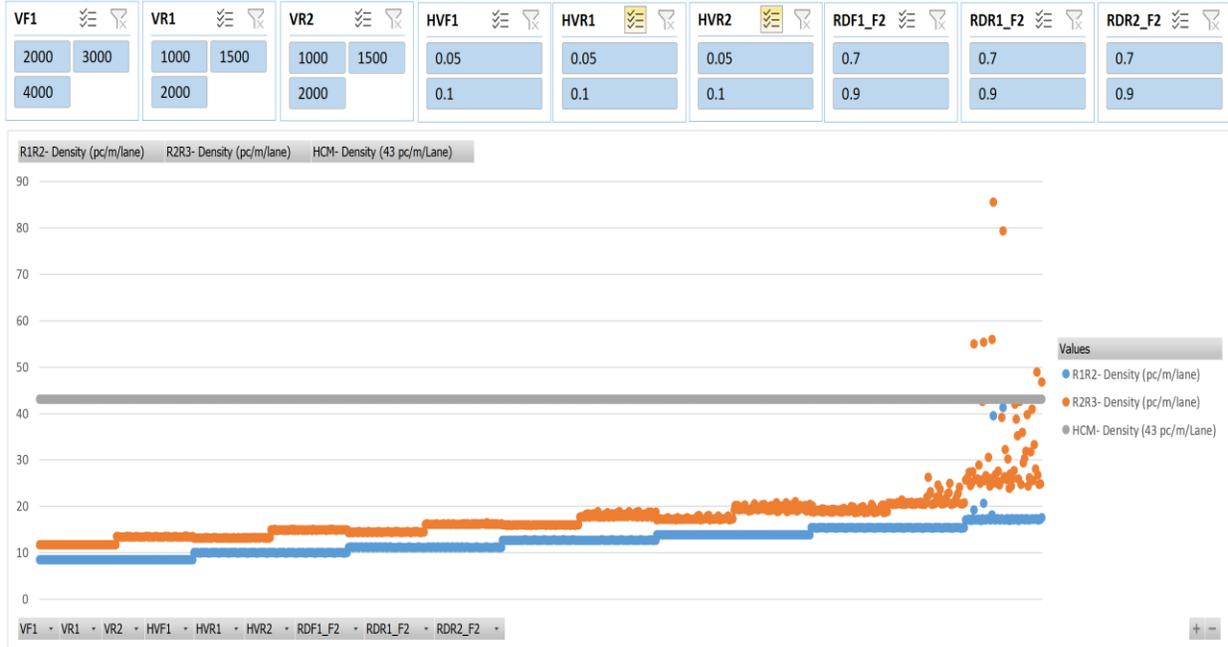


Figure 149: Scenario 18, Density

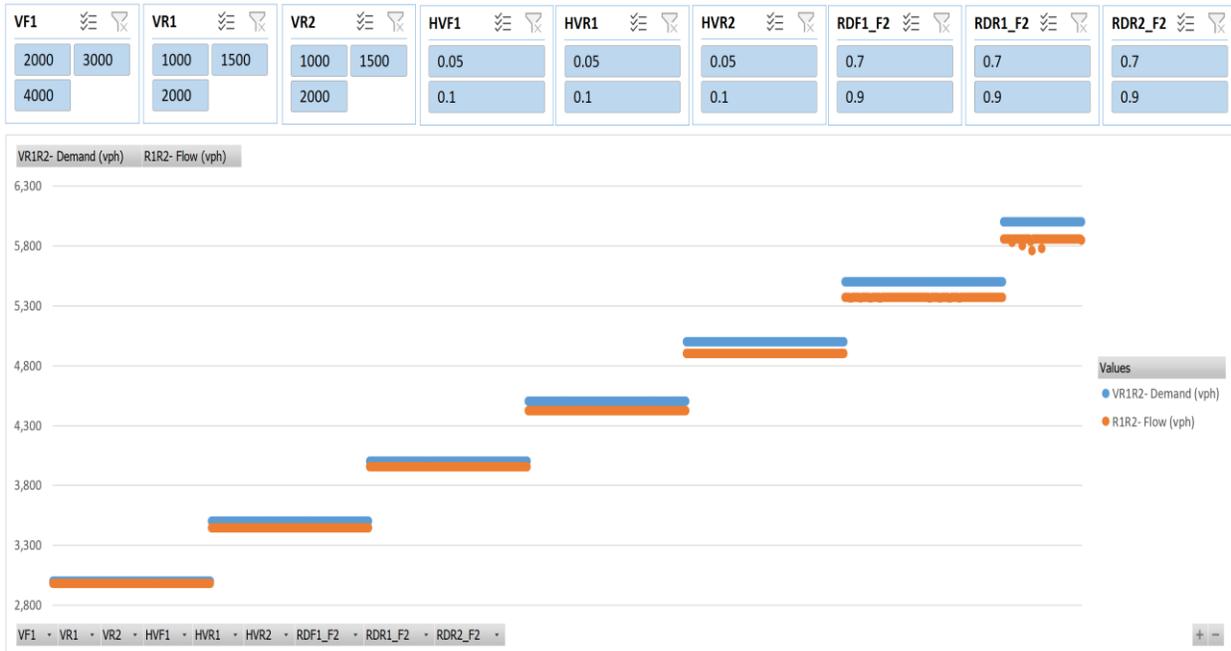


Figure 150: Scenario 18, R1R2 Flow vs. Demand

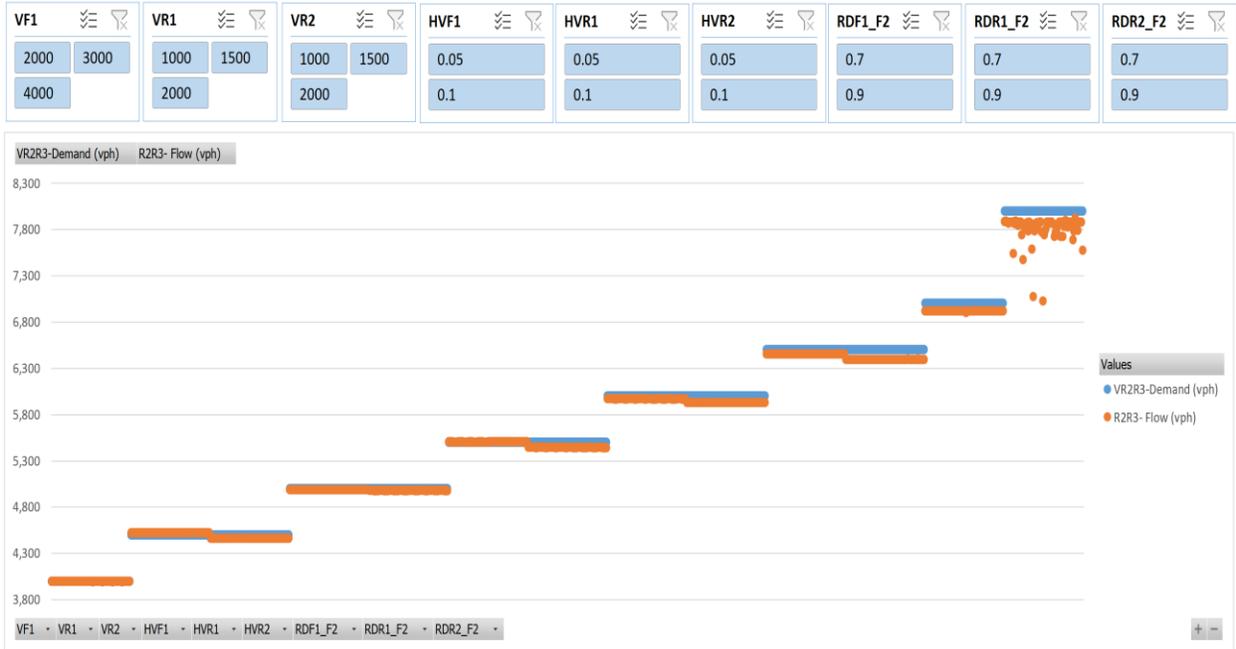


Figure 151: Scenario 18, R2R3 Flow vs. Demand

Scenario Number 19

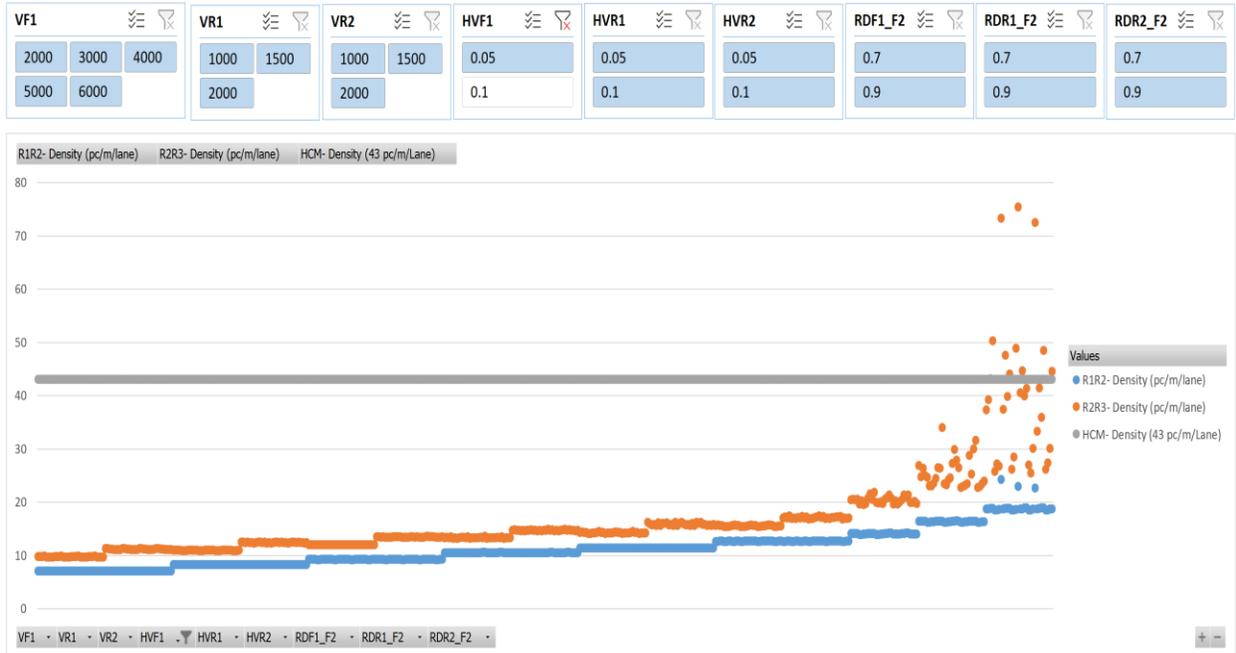


Figure 152: Scenario 19, Density

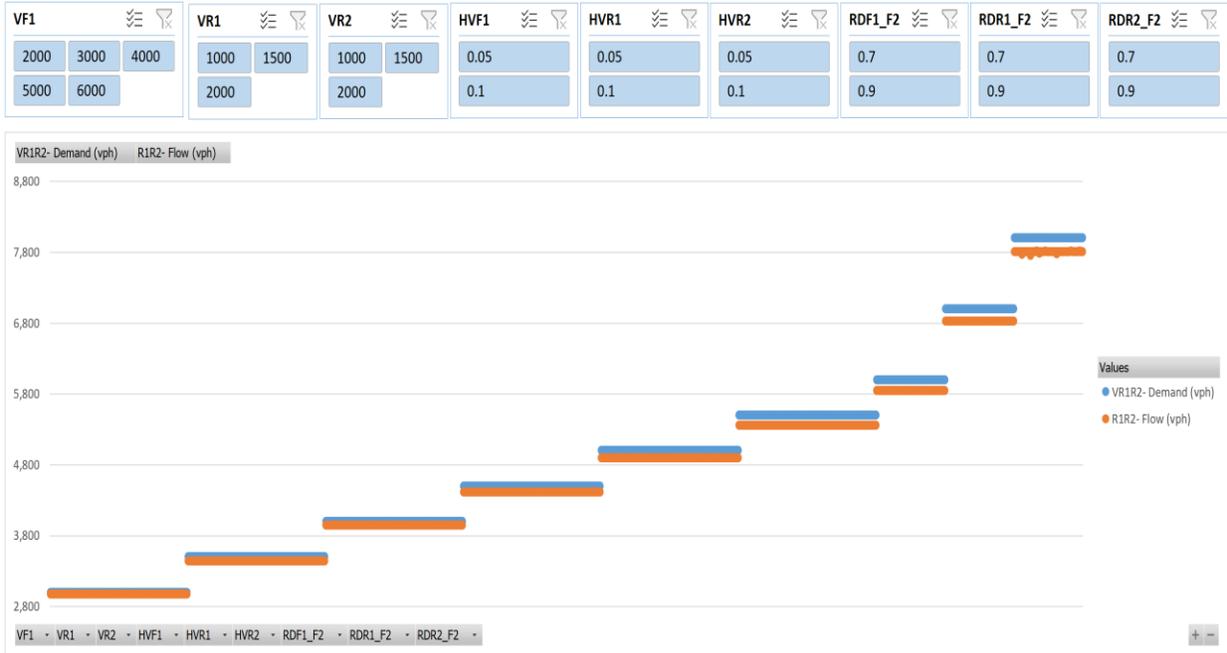


Figure 153: Scenario 19, R1R2 Flow vs. Demand

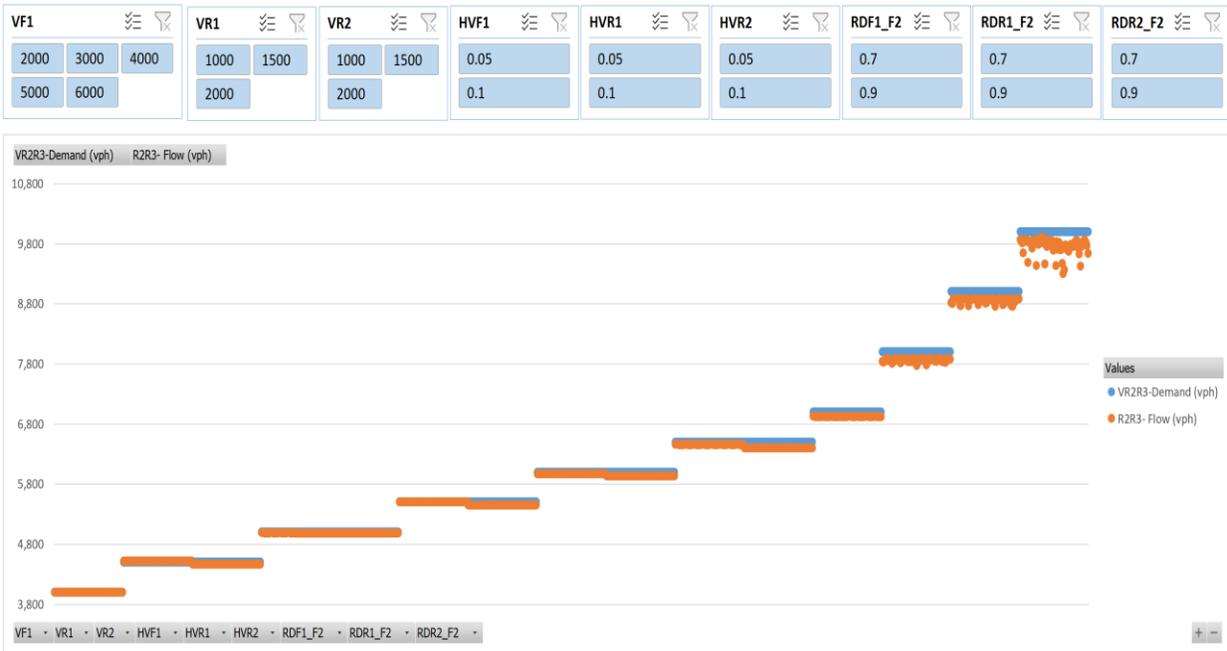


Figure 154: Scenario 19, R2R3 Flow vs. Demand

Scenario Number 20

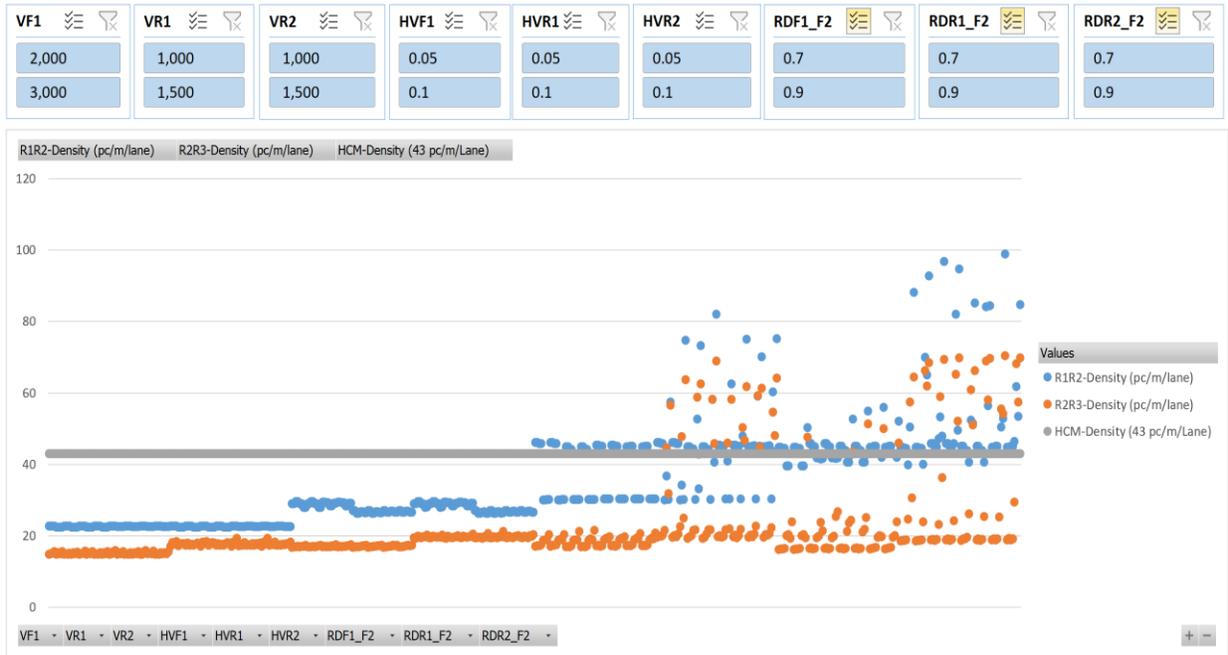


Figure 155: Scenario 20, Density

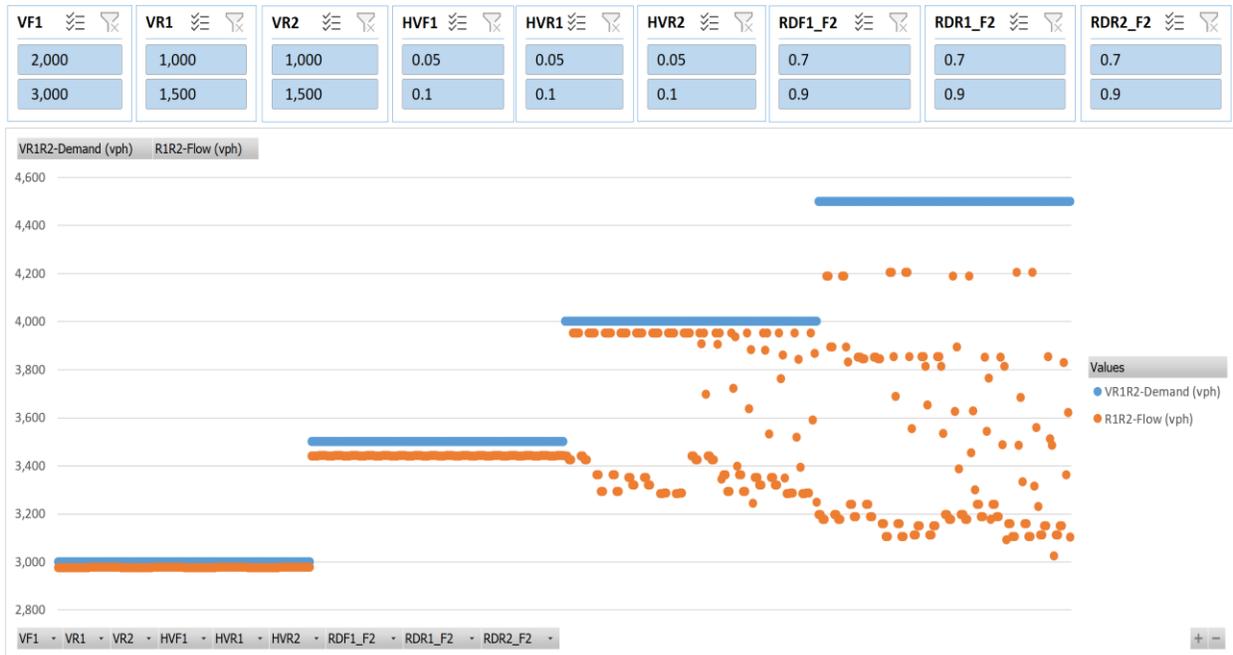


Figure 156: Scenario 20, R1R2 Flow vs. Demand

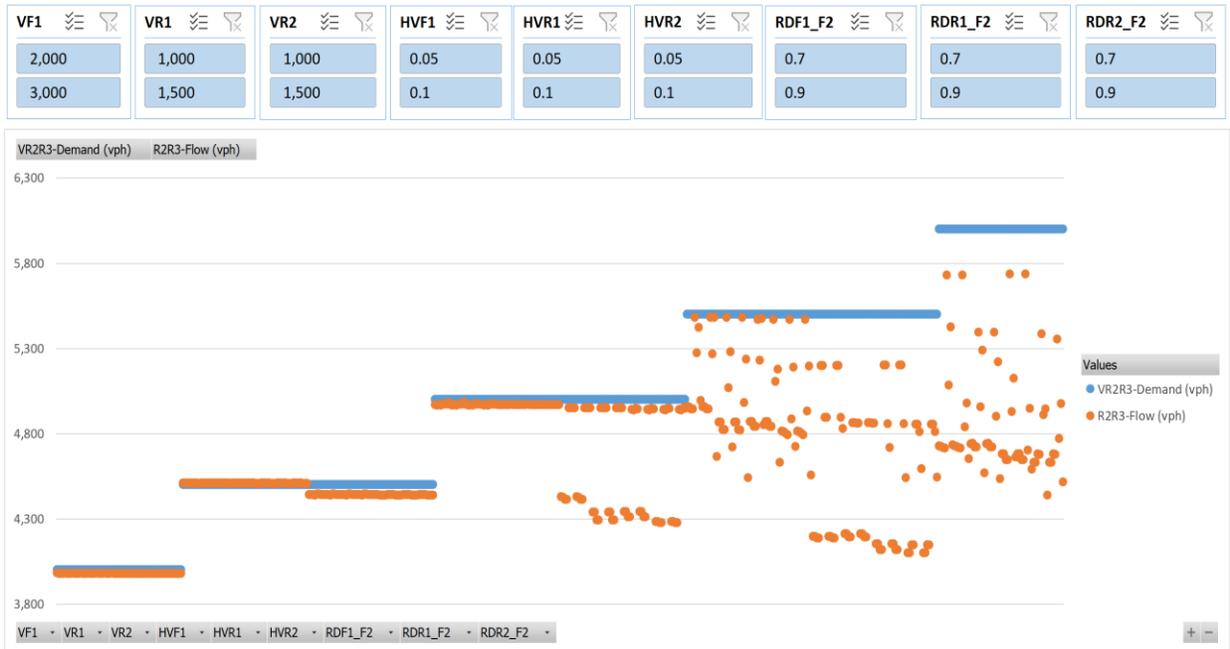


Figure 157: Scenario 20, R2R3 Flow vs. Demand

Scenario Number 21

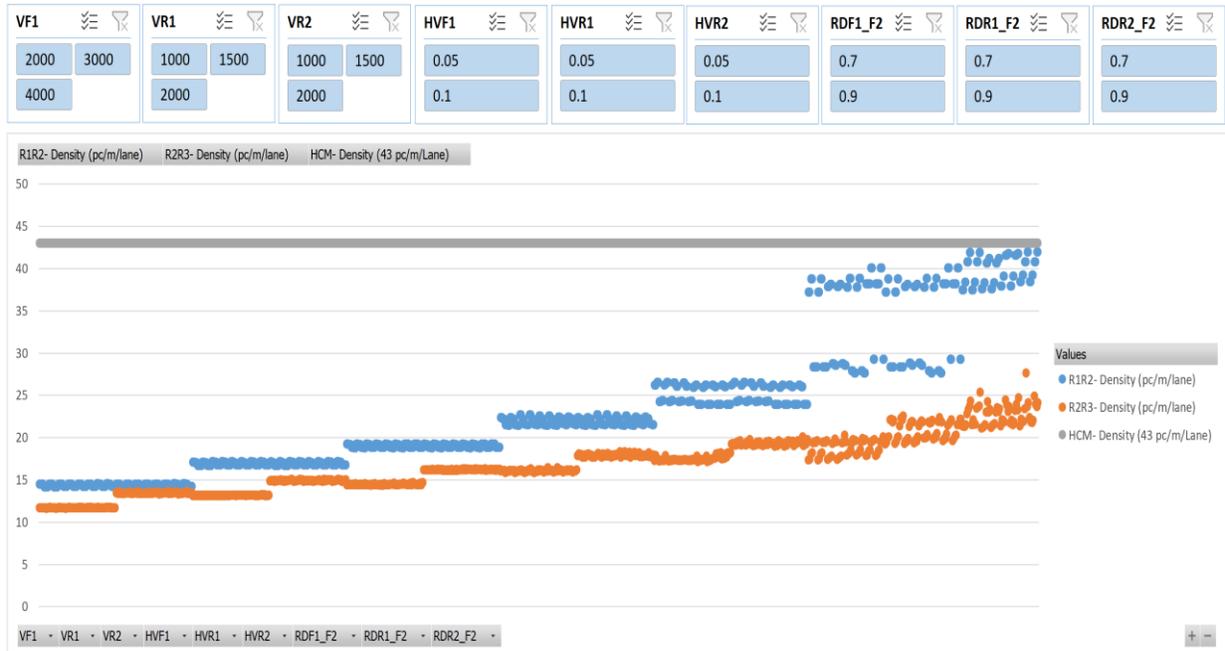


Figure 158: Scenario 21, Density

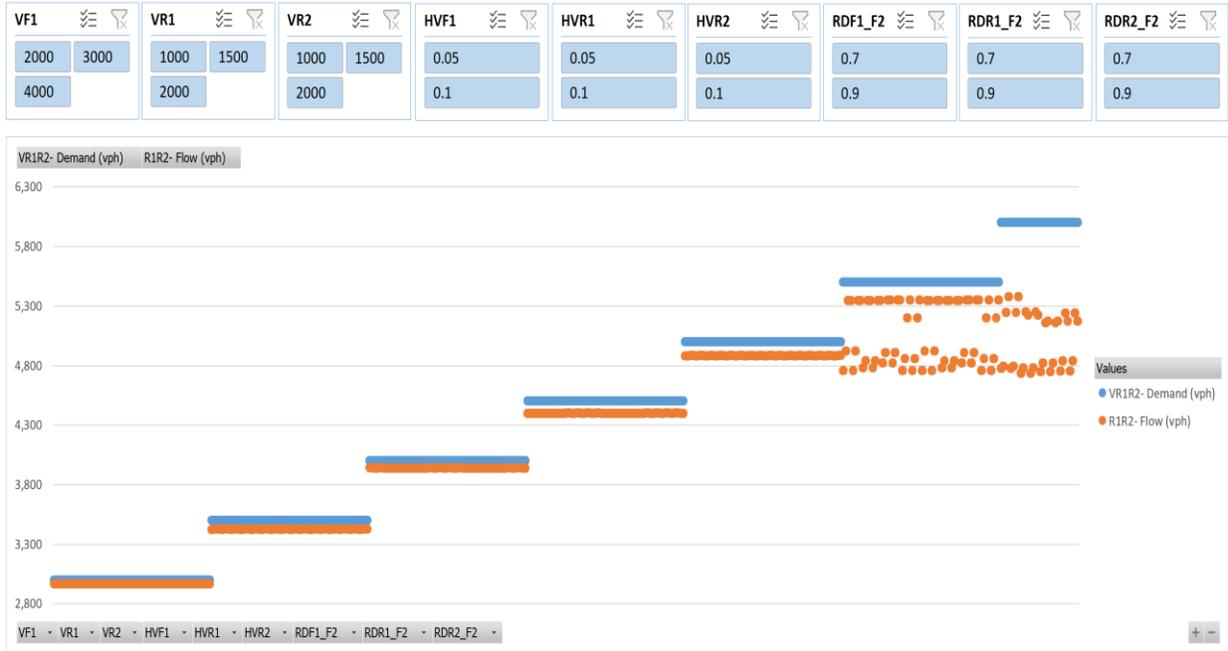


Figure 159: Scenario 21, R1R2 Flow vs. Demand

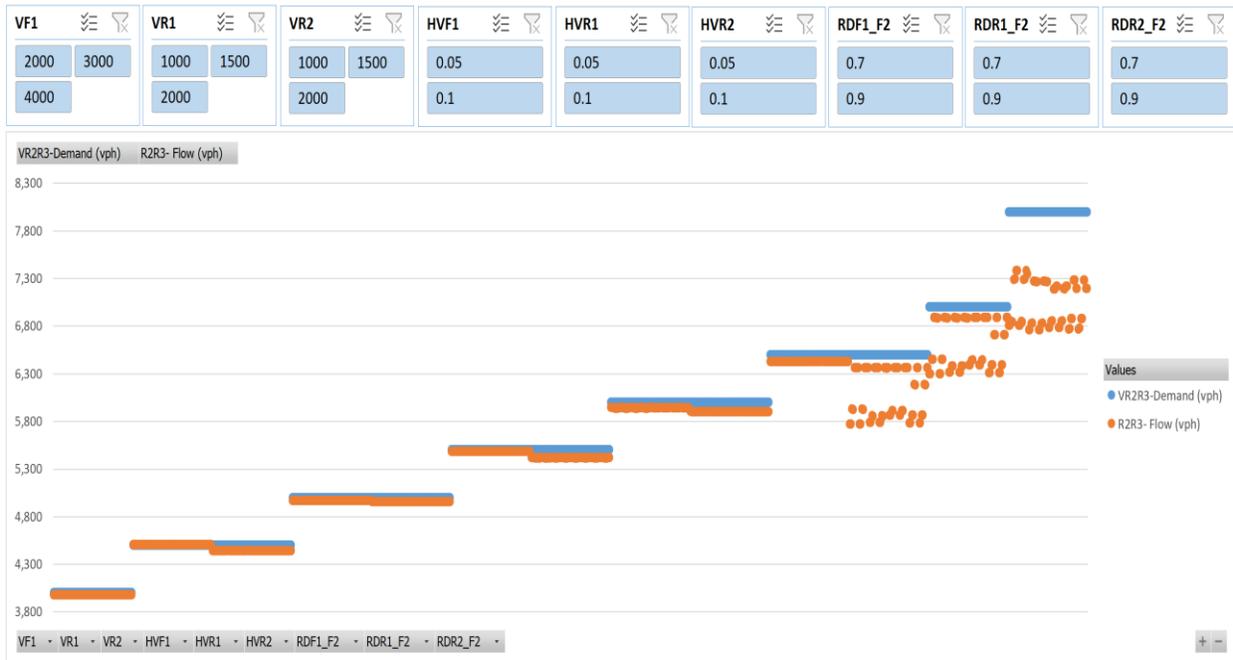


Figure 160: Scenario 21, R2R3 Flow vs. Demand

Scenario Number 22

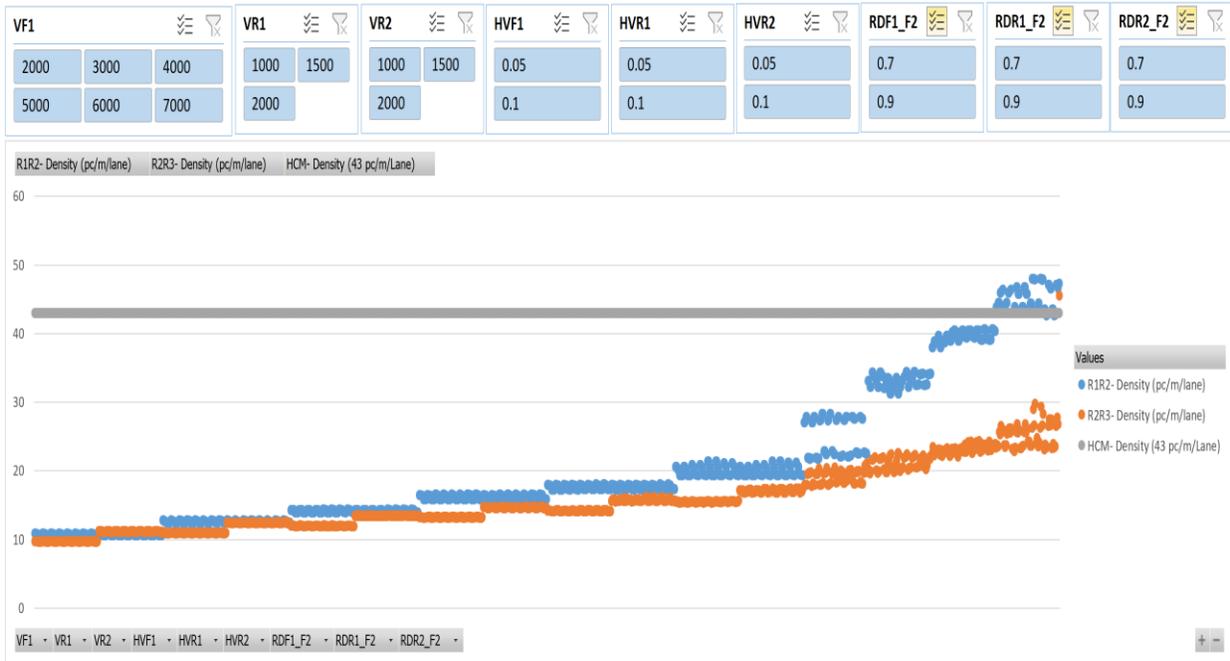


Figure 161: Scenario 22, Density

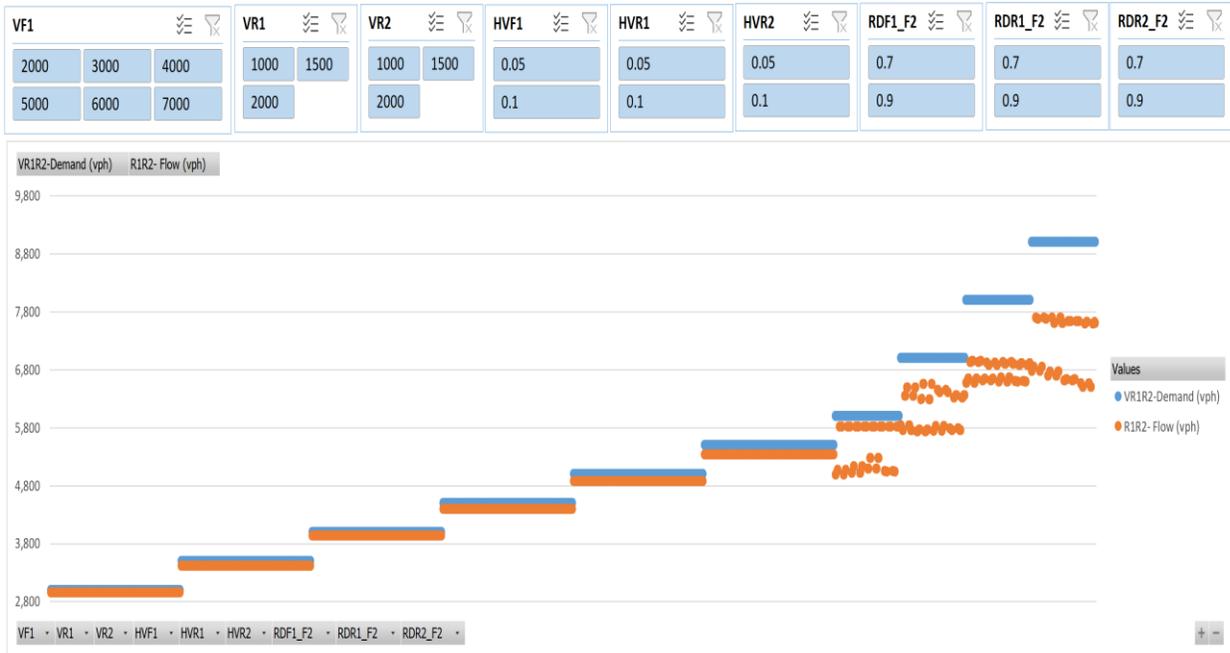


Figure 162: Scenario 22, R1R2 Flow vs. Demand

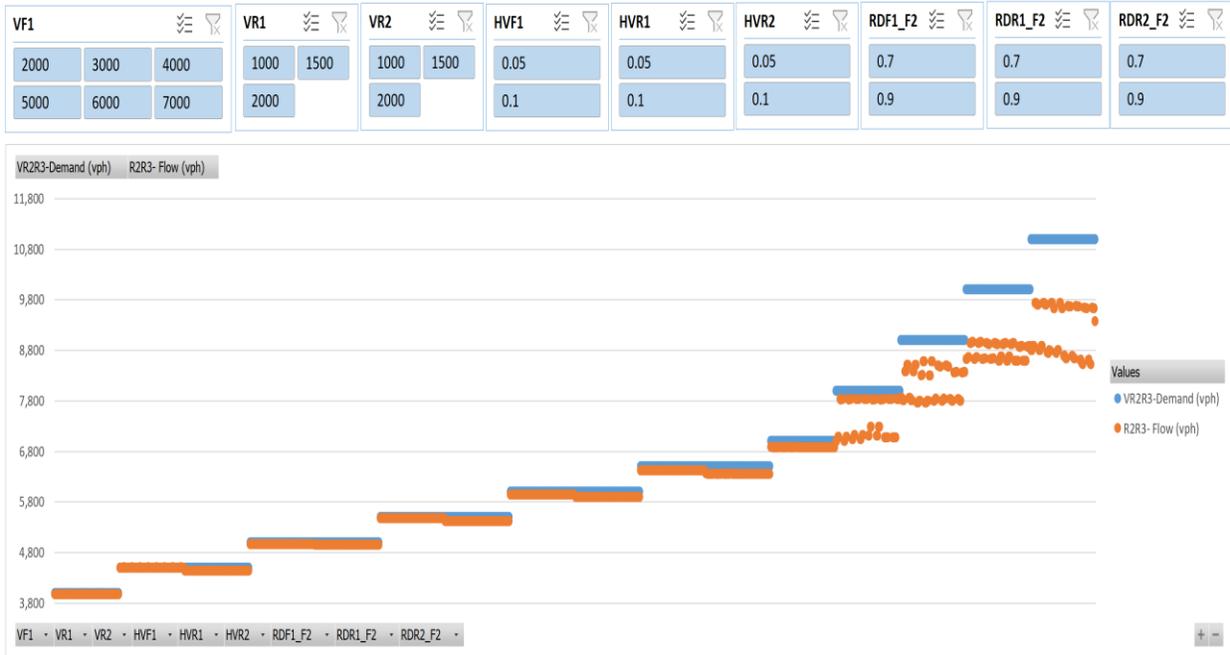


Figure 163: Scenario 22, R2R3 Flow vs. Demand

Scenario Number 23

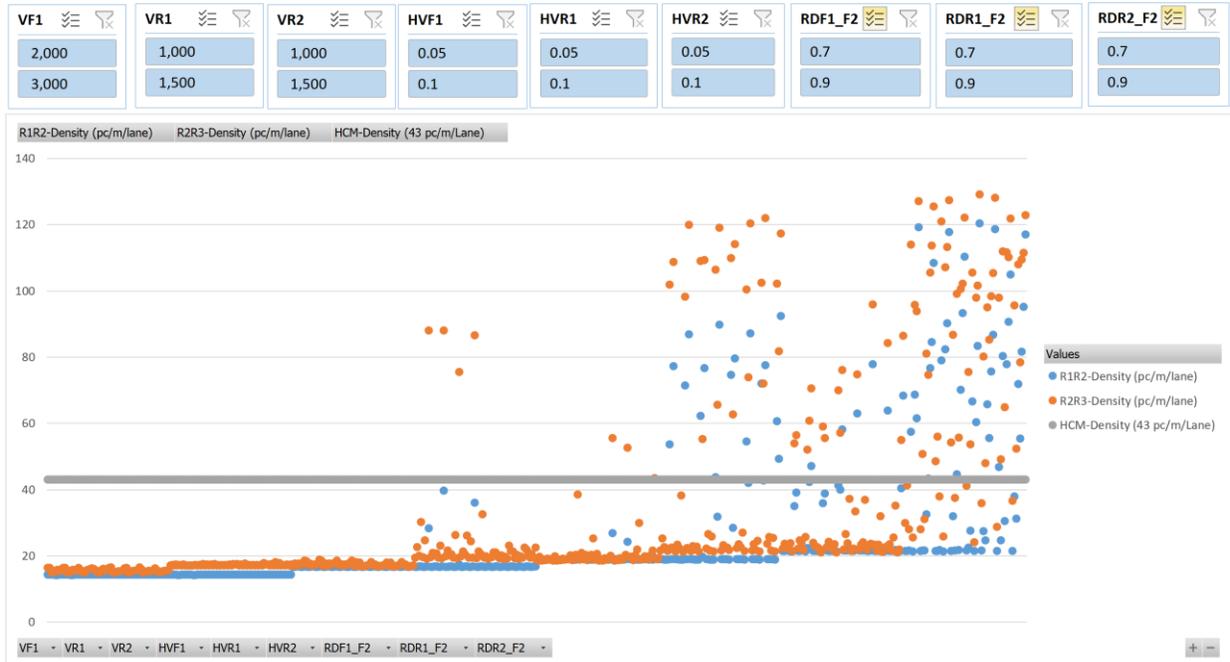


Figure 164: Scenario 23, Density

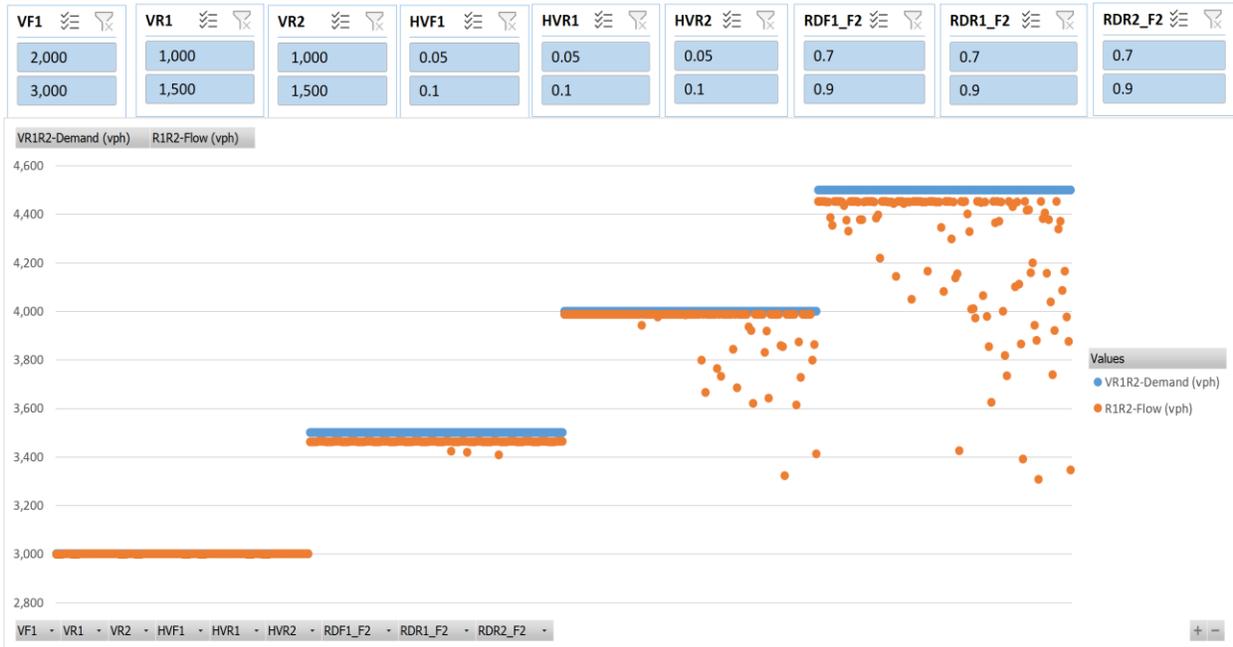


Figure 165: Scenario 23, R1R2 Flow vs. Demand

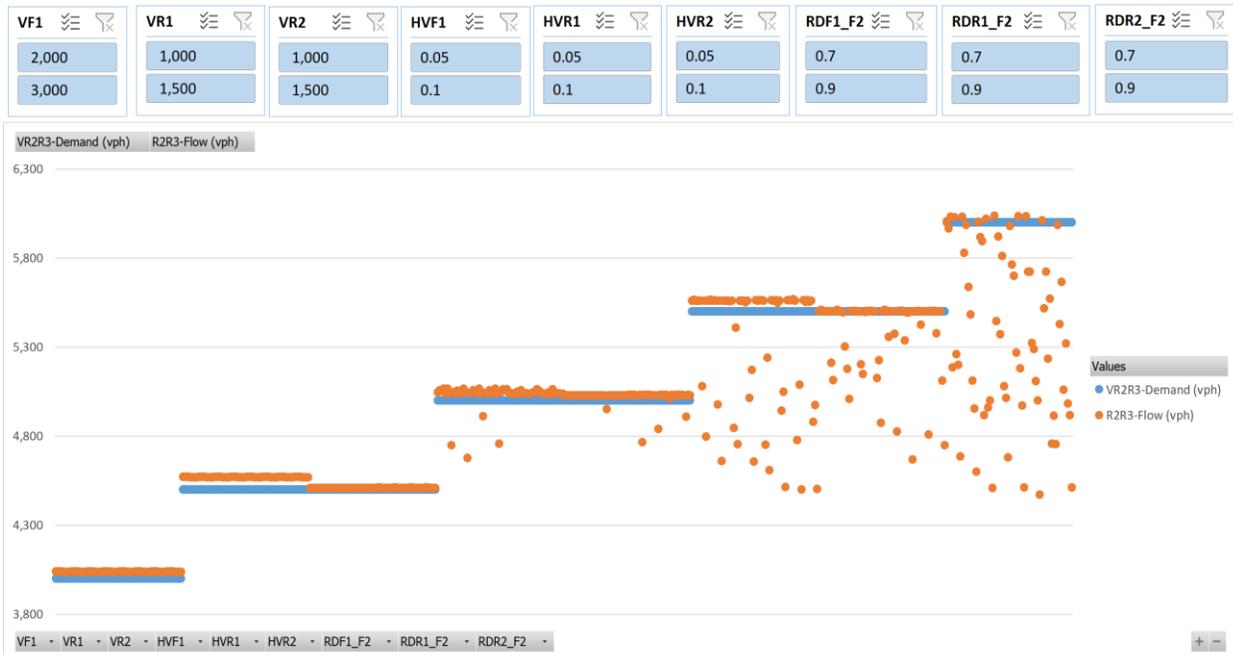


Figure 166: Scenario 23, R2R3 Flow vs. Demand

Scenario Number 24

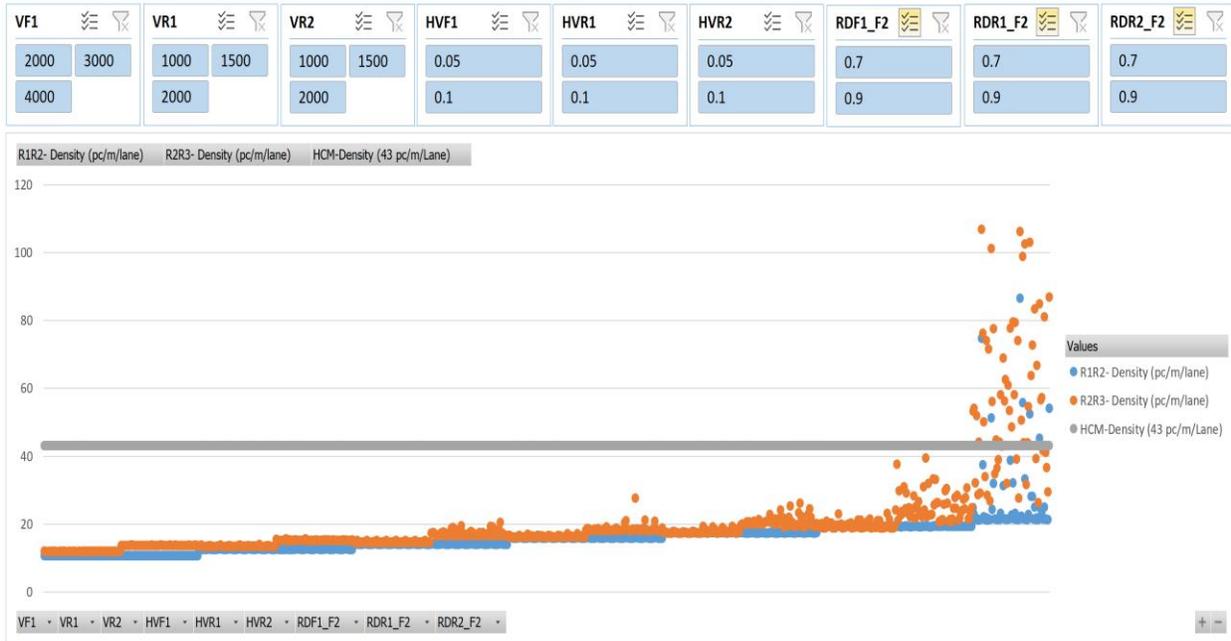


Figure 167: Scenario 24, Density

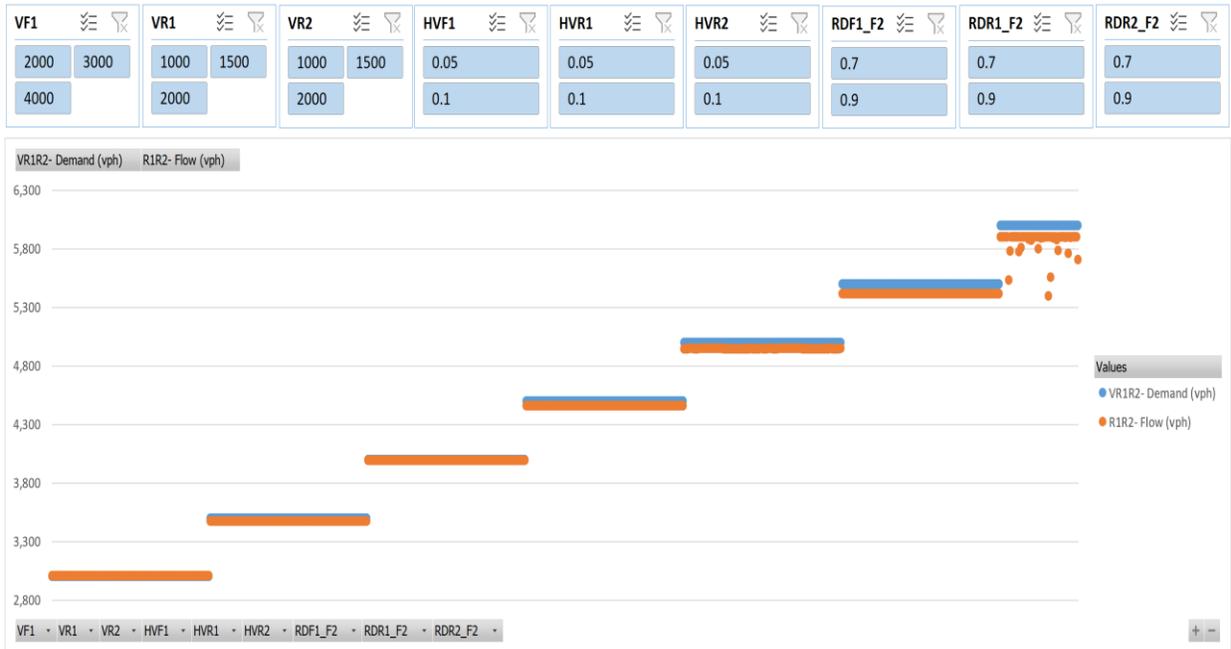


Figure 168: Scenario 24, R1R2 Flow vs. Demand

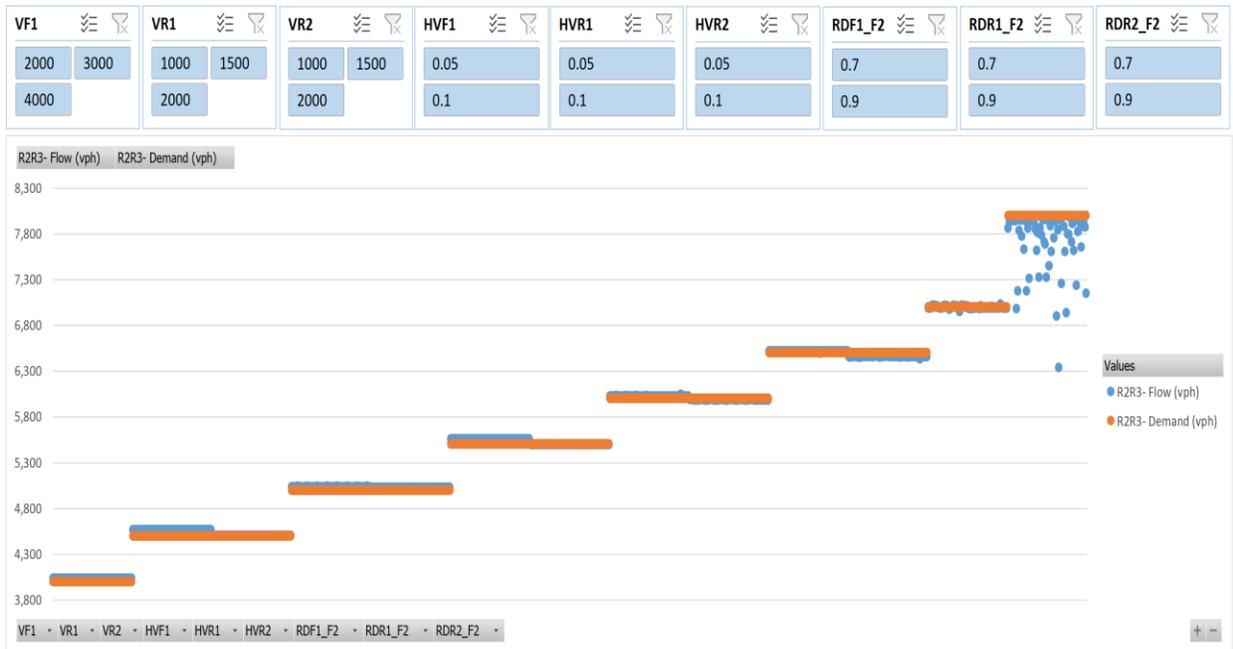


Figure 169: Scenario 24, R2R3 Flow vs. Demand

Scenario Number 25

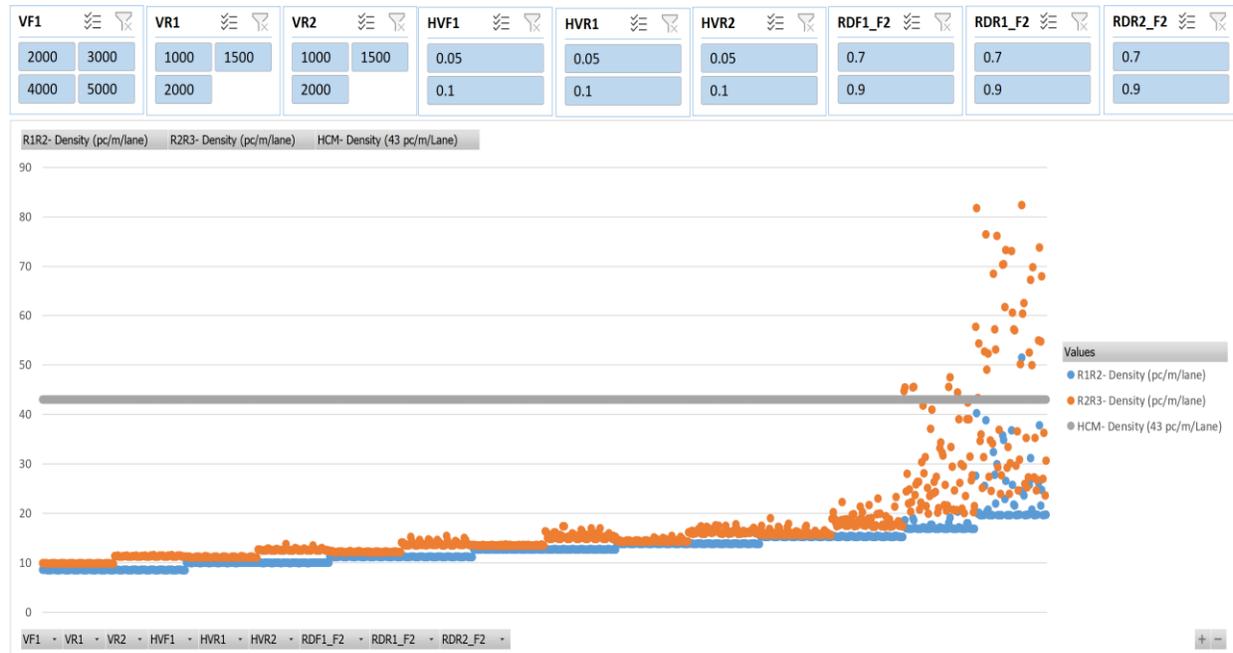


Figure 170: Scenario 25, Density

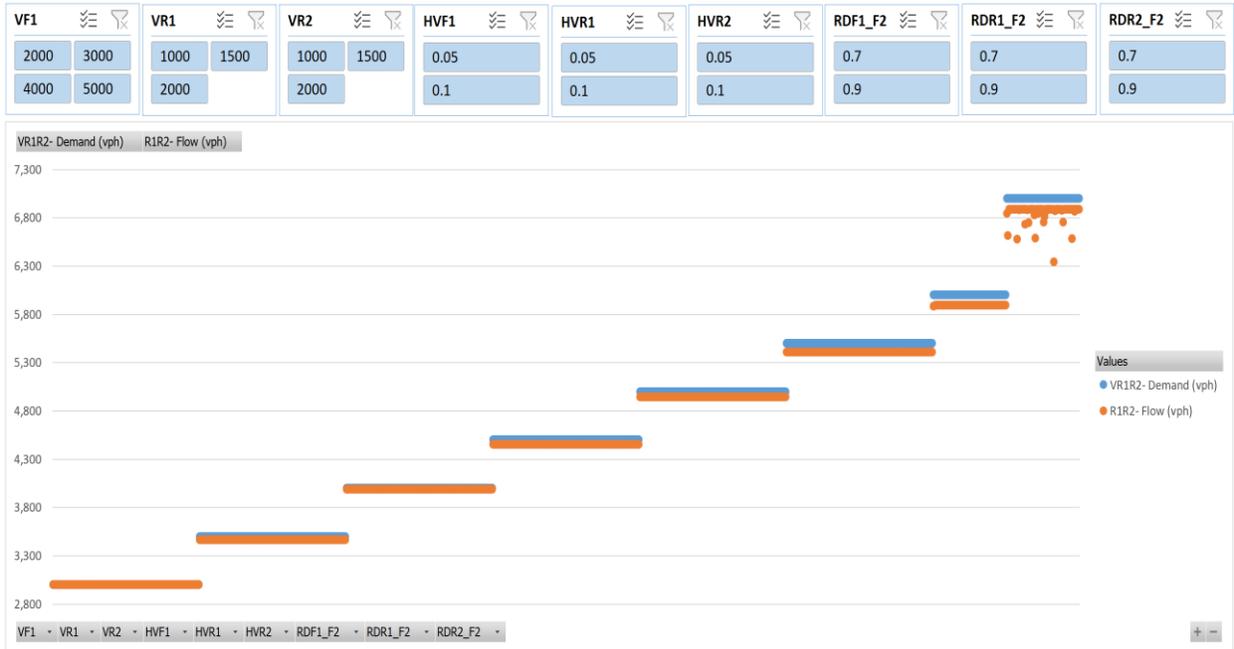


Figure 171: Scenario 25, R1R2 Flow vs. Demand

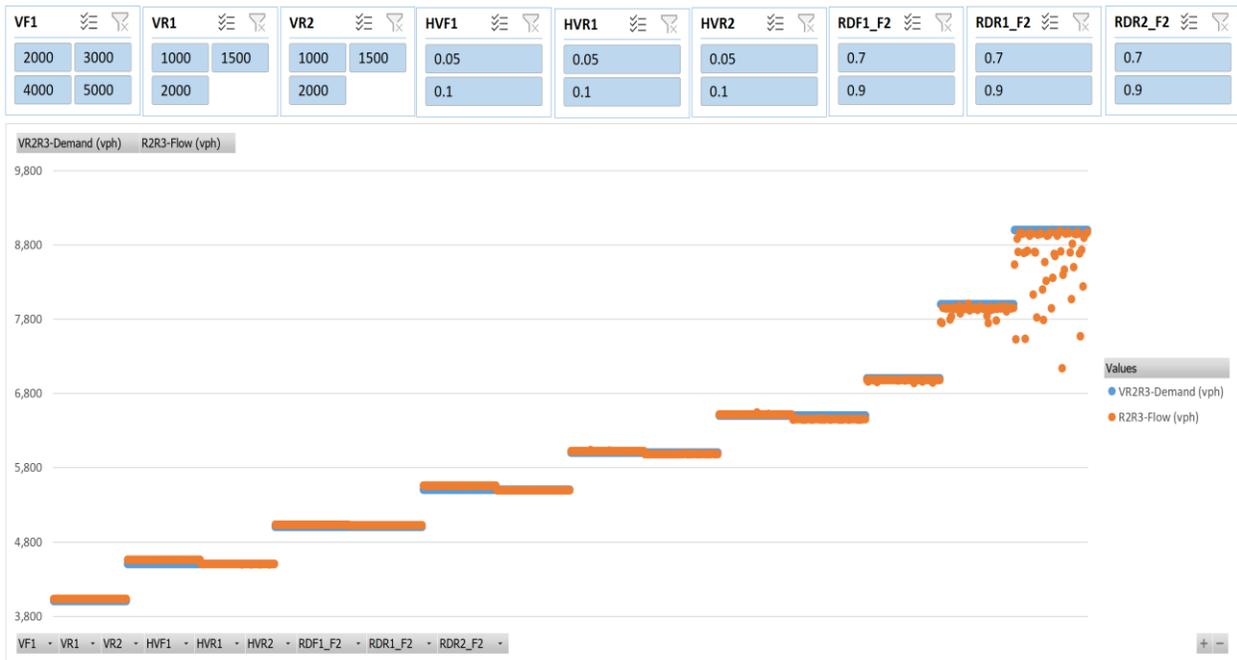


Figure 172: Scenario 25, R2R3 Flow vs. Demand

Scenario Number 26

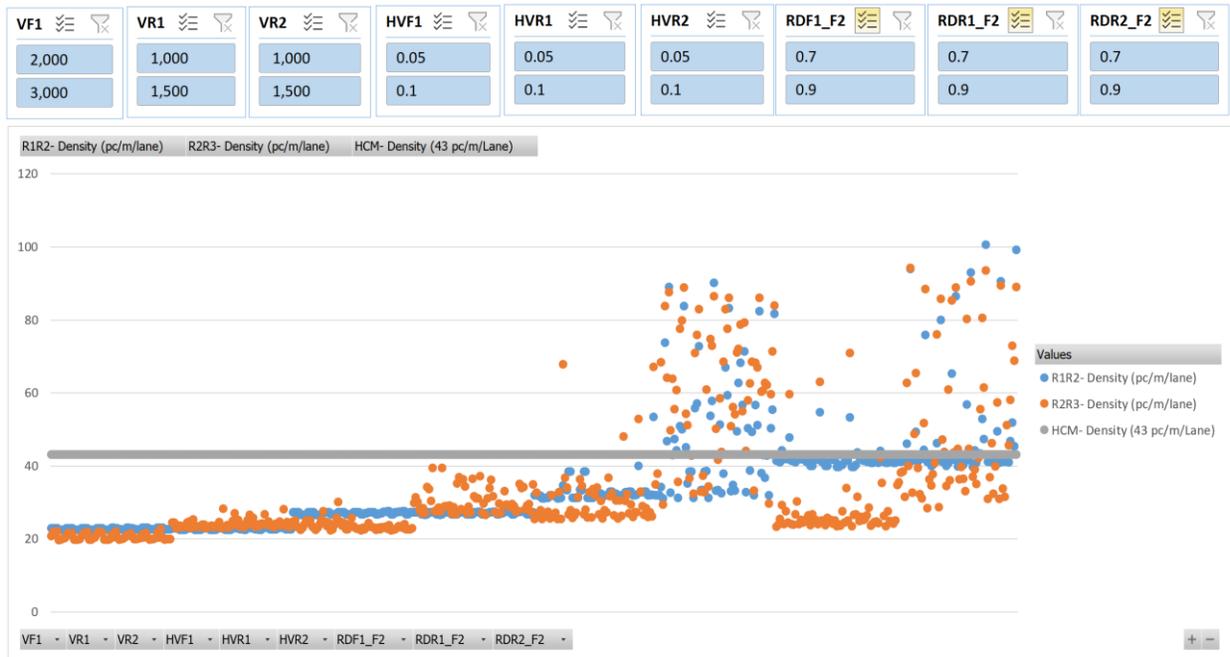


Figure 173: Scenario 26, Density



Figure 174: Scenario 26, R1R2 Flow vs. Demand

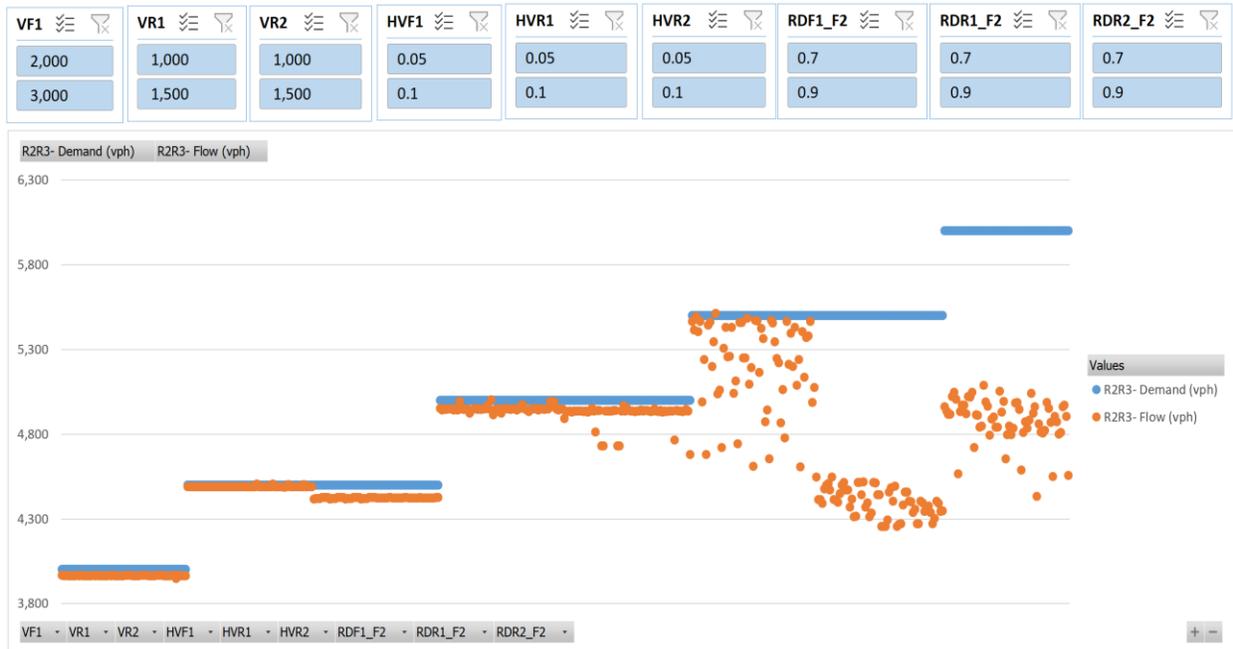


Figure 175: Scenario 26, R2R3 Flow vs. Demand

Scenario Number 27

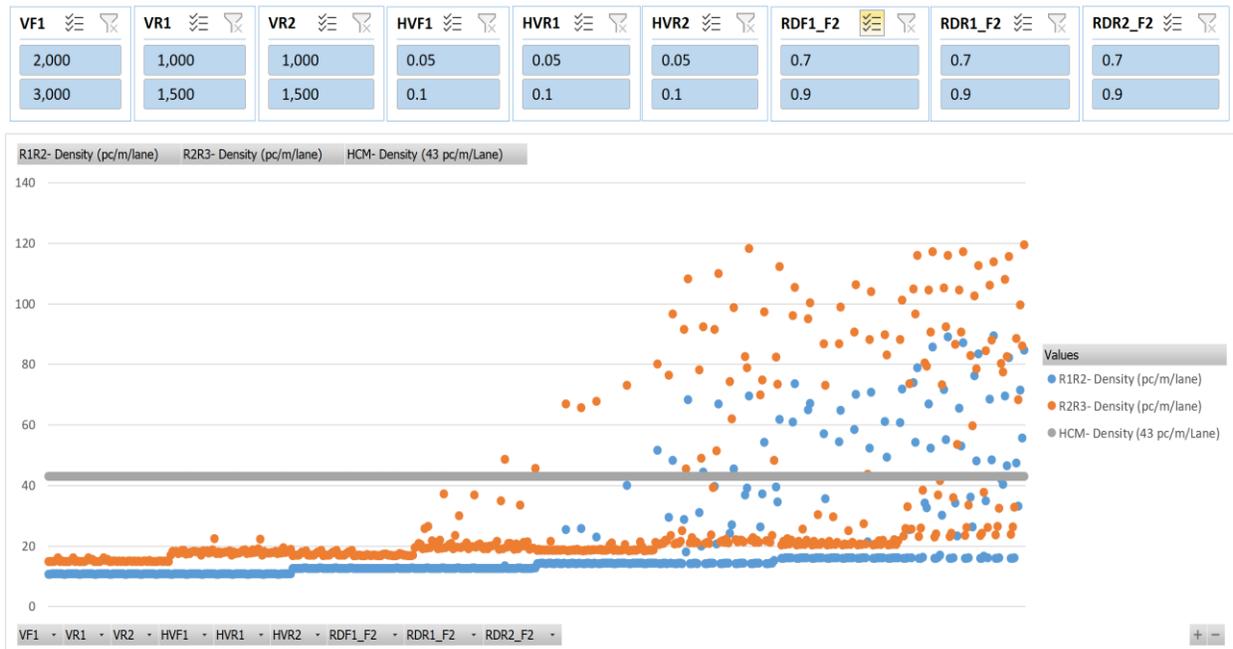


Figure 176: Scenario 27, Density

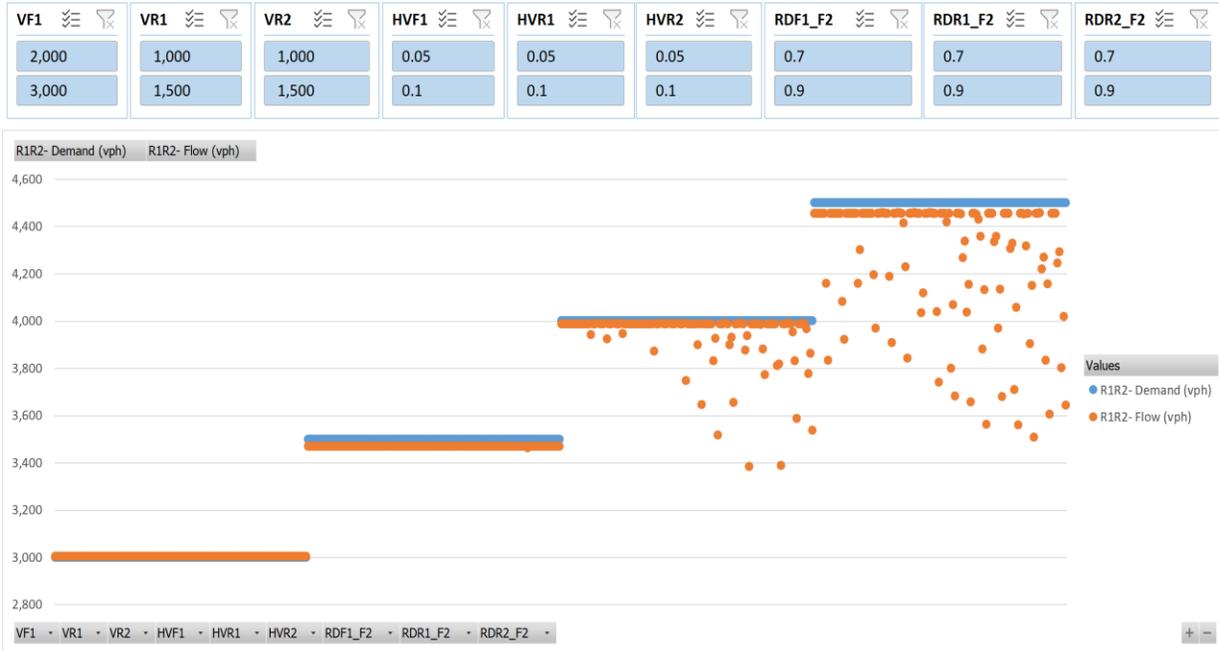


Figure 177: Scenario 27, R1R2 Flow vs. Demand

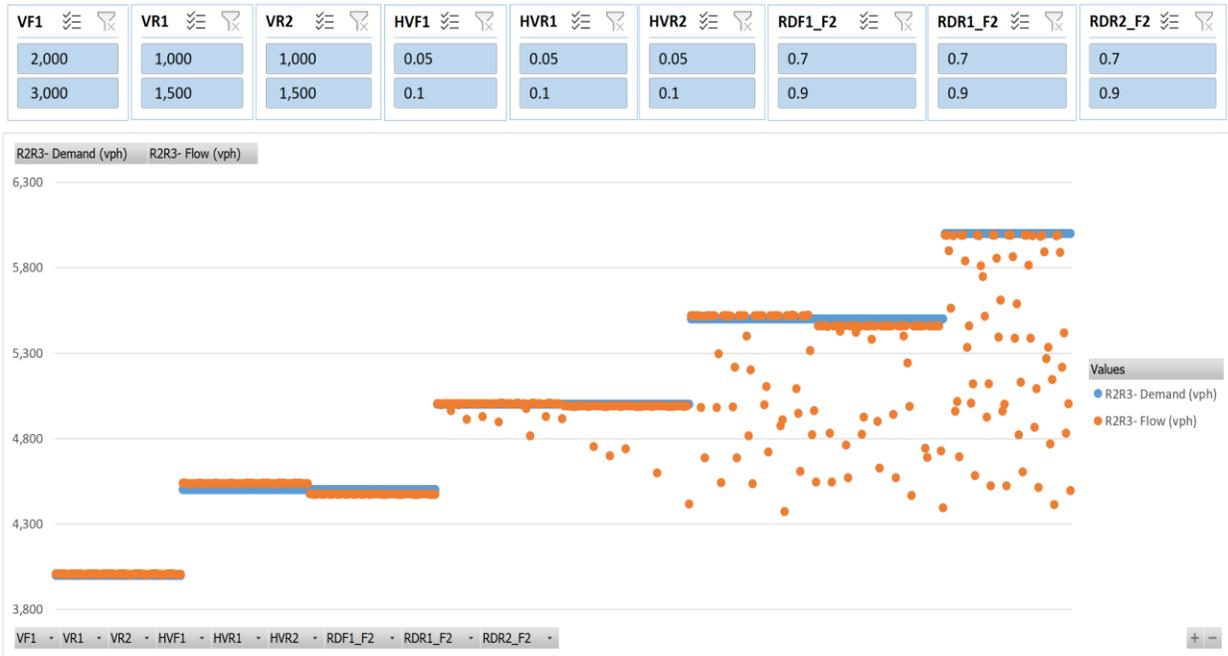


Figure 178: Scenario 27, R2R3 Flow vs. Demand

Scenario Number 28

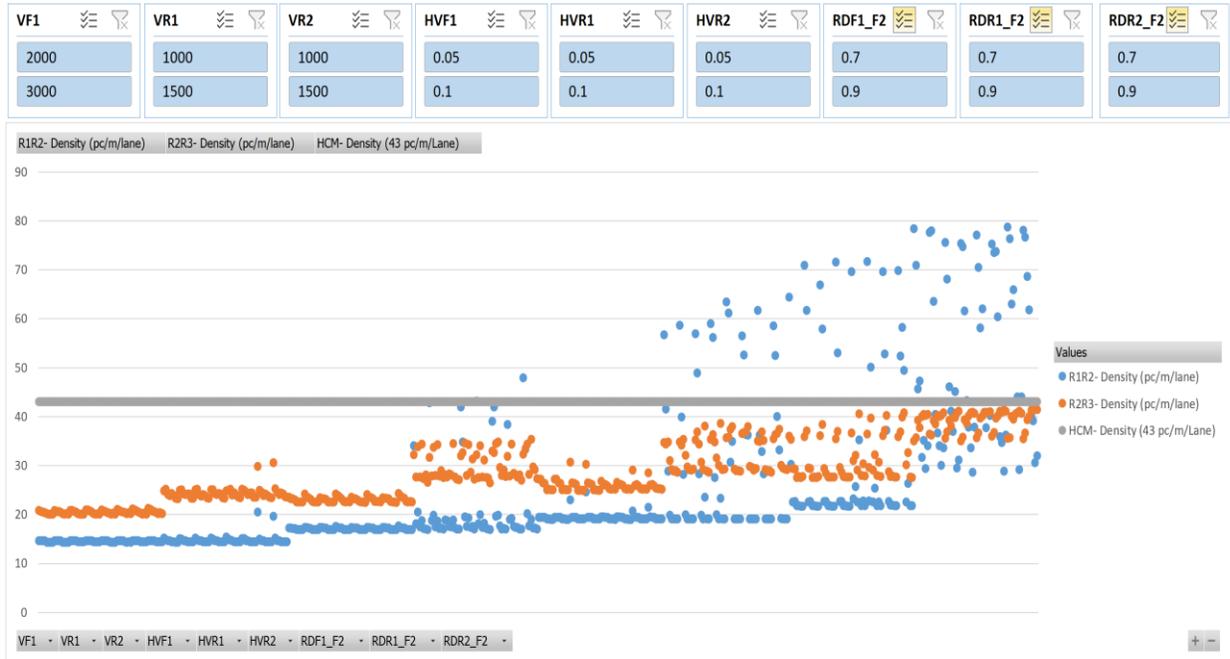


Figure 179: Scenario 28, Density

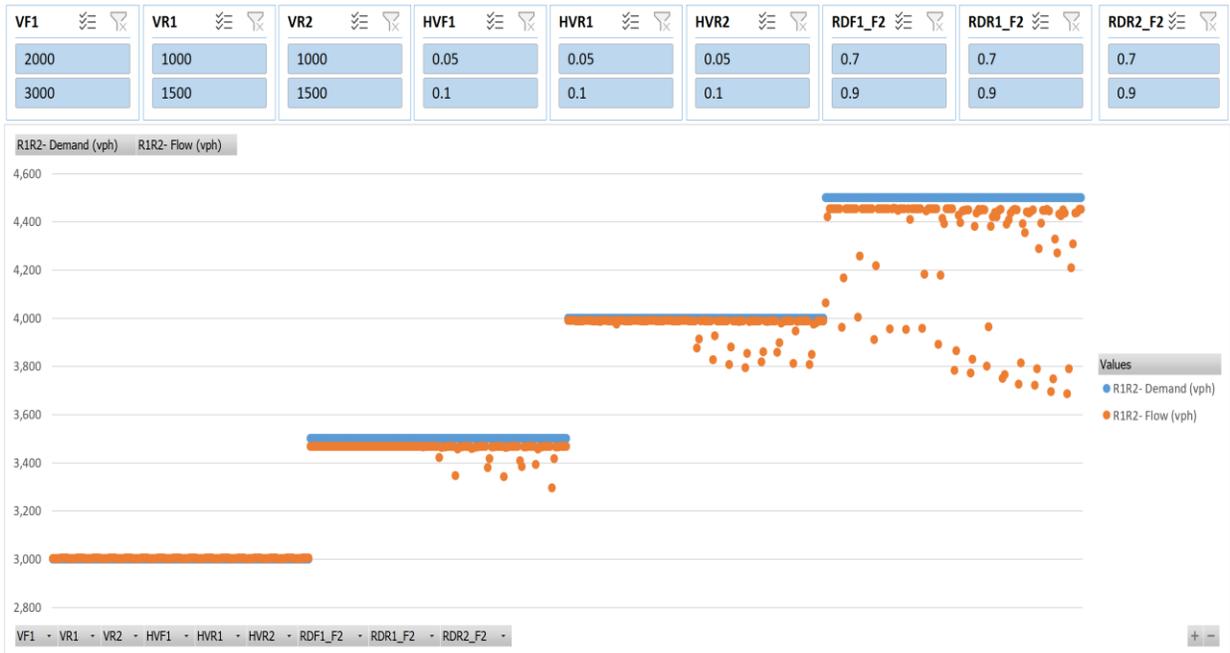


Figure 180: Scenario 28, R1R2 Flow vs. Demand

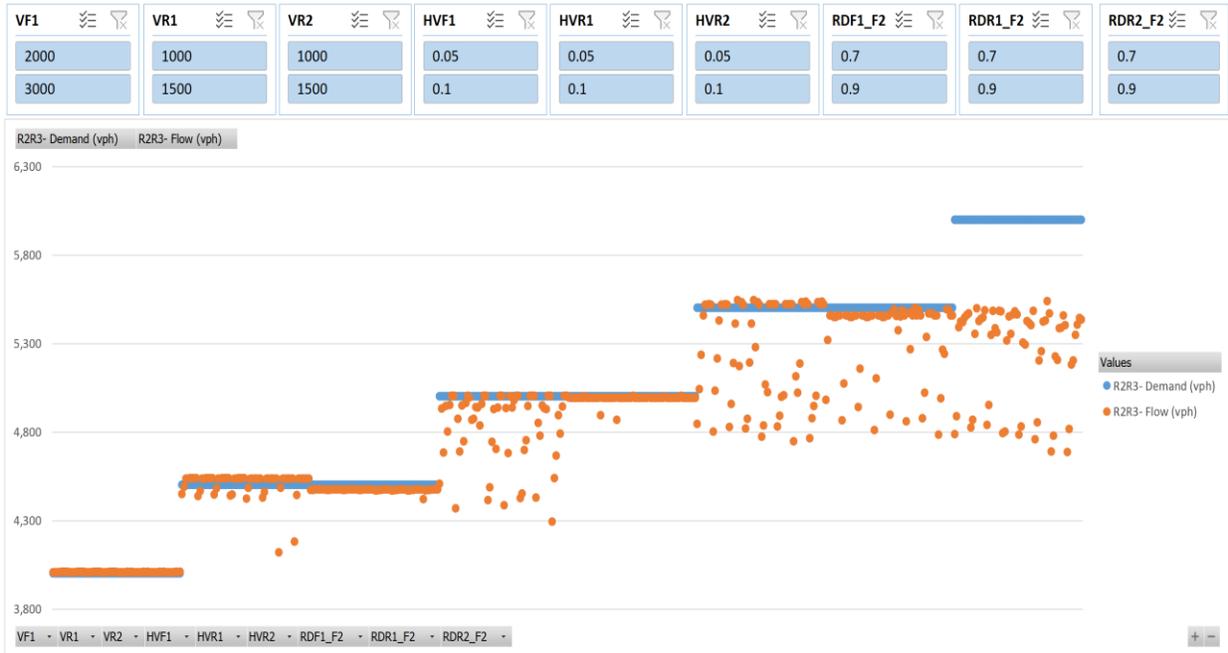


Figure 181: Scenario 28, R2R3 Flow vs. Demand

Scenario Number 29

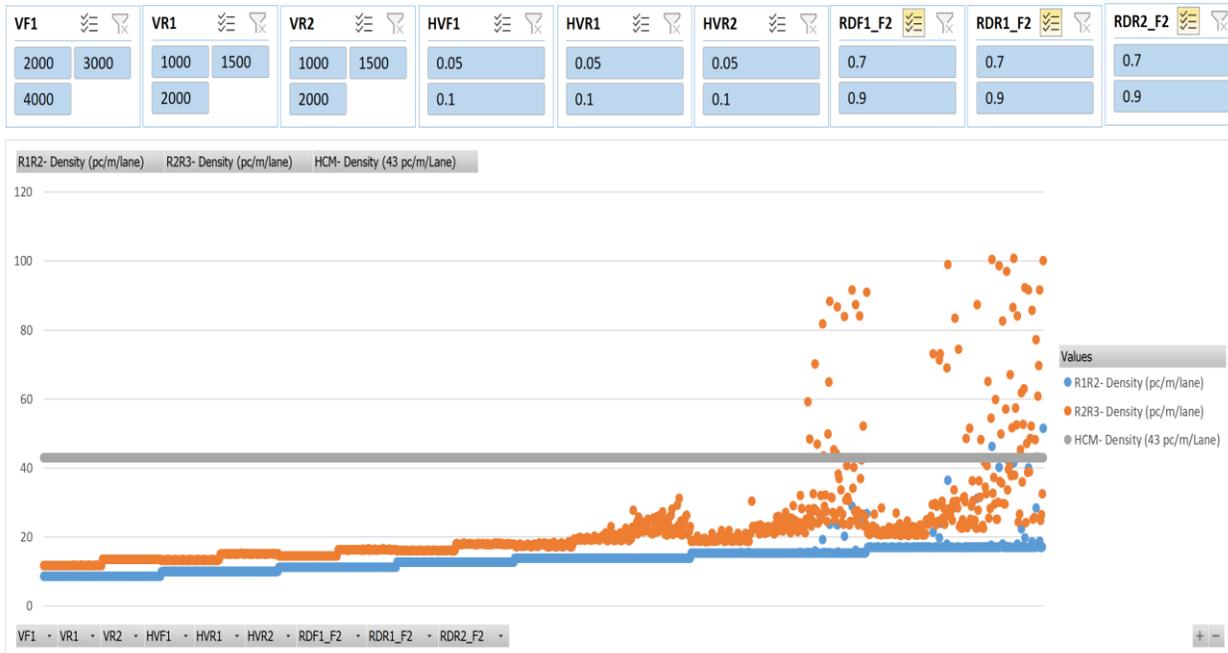


Figure 182: Scenario 29, Density

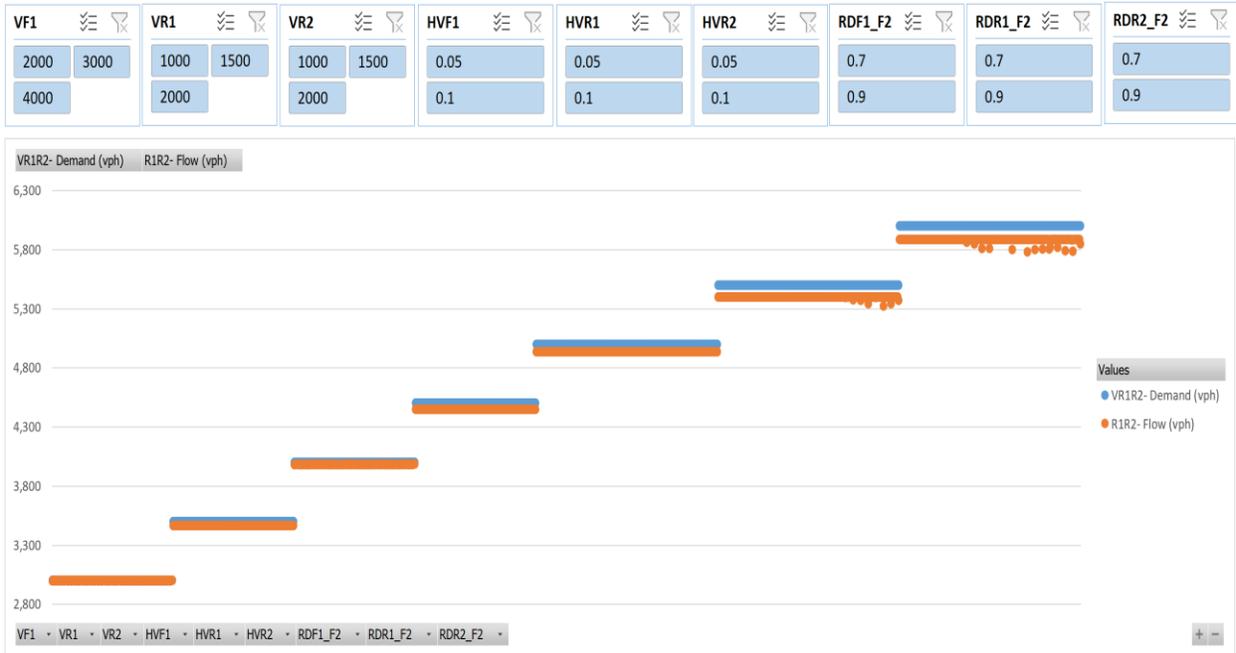


Figure 183: Scenario 29, R1R2 Flow vs. Demand

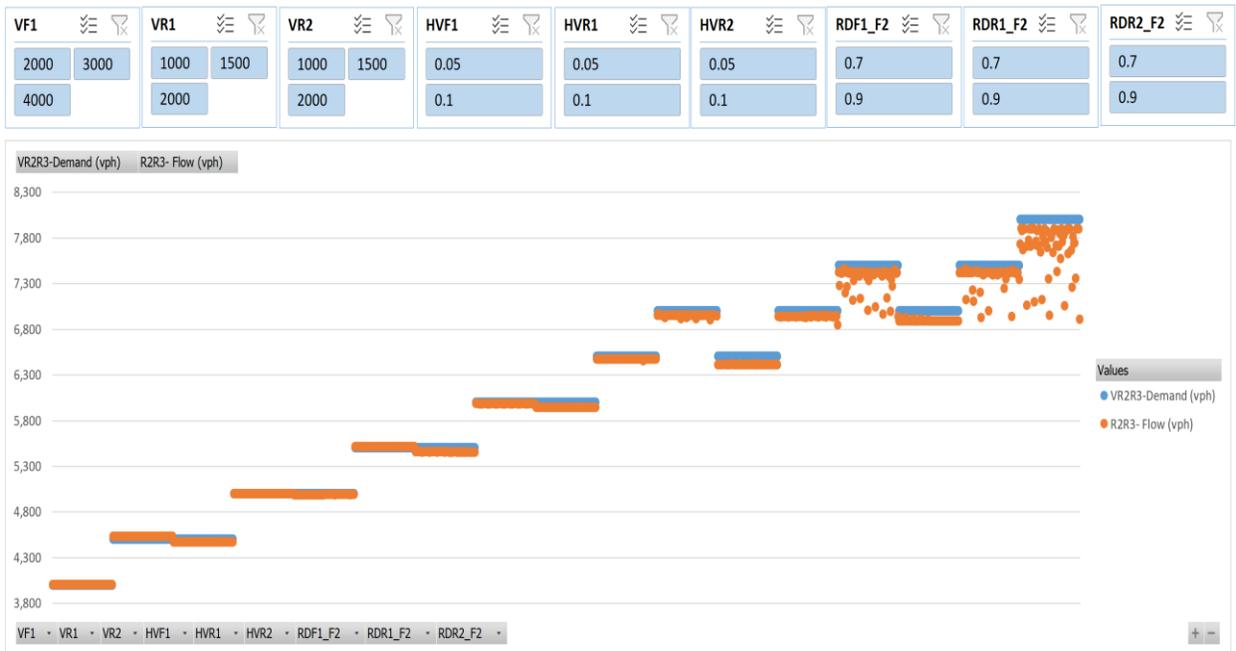


Figure 184: Scenario 29, R2R3 Flow vs. Demand

Scenario Number 30

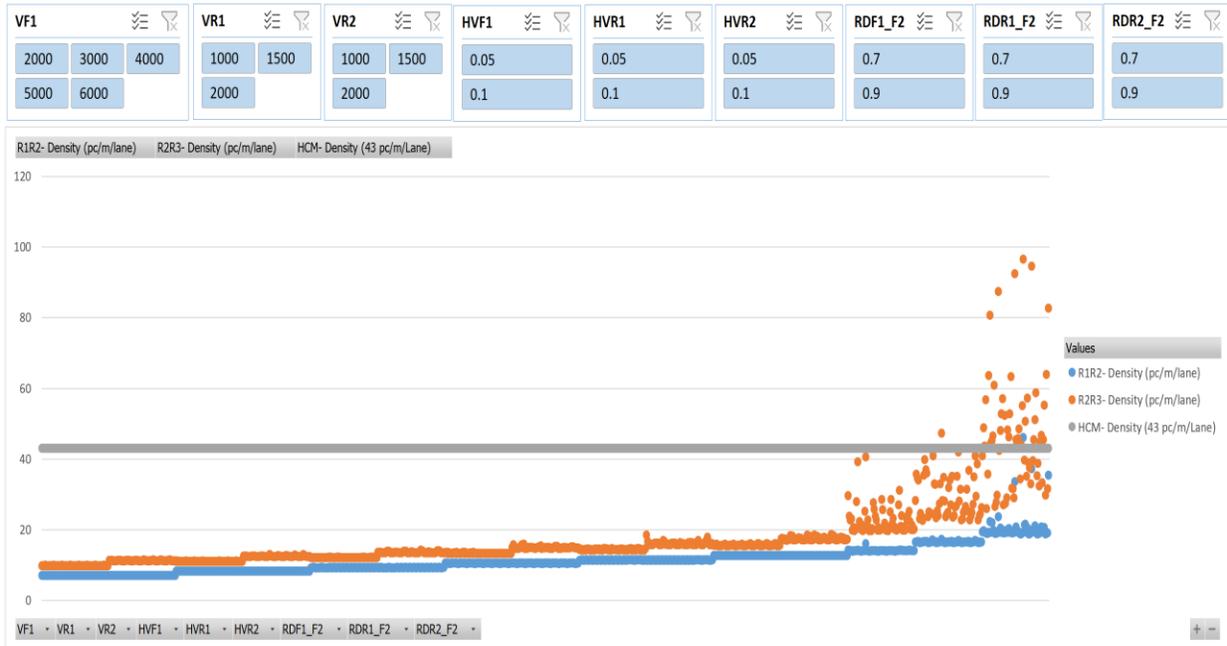


Figure 185: Scenario 30, Density

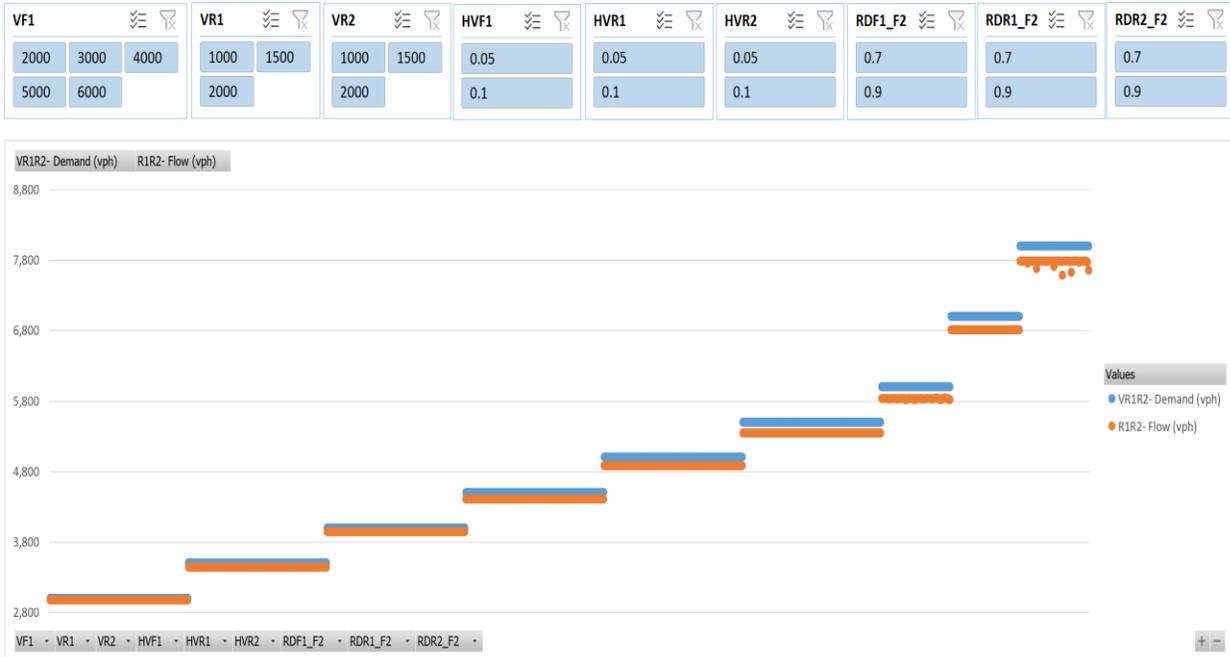


Figure 186: Scenario 30, R1R2 Flow vs. Demand

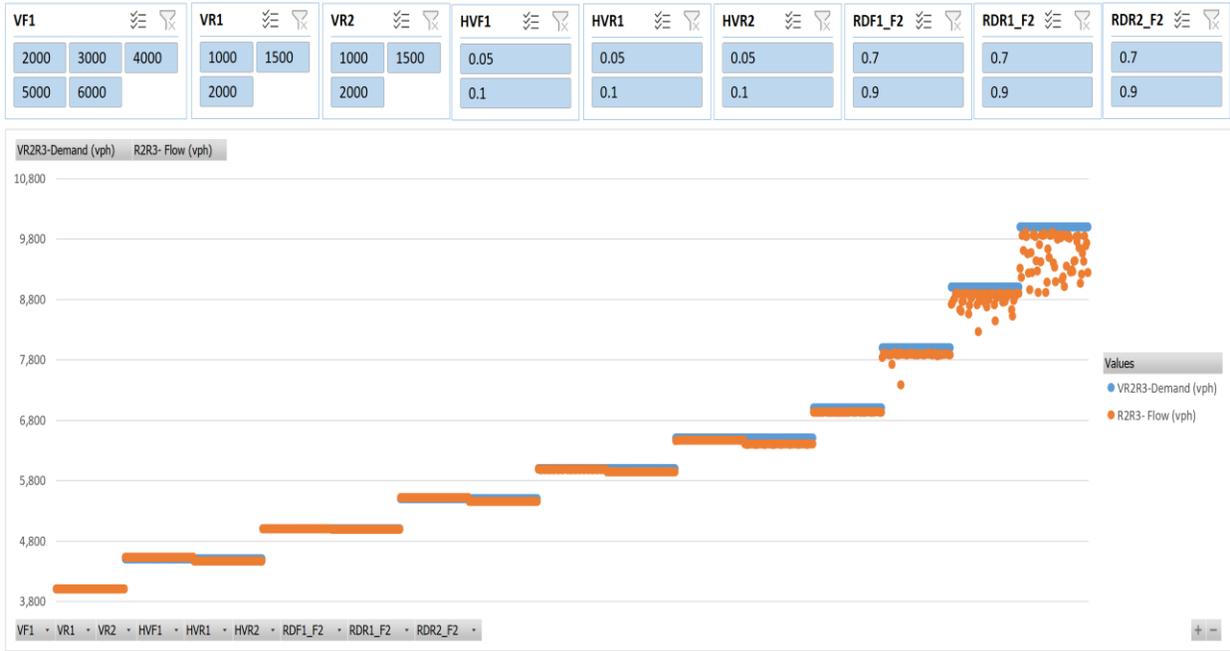


Figure 187: Scenario 30, R2R3 Flow vs. Demand

Scenario Number 31

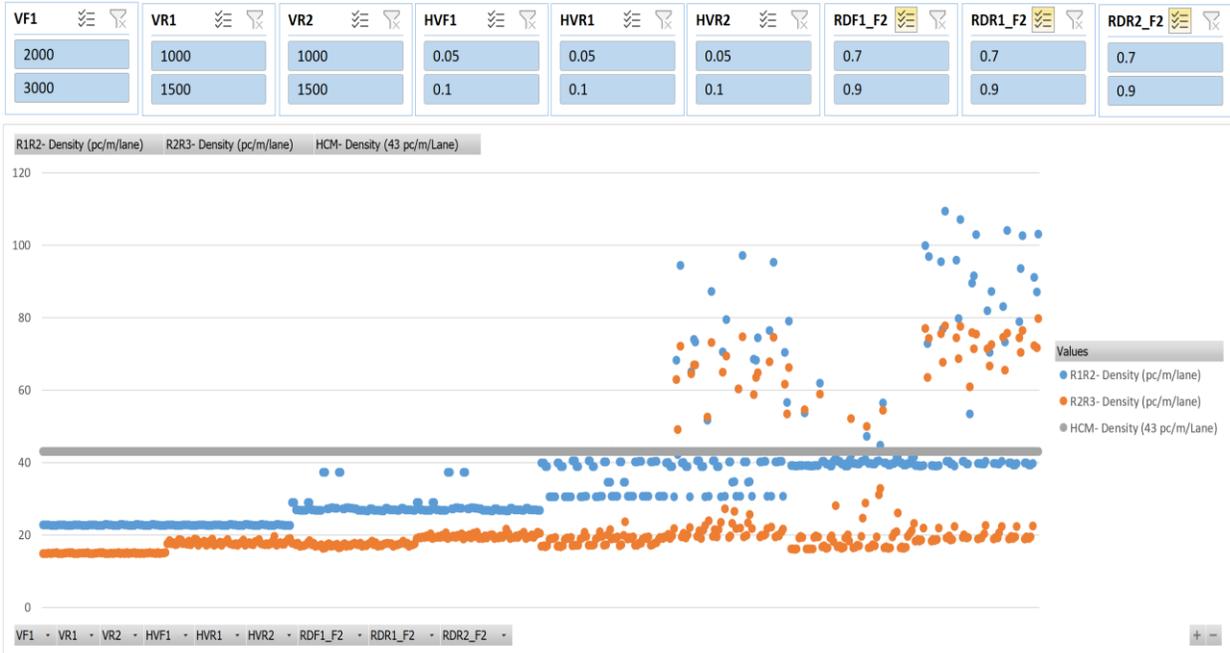


Figure 188: Scenario 31, Density

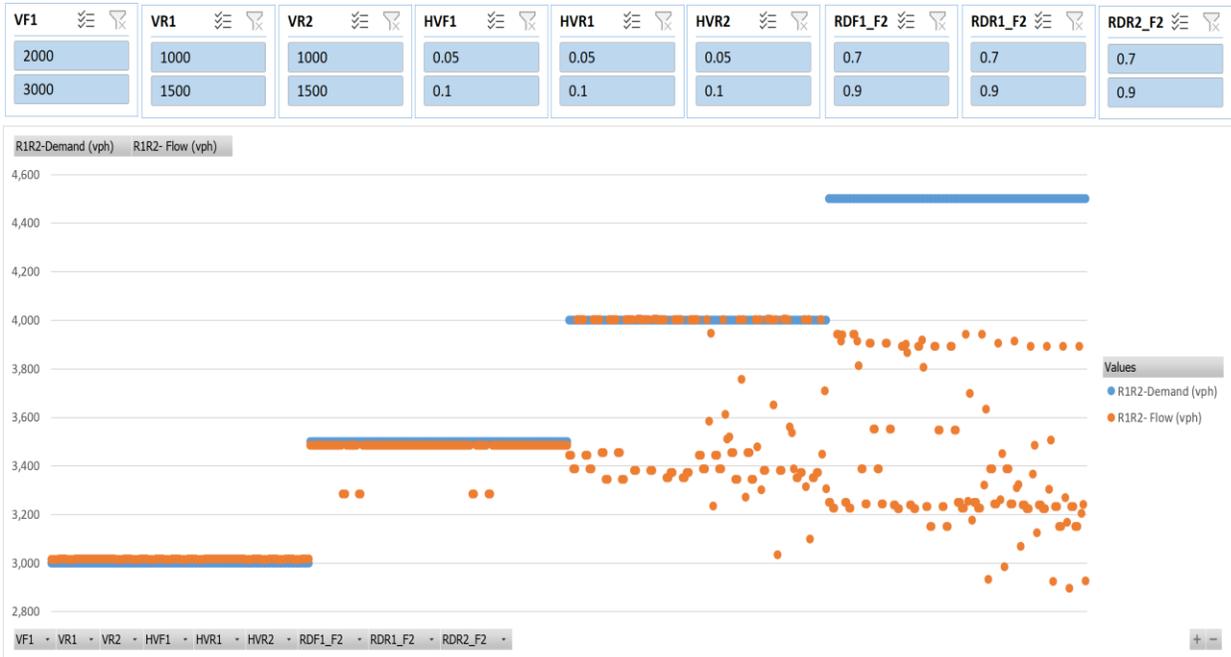


Figure 189: Scenario 31, R1R2 Flow vs. Demand

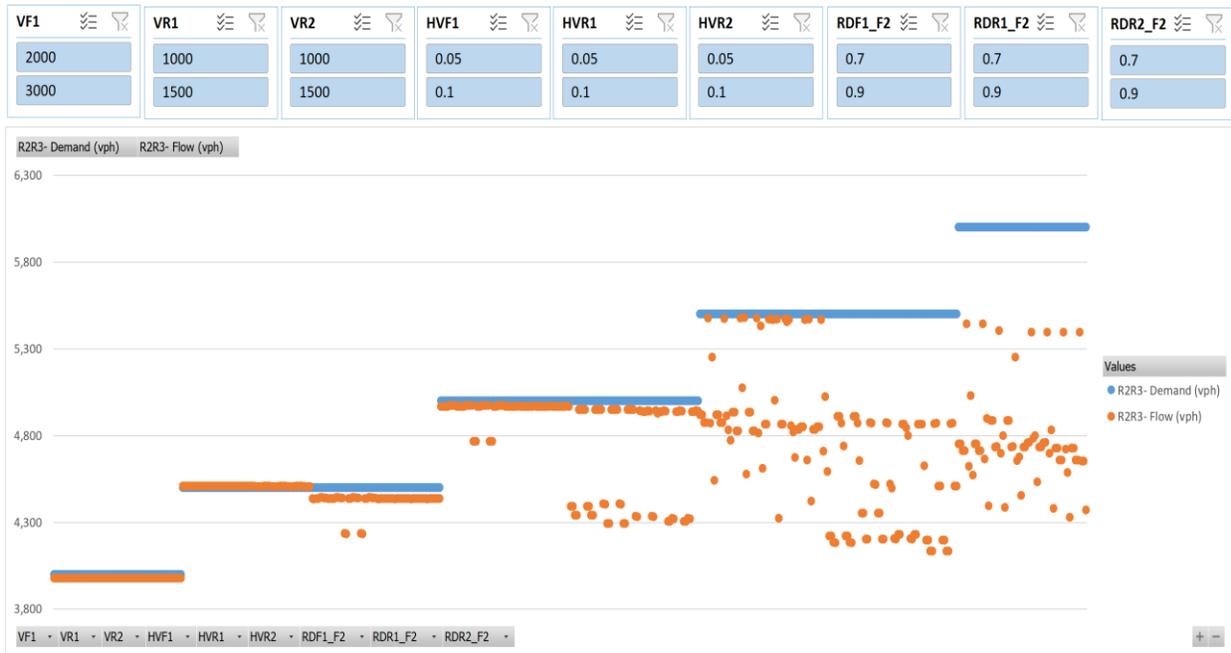


Figure 190: Scenario 31, R2R3 Flow vs. Demand

Scenario Number 32

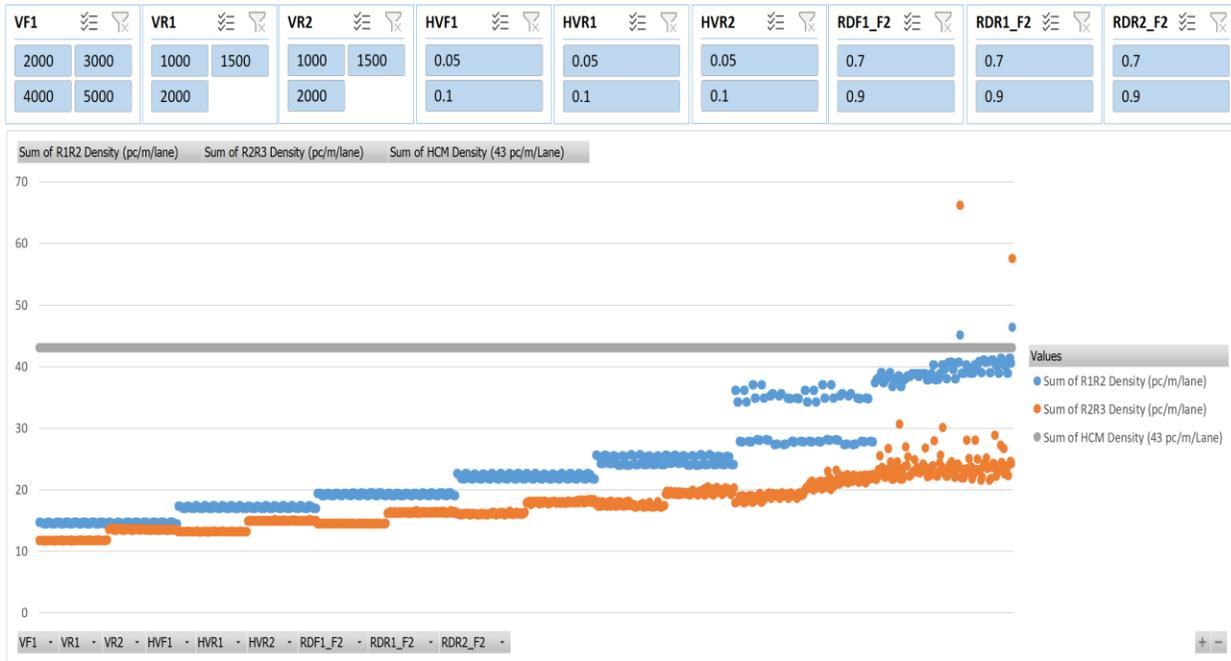


Figure 191: Scenario 32, Density

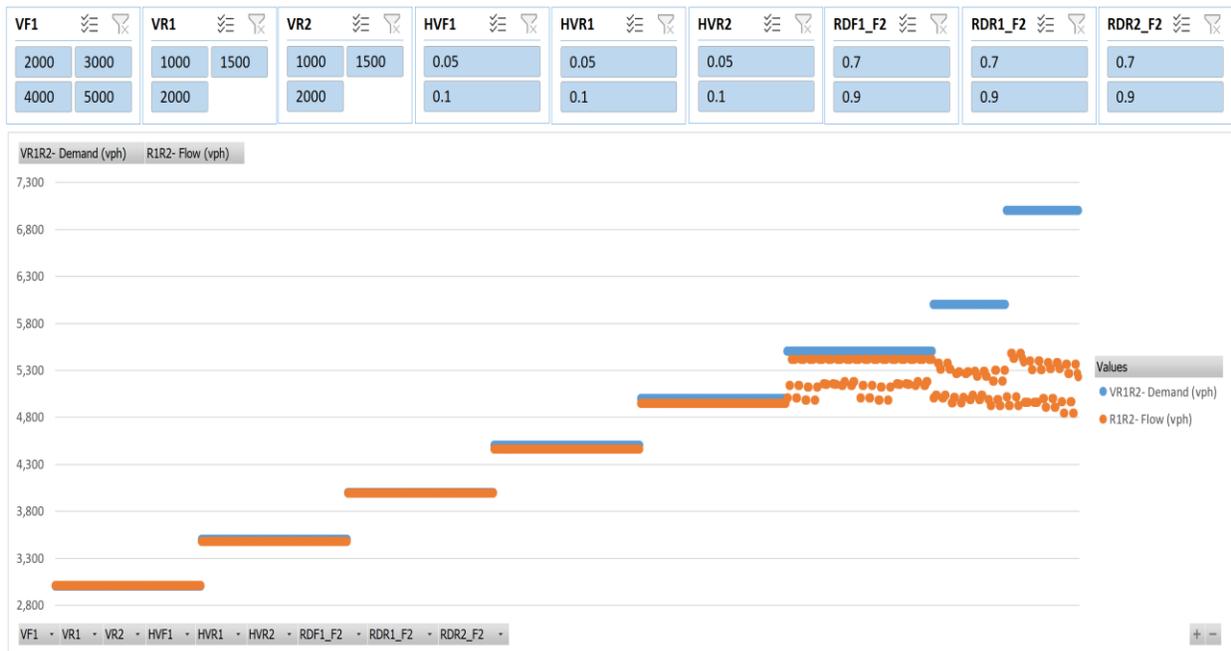


Figure 192: Scenario 32, R1R2 Flow vs. Demand

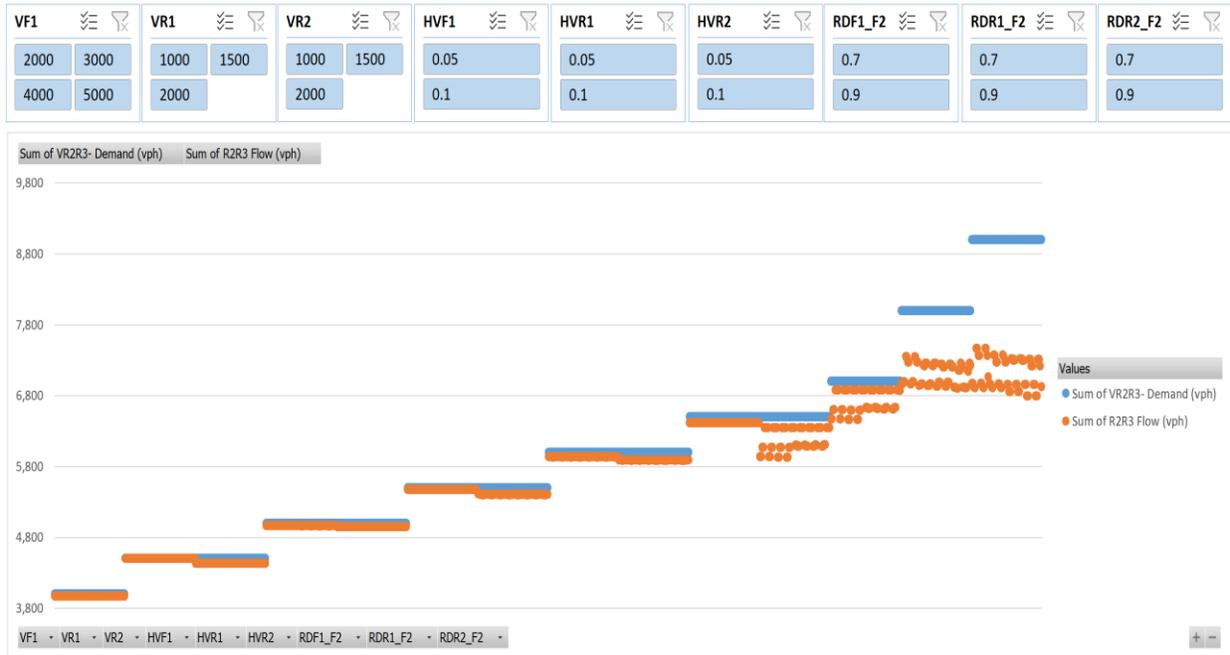


Figure 193: Scenario 32, R2R3 Flow vs. Demand

Scenario Number 33

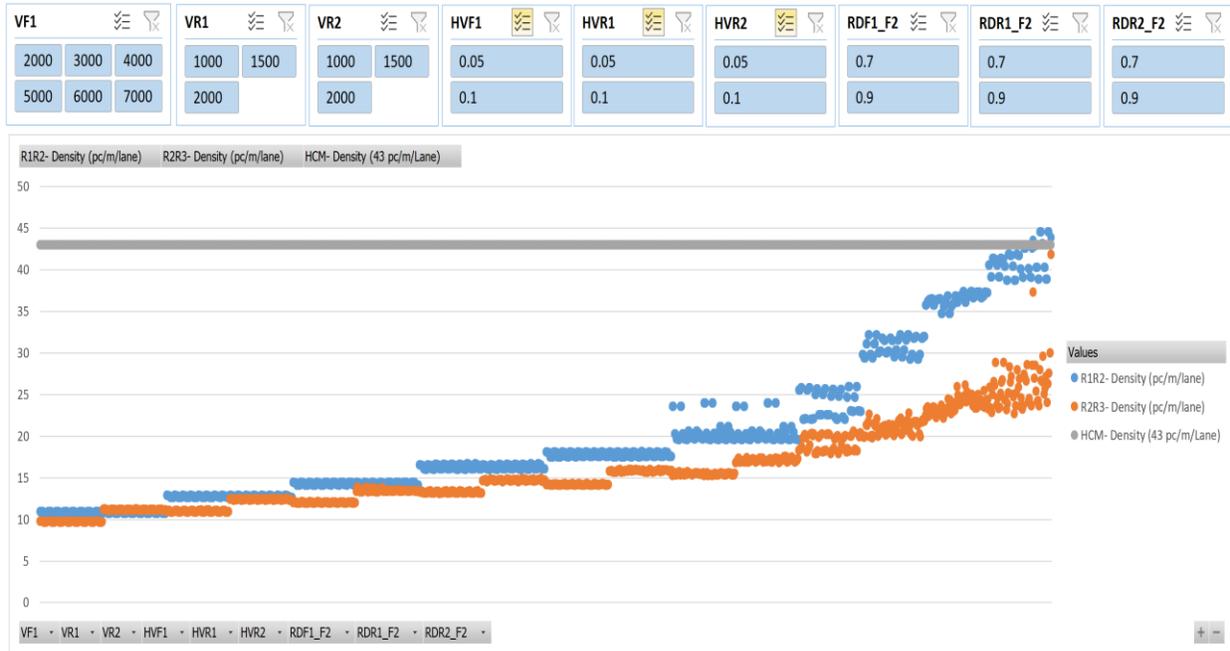


Figure 194: Scenario 33, Density

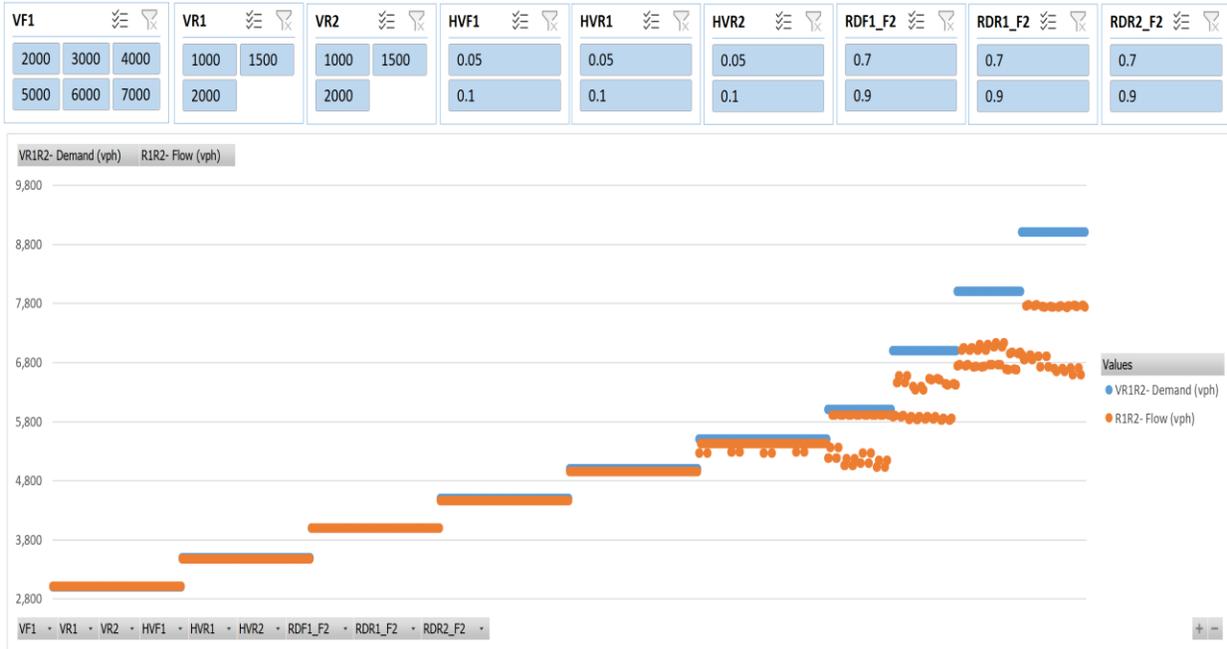


Figure 195: Scenario 33, R1R2 Flow vs. Demand

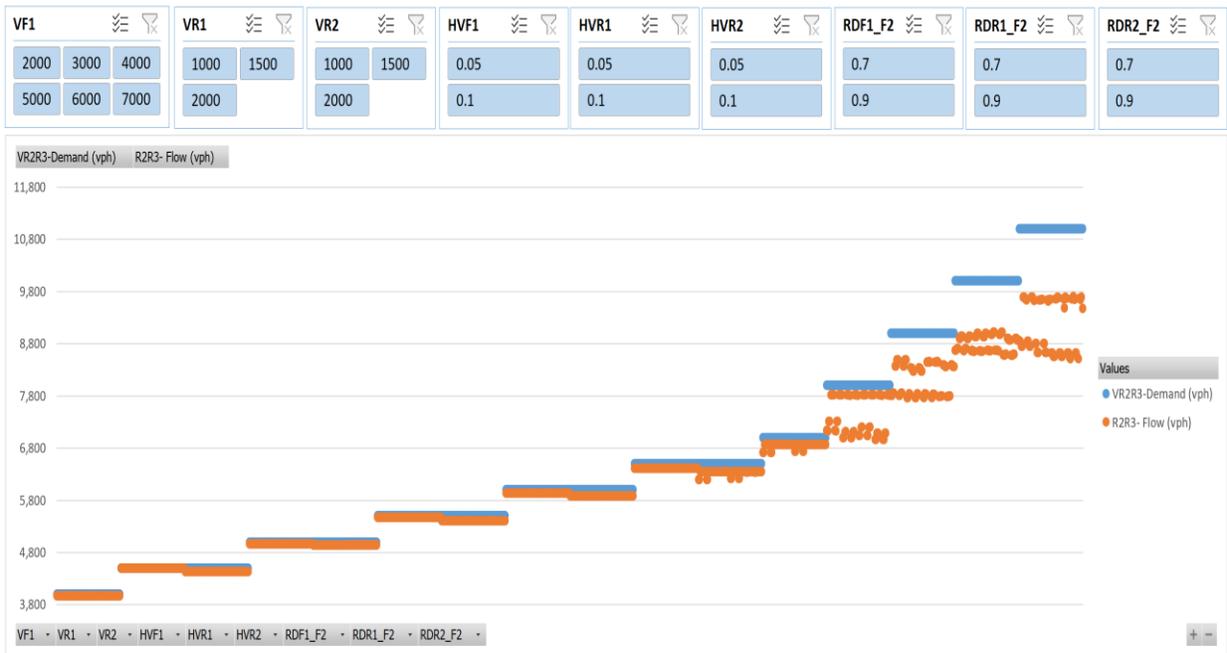


Figure 196: Scenario 33, R2R3 Flow vs. Demand

Scenario Number 34

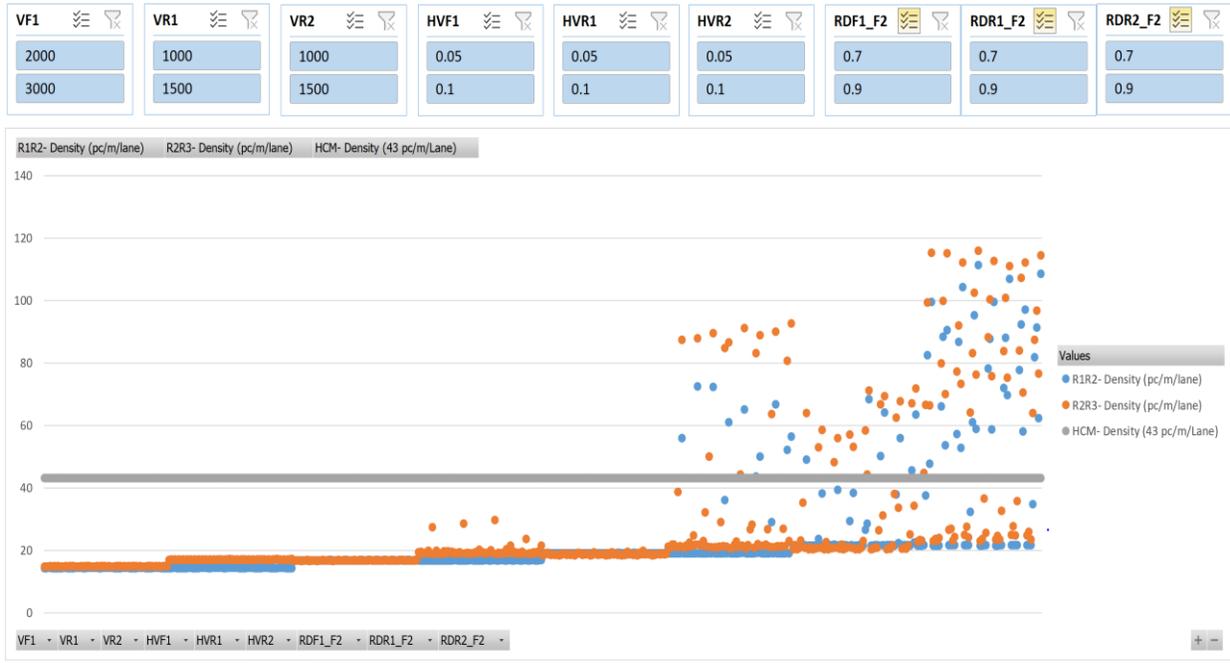


Figure 197: Scenario 34, Density

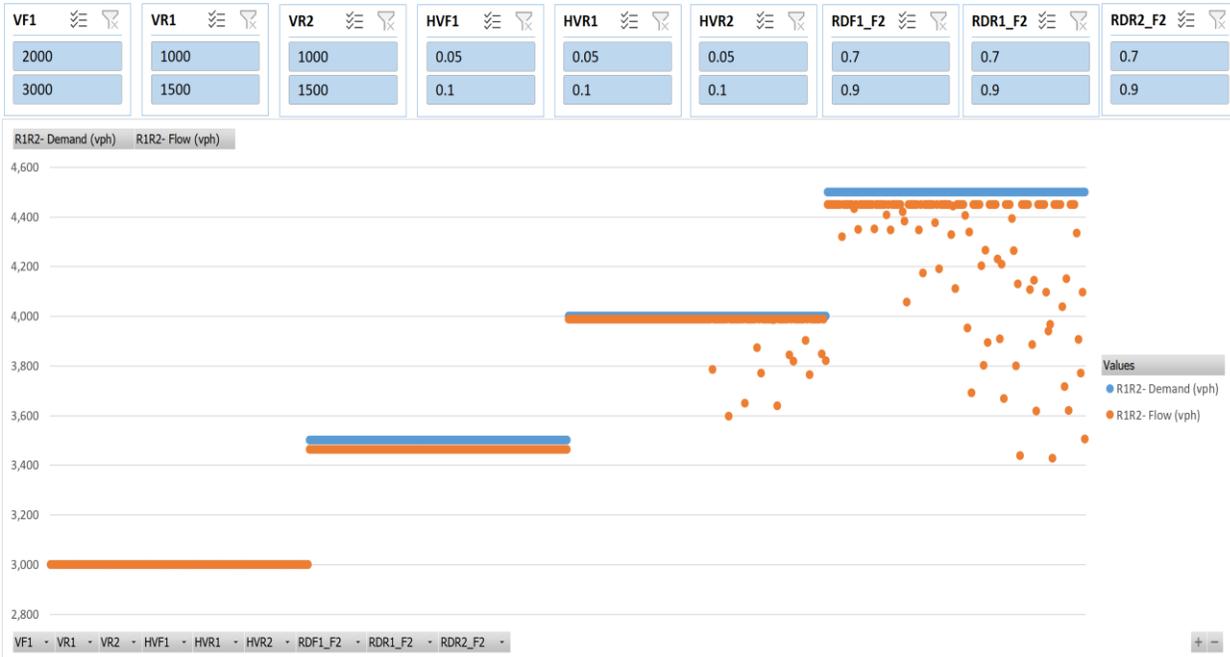


Figure 198: Scenario 34, R1R2 Flow vs. Demand

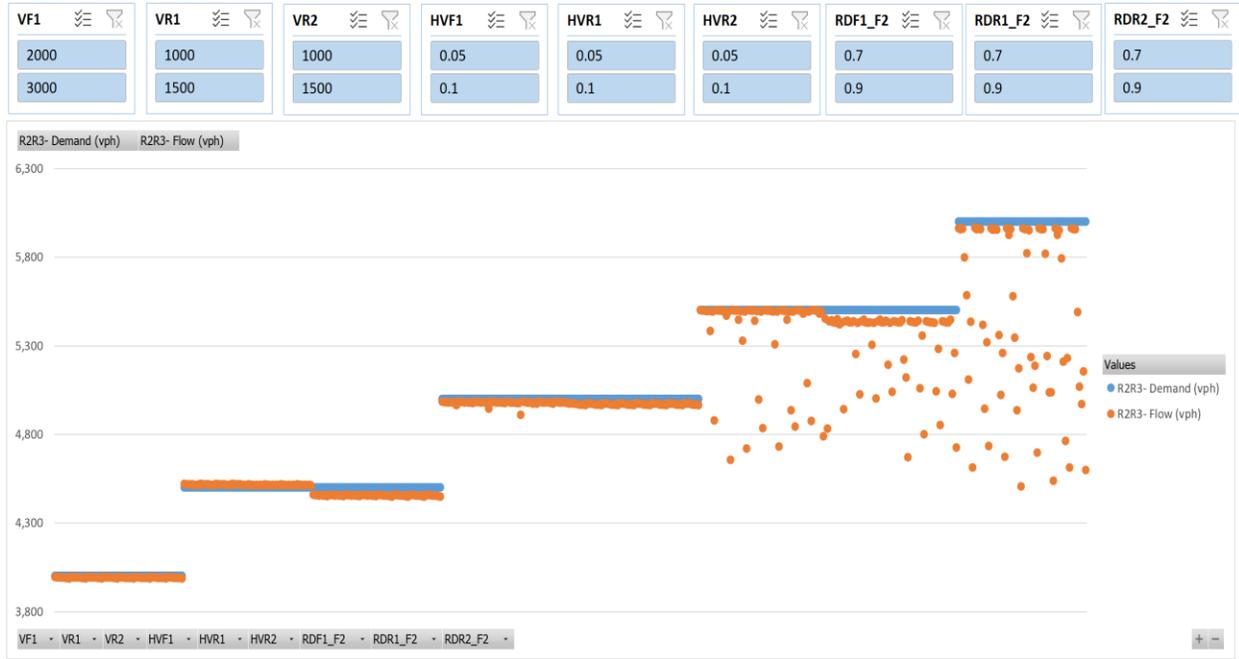


Figure 199: Scenario 34, R2R3 Flow vs. Demand

Scenario Number 35

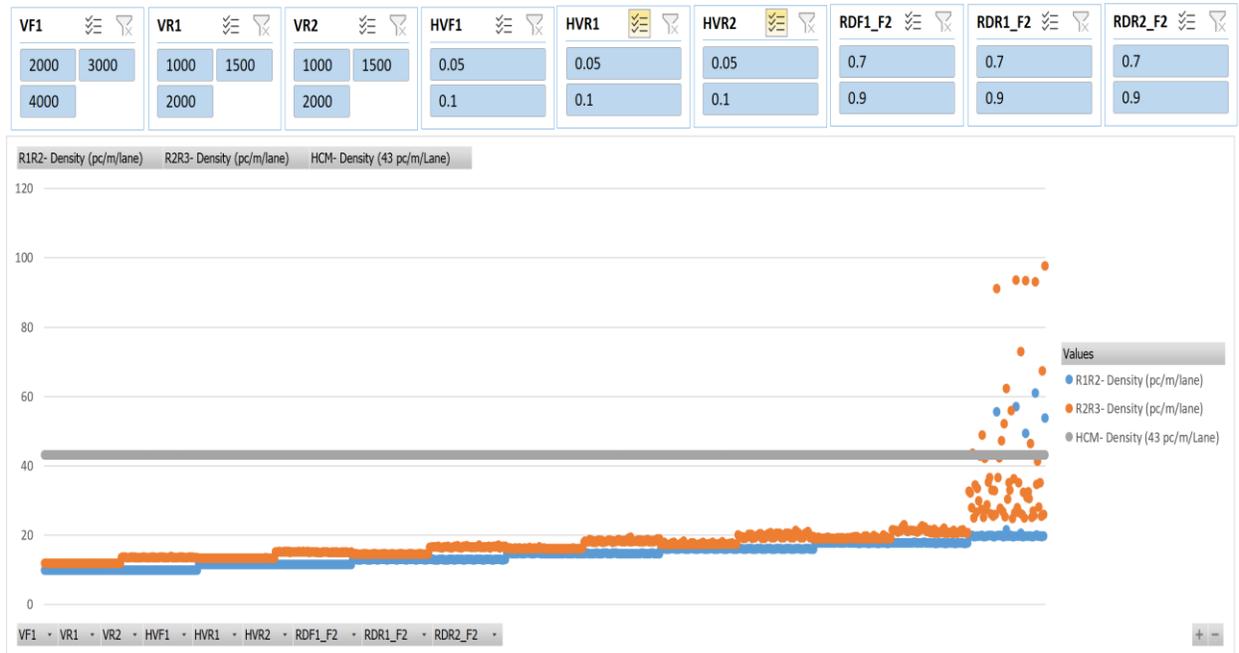


Figure 200: Scenario 35, Density

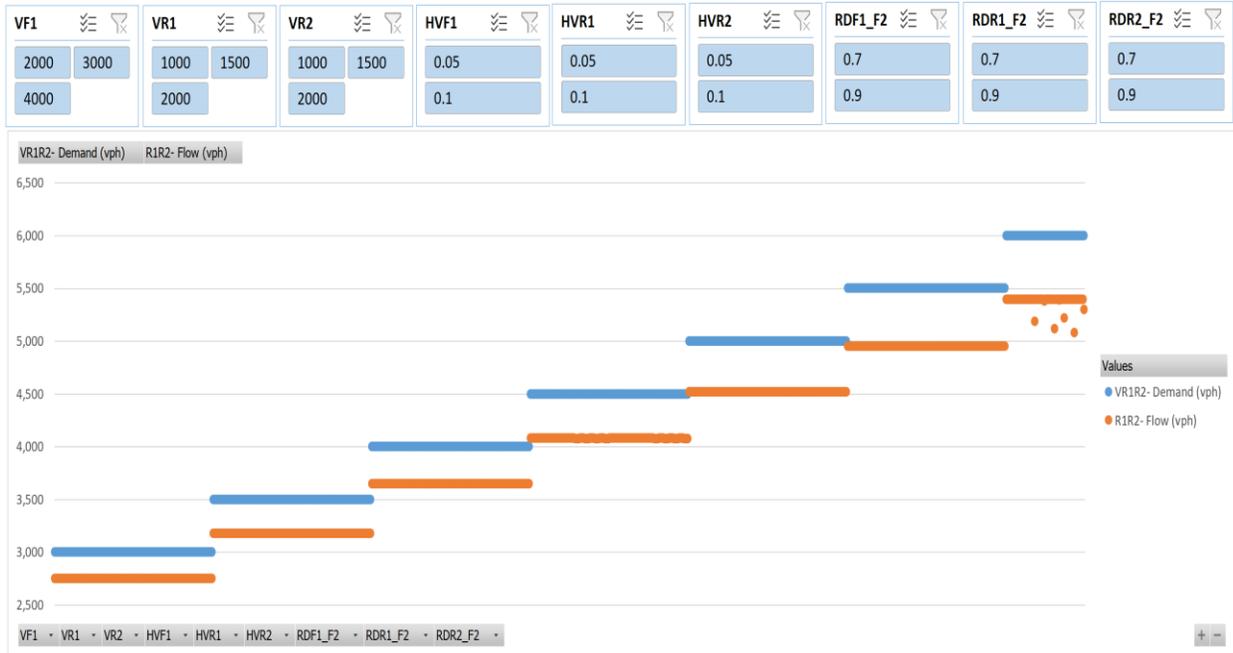


Figure 201: Scenario 35, R1R2 Flow vs. Demand

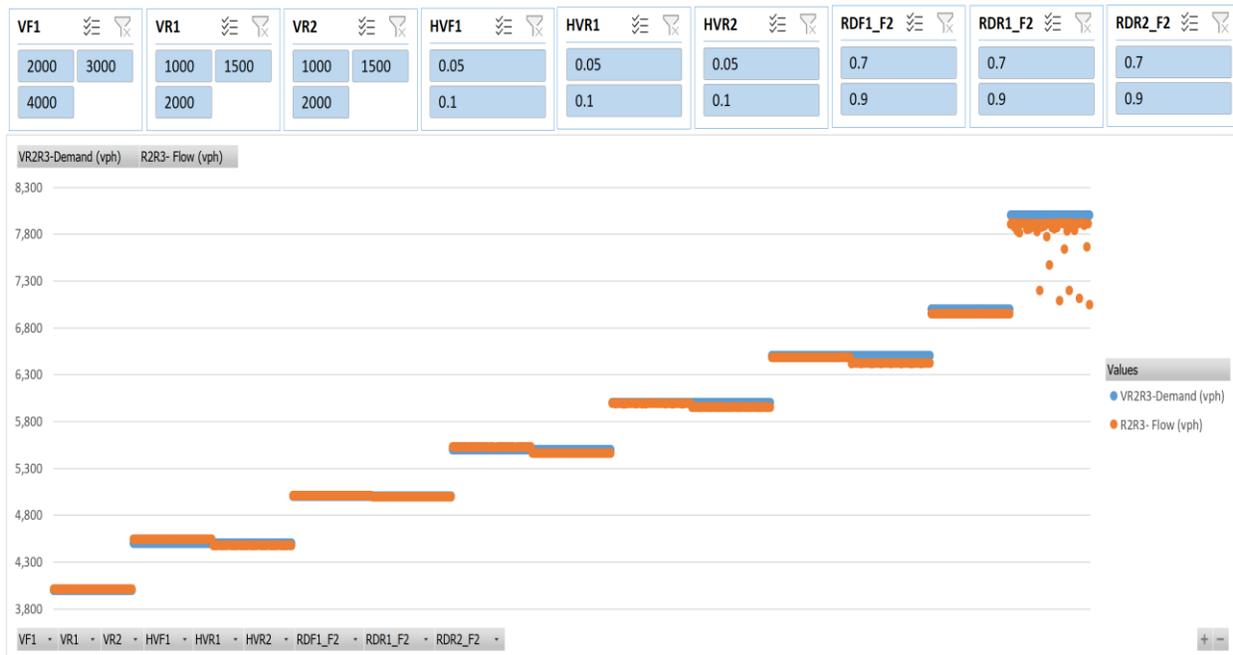


Figure 202: Scenario 35, R2R3 Flow vs. Demand

Scenario Number 36

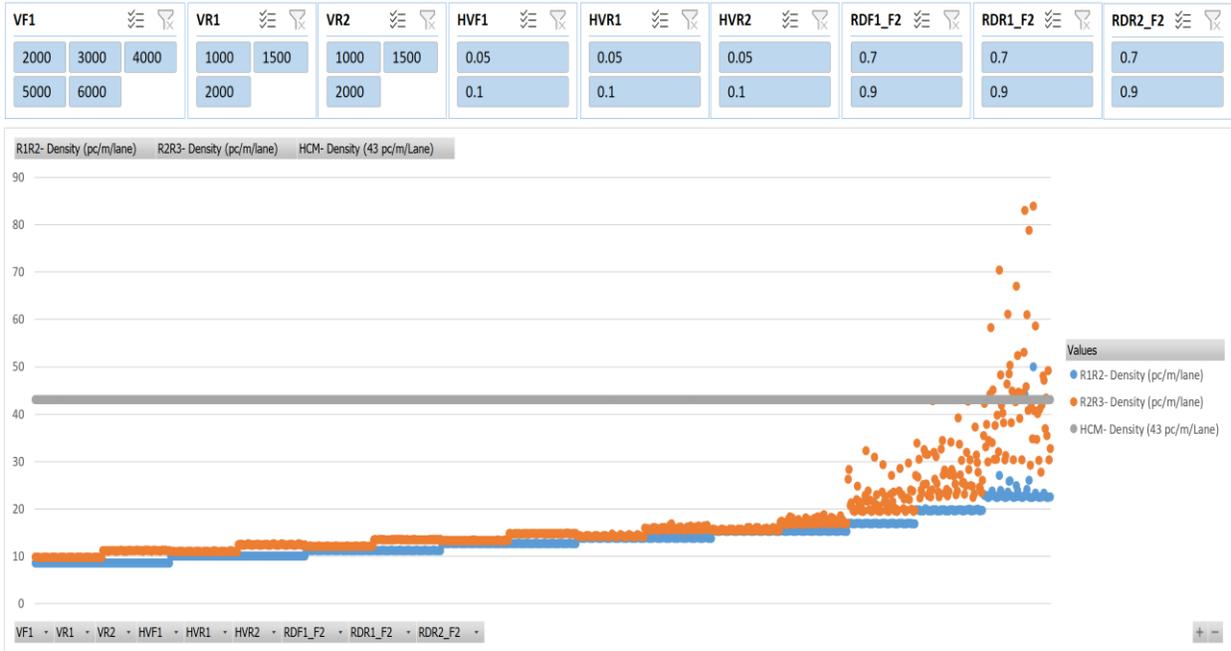


Figure 203: Scenario 36, Density

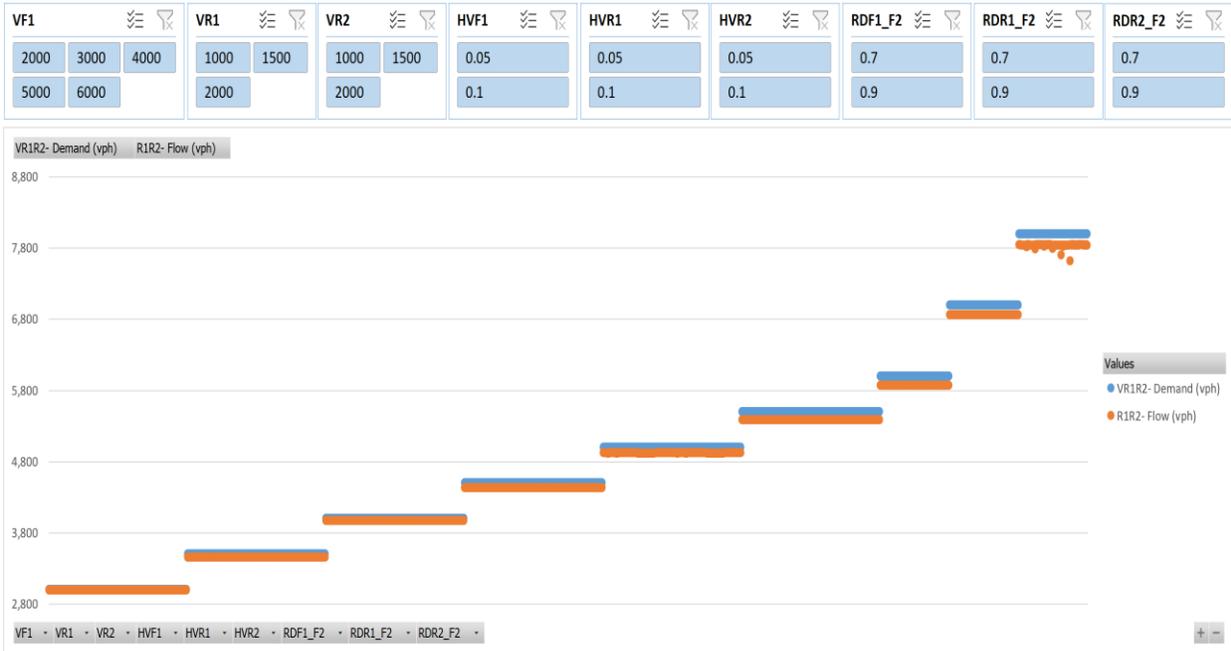


Figure 204: Scenario 36, R1R2 Flow vs. Demand

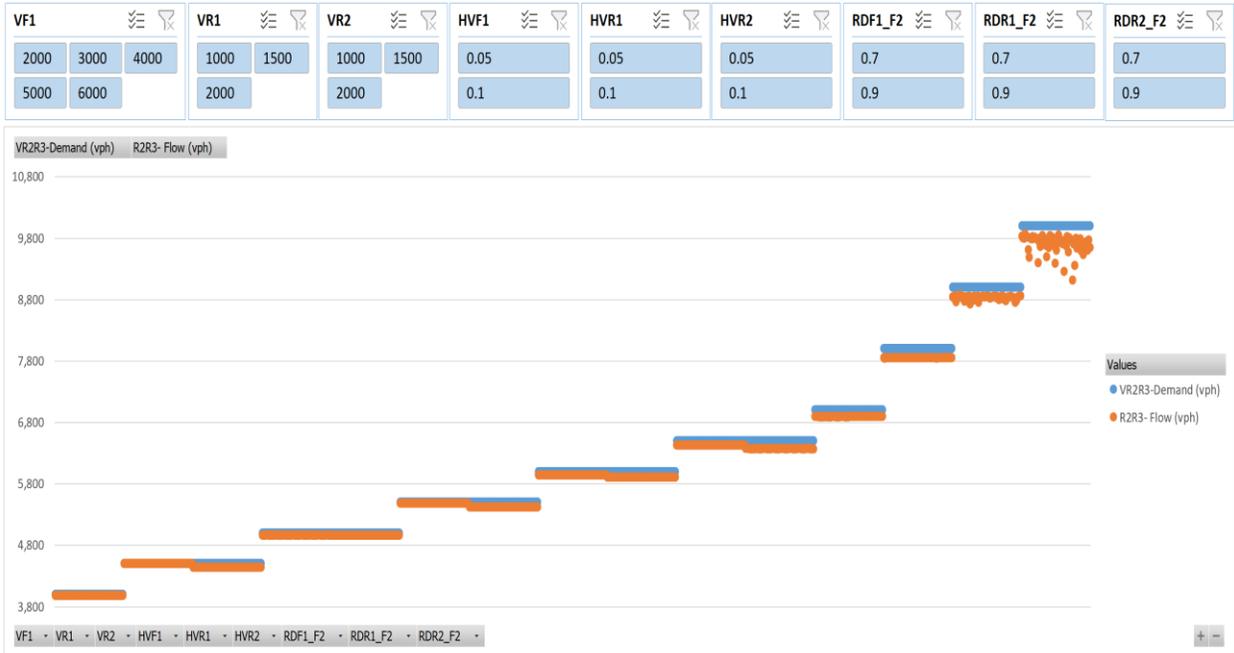


Figure 205: Scenario 36, R2R3 Flow vs. Demand

Scenario Number 37

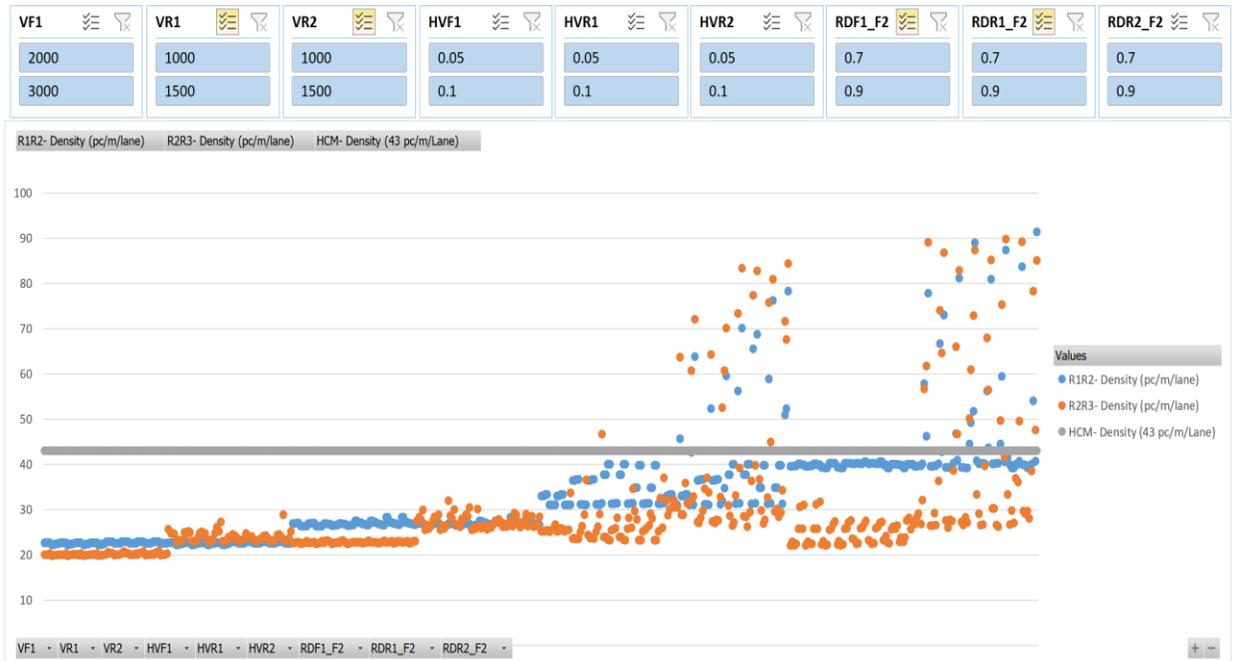


Figure 206: Scenario 37, Density



Figure 207: Scenario 37, R1R2 Flow vs. Demand



Figure 208: Scenario 37, R2R2 Flow vs. Demand

Scenario Number 38

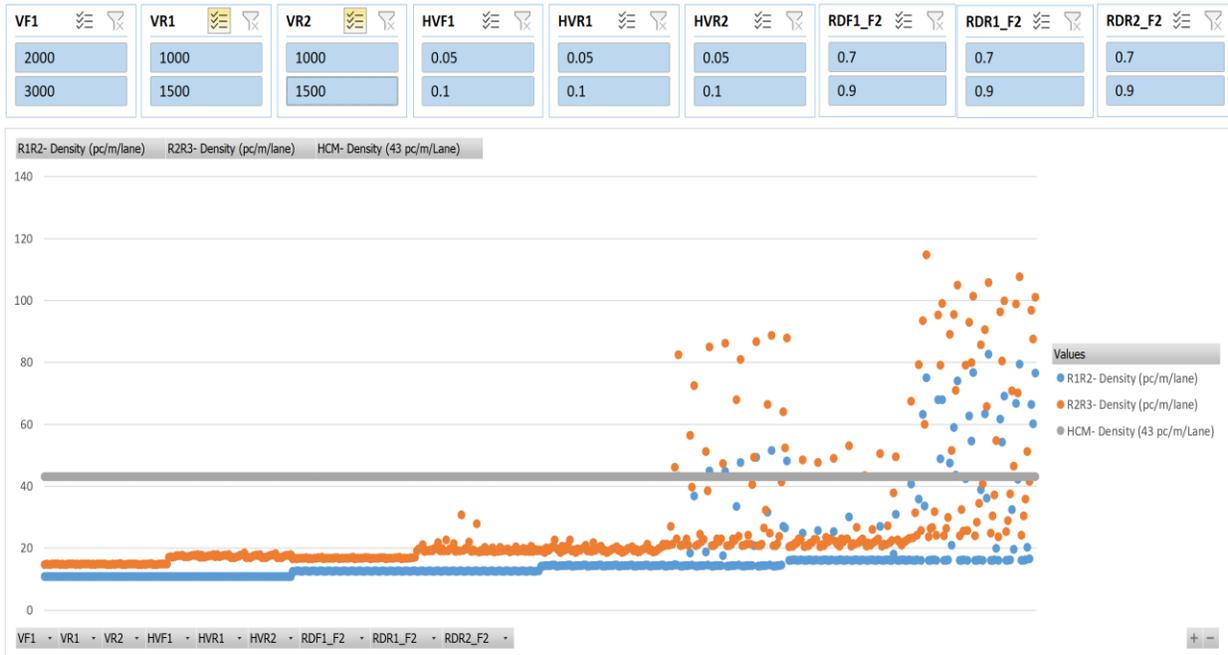


Figure 209: Scenario 38, Density

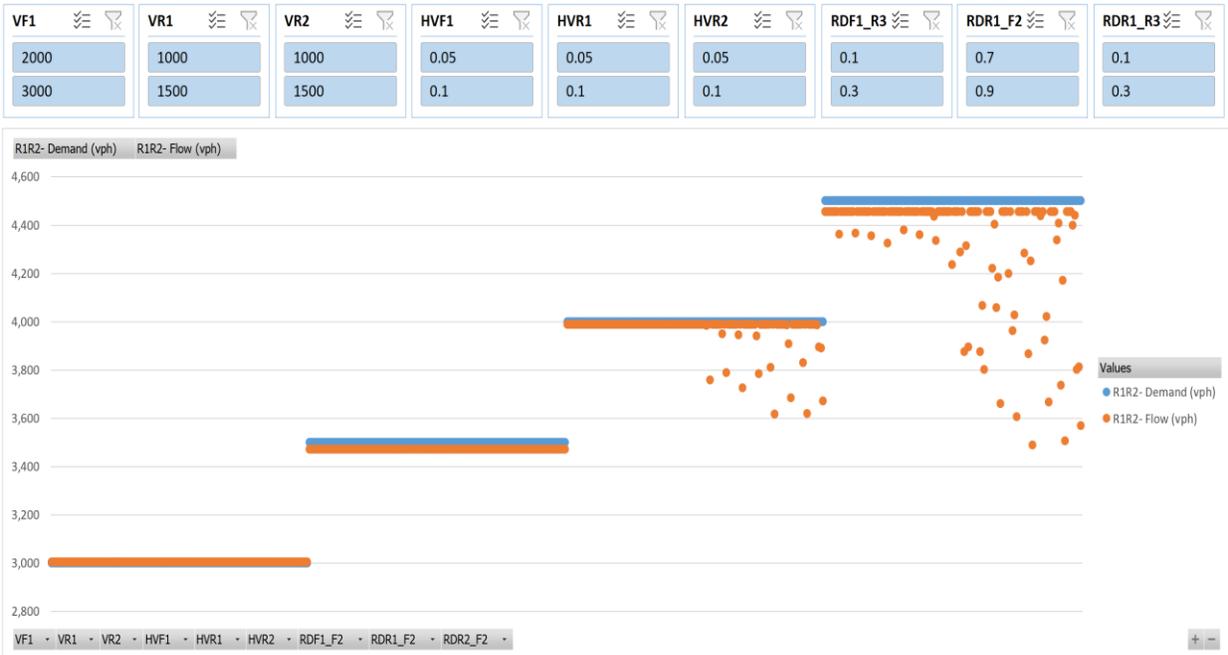


Figure 210: Scenario 38, R1R2 Flow vs. Demand

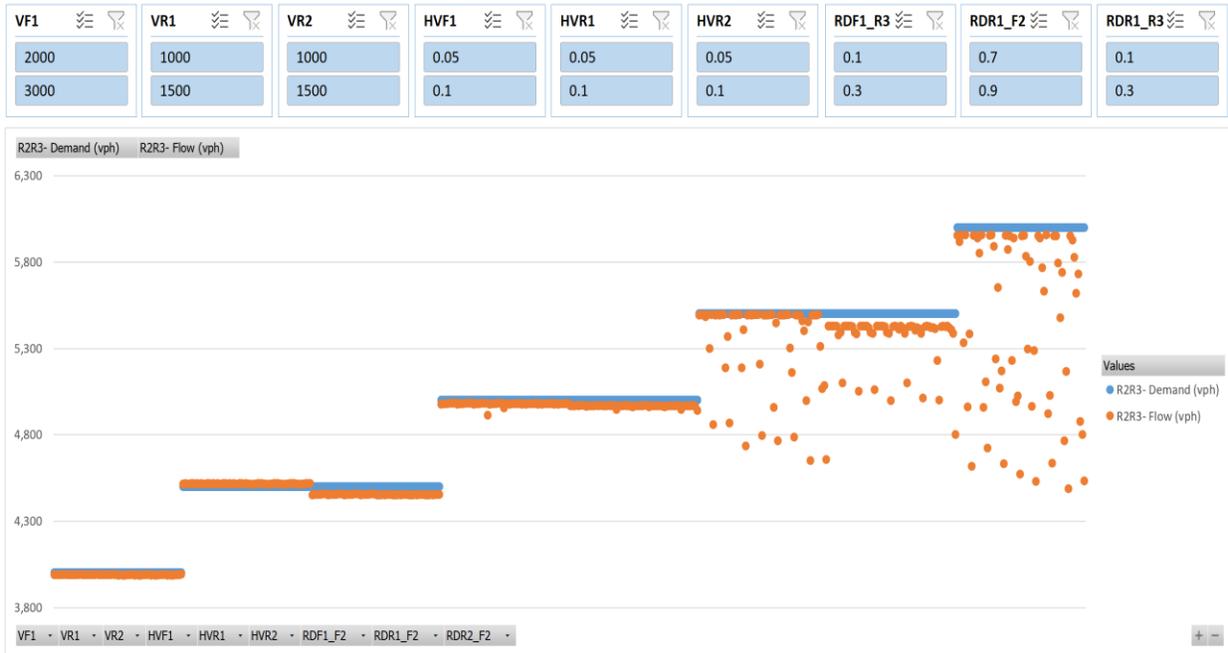


Figure 211: Scenario 38, R2R3 Flow vs. Demand

Scenario Number 39

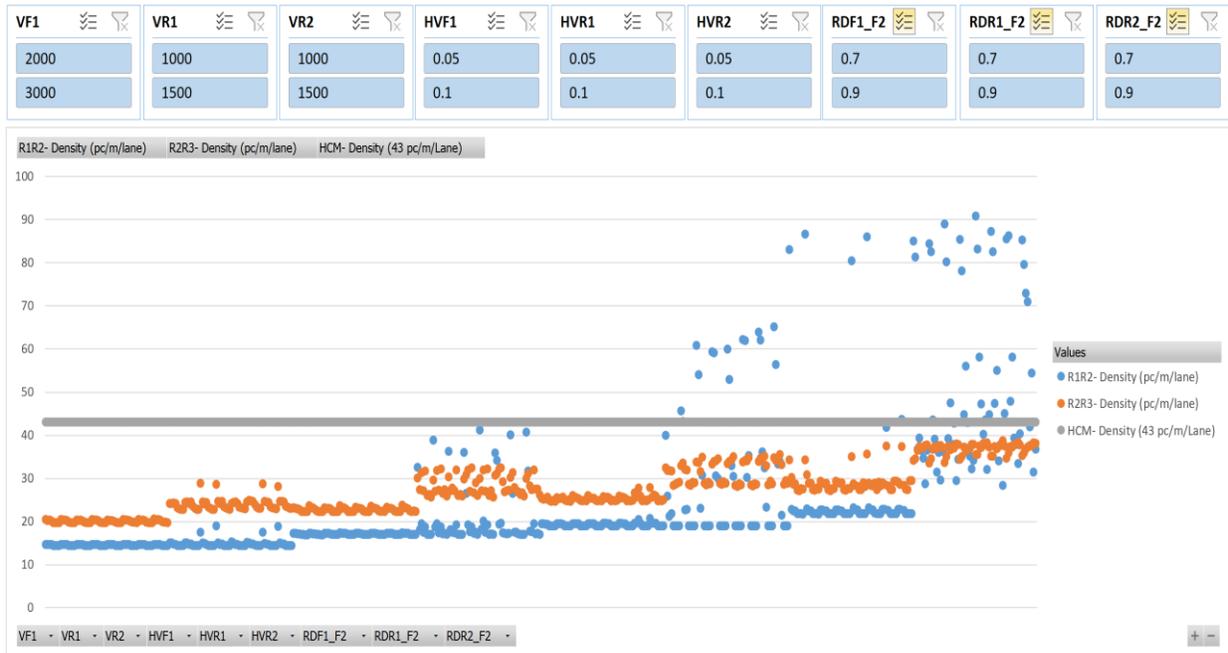


Figure 212: Scenario 39, Density

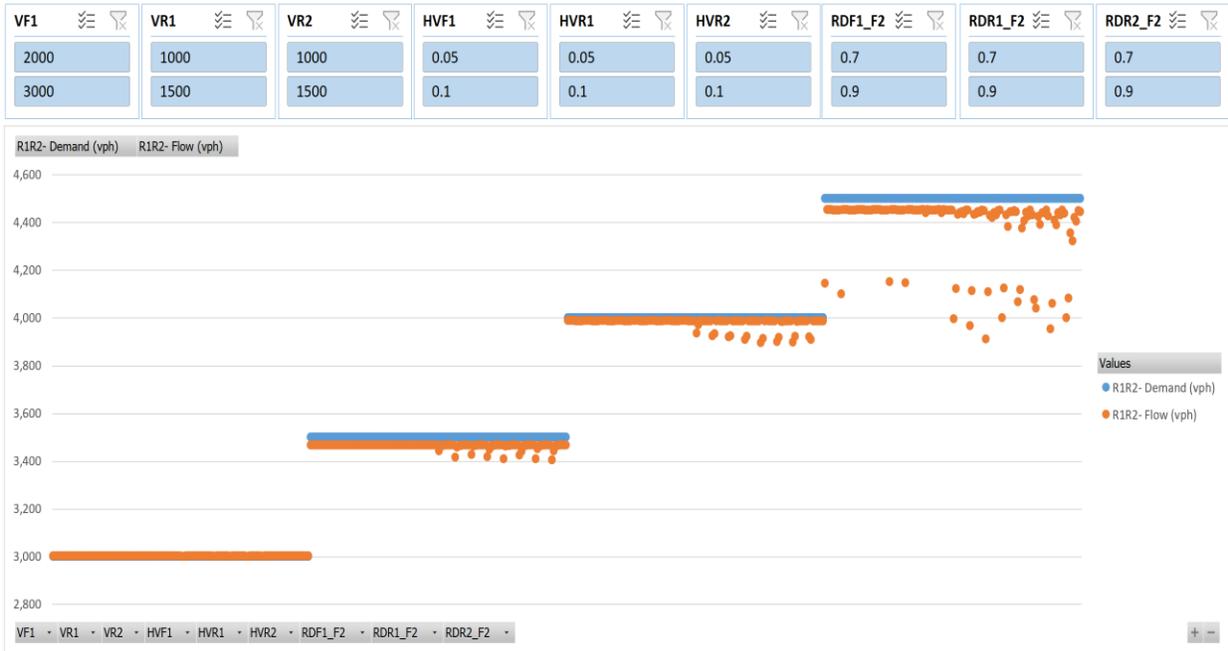


Figure 213: Scenario 39, R1R2 Flow vs. Demand

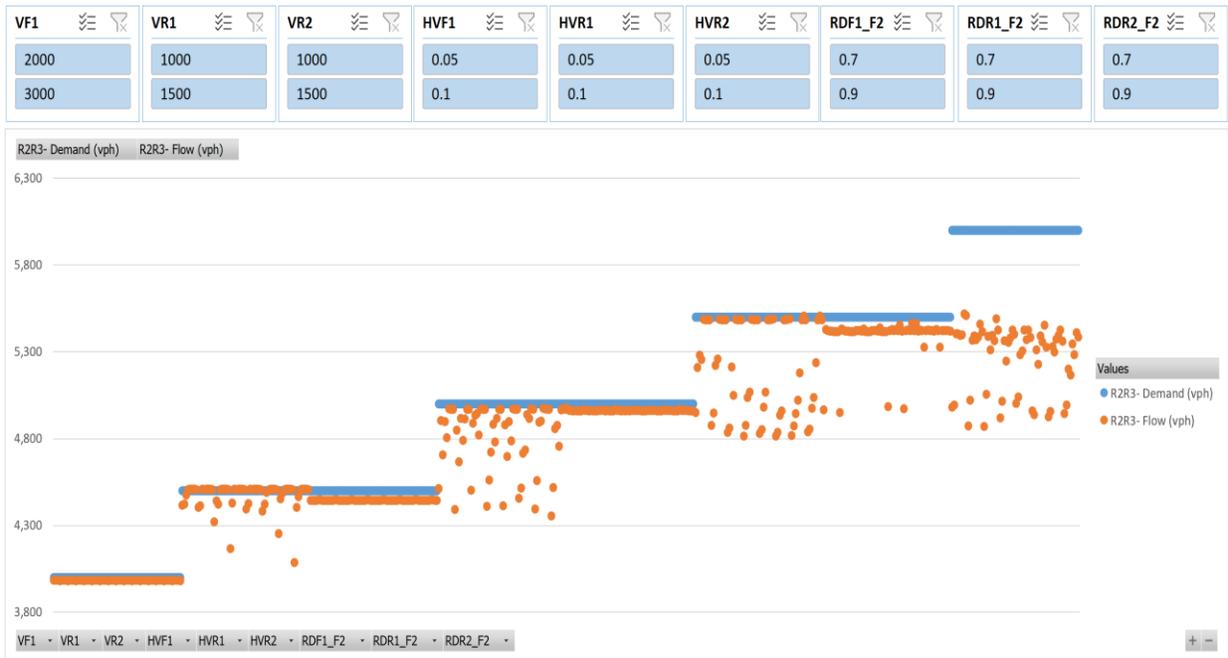


Figure 214: Scenario 39, R2R3 Flow vs. Demand

Scenario Number 40

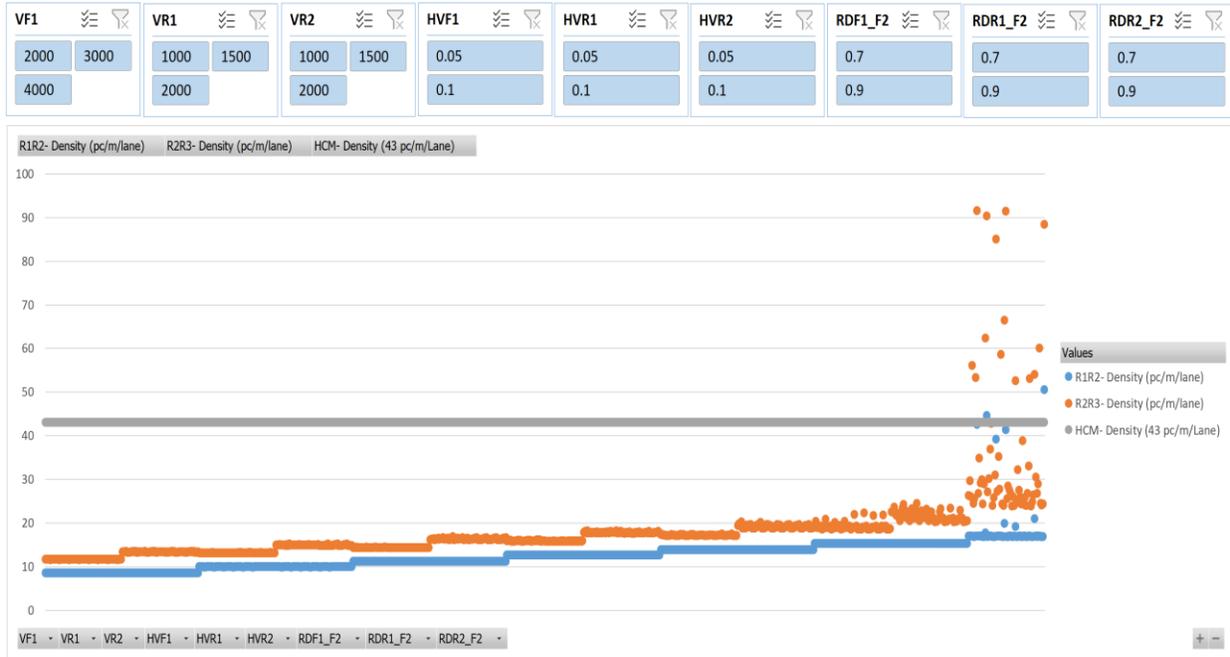


Figure 215: Scenario 40, Density

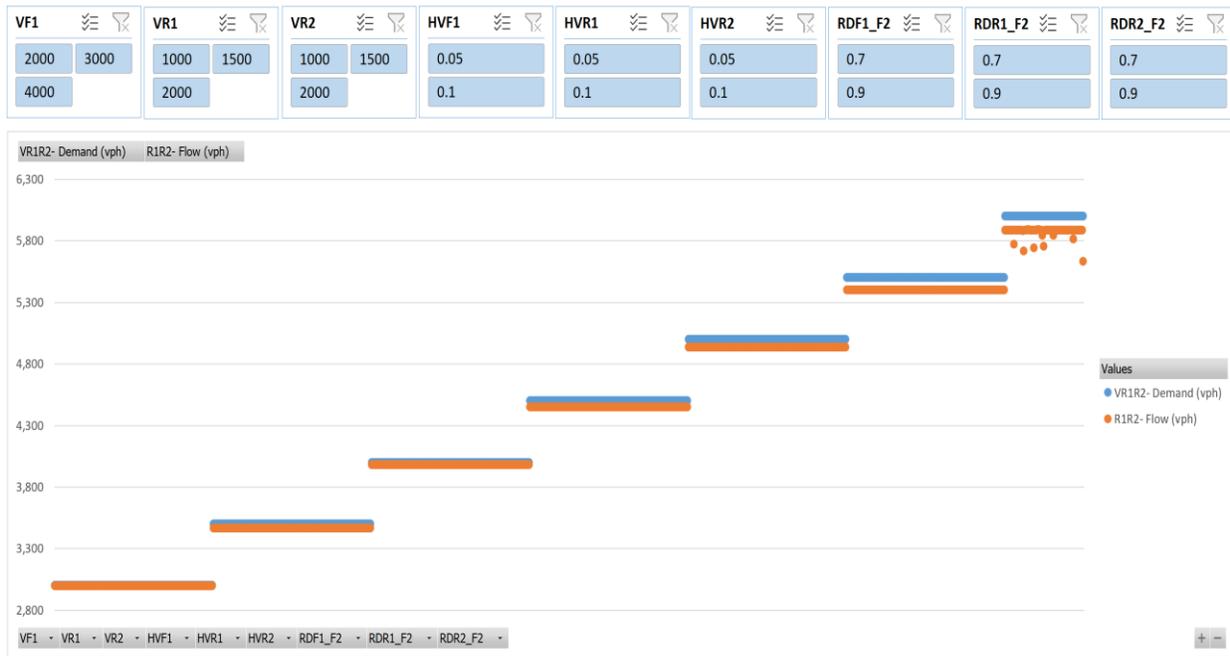


Figure 216: Scenario 40, R1R2 Flow vs. Demand

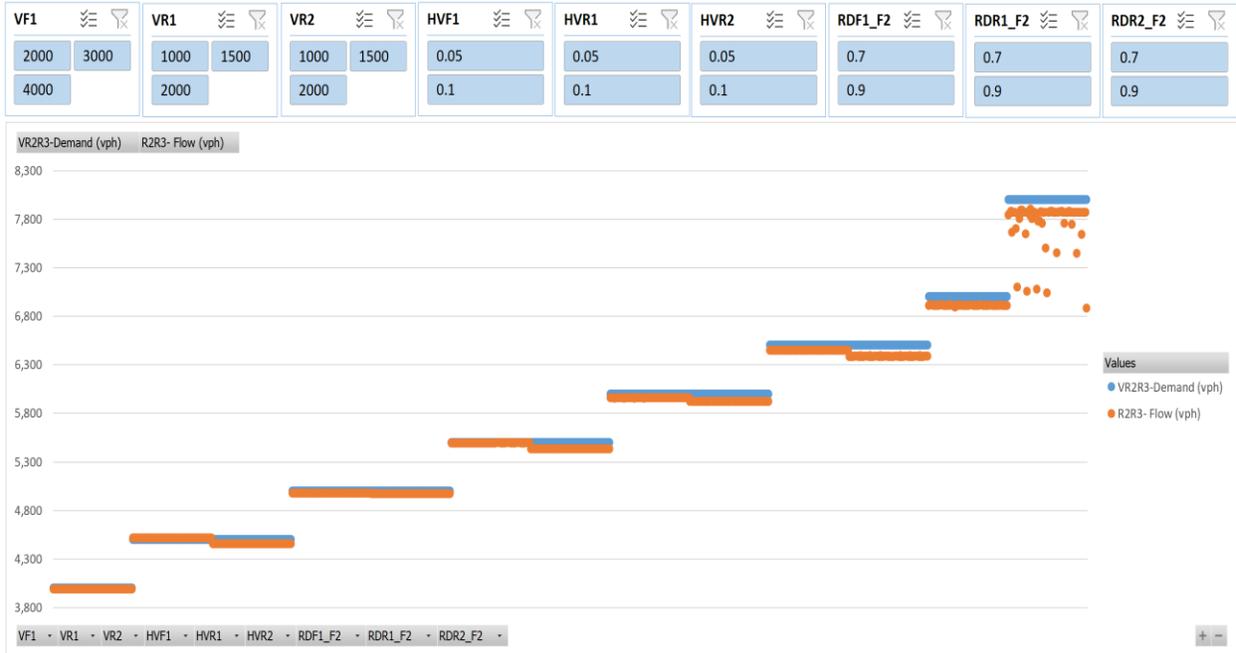


Figure 217: Scenario 40, R2R3 Flow vs. Demand

Scenario Number 41

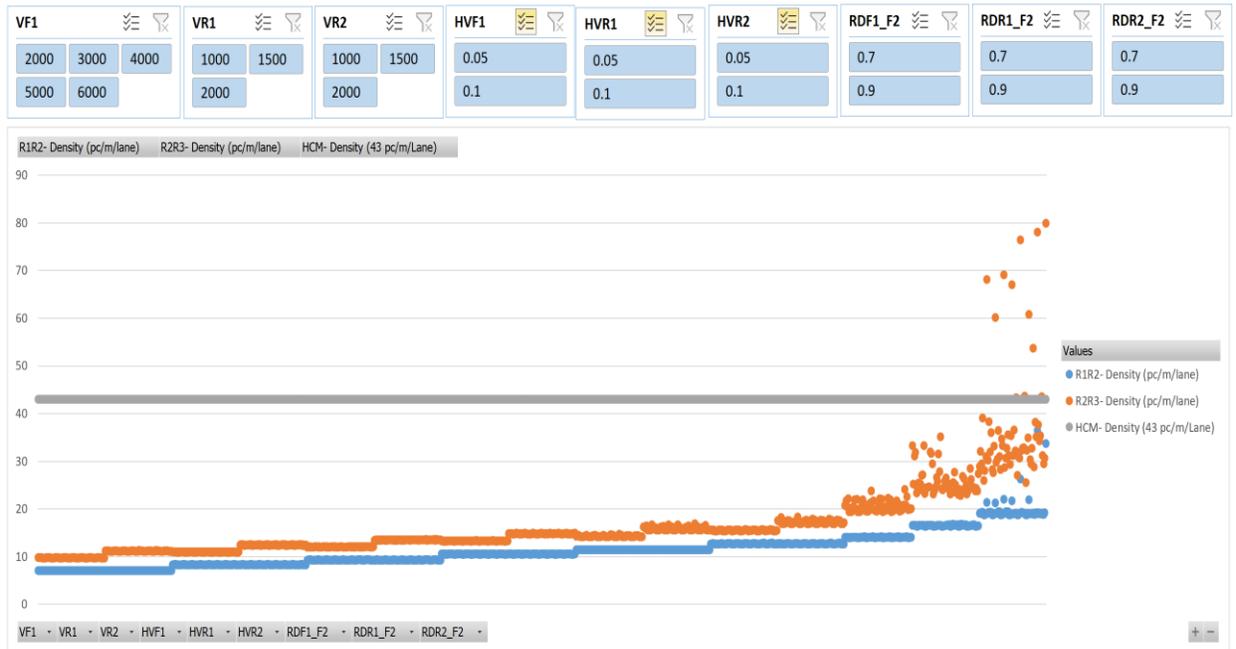


Figure 218: Scenario 41, Density

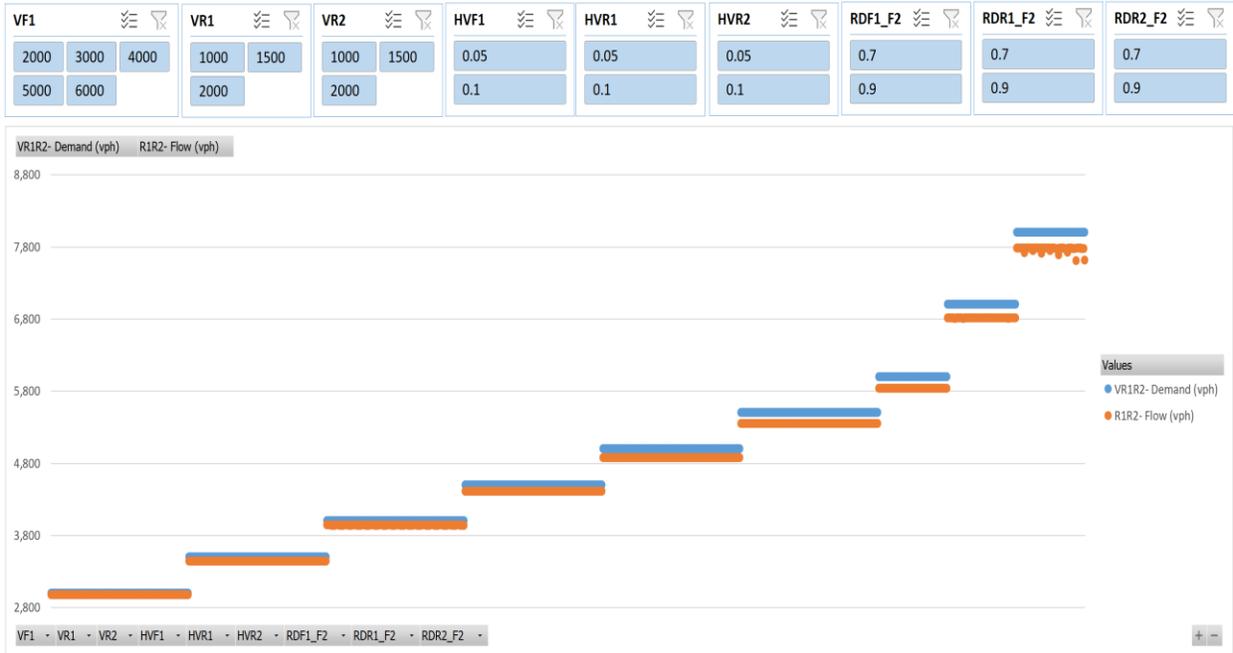


Figure 219: Scenario 41, R1R2 Flow vs. Demand

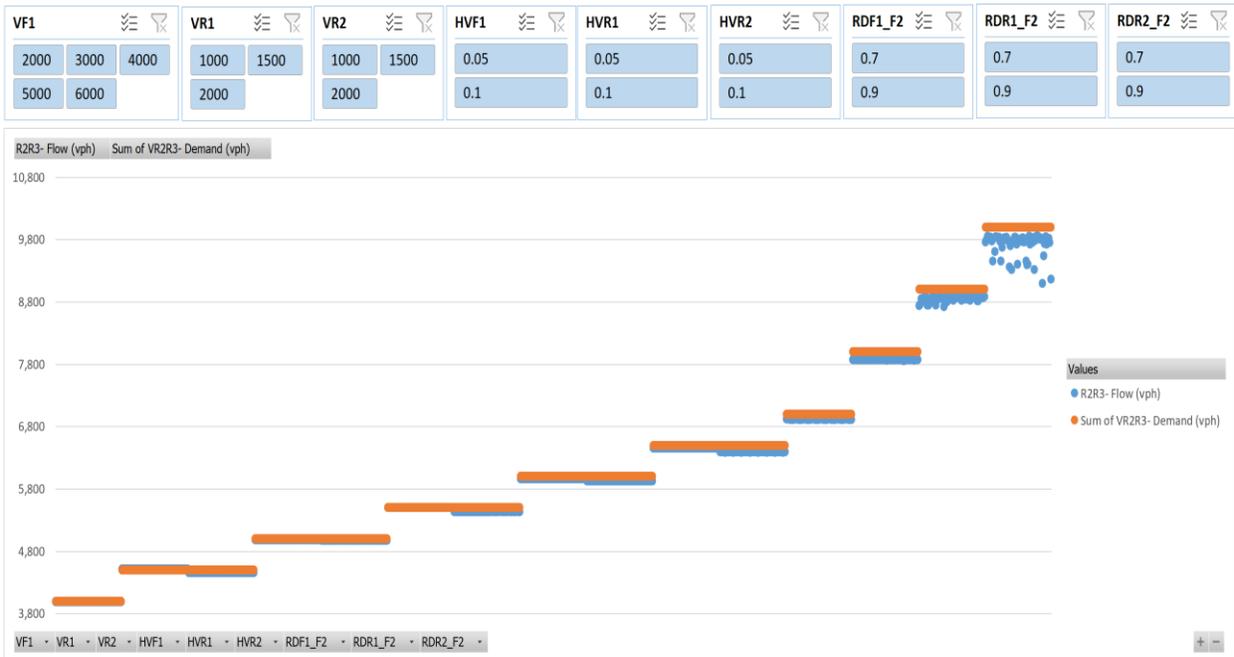


Figure 220: Scenario 41, R2R3 Flow vs. Demand

Scenario Number 42

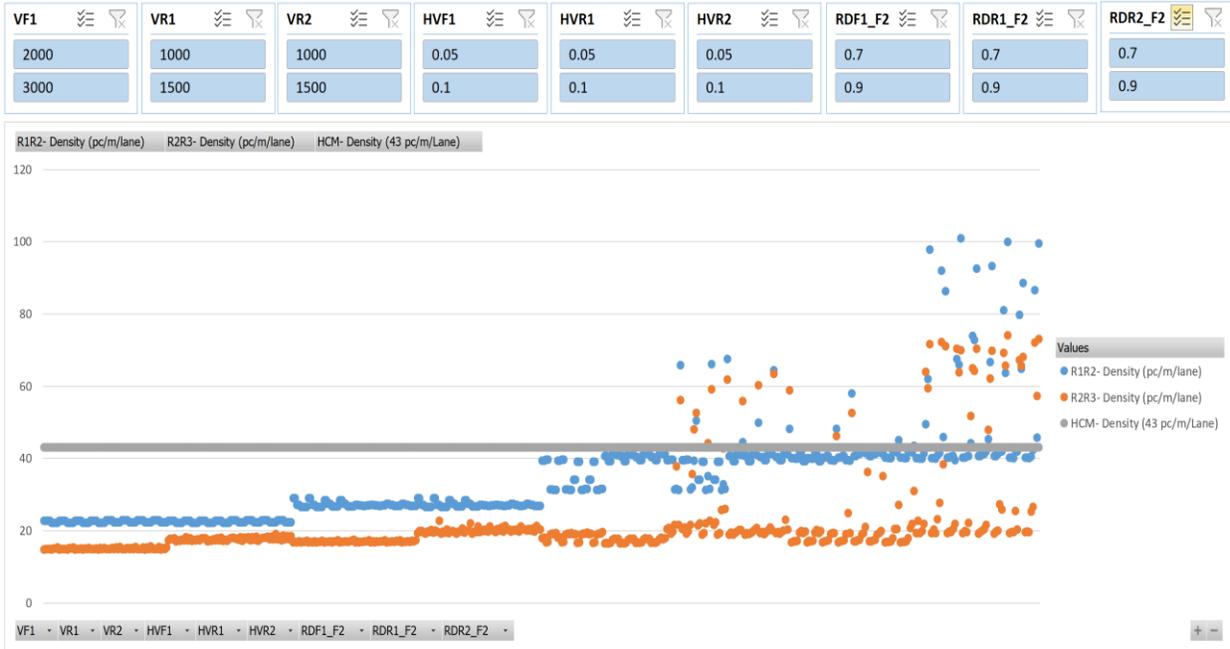


Figure 221: Scenario 42, Density

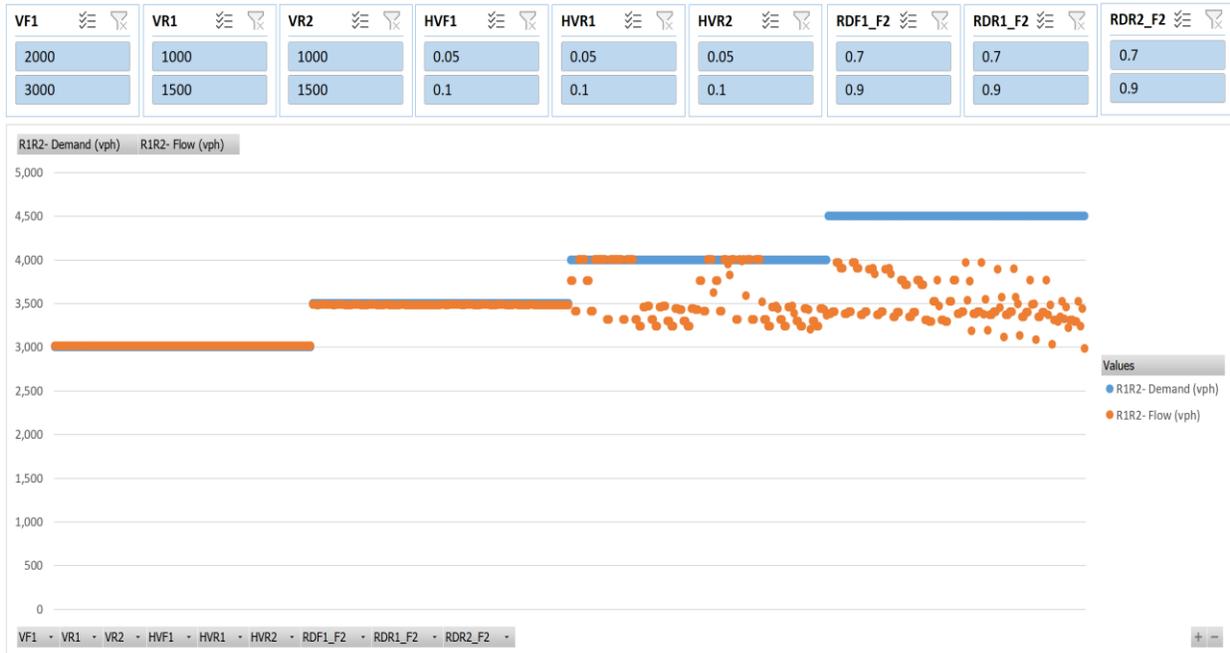


Figure 222: Scenario 42, R1R2 Flow vs. Demand

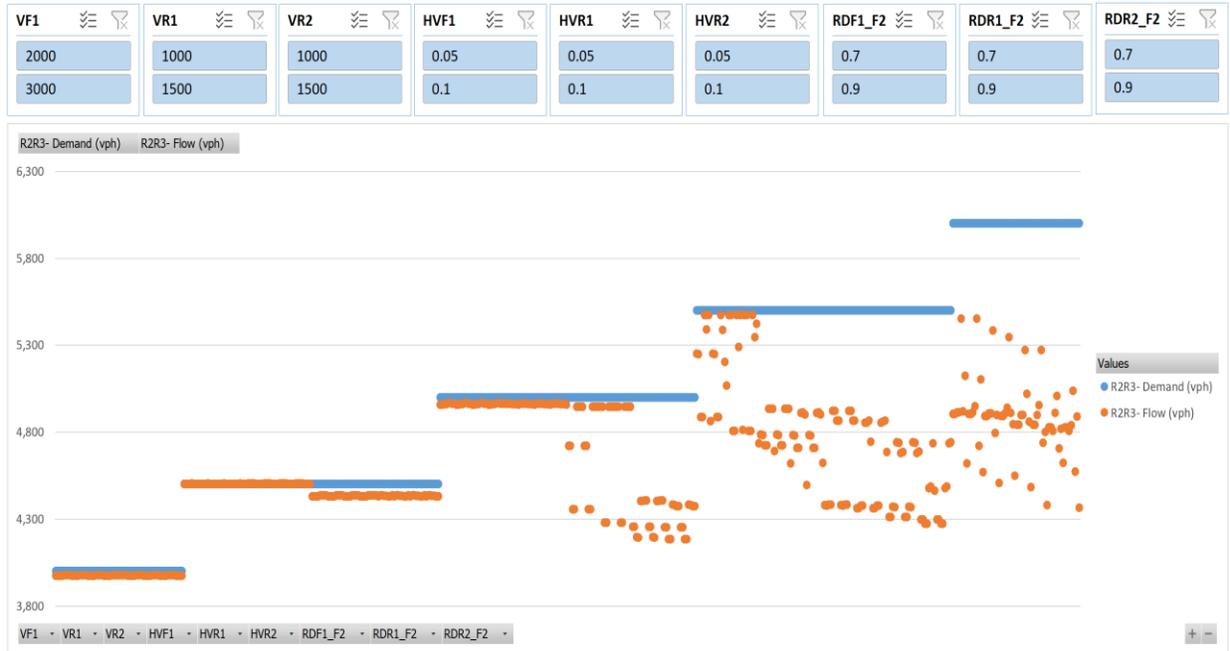


Figure 223: Scenario 42, R2R3 Flow vs. Demand

Scenario Number 43

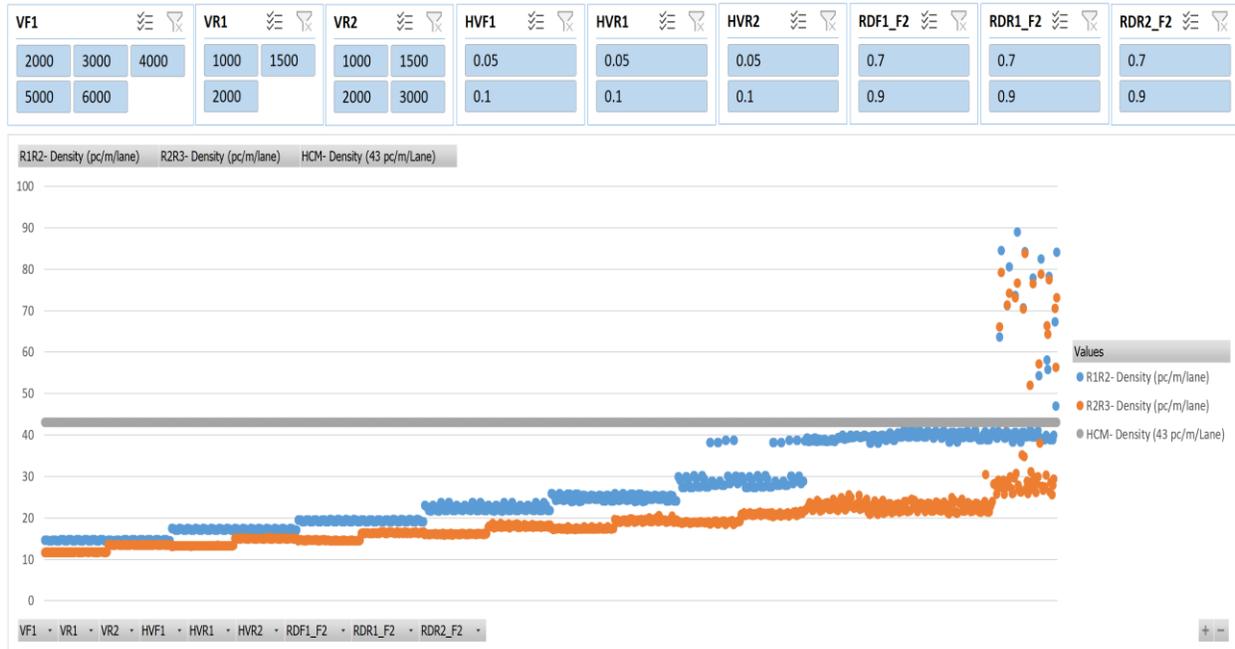


Figure 224: Scenario 43, Density

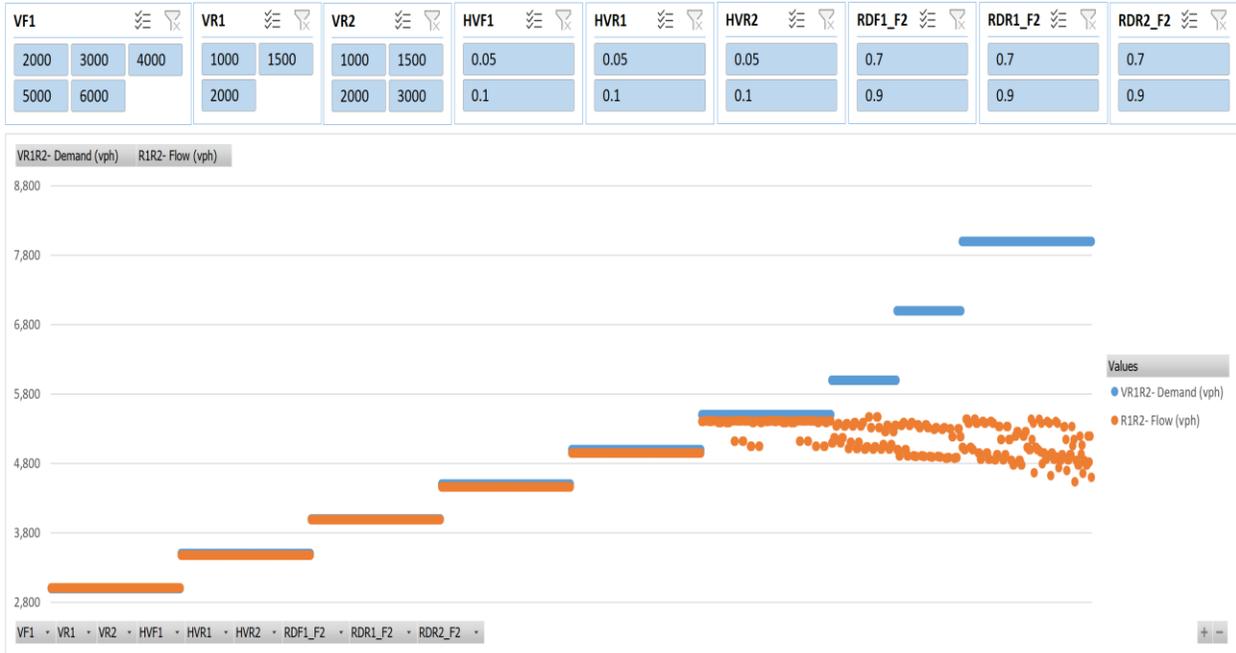


Figure 225: Scenario 43, R1R2 Flow vs. Demand

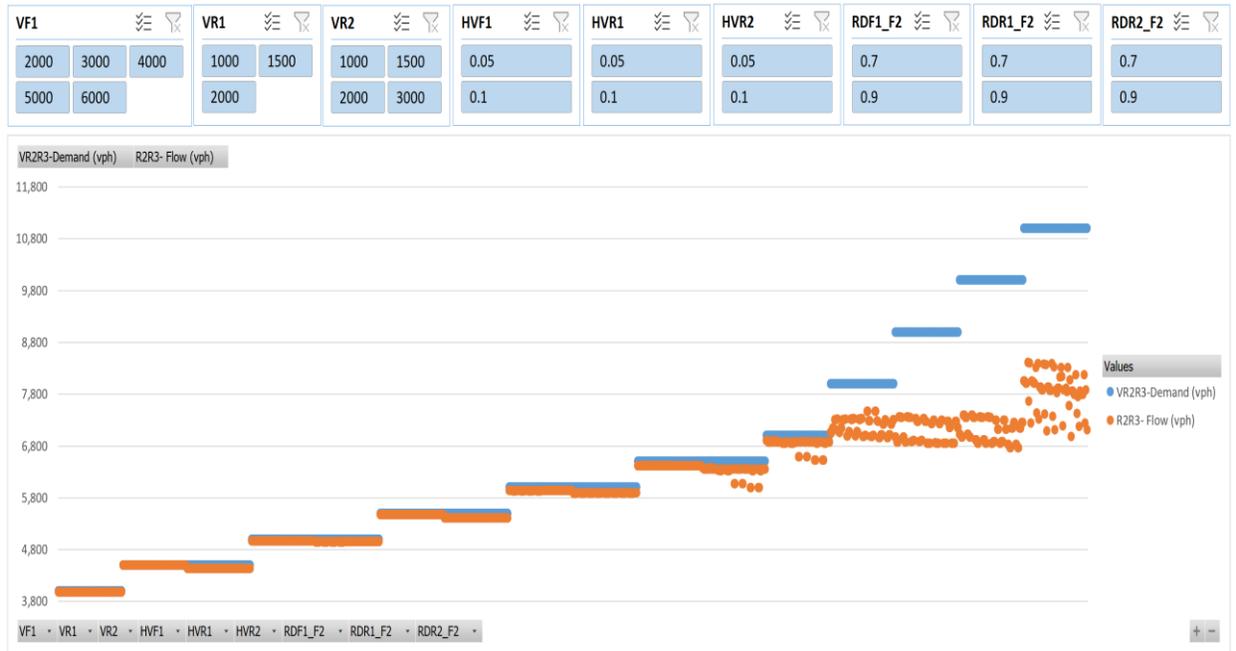


Figure 226: Scenario 43, R2R3 Flow vs. Demand

Scenario Number 44

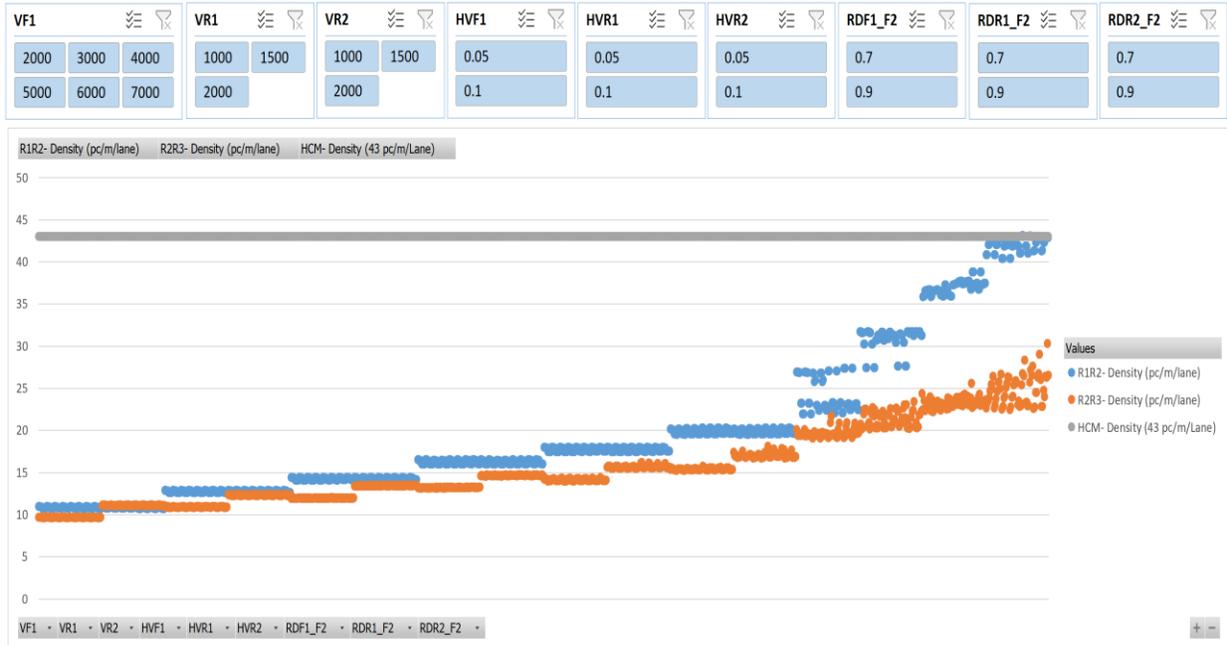


Figure 227: Scenario 44, Density

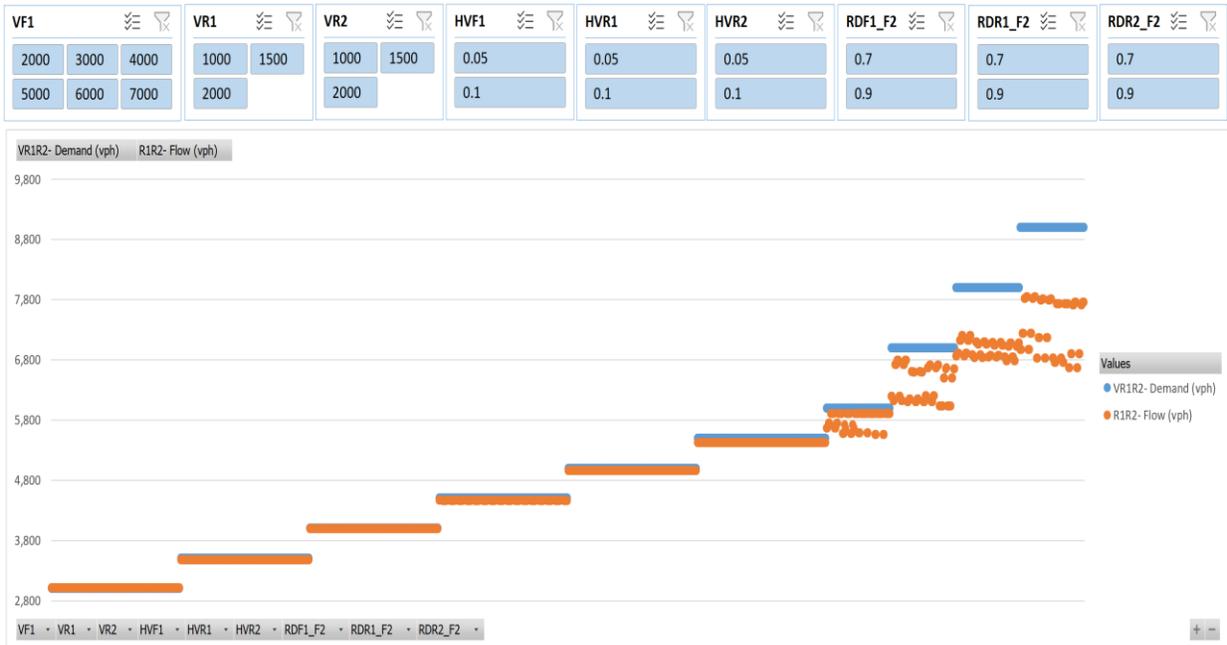


Figure 228: Scenario 44, R1R2 Flow vs. Demand

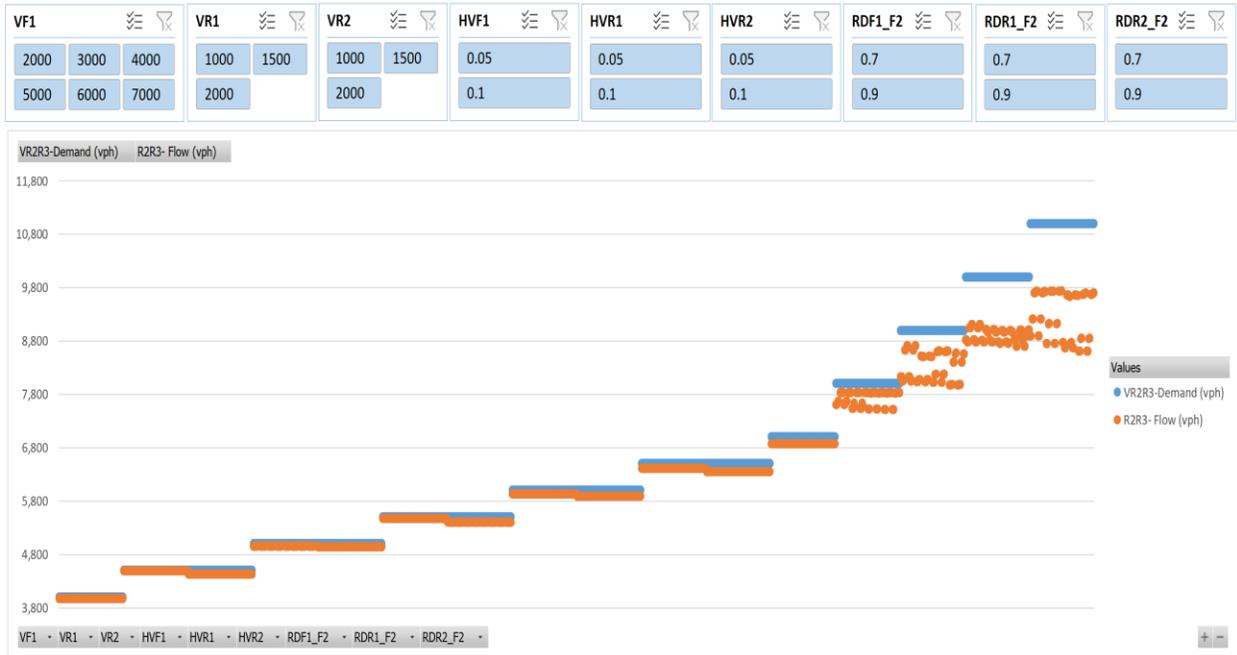


Figure 229: Scenario 44, R2R3 Flow vs. Demand

APPENDIX C; MOST SIGNIFICANT FLOWS

R1R2 Segment

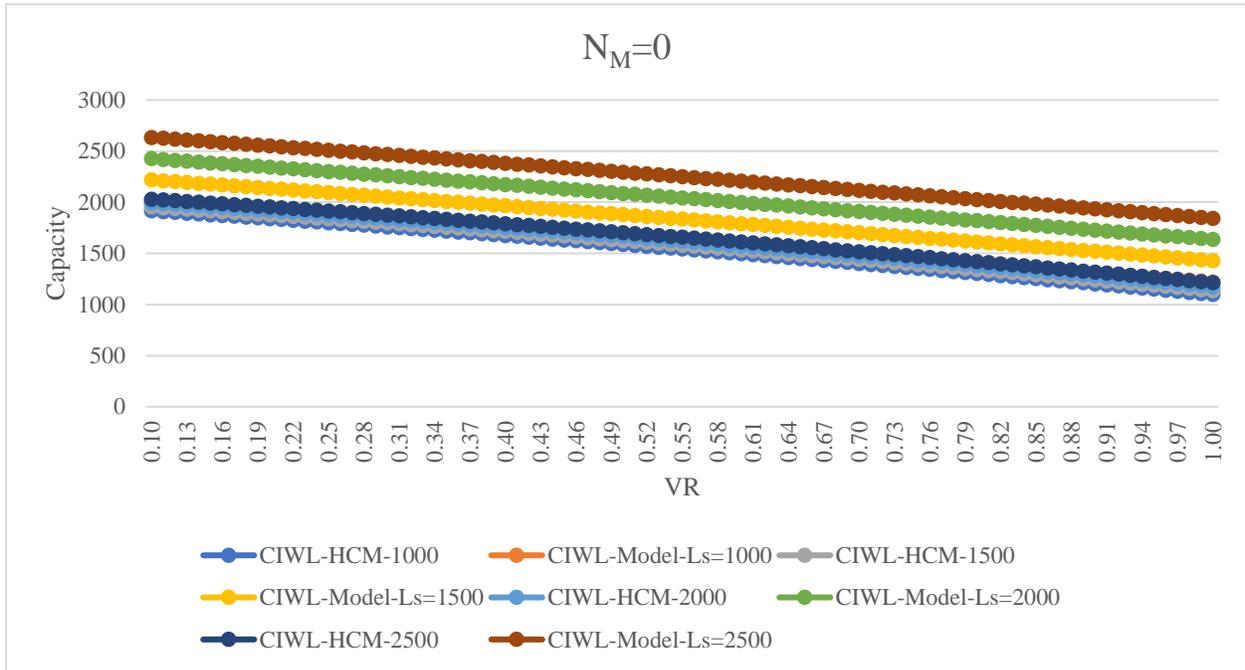


Figure 230: R1R2 Segment- Removing (F1-F2)- $N_M=0$

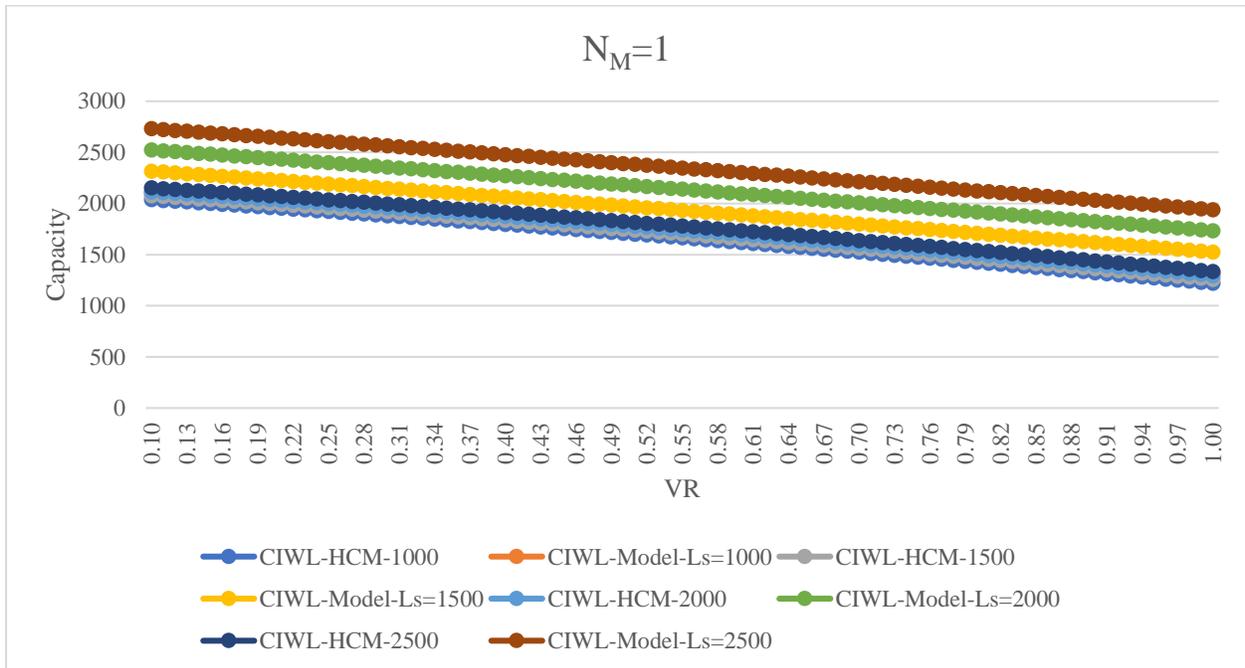


Figure 231: R1R2 Segment- Removing (F1-F2), $N_M=1$

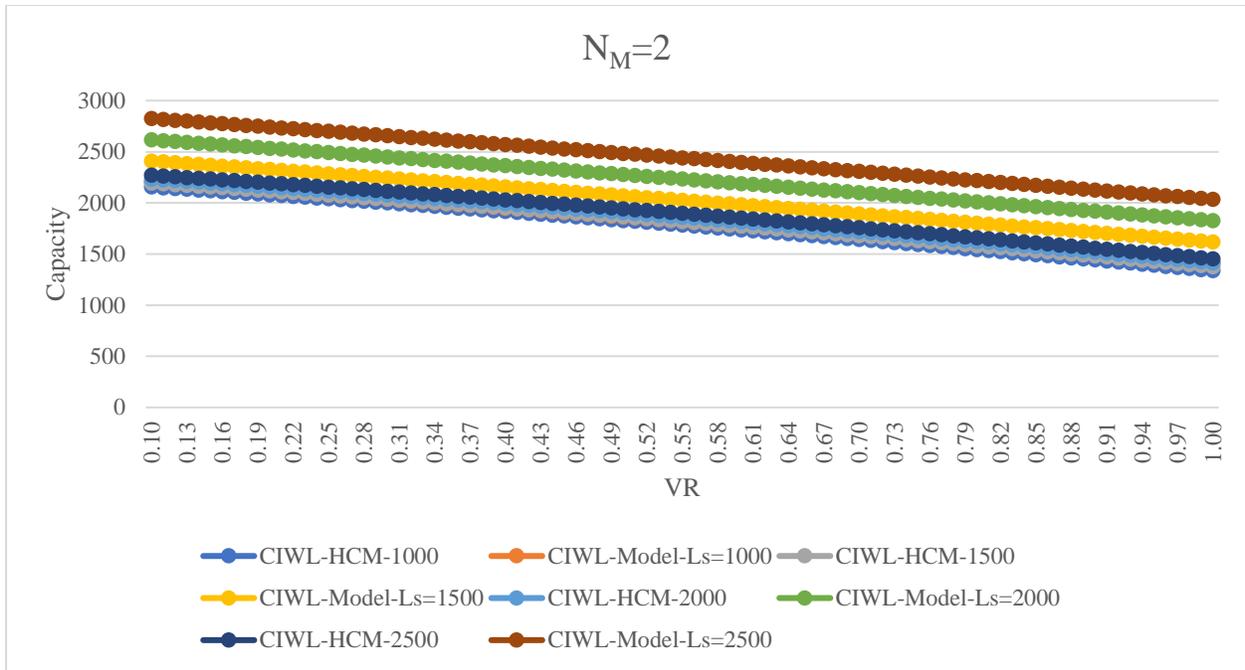


Figure 232: R1R2 Segment- Removing (F1-F2), $N_M=2$

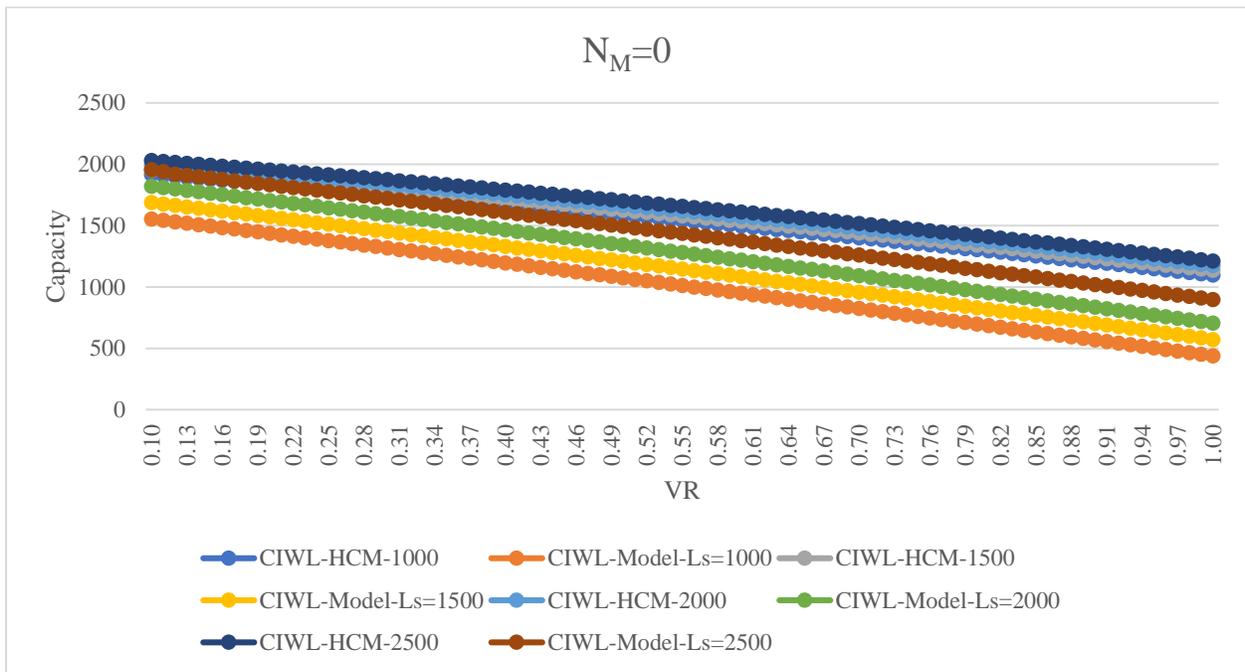


Figure 233: R1R2 Segment- Removing (F1-R3), $N_M=0$

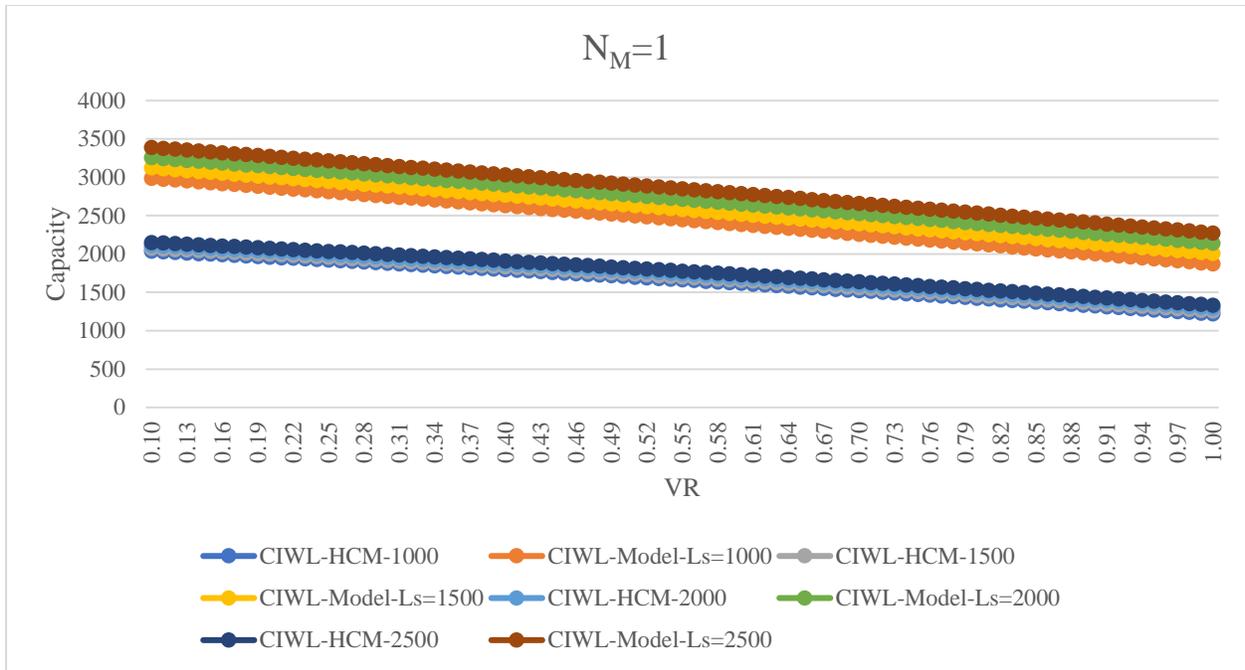


Figure 234: R1R2 Segment- Removing (F1-R3), $N_M=1$

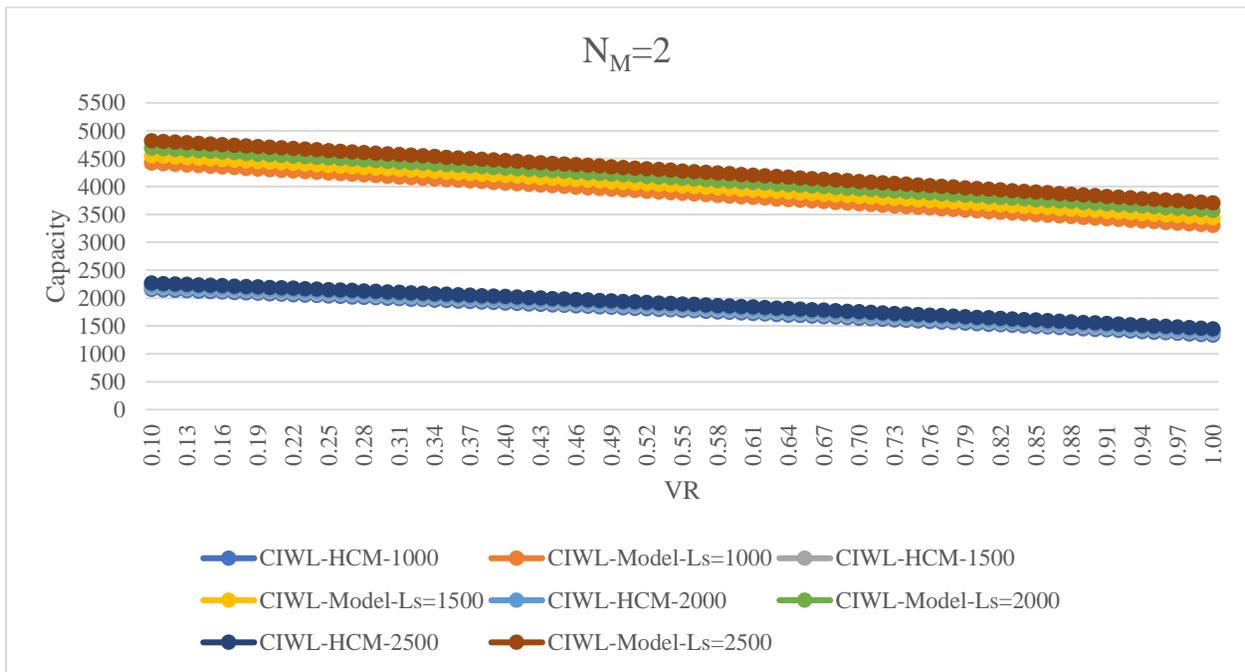


Figure 235: R1R2 Segment- Removing (F1-R3), $N_M=2$

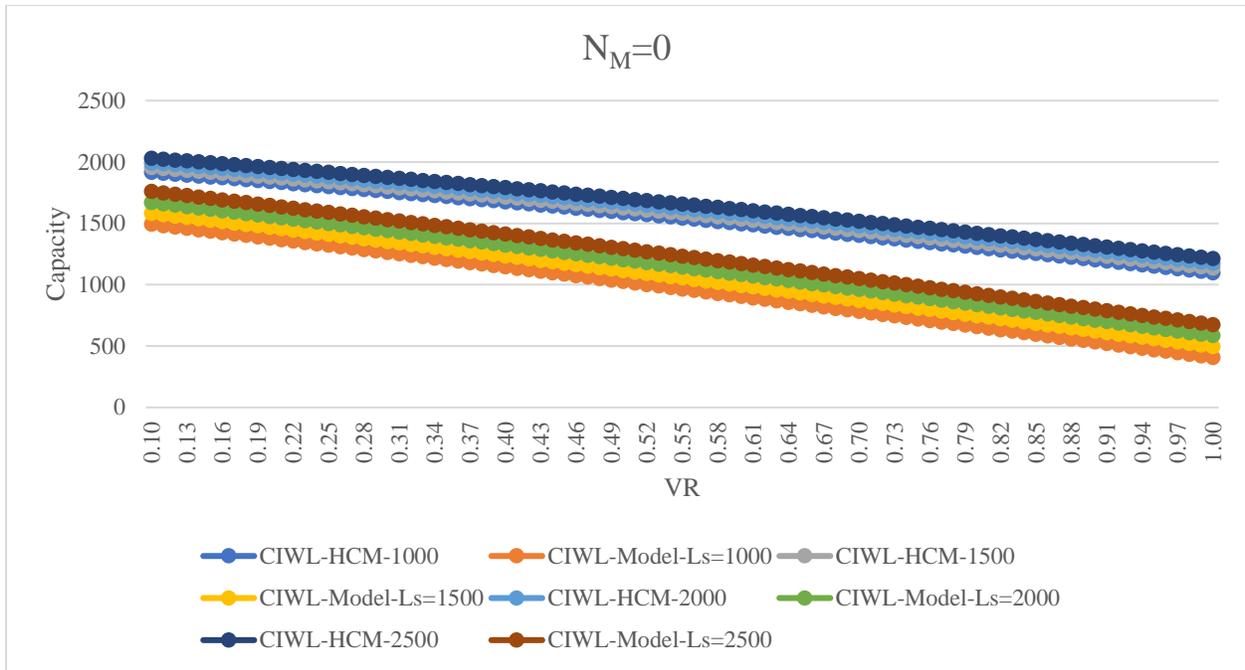


Figure 236: R1R2 Segment- Removing (R1-F2), $N_M=0$

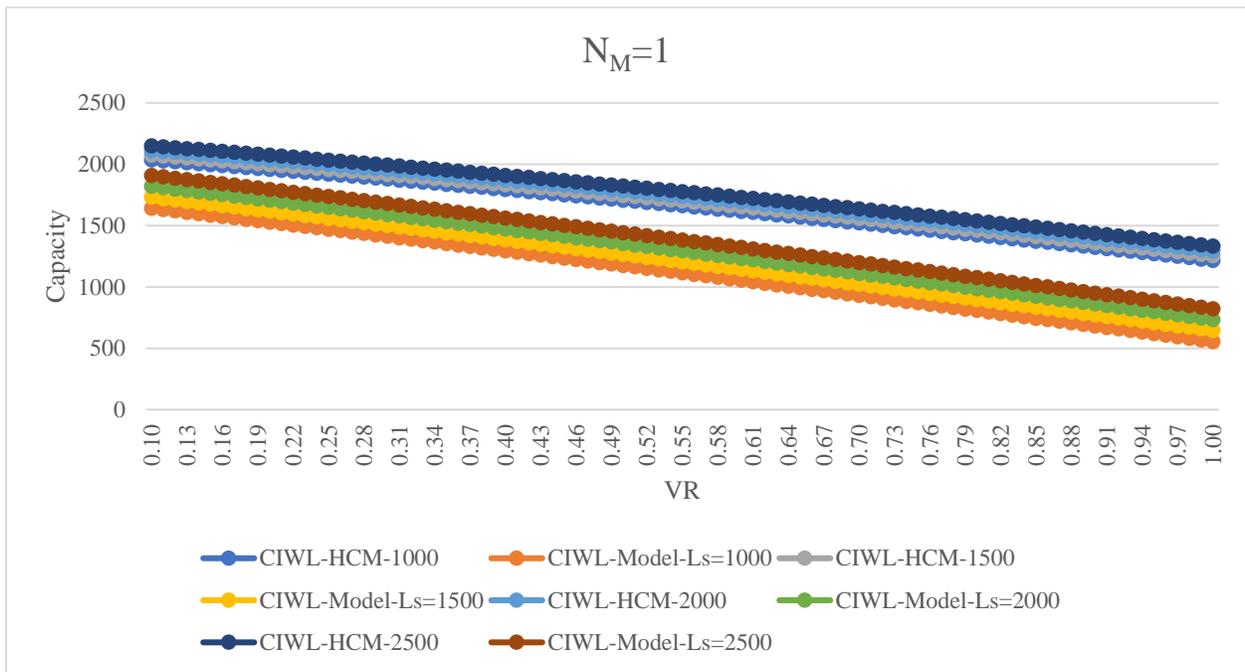


Figure 237: R1R2 Segment- Removing (R1-F2), $N_M=1$

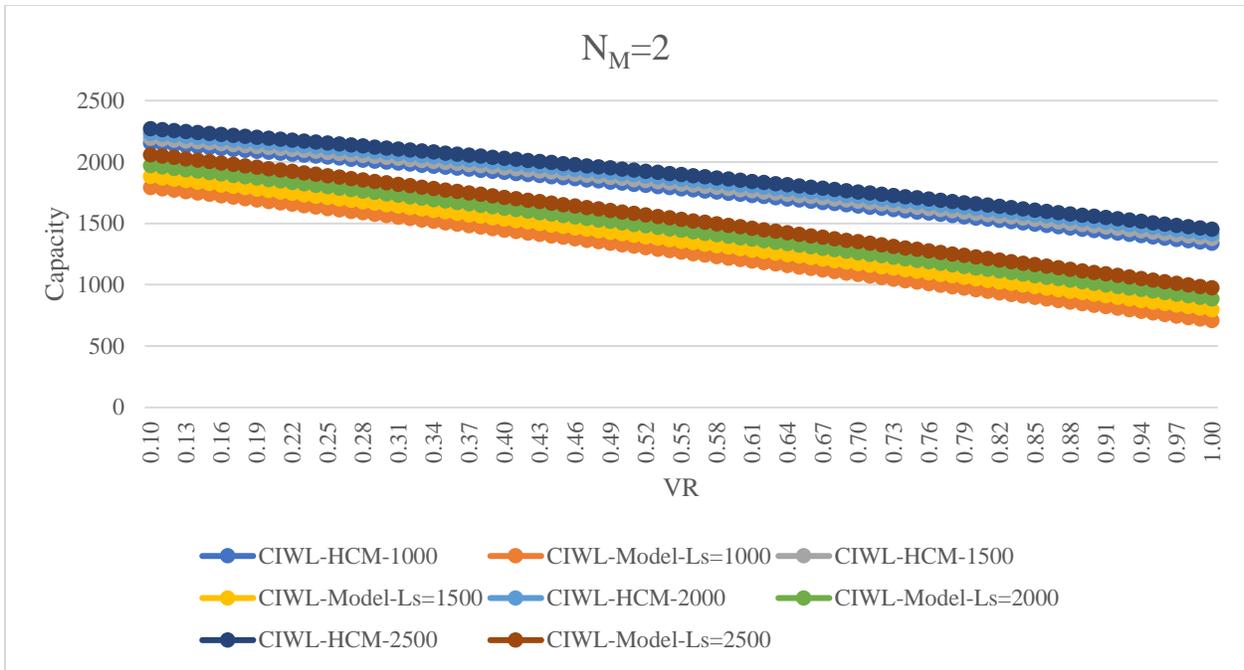


Figure 238: R1R2 Segment- Removing (R1-F2), $N_M=2$

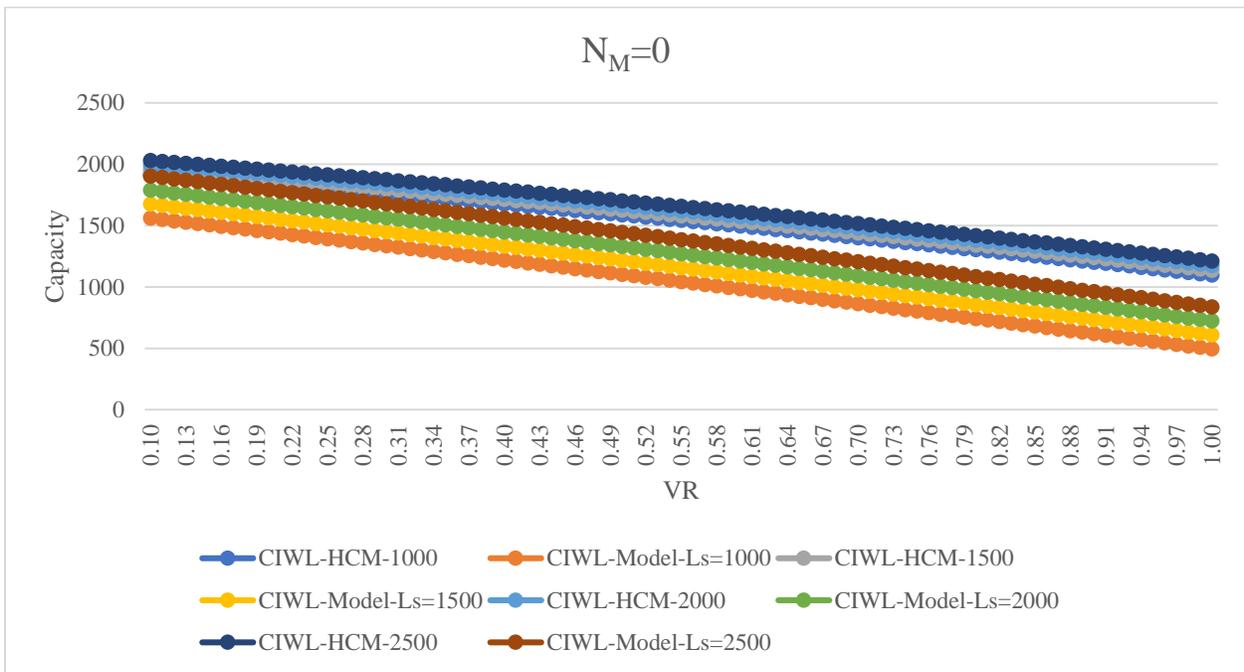


Figure 239: R1R2 Segment- Removing (R1-R3), $N_M=0$

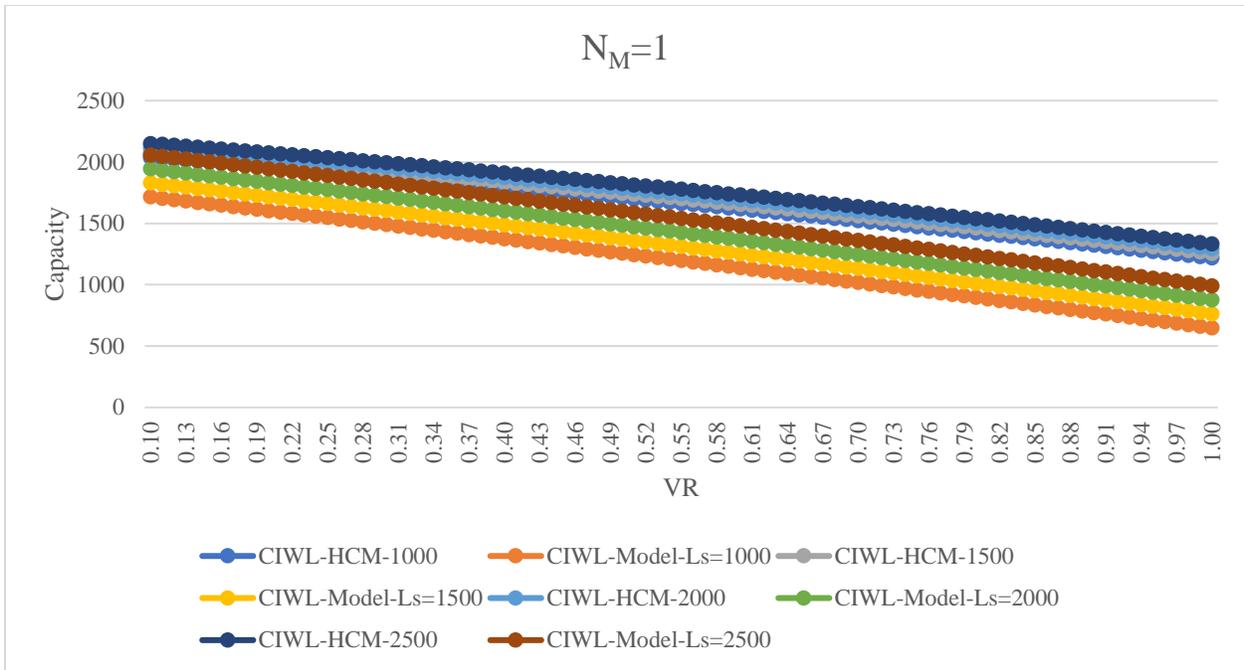


Figure 240: R1R2 Segment- Removing (R1-R3), $N_M=1$

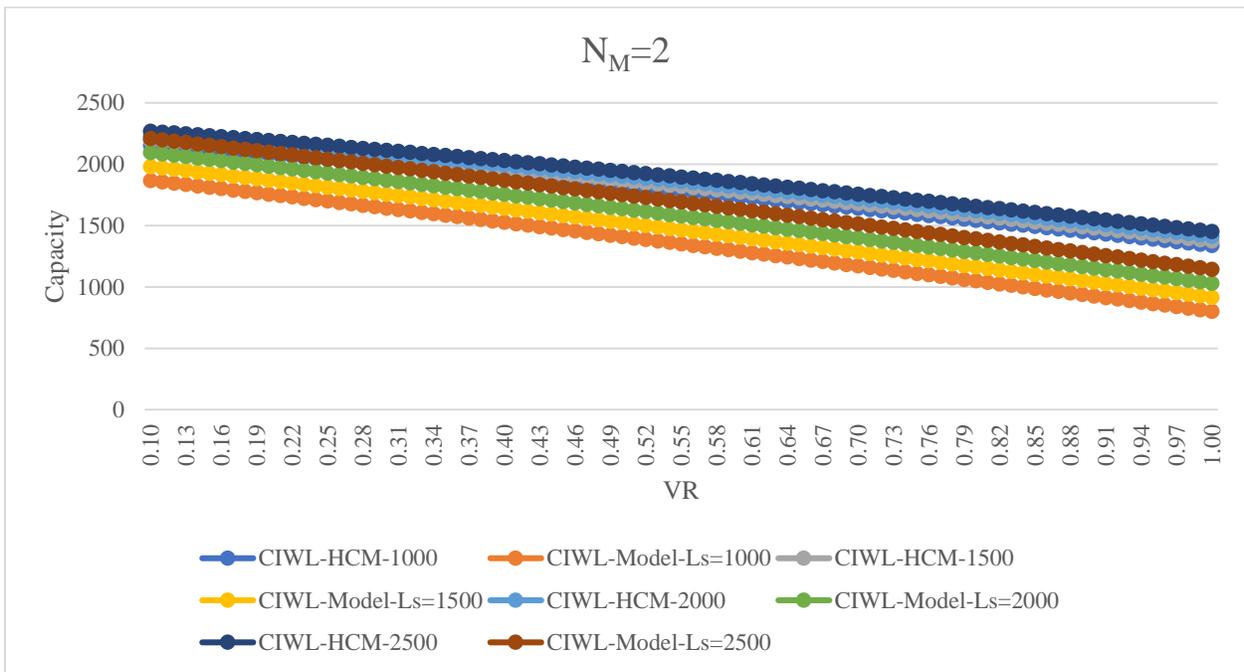


Figure 241: R1R2 Segment- Removing (R1-R3), $N_M=2$

R2R3 segment

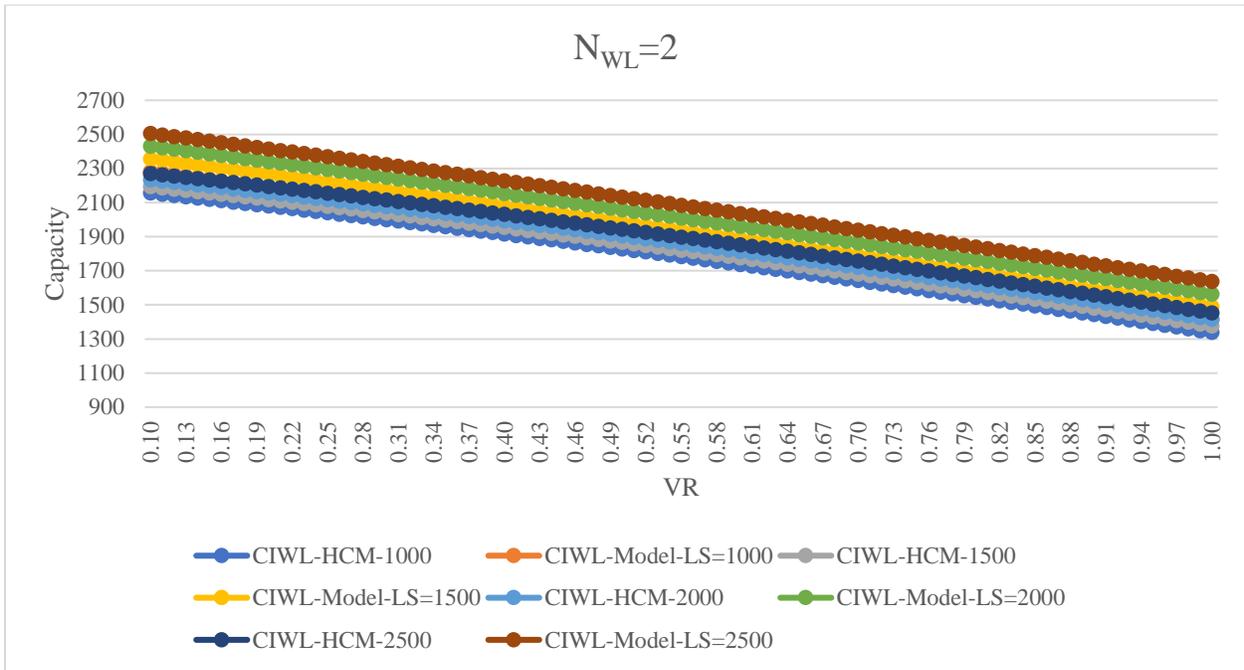


Figure 242: R2R3 Segment- Removing (F1-F2), $N_{WL}=2$

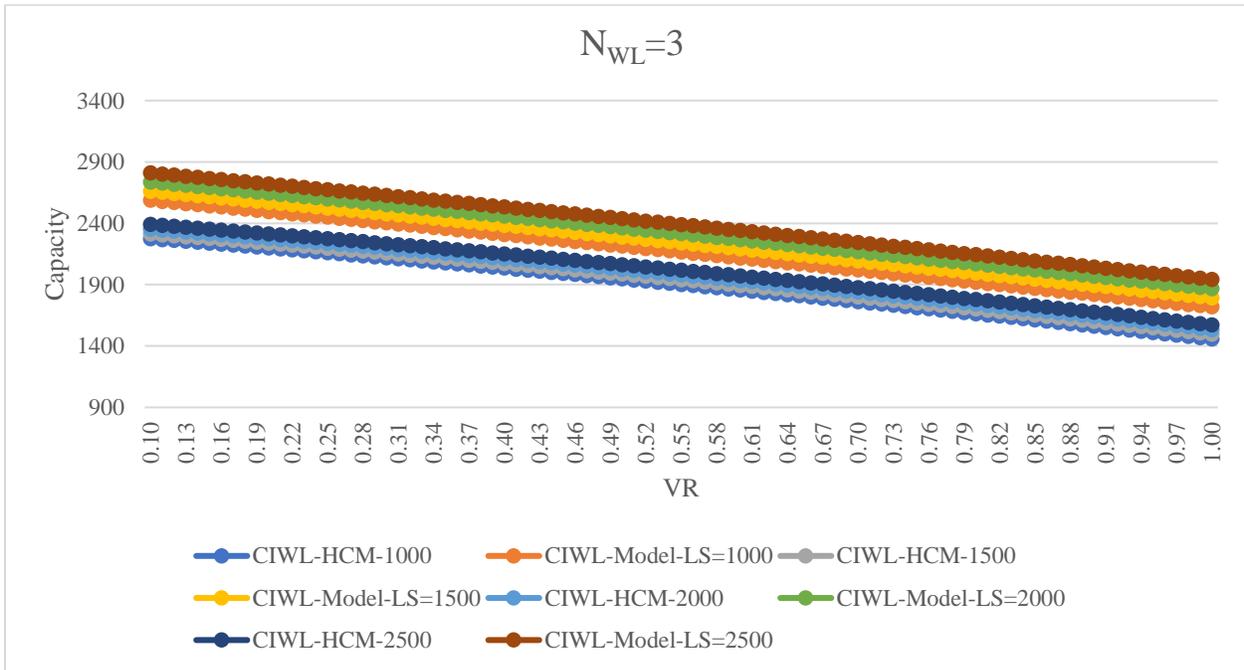


Figure 243: R2R3 Segment- Removing (F1-F2), $N_{WL}=3$

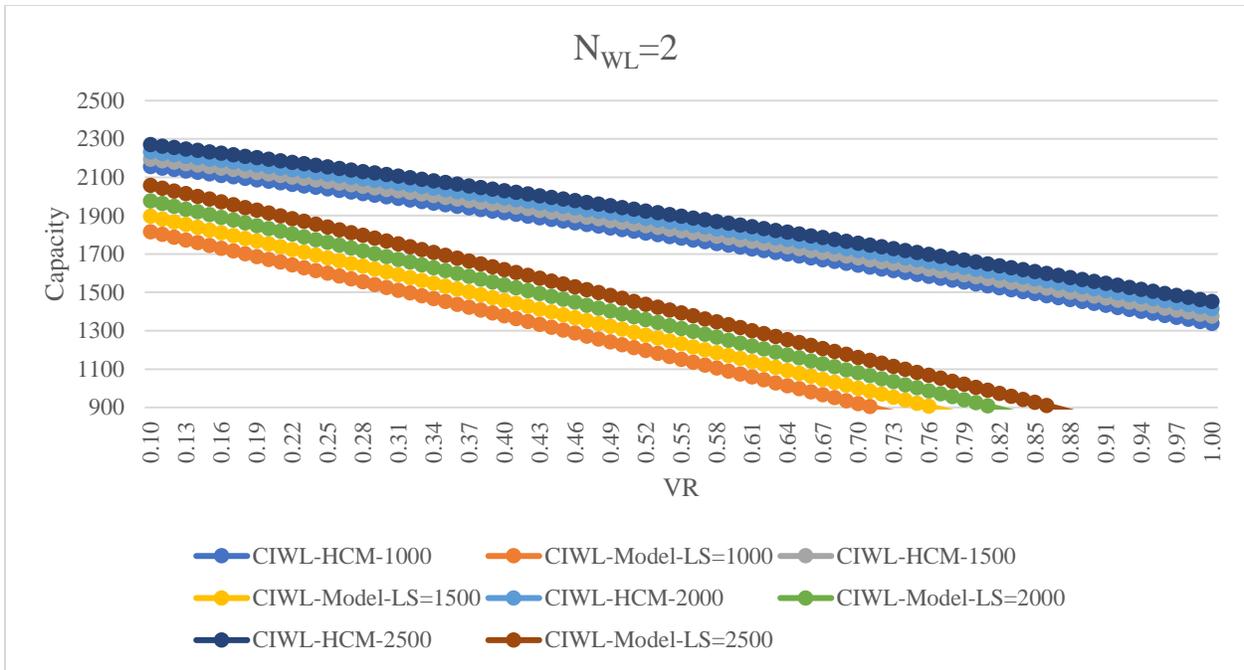


Figure 244: R2R3 Segment- Removing (F1-R3), $N_{WL}=2$

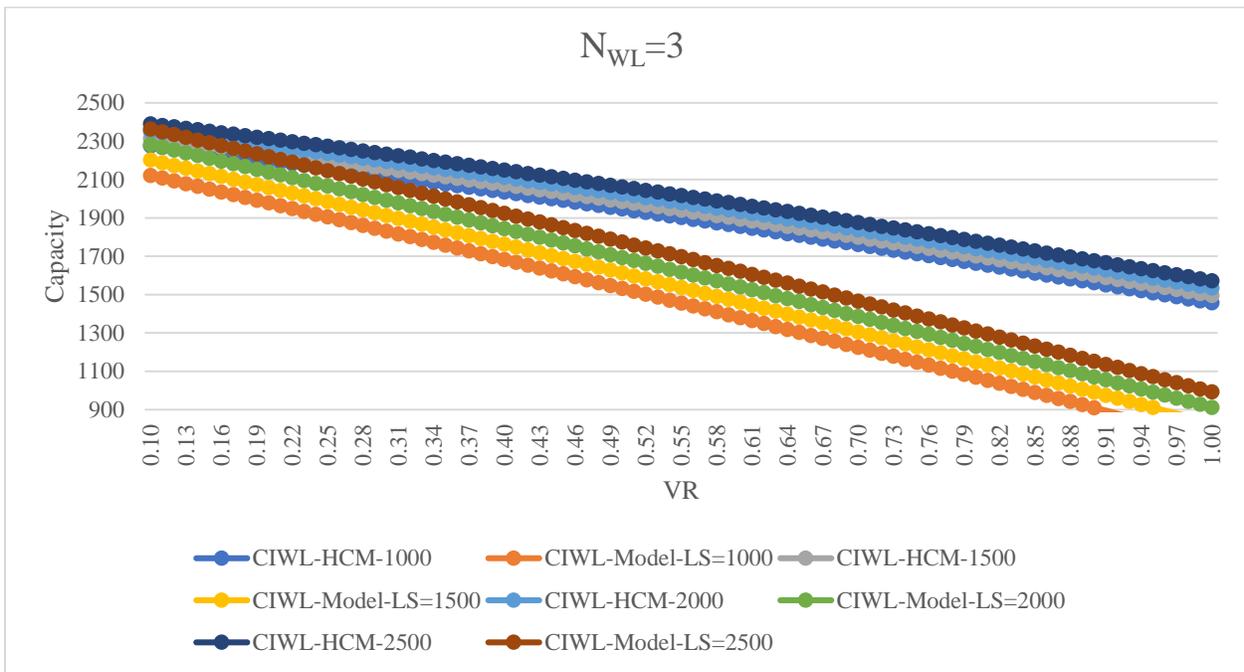


Figure 245: R2R3 Segment- Removing (F1-R3), $N_{WL}=3$

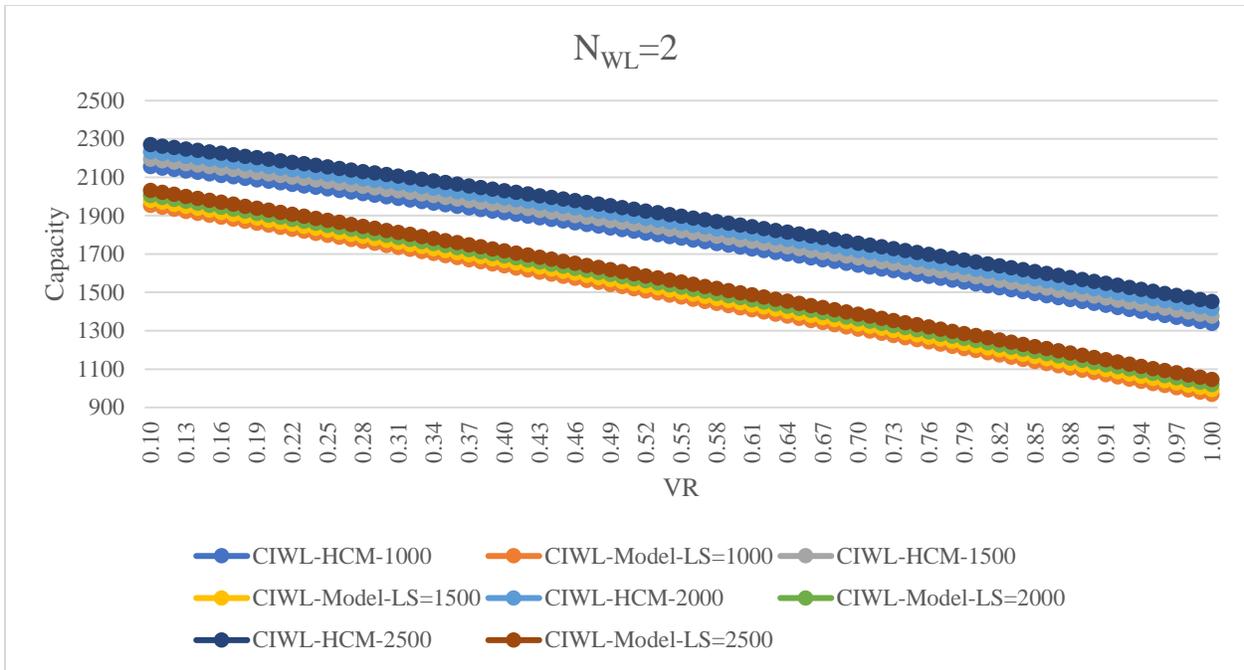


Figure 246: R2R3 Segment- Removing (R1-F2), $N_{WL}=2$

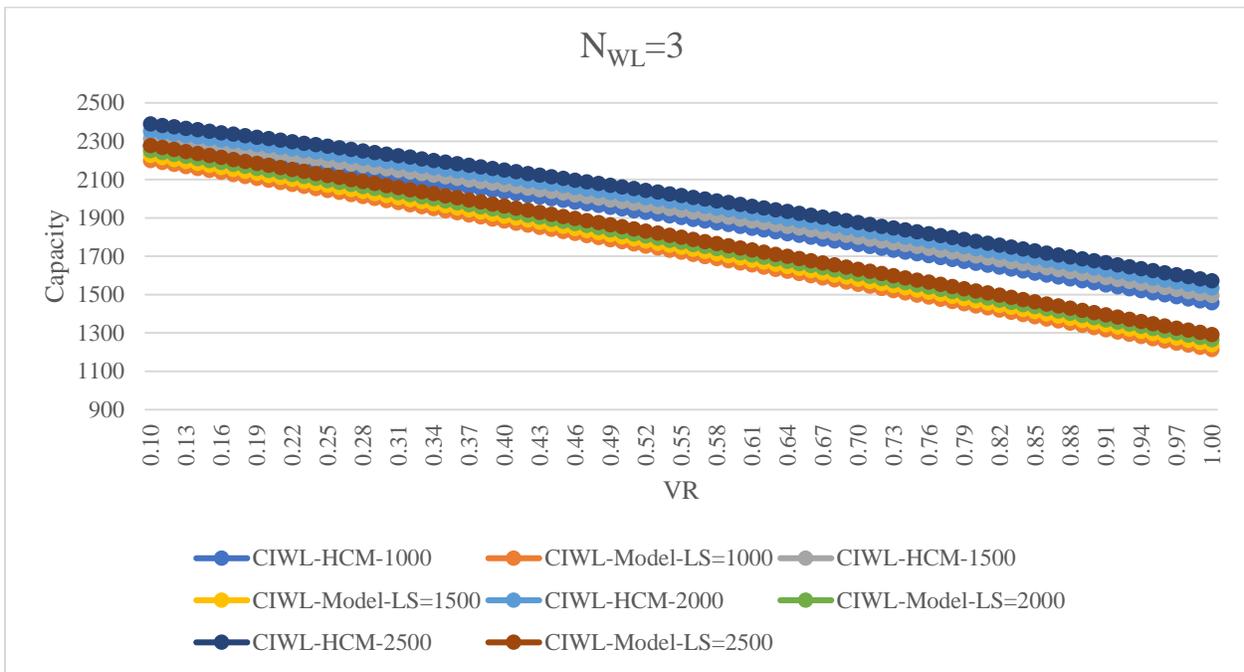


Figure 247: R2R3 Segment- Removing (R1-F2), $N_{WL}=3$

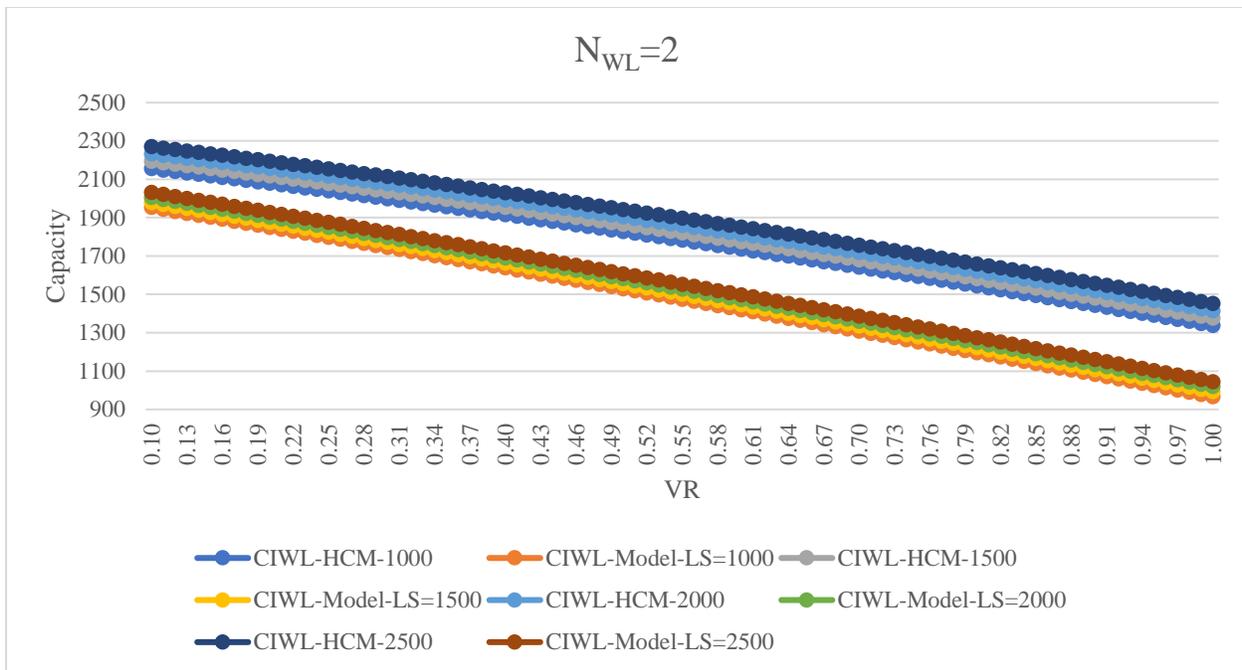


Figure 248: R2R3 Segment- Removing (R1-R3), $N_{WL}=2$

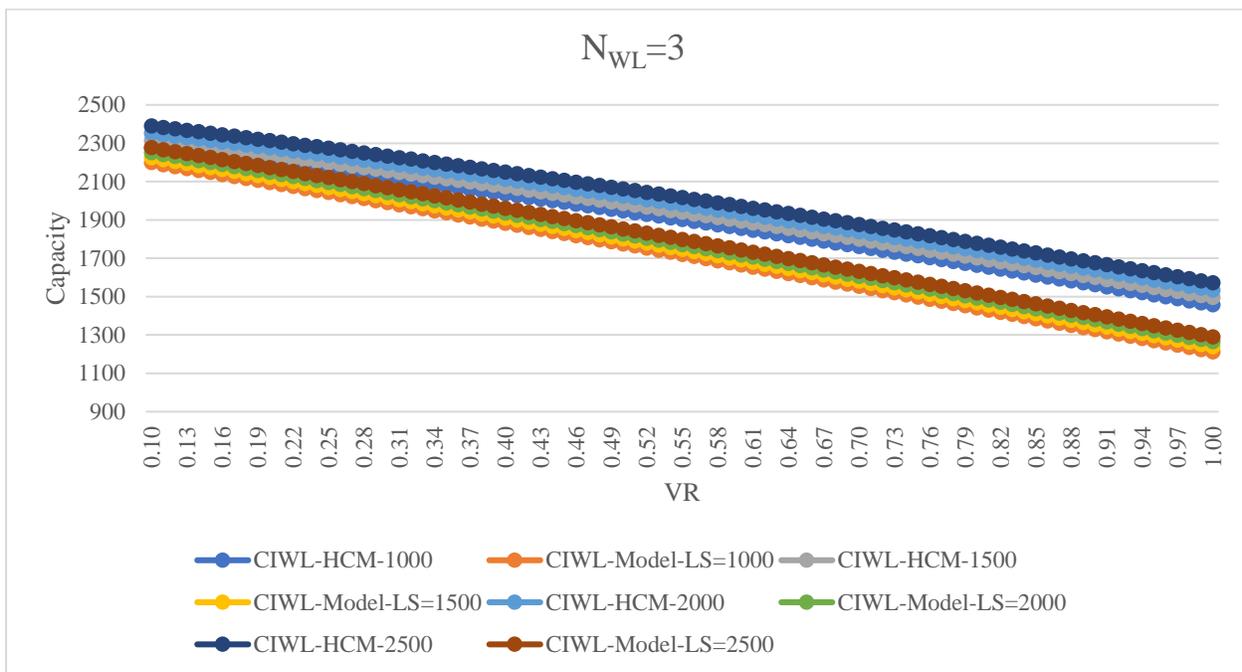


Figure 249: R2R3 Segment- Removing (R1-R3), $N_{WL}=3$

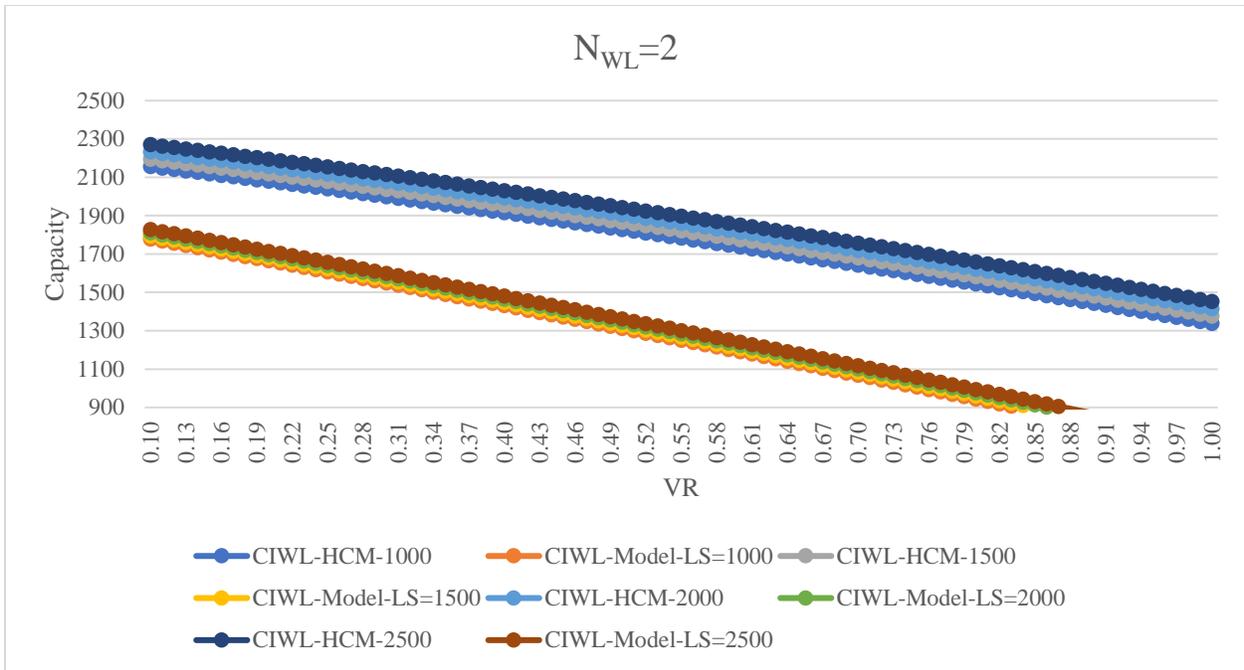


Figure 250: R2R3 Segment- Removing (R2-F2), $N_{WL}=2$

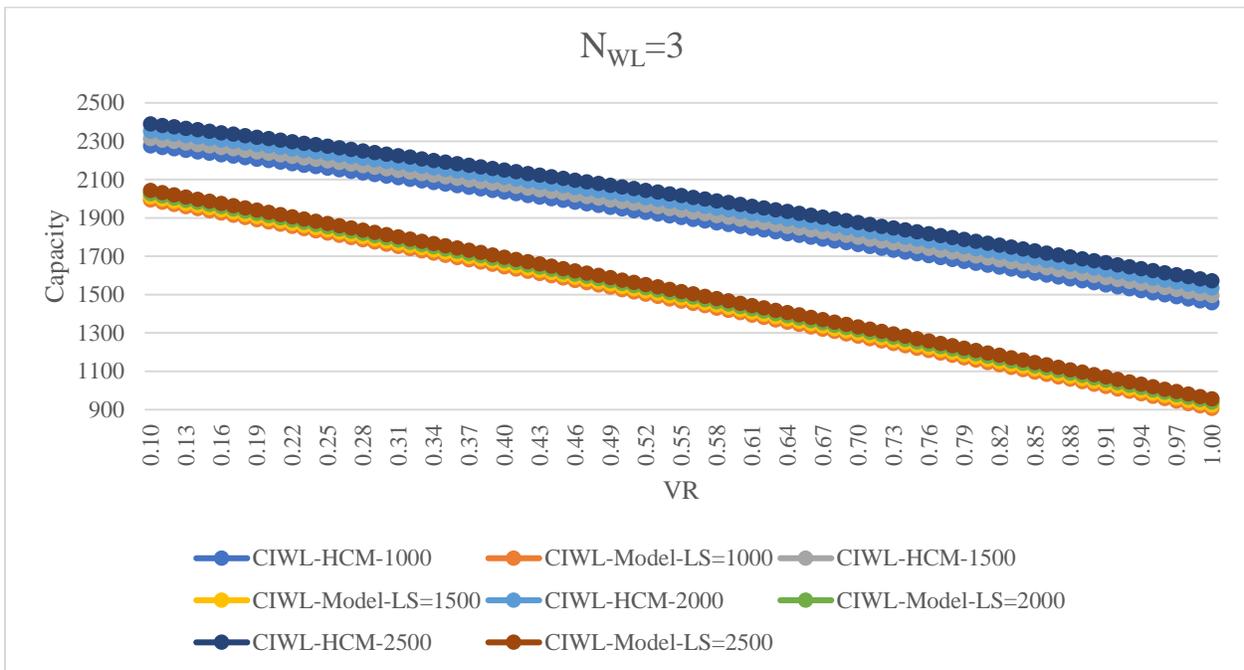


Figure 251: R2R3 Segment- Removing (R2-F2), $N_{WL}=3$

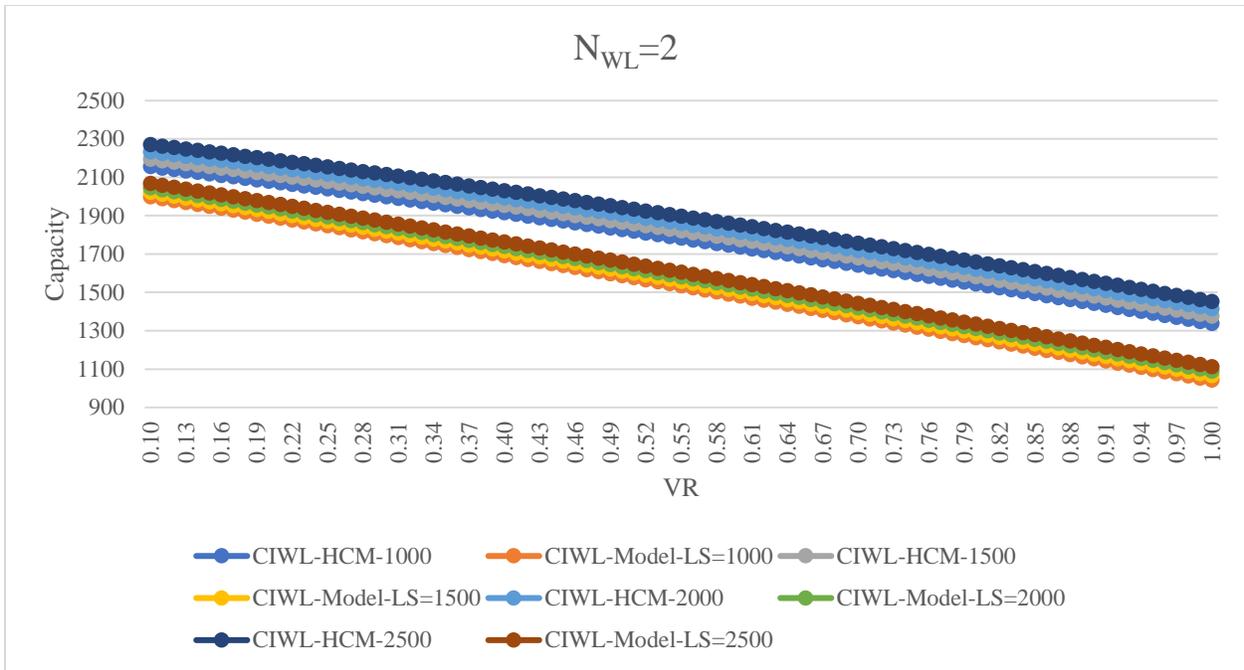


Figure 252: R2R3 Segment- Removing (R2-R3), $N_{WL}=2$

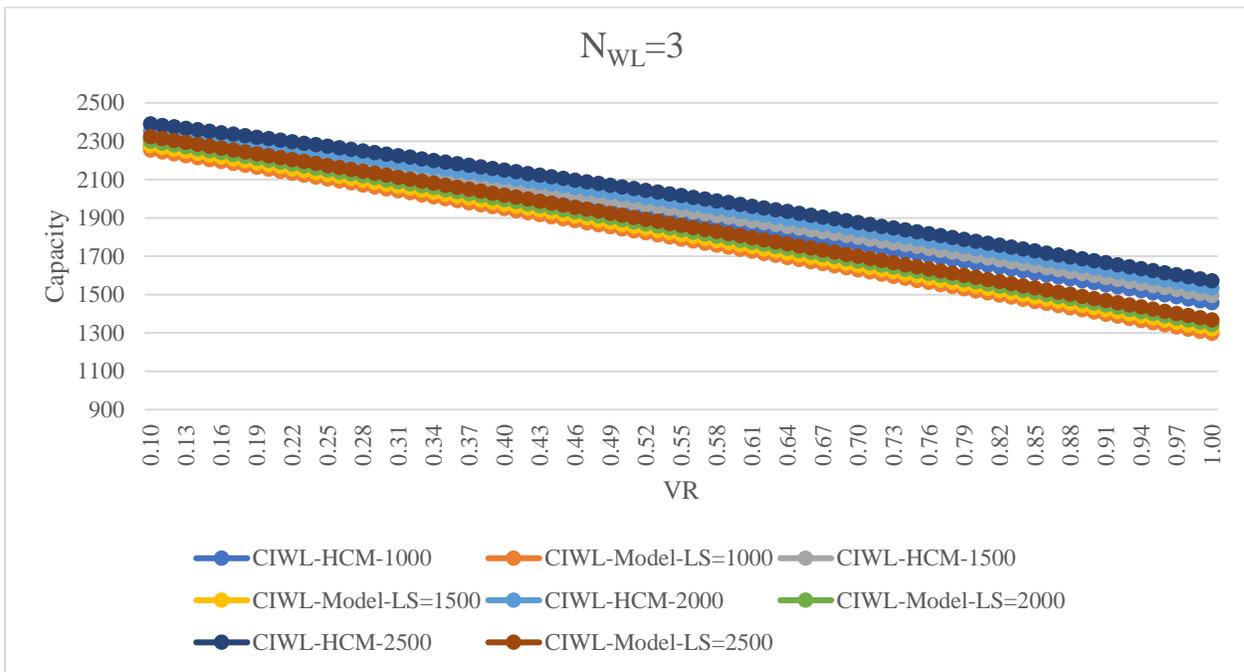


Figure 253: R2R3 Segment- Removing (R2-R3), $N_{WL}=3$